Electronic Supporting Information (ESI)

Salt Complexation Drives Liquid Crystalline Self-Assembly in Crown Ether–Amino Acid Hybrids

Aileen R. Raab,*[a] Tanja Robin Grießer,[a] Daniel Rück,[a] Zhuoqing Li,[b,c] Anna Zens,[a] Johanna R. Bruckner,*[f] Patrick Huber,[b,c] Andreas Schönhals,[d,e] Paulina Szymoniak,*[d] and Sabine Laschat*[a]

a *Universität Stuttgart, Institut für Organische Chemie, Pfaffenwaldring 55, 70569 Stuttgart, Germany.*

b *Hamburg University of Technology, Institute for Materials and X-ray Physics, Denickestr. 15, 21073 Hamburg, Germany*

c *Centre for X-ray and Nano Science CXNS, Deutsches Elektronen-Synchrotron DESY, Notkestr. 85, 22607 Hamburg, Germany*

d *Bundesanstalt für Materialforschung und -prüfung, Unter den Eichen 87, 12205 Berlin, Germany.*

e *Technische Universität Berlin, Institut für Chemie, Straße des 17. Juni 135, 10623 Berlin, Germany.*

f *Universität Stuttgart, Institut für Physikalische Chemie, Pfaffenwaldring 55, 70569 Stuttgart, Germany.*

Acknowledgement

Generous financial support by the Deutsche Forschungsgemeinschaft (DFG grant # LA 907/21-1; HU 850/13-1; SCHO 470/26-1) and DFG (INST 41/897-1 FUGG for 700 MHz NMR, INST 41/1136-1 FUGG for Orbitrap LC-MS), the Carl-Schneider Stiftung Aalen (shared instrumentation grant) and the Ministerium für Wissenschaft, Forschung und Kunst des Landes Baden-Württemberg are gratefully acknowledged.

Table of Contents

1 Materials and Equipment

All **chemicals** were, unless otherwise stated, used without further purification. The eluents for chromatography (acetone, dichloromethane, low boiling hexanes, and ethyl acetate EtOAc) were distilled prior to use. For spectroscopic and spectrometric analysis, the samples were dissolved in deuterated solvents from Eurisotop.

^{1}H **NMR spectra** were measured using the *Bruker Avance 300 NMR*, *Bruker Avance III HD 400 NanoBay NMR*, *Bruker Avance 500 NMR* and *Bruker Avance III HD 700 NMR* spectrometers at 300 MHz, 400 MHz and 700 MHz, ^{13}C NMR spectra at 101 MHz, 126 MHz and 176 MHz respectively. ^{19}F NMR spectra were measured using the *Bruker Avance III HD 400 NanoBay NMR* spectrometer at 376 MHz. To assign the signals of the ^{1}H and ^{13}C NMR spectra, COSY, HSQC, and HMBC measurements were carried out.

FT-IR spectra were measured on a Bruker Vektor 22 with a MKII Golden Gate Single Reflection Diamond ATR. Absorption bands were rounded to integer wavenumbers / cm^{-1} and the absorption intensities were classified as follows: w (weak), m (medium), s (strong), vs (very strong).

Mass spectra (MS) and high-resolution mass spectra (HRMS) were measured by electrospray ionisation (ESI) using a Thermo Fisher Scientific Exactive Plus Orbitrap mass spectrometer. For **thin layer chromatography**, silica gel 60 F254 glass plates (layer thickness of 0.20 mm) on aluminium (pore size 60 Å) and *POLYGRAM® SIL G/UV$_{254}$* silica gel glass plates (40 mm x 80 mm, layer thickness of 0.20 mm) on aluminium from Macherey-Nagel were used. Column chromatography was performed using silica gel *SilicaFlash® F60* (particle diameter of 40 – 63 µm) from *SiliCycle*.

A **polarizing optical microscope** (POM) Olympus BX 50, equipped with a Linkam LTS350 heating stage was used. Temperature regulation was carried out with the control units TP93 and LNP from Linkam ($\Delta T = \pm 1$ K). Photographs were saved with a digital camera ZEISS Axiocam 105 color using the software ZEISS ZEN core from ZEISS microscopy.

For **differential scanning calorimetry** (DSC), a DSC288e and a DSC3 from Mettler Toledo was employed. The instruments were calibrated with indium. The compounds were analysed in 40 µL sealed aluminium pans from *Thepro GbR* with heating and cooling rates of 5 K/min and a nitrogen flow of 30 mL/min. Phase transition temperatures and enthalpies were determined by onset values with a linear baseline correction using the software STARe 14.00 and STARe 16.40.

Fast Scanning Calorimetry (FSC) was conducted using a power-compensated Flash DSC 1 (Mettler Toledo, Switzerland).[1] FSC is based on adiabatic chip calorimetry, which allows for heating rates of 10 K/s to 10^4 K/s due to the microfabricated UFS2 chip sensor which is used

as sample cell. The cooling rates are one order of magnitude lower. The used sample masses were in the range from 200 ng to 500 ng. A Huber TC 100 intracooler was used to control the base temperature of the sensors. The sample cell was purged with N_2 with a flow rate of 40 ml/min. The sample was prepared directly on chip by heating it up to temperature above the clearing temperature. To have the same thermal history for all heating rates, the sample were cooled at a cooling rate of 10^3 K/s rate prior to the heating run which was carried out at different heating rates.

Measurements of the **X-ray diffraction** were performed using a Bruker AXS Nanostar C with a ceramic tube generator (1500 W) having cross-coupled Goebel mirrors providing monochromatic Cu Kα radiation (1.5405 Å). Diffraction patterns were recorded with Bruker HI-STAR or VÅNTEC 500 detectors. Calibration was carried out using the diffraction pattern of silver behenate at room temperature. The compounds were examined in sealed glass capillaries from Hilgenberg GmbH (external diameter of 0.7 mm, wall thickness 0.01 mm). Measured values were analysed with the software SAXS from Bruker. The diffraction patterns were further processed using the software Datasqueeze, Origin 2023Pro and Origin 2024Pro from OriginLab.

To investigate the molecular mobility und the electrical conductivity **broadband dielectric spectroscopy** was carried out for selected samples. The complex dielectric function ε*(f) was measured by a high-resolution Alpha analyzer (Novocontrol, Montabaur, Germany) interfaced to a sample holder with an active head in the frequency range form 10^{-1} Hz to 10^6 Hz. The measurement was carried in parallel plate geometry. The sample was prepared between two gold-plated stainless-steel electrodes by melting the material at temperatures above the clearing point. The distance of the electrodes was maintained by fused silica spacers with a thickness of 50 µm. Isothermal frequency scans were carried out at temperatures between –140 °C and values above the clearing point depending on the samples. The temperature of the sample was controlled by Quatro cryostat (Novocontrol) with a stability of 0.1 K. The length of the investigated molecules was determined by the software Chem3D 21.0.0 from PerkinElmer employing a MM2 optimization.

2 Synthesis

Darzens halogenation for the preparation of the crown ether building block[2,3]

Pentaethyleneglycol (1.16 mL, 5.48 mmol) was dissolved in pyridine (1.00 mL, 12.4 mmol) under nitrogen atmosphere and cooled with an ice bath. Thionyl chloride (0.91 mL, 12.5 mmol) was added dropwise to the solution and the reaction mixture was stirred for 1 d at 50 °C. Water (20 mL) was added to the reaction mixture, which was subsequently extracted with 4 x 30 mL diethylether. The combined organic phase was dried over $MgSO_4$ to obtain the dichloride **4** as yellow oil.

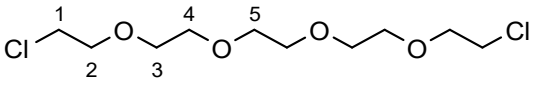

4
$C_{10}H_{20}Cl_2O_4$
(275.17)

Yellow oil (100 %, 1.51 g, 5.48 mmol).

^{1}**H-NMR** (300 MHz, $CDCl_3$): δ = 3.59 – 3.65 (m, 4H, Cl-C*H*$_2$-CH$_2$-O), 3.63 – 3.71 (m, 12H, CH_2), 3.71 – 3.78 (m, 4H, Cl-CH$_2$-C*H*$_2$-O) ppm.

^{13}**C-NMR** (101 MHz, $CDCl_3$): δ = 42.84 (Cl-*C*H$_2$-CH$_2$-O), 70.72 (Cl-(CH$_2$)$_2$-O-*C*H$_2$), 70.79 (O-(CH$_2$)$_2$-O), 71.48 (Cl-CH$_2$-*C*H$_2$-O) ppm.

The spectroscopic data were in accordance with the literature.[2]

Williamson etherification for the preparation of the crown ether building block[4]

Sodium carbonate (0.38 g, 3.6 mmol) and sodium iodide (0.05 g, 0.3 mmol) were suspended in abs. dimethylformamide (20 mL) and heated to 130 °C. A solution of 1,14-dichloro-3,6,9,12-tetraoxatetradecane **4** (0.50 g, 1.82 mmol) and ethyl 3,4-dihydroxybenzoate (0.33 g, 1.8 mmol) in abs. dimethylformamide (5 mL) were added dropwise to the suspension and stirred at 130 °C for 1 d. The solvent was removed, and the remaining crude product was dissolved in 70 mL CH_2Cl_2. The organic phase was washed with 2 x 20 mL 10 % NaOH solution. The solvent was removed and the remnant brown solid was extracted with hot *n*-hexane to obtain the crown ether **5** as colourless solid.

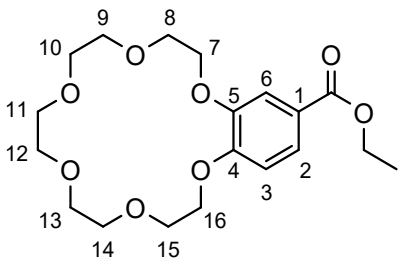

5
$C_{19}H_{28}O_8$
(384.43)

Colourless solid (72 %, 0.50 g, 1.3 mmol).

^{1}**H-NMR** (300 MHz, $CDCl_3$): δ = 1.34 (t, *J* = 7.1 Hz, 3H, CH_3), 3.57 – 3.79 (m, 12H, 9-H – 14-H), 3.84 – 3.96 (m, 4H, 8-H, 15-H), 4.10 – 4.22 (m, 4H, 7-H, 16-H), 4.25 – 4.38 (m, 2H, CH_3-C*H*$_2$), 6.83 (d, *J* = 8.4 Hz, 1H, 3-H), 7.51 (d, *J* = 2.0 Hz, 1H, 6-H), 7.62 (dd, *J* = 2.0 Hz, 8.4 Hz, 1H, 2-H) ppm.

^{13}**C-NMR** (101 MHz, $CDCl_3$): δ = 14.54 (CH_3), 60.91 (CH_2), 69.11, 69.40 (C-7, C-16), 69.59, 69.70 (C-8, C-15), 70.88, 70.93, 71.01, 71.13, 71.16 (C-9 – C-14), 112.44 (C-3), 114.87 (C-6), 123.47 (C-4), 124.00 (C-2), 148.53 (C-5), 153.16 (C-1), 166.54 (COO) ppm.

The spectroscopic data were in accordance with the literature.[4]

Saponification of the crown ether building block

Ethyl 2,3,5,6,8,9,11,12,14,15-decahydrobenzo[b][1,4,7,10,13,16]hexaoxacyclooctadecine-18-carboxylate **5** (4.88 g, 12.7 mmol) was dissolved in MeOH (200 mL) and 0.1 M NaOH solution (80 mL, 8.0 mmol) was added. The solution was stirred for 3 h under reflux. The reaction mixture was extracted with 100 mL CH_2Cl_2. The aqueous phase was acidified with conc. HCl and subsequently extracted with 5 x 100 mL CH_2Cl_2. The combined organic phases were dried over $MgSO_4$ to obtain **[18]c-6-OH** as colourless solid.

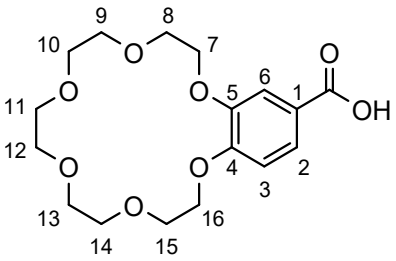

[18]c-6-OH
$C_{17}H_{24}O_8$
(356.37)

Colourless solid (95 %, 4.29 g, 12.0 mmol).

^{1}**H-NMR** (300 MHz, DMSO-d_6): δ = 3.49 – 3.65 (m, 12H, 9-H – 14-H), 3.72 – 3.80 (m, 4H, 8-H, 15-H), 4.05 – 4.24 (m, 4H, 7-H, 16-H), 7.00 – 7.11 (m, 1H, 3-H), 7.40 – 7.48 (m, 1H, 6-H), 7.51 – 7.59 (m, 1H, 2-H) ppm.

^{13}**C-NMR** (101 MHz, DMSO-d_6): δ = 68.08, 68.15, 68.48, 68.57, 69.70, 69.77, 69.79, 69.89 (C-7 – C-16), 111.91 (C-3), 113.02 (C-6), 122.92 (C-1), 123.21 (C-2), 147.58 (C-5), 152.02 (C-4), 167.07 (COOH) ppm.

The spectroscopic data were in accordance with the literature.[4]

Preparation of the catalyst[5]

4-Dimethylaminopyridine (2.00 g, 16.4 mmol) was solved in THF (20 mL) and mixed with *para*-toluenesulfonic acid (3.27 g, 19.0 mmol) solved in THF (27 mL). The product precipitates as colourless solid and was filtered off after 1 d.

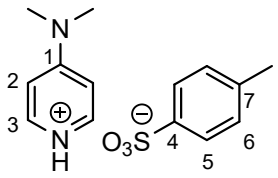

DPTS
$C_{14}H_{18}N_2O_3S$
(294.37)

Colourless solid (83 %, 4.65 g, 15.8 mmol).

^{1}**H-NMR** (300 MHz, $CDCl_3$) δ = 2.34 (s, 3H, CH_3), 3.21 (d, *J* = 1.9 Hz, 6H, NCH_3), 6.74 (d, *J* = 7.0 Hz, 2H, 2-H), 7.17 (d, *J* = 7.9 Hz, 2H, 6-H), 7.78 – 7.90 (m, 2H. 5-H), 8.12 – 8.33 (m, 2H, 3-H) ppm.

^{13}**C-NMR** (101 MHz, $CDCl_3$): δ = 21.46 (CH_3), 40.25 (NCH_3), 106.87 (C-2), 126.15 (C-5), 128.88 (C-6), 139.90 (C-4), 139.92 (C-7), 142.79 (C-3), 157.47 (C-1) ppm.

The spectroscopic data were in accordance with the literature.[5]

Pictet-Spengler reaction[6]

To L-DOPA **2** (2.39 g, 12.1 mmol) 6 mL 0.5 N H_2SO_4 was added to dissolve the substrate. Then formaldehyde solution (37 %, 1.0 mL, 12.9 mmol) was added dropwise and the reaction was stirred for 8 h at room temperature. Saturated $NaHCO_3$ solution was added dropwise to the solution until solid precipitated at pH = 7. The precipitate was filtered off and dried under vacuum to obtain the product.

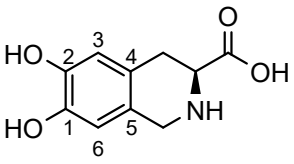

3
$C_{10}H_{11}NO_4$
(209.20)

Light brown solid (77 %, 1.94 g, 9.27 mmol).

^{1}H-NMR (400 MHz, D_2O): δ = 2.67 – 3.53 (m, 2H, HNCHCH_2), 3.90 – 4.28 (m, 3H, HNC*H*, HNCH_2), 6.73 (s, 1H, 3-H), 6.79 (s, 1H, 6-H) ppm.

MS (ESI): *m/z* ($C_{10}H_{11}NO_4$) calcd. 208.0615 $[M - H]^-$, found: 208.06.

HRMS (ESI): *m/z* ($C_{10}H_{11}NO_4$) calcd. 208.0615 $[M - H]^-$, found: 208.0614.

The spectroscopic data was in accordance with literature.[6]

GP1: Boc Protection of the amino unit[7]

The respective amino acid (2.5 mmol) and di-*tert*-butyldicarbonate (0.84 g, 3.9 mmol) were dissolved in 20 ml of an acetone/water mixture (V / V = 1 : 1). Triethylamine (0.60 mL, 4.3 mmol) was added and the mixture was stirred for 24 h at room temperature. Saturated $NaHCO_3$ solution (20 mL) was added to the mixture, which was subsequently extracted with 2 x 25 mL ethyl acetate. The aqueous phase was acidified to pH = 1 using concentrated hydrochloric acid and extracted with 3 x 40 mL ethyl acetate. The organic phase was washed with brine (60 mL) and dried over $MgSO_4$. The solvent was removed under reduced pressure to yield the product.

(*S*)-2-((tert-butoxycarbonyl)amino)-3-(3,4-dihydroxyphenyl)propanoic acid (Boc-DOPA)

According to GP1: L-DOPA **2** (0.50 g, 2.5 mmol), di-*tert*-butyldicarbonate (0.84 g, 3.9 mmol), triethylamine (0.60 mL, 4.3 mmol), 10 ml acetone, 10 mL water.

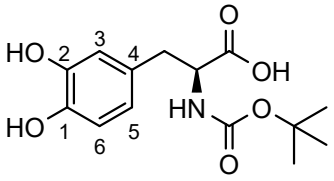

Boc-DOPA
$C_{14}H_{19}NO_6$
(297.31)

Off-white to brown solid (97 %, 0.73 mg, 2.5 mmol).

^{1}H-NMR (400 MHz, DMSO-d_6): δ = 1.33 (s, 9H, $C(CH_3)_3$), 2.56 – 2.93 (m, 2H, HNCHC*H*$_2$), 3.87 – 4.08 (m, 1H, HNC*H*), 6.48 (dd, *J* = 1.9 Hz, 8.2 Hz, 5-H), 6.56 – 6.69 (m, 1H, 3-H, NH), 6.89 (d, *J* = 8.2 Hz, 1H, 6-H), 8.83 (s, 3H, OH, COOH) ppm.

^{13}C-NMR (101 MHz, DMSO-d_6): δ = 28.29 ($C(CH_3)_3$), 36.08 (HNCH*C*H$_2$), 55.66 (HNCH), 78.17 ($C(CH_3)_3$), 115.41 (C-6), 116.61 (C-3), 119.95 (C-5), 128.82 (C-4), 143.88 (C-1), 144.97 (C-2), 155.56 (N(C=O)), 173.90 (C=O) ppm.

The spectroscopic data was in accordance with literature.[8]

(*S*)-2-(tert-butoxycarbonyl)-6,7-dihydroxy-1,2,3,4-tetrahydroisoquinoline-3-carboxylic acid (Boc-THIQ)

According to GP1: Amino acid **3** (1.25 g, 5.98 mmol), di-*tert*-butyldicarbonate (2.23 g, 10.2 mmol), triethylamine (1.2 mL, 8.6 mmol), 125 mL acetone, 125 mL water.

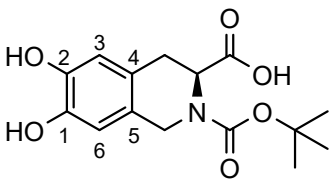

Boc-THIQ
$C_{15}H_{19}NO_6$
(309.32)

Light yellow solid (90 %, 1.67 g, 5.40 mmol).

^{1}H-NMR (400 MHz, DMSO-d_6): δ = 1.33 – 1.49 (m, 9H, CH_3), 2.77 – 3.02 (m, 2H, HNCHCH_2), 4.14 – 4.47 (m, 2H, HNCH_2), 4.82 – 4.53 (m, 1H, CH_2C*H*), 6.44 – 6.61 (m, 2H, 3-H, 6-H) ppm.

^{13}C-NMR (101 MHz, DMSO-d_6): δ = 21.37 (d, *J* = 29.1 Hz, HNCH*C*H_2), 28.49 (d, *J* = 14.2 Hz, C(*C*H_3)$_3$), 53.43 (d, *J* = 167.2 Hz, HNCH), 60.22 (HNCH_2), 79.76 (d, *J* = 17.0 Hz, *C*(CH_3)), 113.54 (d, *J* = 23.6 Hz, C-6), 115.44 (d, *J* = 20.4 Hz, C-3), 123.32 (d, *J* = 25.8 Hz,C-5), 123.52 (d, *J* = 168.7 Hz, C-4), 144.45 (d, *J* = 2.9 Hz, C-1), 144.49 (d, *J* = 20.9 Hz, C-2), 154.75 (N(C=O)), 174.32 – 169.84 (m, C=O) ppm.

FT-IR (ATR): ν = 3293 (m), 2978 (m), 2925 (m), 2853 (w), 1666 (s), 1526 (m), 1456 (m), 1406 (s), 1368 (s), 1284 (s), 1250 (s), 1228 (s), 1155 (vs), 1126 (s), 1095 (m), 1035 (w), 1002 (w), 913 (w), 869 (m), 775 (w), 686 (w), 571 (w) cm^{-1}.

MS (ESI): *m/z* ($C_{15}H_{19}NO_6$) calcd. 310.1286 $[M + H]^-$, found: 310.13.

HRMS (ESI): *m/z* ($C_{15}H_{19}NO_6$) calcd. 310.1286 $[M + H]^+$, found: 310.1278.

GP2: Alkylation of the Boc-protected amines[9]

Acetonitrile (250 mL) was degassed for 30 min. Under nitrogen atmosphere the respective Boc-protected amino acid (8.20 mmol), sodium iodide (0.17 g, 1.1 mmol) and potassium carbonate (8.06 g, 58.3 mmol) were added and stirred under reflux for 1 h. The respective 1-bromoalkane (33 mmol) was added and the reaction mixture was stirred under reflux for 4 d. After filtering off the inorganic reactants the solvent was removed under reduced pressure. The crude product was purified by column chromatography.

Dodecyl (*S*)-3-(3,4-bis(dodecyloxy)phenyl)-2-((tert-butoxycarbonyl)amino)propanoate (Boc-DOPA(12))

According to GP2: **Boc-DOPA** (2.44 g, 8.23 mmol), potassium carbonate (8.06 g, 58.3 mmol), sodium iodide (0.17 g, 1.1 mmol), 1-bromododecane (8.0 mL, 50 mmol), acetonitrile (250 mL); purification: column chromatography (silica, petroleum ether / ethyl acetate, 50 : 1→30 : 1→5 : 1).

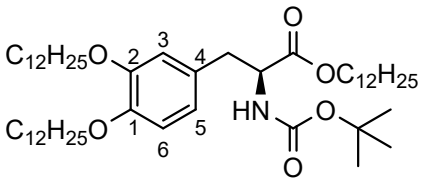

Boc-DOPA(12)
$C_{50}H_{91}NO_6$
(802.28)

Colourless solid (74 %, 4.85 g, 6.05 mmol).

^{1}H-NMR (400 MHz, $CDCl_3$): δ = 0.88 (t, *J* = 6.8 Hz, 9H, CH_3), 1.22 – 1.38 (m, 50H, CH_2), 1.39 – 1.50 (m, 13H, C*H*$_2$CH$_2$CH$_2$OAr, C(CH$_3$)$_3$), 1.53 – 1.64 (m, 2H, C*H*$_2$CH$_2$O(C=O)) 1.73 – 1.85 (m, 4H, C*H*$_2$CH$_2$OAr), 2.98 – 3.03 (m, 2H, HNCHC*H*$_2$), 3.90 – 3.98 (m, 4H, CH$_2$OAr), 4.08 (t, *J* = 6.7 Hz, 2H, CH$_2$O(C=O)), 4.47 – 4.58 (m, 1H, HNC*H*), 4.95 (d, *J* = 8.3 Hz, 1H, NH), 6.59 – 6.68 (m, 2H, 3-H, 5-H), 6.78 (d, *J* = 8.0 Hz, 1H, 6-H) ppm.

^{13}C-NMR (126 MHz, $CDCl_3$): *δ* = 14.25 (CH_3), 22.83, 26.01, 26.20, 26.22 (CH_2), 28.46 (C(*C*H$_3$)$_3$), 28.65, 29.39, 29.49, 29.50, 29.60, 29.61, 29.65, 29.75, 29.79, 29.81, 29.85, 29.86, 32.07 (CH_2), 37.98 (HNCH*C*H$_2$), 54.62 (HNCH), 65.62 ((C=O)O*C*H$_2$), 69.36, 69.43 (OCH$_2$), 79.89 (*C*(CH$_3$)$_3$), 113.97 (C-6), 115.13 (C-3), 121.72 (C-5), 128.65 (C-4), 148.33 (C-1), 149.17 (C-2), 155.22 (N(C=O)), 172.20 (C=O) ppm.

FT-IR (ATR): ν = 3345 (w), 2917 (vs), 2849 (vs), 1733 (m), 1691 (vs), 1589 (w), 1531 (s), 1517 (s), 1467 (m), 1428(w), 1390 (w), 1368 (w), 1341 (w), 1322 (w), 1259 (s), 1233 (s), 1168 (vs), 1138 (s), 1059 (m), 849 (w), 795 (m), 722 (w), 672 (w) cm^{-1}.

MS (ASAP): *m/z* ($C_{50}H_{91}NO_6$) calcd. 801.6846 $[M]^+$, found: 801.68.

HRMS (ASAP): *m/z* ($C_{50}H_{91}NO_6$) calcd. 801.6846 $[M]^+$, found: 801.6838.

The spectroscopic data was previously reported by Z. Li *et al*.[10]

Tetradecyl (*S*)-3-(3,4-bis(tetradecyloxy)phenyl)-2-((tert butoxycarbonyl)amino)-propanoate (Boc-DOPA(14))

According to GP2: **Boc-DOPA** (2.04 g, 6.88 mmol), potassium carbonate (7.98 g, 57.8 mmol), sodium iodide (0.15 g, 1.0 mmol), 1-bromotetradecane (8.0 mL, 27 mmol), acetonitrile (250 mL); purification: column chromatography (silica, petroleum ether / ethyl acetate, 50 : 1→30 : 1→5 : 1).

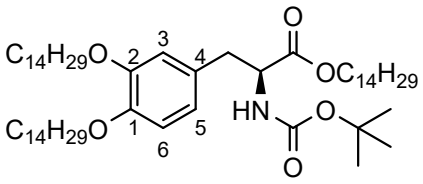

Boc-DOPA(14)
$C_{56}H_{103}NO_6$
(886.44)

Colourless solid (79 %, 4.85 g, 5.47 mmol).

^{1}H-NMR (400 MHz, $CDCl_3$): δ = 0.84 – 0.93 (m, 9H, CH_3), 1.21 – 1.38 (m, 62H, CH_2, 1.42 (s, 9H, C(CH$_3$)$_3$), 1.44 – 1.50 (m, 4H, C*H*$_2$CH$_2$CH$_2$OAr), 1.53 – 1.63 (m, 2H, C*H*$_2$CH$_2$O(C=O)) 1.73 – 1.85 (m, 4H, C*H*$_2$CH$_2$OAr), 2.97 – 3.03 (m, 2H, HNCHC*H*$_2$), 3.90 – 3.97 (m, 4H, CH$_2$OAr,), 4.08 (t, 2H, CH$_2$O(C=O)), 4.46 – 4.57 (m, 1H, HNC*H*), 4.89 – 4.99 (m, 1H, NH), 6.58 – 6.67 (m, 2H, 3-H, 5-H), 6.78 (d, *J* = 8.0 Hz, 1H, 6-H) ppm.

^{13}C-NMR (176 MHz, $CDCl_3$): δ = 14.28 (CH_3), 22.86, 26.03, 26.22, 26.24, 28.50, 28.68, 29.41, 29.50, 29.53, 29.62, 29.64, 29.68, 29.78, 29.82, 29.83, 29.85, 29.87, 29.88, 29.90, 32.09 (CH_2), 38.00 (HNCH*C*H_2), 54.64 (HNCH), 65.64 ((C=O)O*C*H_2), 69.38, 69.45 (ArOCH_2), 79.93 (*C*$(CH_3)_3$), 113.97 (C-6), 115.13 (C-3), 121.73 (C-5), 128.65 (C-4), 148.35 (C-1), 149.19 (C-2), 155.23 (N(C=O)), 172.22 (C=O) ppm.

The spectroscopic data is in accordance with literature.[8]

Hexadecyl (*S*)-3-(3,4-bis(hexadecyloxy)phenyl)-2-((tert-butoxycarbonyl)amino)propanoate (Boc-DOPA(16))

According to GP2: **Boc-DOPA** (2.04 g, 6.88 mmol), potassium carbonate (5.98 g, 43.3 mmol), sodium iodide (0.15 g, 1.0 mmol), 1-bromohexadecane (8.0 mL, 26 mmol), acetonitrile (250 mL); purification: column chromatography (silica, petroleum ether / ethyl acetate, 50 : 1→30 : 1→5 : 1).

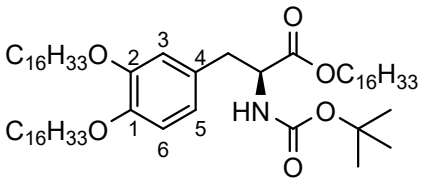

Boc-DOPA(16)
$C_{62}H_{115}NO_6$
(970.60)

Colourless solid (67 %, 4.50 g, 4.64 mmol).

^{1}H-NMR (400 MHz, $CDCl_3$): δ = 0.88 (t, *J* = 6.8 Hz, 9H, CH_3), 1.19 – 1.39 (m, 74H, CH_2), 1.42 (s, 9H, $C(CH_3)_3$), 1.44 – 1.50 (m, 4H, C*H*$_2$CH$_2$CH$_2$OAr), 1.53 – 1.66 (m, 2H, C*H*$_2$CH$_2$O(C=O)) 1.73 – 1.86 (m, 4H, C*H*$_2$CH$_2$OAr), 3.00 (d, *J* = 5.0 Hz, 2H, HNCHC*H*$_2$), 3.88 – 4.02 (m, 4H, CH_2OAr), 4.08 (t, *J* = 6.7 Hz, 2H, CH_2O(C=O)), 4.44 – 4.59 (m, 1H, HNC*H*), 4.95 (d, *J* = 8.3 Hz, 1H, NH), 6.58 – 6.68 (m, 2H, 3-H, 5-H), 6.78 (d, d, *J* = 8.0 Hz, 1H, 6-H) ppm.

^{13}C-NMR (101 MHz, $CDCl_3$): δ = 14.26 (CH_3), 22.84, 26.03, 26.22, 26.24, 28.48, 28.68, 29.41, 29.52, 29.62, 29.63, 29.67, 29.77, 29.82, 29.87, 32.08 (CH_2), 38.02 (HNCH*C*H_2), 54.65 (HNCH), 65.63 ((C=O)O*C*H_2), 69.42, 69.50 (CH_2OAr), 79.89 (*C*$(CH_3)_3$), 114.09 (C-6), 115.23 (C-3), 121.76 (C-5), 128.71 (C-4), 148.40 (C-1), 149.25 (C-2), 155.30 (N(C=O)), 172.21 (C=O) ppm.

FT-IR (ATR): ν = 2921 (s), 2852 (s), 1711 (m), 1589 (w), 1512 (m), 1467 (m), 1391 (w), 1366 (w), 1350 (w), 1260 (m), 1234 (m), 1167 (m), 1139 (m), 1060 (w), 1021 (w), 907 (s), 731 (vs), 648 (w) cm^{-1}.

MS (ASAP): *m/z* ($C_{62}H_{115}NO_6$) calcd. 969.8719 $[M]^+$, found: 969.9.

HRMS (ASAP): *m/z* ($C_{62}H_{115}NO_6$) calcd. 969.8719 $[M]^+$, found: 969.8713.

The spectroscopic data was previously reported by Z. Li *et al*.[10]

2-(*Tert*-butyl) 3-tetradecyl (*S*)-6,7-bis(tetradecyloxy)-3,4-dihydroisoquinoline-2,3(1H)-dicarboxylate (Boc-THIQ(14))

According to GP2: **Boc-THIQ** (2.13 g, 6.89 mmol), potassium carbonate (9.33 g, 67.5 mmol), sodium iodide (0.22 g, 1.5 mmol), 1-bromotetradecane (8.0 mL, 27 mmol), acetonitrile (250 mL); purification: column chromatography (silica, petroleum ether / ethyl acetate, 70 : 1).

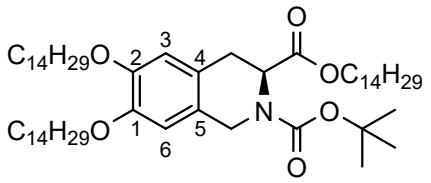

Boc-THIQ(14)
$C_{57}H_{103}NO_6$
(898.45)

Colourless solid (79 %, 4.87 g, 5.42 mmol).

^{1}H-NMR (400 MHz, $CDCl_3$): δ = 0.88 (t, *J* = 6.8 Hz, 9H, CH_3), 1.18 – 1.40 (m, 66H, CH_2), 1.41 – 1.44 (m, 11H, $C(CH_3)_3$, $CH_2CH_2O(C=O)$) 1.72 – 1.86 (m, 4H, CH_2CH_2OAr), 2.98 – 3.24 (m, 2H, $NCHCH_2$), 3.89 – 4.06 (m, 6H, CH_2OAr, $CH_2O(C=O)$), 4.34 – 4.67 (m, 2H, CH_2N), 5.17 – 4.74 (m, 1H, CHN), 6.67 – 6.54 (m, 2H, 3-H, 6-H) ppm.

^{13}C-NMR (101 MHz, $CDCl_3$): δ = 14.18 (CH_3), 22.80, 25.88, 25.89, 26.19, 27.01, (CH_2) 28.43 ($C(CH_3)_3$), 28.52, 28.67, 28.72, 29.31, 29.46, 29.49, 29.57, 29.61, 29.63, 29.74, 29.77, 29.79, 29.83, 32.05 (CH_2), 44.16 (d, *J* = 49.4 Hz, $NCHCH_2$), 52.64 (NCH_2), 54.42 (NCH), 65.20 ($CH_2O(C=O)$), 69.45, 69.57 (OCH_2), 80.38 ($C(CH_3)_3$), 111.84 (d, *J* = 32.5 Hz, C-6), 113.83 (d, *J* = 17.5 Hz, C-3), 124.05 (d, *J* = 16.0 Hz, C-4), 125.38 (d, *J* = 118.8 Hz, C-5), 148.06 (d, *J* = 8.1 Hz, C-1), 148.35 (d, *J* = 6.2 Hz, C-2), 155.32 (d, *J* = 70.3 Hz, N(C=O)), 171.82 (d, *J* = 54.1 Hz, C=O) ppm

FT-IR (ATR): ν = 2921 (vs), 2852 (vs), 1741 (m), 1703 (s), 1613 (w), 1517 (m), 1466 (m), 1391 (s), 1366 (m), 1332 (m), 1267 (m), 1230 (m), 1166 (s), 1127 (m), 1096 (m), 1004 (m), 913 (w), 863 (w), 774 (w), 722 (w) cm^{-1}.

MS (ESI): *m/z* ($C_{57}H_{103}NO_6$) calcd. 898.7858 $[M + H]^+$, found: 898.79; calcd. 920.7678 $[M + Na]^+$, found: 920.77.

HRMS (ESI): *m/z* ($C_{57}H_{103}NO_6$) calcd. 898.7858 $[M + H]^+$, found: 898.7853; calcd. 920.7678 $[M + Na]^+$, found: 920.7675.

2-(Tert-butyl) 3-hexadecyl (*S*)-6,7-bis(hexadecyloxy)-3,4-dihydroisoquinoline-2,3(1H)-dicarboxylate (Boc-THIQ(16))

According to GP2: **Boc-THIQ** (0.51 g, 1.7 mmol), potassium carbonate (2.05 g, 14.9 mmol), sodium iodide (79 mg, 0.53 mmol), 1-bromohexadecane (2.0 mL, 6.5 mmol), acetonitrile (50 mL); purification: column chromatography (silica, petroleum ether / ethyl acetate, 70 : 1).

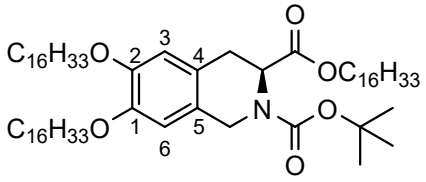

Boc-THIQ(16)
$C_{63}H_{115}NO_6$
(982.61)

Colourless solid (71 %, 1.15 g, 1.17 mmol).

^{1}H-NMR (400 MHz, $CDCl_3$): δ = 0.88 (t, *J* = 6.8 Hz, 9H, CH_3), 1.08 – 1.59 (m, 89H, CH_2, $C(CH_3)$), 1.72 – 1.85 (m, 4H, C*H*$_2$$CH_2$OAr), 2.99 – 3.22 (m, 2H, NCHC*H*$_2$), 3.85 – 4.09 (m, 6H, CH_2OAr, CH_2O(C=O)), 4.32 – 4.66 (m, 2H, C*H*$_2$N), 4.75 – 5.19 (m, 1H, C*H*N), 6.55 – 6.69 (m, 2H, 3-H, 6-H) ppm.

^{13}C-NMR (126 MHz, $CDCl_3$): δ = 14.08 (CH_3), 22.74, 25.84, 26.15, 26.94, (CH_2) 28.29 ($C(CH_3)_3$), 28.38, 28.63, 28.69, 29.26, 29.42, 29.46, 29.53, 29.56, 29.59, 29.71, 29.74, 29.75, 29.80, 32.00 (CH_2), 44.08 (d, *J* = 60.9 Hz, NCHC*H*$_2$), 52.55 (NCH_2), 54.34 (NCH), 64.99 (*C*H_2O(C=O)), 69.26, 69.39 (CH_2OAr), 80.12 (*C*$(CH_3)_3$), 111.68 (d, *J* = 41.6 Hz, C-6), 113.69 (d, *J* = 21.4 Hz, C-3), 123.92 (d, *J* = 19.4 Hz, C-4), 125.28 (d, *J* = 151.5 Hz, C-5), 148.00 (d, *J* = 9.9 Hz, C-1), 148.31 (d, *J* = 8.1 Hz, C-2), 155.17 (d, *J* = 90.3 Hz, N(C=O)), 171.58 (d, *J* = 67.8 Hz, C=O) ppm

FT-IR (ATR): ν = 2920 (vs), 2851 (vs), 1739 (m), 1699 (m), 1613 (w), 1517 (w), 1467 (m), 1392 (m), 1366 (m), 1335 (w), 1268 (m), 1231 (m), 1166 (m), 1128 (w), 1097 (w), 1004 (w), 909 (m), 734 (s), 648 (w) cm^{-1}.

MS (ESI): *m/z* ($C_{63}H_{115}NO_6$) calcd. 1004.8617 $[M + Na]^+$, found: 1004.86.

HRMS (ESI): *m/z* ($C_{63}H_{115}NO_6$) calcd. 982.8798 $[M + H]^+$, found: 982.8787; calcd. 1004.8617 $[M + Na]^+$, found: 1004.8608.

GP3: Removal of the Boc-protection group[11]

The respective Boc-protected amino acid (0.50 mmol) was dissolved in CH_2Cl_2 (10 mL). Trifluoroacetic acid (0.40 mL, 5.2 mmol) was added and the reaction was stirred for 18 h. More CH_2Cl_2 (10 mL) was added, and the reaction mixture was neutralized with Amberlyst 21. The base was filtered off and the solvent was removed under reduced pressure to afford the product as a white solid without further purification.

Dodecyl (*S*)-2-amino-3-(3,4-bis(dodecyloxy)phenyl)propanoate (DOPA(12))

According to GP3: **Boc-DOPA(12)** (0.40 g, 0.50 mmol), trifluoroacetic acid (0.40 mL, 5.2 mmol), CH_2Cl_2 (10 mL).

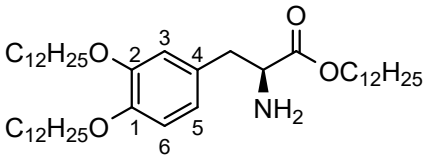

DOPA(12)
$C_{45}H_{83}NO_4$
(702.16)

Colourless solid (quantitative, 0.35 g, 0.50 mmol).

^{1}H-NMR (300 MHz, $CDCl_3$): δ = 0.83 – 0.92 (m, 9H, CH_3), 1.17 – 1.69 (m, 56H, CH_2), 1.71 – 1.87 (m, 4H, C*H*$_2$CH$_2$OAr), 2.71 – 2.87 (m, 1H, H_2NCHC*H*$_2$), 2.94 – 3.06 (m, 1H, H_2NCHC*H*$_2$), 3.62 – 3.72 (m, 1H, H_2NC*H*), 3.95 (t, *J* = 6.6 Hz, 4H, CH_2OAr), 4.09 (t, *J* = 6.7 Hz, 2H, CH_2O(C=O)), 6.66 – 6.75 (m, 2H, 3-H, 5-H), 6.80 (d, *J* = 8.0 Hz, 1H, 6-H) ppm.

The N-H signals could not be detected.

^{13}C NMR (126 MHz, $CDCl_3$): δ = 14.27 (CH_3), 22.84, 26.06, 26.21, 26.23, 28.73, 29.41, 29.51, 29.52, 29.61, 29.63, 29.67, 29.76, 29.80, 29.81, 29.87, 32.08 (CH_2), 40.36 (H_2NCH*C*H$_2$), 55.91 (H_2NCH), 65.41 (*C*H$_2$O(C=O)), 69.44, 69.52 (CH_2OAr), 114.19 (C-6), 115.15 (C-3), 121.76 (C-5), 148.30 (C-1), 149.35 (C-2) ppm.

The quaternary C-4 signal and the quaternary carbonyl C signal could not be detected.

FT-IR (ATR): ν = 2955 (m), 2917 (vs), 2850 (s), 1745 (m), 1590 (w), 1519 (m), 1468 (m), 1427 (w), 1395 (w), 1271 (m), 1235 (m), 1188 (w), 1139 (m), 722 (w) cm^{-1}.

MS (ESI): *m/z* ($C_{45}H_{83}NO_4$) calcd. 702.6395 [M + Na]$^+$, found: 702.64.

HRMS (ESI): *m/z* ($C_{45}H_{83}NO_4$) calcd. 702.6395 [M + Na]$^+$, found: 702.6393.

The spectroscopic data was previously reported by Z. Li *et al*.[10]

Tetradecyl (*S*)-2-amino-3-(3,4-bis(tetradecyloxy)phenyl)propanoate (DOPA(14))

According to GP3: **Boc-DOPA(14)** (0.77 g, 0.87 mmol), trifluoroacetic acid (0.70 mL, 9.2 mmol), CH_2Cl_2 (18 mL).

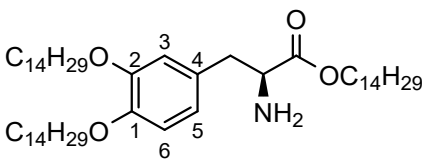

DOPA(14)
$C_{51}H_{95}NO_4$
(786.32)

Colourless solid (97 %, 0.66 g, 0.84 mmol).

^{1}H-NMR (400 MHz, $CDCl_3$): δ = 0.88 (t, *J* = 7.1 Hz, 9H, CH_3), 1.20 – 1.39 (m, 62H, CH_2), 1.39 – 1.51 (m, 4H, C*H*$_2$CH$_2$CH$_2$OAr), 1.57 – 1.66 (m, 2H, C*H*$_2$CH$_2$O(C=O)), 1.73 – 1.86 (m, 4H, C*H*$_2$CH$_2$OAr), 2.72 – 3.07 (m, 2H, H$_2$NCHC*H*$_2$), 3.64 – 3.73 (m, 1H, H$_2$NC*H*), 3.90 – 4.01 (m, 4H, CH_2OAr), 4.09 (t, *J* = 6.8 Hz, 2H, CH_2O(C=O)), 6.65 – 6.75 (m, 2H, 3-H, 5-H), 6.80 (d, *J* = 8.1 Hz, 1H, 6-H) ppm.

The N-H signals could not be detected.

^{13}C-NMR (101 MHz, $CDCl_3$): δ = 14.25 (CH_3), 22.84, 26.06, 26.21, 26.22, 28.75, 29.41, 29.52, 29.61, 29.62, 29.67, 29.75, 29.81, 29.86, 32.08 (CH_2), 40.73 (H$_2$NCH*C*H$_2$), 56.03 (H$_2$NCH), 65.30 (*C*H$_2$O(C=O)), 69.45, 69.55 (CH_2OAr) 114.24 (C-6), 115.21 (C-3), 121.75 (C-5), 129.89 (C-4), 148.28 (C-1), 149.35 (C-2), 175.21 (C=O) ppm.

MS (ESI): *m/z* ($C_{51}H_{95}NO_4$) calcd. 786.7334 $[M + Na]^+$, found: 786.73.

HRMS (ESI): *m/z* ($C_{51}H_{95}NO_4$) calcd. 786.7334 $[M + H]^+$, found: 786.7338.

The spectroscopic data is in accordance with literature.[8]

Hexadecyl (*S*)-2-amino-3-(3,4-bis(hexadecyloxy)phenyl)propanoate (DOPA(16))

According to GP3: **Boc-DOPA(16)** (0.32 g, 0.33 mmol), trifluoroacetic acid (0.25 mL, 3.3 mmol), CH_2Cl_2 (10 mL).

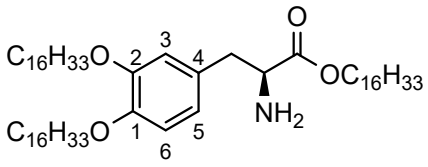

DOPA(16)
$C_{57}H_{107}NO_4$
(870.49)

Colourless solid (82 %, 235 mg, 0.270 mmol).

^{1}H-NMR (400 MHz, $CDCl_3$): δ = 0.88 (t, *J* = 6.7 Hz, 9H, CH_3), 1.17 – 1.40 (m, 72H, CH_2), 1.40 – 1.51 (m, 6H, C*H*$_2$CH$_2$CH$_2$O(C=O), C*H*$_2$CH$_2$CH$_2$OAr), 1.52 – 1.69 (m, 2H, C*H*$_2$CH$_2$O(C=O)), 1.73 – 1.86 (m, 4H, C*H*$_2$CH$_2$OAr), 2.74 – 2.84 (m, 1H, H$_2$NCHC*H*$_2$), 2.95 – 3.05 (m, 1H, H$_2$NCHC*H*$_2$), 3.65 – 3.72 (m, 1H, H$_2$NC*H*), 3.91 – 4.01 (m, 4H, CH_2OAr), 4.09 (t, *J* = 6.8 Hz, 2H, CH_2O(C=O)), 6.59 – 6.75 (m, 2H, 3-H, 5-H), 6.75 – 6.83 (m, 1H, 6-H) ppm.

The N-H signals could not be detected.

^{13}C-NMR (101 MHz, $CDCl_3$): δ = 14.27 (CH_3), 22.85, 26.07, 26.23, 28.76, 29.42, 29.52, 29.63, 29.68, 29.82, 29.87, 32.08 (CH_2), 40.81 (H$_2$NCH*C*H$_2$), 56.07 (H$_2$NCH), 65.29 (*C*H$_2$O(C=O)), 69.56 (CH_2OAr) 114.25 (C-6), 115.23 (C-3), 121.75 (C-5), 129.90 (C-4), 148.28 (C-1), 149.57 (C-2), 175.30 (C=O) ppm.

FT-IR (ATR): ν = 2955 (m), 2916 (vs), 2849 (vs), 1736 (w), 1590 (w), 1517 (w), 1468 (m), 1429 (w), 1392 (w), 1267 (w), 1236 (w), 1168 (w), 1139 (w), 1067 (w), 1016 (w), 722 (w) cm^{-1}.

MS (ESI): *m/z* ($C_{57}H_{107}NO_4$) calcd. 870.8273 $[M + H]^+$, found: 870.83.

HRMS (ESI): *m/z* ($C_{57}H_{107}NO_4$) calcd. 870.8273 $[M + H]^+$, found: 870.8253.

The spectroscopic data was previously reported by Z. Li *et al*.[10]

Tetradecyl (*S*)-6,7-bis(tetradecyloxy)-1,2,3,4-tetrahydroisoquinoline-3-carboxylate (THIQ(14))

According to GP3: **Boc-THIQ(14)** (3.86 g, 4.29 mmol), trifluoroacetic acid (3.20 mL, 41.8 mmol), CH_2Cl_2 (50 mL).

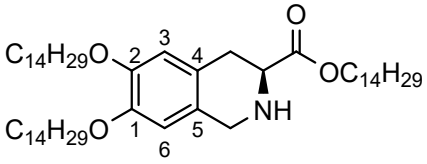

THIQ(14)
$C_{52}H_{95}NO_4$
(798.34)

Colourless solid (92 %, 3.16 g, 3.95 mmol).

^{1}H-NMR (700 MHz, $CDCl_3$): δ = 0.87 (t, *J* = 7.1 Hz, 9H, CH_3), 1.15 – 1.38 (m, 66H, CH_2), 1.38 – 1.51 (m, 4H, C*H*$_2$CH$_2$OAr), 1.57 – 1.69 (m, 2H, C*H*$_2$CH$_2$O(C=O)), 2.85 – 3.09 (m, 2H, HNCHC*H*$_2$), 3.74 – 3.89 (m, 1H, HNC*H*), 3.89 – 4.02 (m, 4H, CH_2OAr), 4.00 – 4.23 (m, 4H, HNC*H*$_2$, CH_2O(C=O)), 6.53 (s, 1H, 3-H), 6.59 (s, 1H, 6-H) ppm.

The N-H signal could not be detected.

^{13}C-NMR (176 MHz, $CDCl_3$): δ = 14.24 (CH_3), 22.81, 25.94, 26.17, 28.64, 29.36, 29.44, 29.51, 29.58, 29.64, 29.73, 29.79, 29.81, 29.82, 29.86, 30.47, 32.06 (CH_2), 46.12 (HNCH*C*H$_2$), 55.56 (HNCH$_2$), 63.08 (HNCH), 65.73 (*C*H$_2$O(C=O)), 69.49, 69.53 (CH_2OAr), 111.49 (C-6), 114.29 (C-3), 124.37 (C-4), 124.99 (C-5), 148.14 (C-1), 148.20 (C-2), 172.05 (C=O) ppm

FT-IR (ATR): ν = 2922 (s), 2853 (m), 1737 (w), 1676 (w), 1611 (w), 1515 (w), 1466 (m), 1244 (m), 1200 (m), 1124 (w), 1024 (w), 907 (s), 730 (vs), 647 (w) cm^{-1}.

MS (ESI): *m/z* ($C_{52}H_{95}NO_4$) calcd. 798.7334 $[M + H]^+$, found: 798.73.

HRMS (ESI): *m/z* ($C_{52}H_{95}NO_4$) calcd. 798.7334 $[M + H]^+$, found: 798.7329.

Hexadecyl (*S*)-6,7-bis(hexadecyloxy)-1,2,3,4-tetrahydroisoquinoline-3-carboxylate (THIQ(16))

According to GP3: **Boc-THIQ(16)** (4.42 g, 4.50 mmol), trifluoroacetic acid (3.8 mL, 50 mmol), CH_2Cl_2 (50 mL).

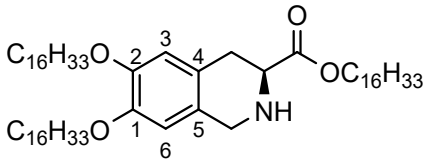

THIQ(16)
$C_{58}H_{107}NO_4$
(882.50)

Colourless solid (80 %, 3.17 g, 3.59 mmol).

^{1}H-NMR (400 MHz, $CDCl_3$): δ = 0.86 – 0.95 (m, 9H, CH_3), 1.20 – 1.41 (m, 74H, CH_2), 1.41 – 1.53 (m, 4H, C*H*$_2$CH$_2$CH$_2$OAr), 1.63 – 1.75 (m, 2H, C*H*$_2$CH$_2$O(C=O)), 1.76 – 1.87 (m, 4H, C*H*$_2$CH$_2$OAr), 2.86 – 3.07 (m, 2H, HNCHC*H*$_2$), 3.75 – 3.82 (m, 1H, HNC*H*), 3.91 – 4.00 (m, 4H, CH$_2$OAr), 4.02 – 4.15 (m, 2H, HNC*H*$_2$,),4.15 – 4.23 (m, 2H, CH$_2$O(C=O)), 6.53 (s, 1H, 3-H), 6.59 (s, 1H, 6-H) ppm.

The N-H signal could not be detected.

^{13}C-NMR (176 MHz, $CDCl_3$): δ = 14.28 (CH_3), 22.86, 26.00, 26.20, 28.70, 29.38, 29.44, 29.46, 29.52, 29.59, 29.66, 29.75, 29.81, 29.83, 29.84, 29.86, 29.87, 30.85, 32.09 (CH_2), 46.50 (HNCH*C*H$_2$), 55.81 (HNCH$_2$), 65.63 (HNCH), 69.55 (*C*H$_2$O(C=O)), 69.59 (CH$_2$OAr), 111.59 (C-6), 114.45 (C-3), 124.71 (C-4), 124.97 (C-5), 148.11 (C-1), 162.51 (d, *J* = 35.0 Hz, N(C=O)), 172.51 (C=O) ppm.

The quaternary C-2 signal could not be detected.

FT-IR (ATR): ν = 2955 (m), 2914 (vs), 2848 (vs), 1736 (m), 1611 (w), 1520 (m), 1467 (m), 1426 (w), 1392 (w), 1362 (w), 1329 (w), 1248 (s), 1219 (m), 1192 (m), 1176 (m), 1128 (m), 1073 (w), 908 (m), 722 (m), 647 (w), 627 (w), 578 (w) cm^{-1}.

MS (ESI): *m/z* ($C_{58}H_{107}NO_4$) calcd. 882.8273 [M + H]$^+$, found: 882.83.

HRMS (ESI): *m/z* ($C_{58}H_{107}NO_4$) calcd. 882.8273 [M + H]$^+$, found: 882.8265.

GP4: Introduction of [18]c-6-OH to the amine[12]

The crown ether building block **[18]c-6-OH** (0.13 g, 0.37 mmol), 1-ethyl-3-(3-dimethylaminopropyl)carbodiimide hydrochloride (EDC · HCl, 0.12 g, 0.61 mmol) and hydroxybenzotriazole monohydrate (HOBt · H_2O, 0.052 g, 0.34 mmol) were dissolved in 150 mL CH_2Cl_2 and stirred at room temperature for 1 h. Then the respective deprotected aminoacid (0.31 mmol), DPTS (0.090 g, 0.31 mmol) and triethylamine (1.3 mL, 0.92 mmol)

were added and the reaction mixture was refluxed for 2 d. The solution was washed with water and dried over $MgSO_4$. The solvent was removed and the crude product was purified by column chromatography (SiO_2, 15 : 1 CH_2Cl_2 / MeOH) to yield the product as a colourless to slightly yellow solid.

c-DOPA(12)

According to GP4: **[18]c-6-OH** (0.13 g, 0.37 mmol), EDC · HCl (0.12 g, 0.63 mmol), HOBt · H_2O (0.052 g, 0.34 mmol), **DOPA(12)** (0.22 g, 0.31 mmol), DPTS (0.090 g, 0.31 mmol), triethylamine (1.3 mL, 0.93 mmol), CH_2Cl_2 (150 mL).

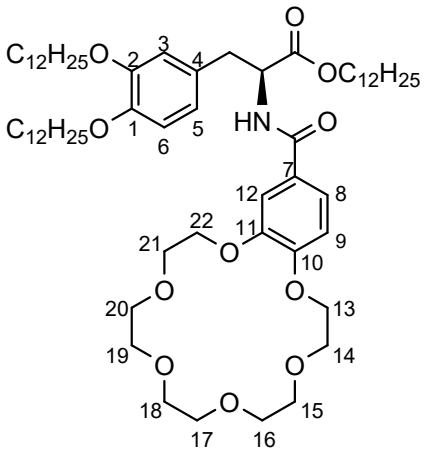

c-DOPA(12)
$C_{62}H_{105}NO_{11}$
(1040.52)

Off-white solid (73 %, 0.238 g, 0.229 mmol).

^{1}H-NMR (700 MHz, $CDCl_3$): δ = 0.87 (t, *J* = 7.0 Hz, 9H, CH_3), 1.17 – 1.47 (m, 54H, CH_2), 1.59 – 1.65 (m, 2H, C*H*$_2$CH$_2$O(C=O)), 1.71 – 1.81 (m, 4H, C*H*$_2$CH$_2$OAr), 3.12 – 3.17 (m, 2H, HNCHC*H*$_2$), 3.66 – 3.78 (m, 12H, 15-H, 16-H, 17-H, 18-H, 19-H, 20-H), 3.81 – 3.96 (m, 8H, 13-H, 14-H, 21-H, 22-H), 4.07 – 4.15 (m, 2H, CH_2O(C=O)), 4.15 – 4.20 (m, 4H, CH_2OAr), 4.95 – 5.00 (m, 1H, HNC*H*), 6.50 (d, *J* = 7.5 Hz, 1H, NH), 6.59 – 6.64 (m, 2H, 3-H, 6-H), 6.76 (d, *J* = 8.1 Hz, 1H, 5-H), 6.81 (d, *J* = 8.4 Hz, 1H, 9-H), 7.19 (dd, *J* = 2.0 Hz, 8.4 Hz, 1H, 8-H), 7.35 (d, *J* = 2.0 Hz, 1H, 12-H) ppm.

^{13}C-NMR (176 MHz, $CDCl_3$): δ = 14.24 (CH_3), 22.80 (CH_3C*H*$_2$), 26.01, 26.18, 28.63, 29.37, 29.43, 29.46, 29.48, 29.50, 29.58, 29.64, 29.72, 29.76, 29.78, 29.82, 29.85, 32.03 (CH_2), 37.58 (HNCH*C*H$_2$), 53.72 (HNCH), 65.84 (*C*H$_2$O(C=O)), 68.91, 68.99 (CH_2OAr), 69.29, 69.37, 69.43, 69.50 (C-13, C-14, C-21, C-22), 70.66, 70.72, 70.77, 70.84, 70.92, 70.95 (C-15, C-16, C-17, C-18, C-19, C-20), 112.29 (C-9), 112.77 (C-3), 113.87 (C-12), 115.09 (C-6), 119.99 (C-5), 121.73 (C-8), 126.84 (C-7), 128.51 (C-4), 148.37 (C-1), 148.76 (C-11), 149.18 (C-2), 151.93 (C-10), 166.35 (N(C=O)), 171.99 (C=O) ppm.

FT-IR (ATR): ν = 3277 (w), 2919 (vs), 2850 (s), 1750 (m), 1629 (s), 1603 (w), 1582 (w), 1542 (m), 1511 (s), 1468 (m), 1430 (m), 1392 (w), 1351 (m), 1272 (s), 1227 (s), 1207 (s), 1172 (s), 1134 (vs), 1097 (s), 1055 (s), 995 (m), 946 (m), 871 (m), 812 (m), 786 (w), 761 (w), 721 (m), 684 (w), 650 (w), 628 (w), 566 (w) cm^{-1}.

MS (ESI): *m/z* ($C_{62}H_{105}NO_{11}$) calcd. 1040.7761 $[M + H]^+$, found: 1040.77; calcd. 1057.8026 $[M + NH_4]^+$, found: 1057.80; calcd. 1062.7580 $[M + Na]^+$, found: 1062.75.

HRMS (ESI): *m/z* ($C_{62}H_{105}NO_{11}$) calcd. 1040.7761 $[M + H]^+$, found: 1040.7667.

DSC: Cr 114 [-71.9 kJ mol^{-1}] I (1st heating), I 100 [70.6 kJ mol^{-1}] Cr (1st cooling).

c-DOPA(14)

According to GP4: **[18]c-6-OH** (0.17 g, 0.49 mmol), EDC · HCl (0.15 g, 0.76 mmol), HOBt · H_2O (0.053 g, 0.35 mmol), **DOPA(14)** (0.27 g, 0.35 mmol), DPTS (0.12 g, 0.42 mmol), triethylamine (0.15 mL, 1.1 mmol), CH_2Cl_2 (50 mL); purification by column chromatography (SiO_2, 70 : 1 CH_2Cl_2 / MeOH).

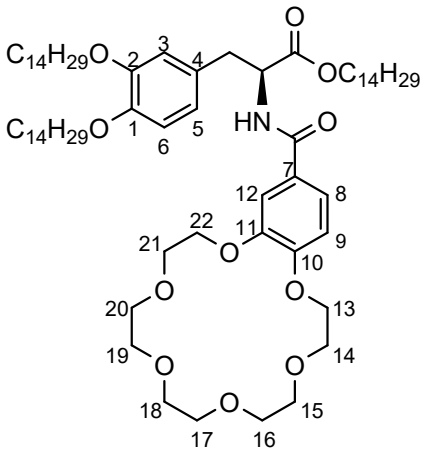

c-DOPA(14)
$C_{68}H_{117}NO_{11}$
(1124.68)

Off-white solid (20 %, 0.08 g, 0.07 mmol).

^{1}H-NMR (400 MHz, $CDCl_3$): δ = 0.88 (t, *J* = 6.7 Hz, 9H, CH_3), 1.20 – 1.50 (m, 66H, CH_2), 1.57 – 1.69 (m, 2H, C*H*$_2$CH$_2$O(C=O)), 1.70 – 1.83 (m, 4H, C*H*$_2$CH$_2$OAr), 3.16 (d, *J* = 5.6 Hz, 2H, HNC*H*), 3.65 – 3.80 (m, 12H, 15-H, 16-H, 17-H, 18-H, 19-H, 20-H), 3.81 – 3.98 (m, 8H, 13-H, 14-H, 21-H, 22-H), 4.06 – 4.16 (m, 2H, CH_2O(C=O)), 4.16 – 4.22 (m, 4H, CH_2OAr), 4.95 – 5.03 (m, 1H, HNC*H*), 6.47 (d, *J* = 7.5 Hz, 1H, NH), 6.58 – 6.66 (m, 2H, 3-H, 6-H), 6.77 (d, *J* = 8.0 Hz, 1H, 5-H), 6.82 (d, *J* = 8.4 Hz, 1H, 8-H), 7.20 (dd, *J* = 2.0 Hz, 8.4 Hz, 1H, 9-H), 7.37 (d, *J* = 2.0 Hz, 1H, 12-H) ppm.

^{13}C-NMR (101 MHz, $CDCl_3$): δ = 14.19 (CH_3), 22.79 (CH_3*C*H$_2$), 26.00, 26.18, 28.63, 29.35, 29.47, 29.58, 29.63, 29.72, 29.76, 29.78, 29.81, 29.83, 32.02 (CH_2), 37.59 (HNCH*C*H$_2$), 53.55

(HNCH), 65.82 (*C*H_2O(C=O)), 68.95, 69.06 (CH_2OAr), 69.33, 69.41, 69.44, 69.52 (C-13, C-14, C-21, C-22), 70.67, 70.73, 70.78, 70.84, 70.93, 70.96 (C-15, C-16, C-17, C-18, C-19, C-20), 112.38 (C-9), 112.84 (C-3), 113.96 (C-12), 115.18 (C-6), 120.00 (C-5), 121.75 (C-8), 126.87 (C-7), 128.56 (C-4), 148.41 (C-1), 148.81 (C-11), 149.22 (C-2), 151.99 (C-10), 166.34 (N(C=O)), 171.96 (C=O) ppm.

FT-IR (ATR): ν = 3271 (w), 2918 (vs), 2850 (vs), 1737 (w), 1713 (m), 1631 (m), 1601 (w), 1511 (m), 1467 (m), 1430 (m), 1349 (w), 1271 (vs), 1212 (m), 1134 (vs), 1054 (m), 948 (w), 873 (w), 813 (w), 763 (w), 722 (w) cm^{-1}.

MS (ESI): *m/z* ($C_{68}H_{117}NO_{11}$) calcd. 1124.8700 $[M + H]^+$, found: 1124.87; calcd. 1146.8519 $[M + Na]^+$, found: 1146.85.

HRMS (ESI): *m/z* ($C_{68}H_{117}NO_{11}$) calcd. 1124.8700 $[M + H]^+$, found: 1124.8694; calcd. 1146.8519 $[M + Na]^+$, found: 1146.8517; calcd. 1162.8259 $[M + K]^+$, found: 1162.8252.

DSC: Cr 112 [-61.7 kJ mol^{-1}] I (1st heating), I 101 [70.0 kJ mol^{-1}] Cr (1st cooling).

c-DOPA(16)

According to GP4: **[18]c-6-OH** (0.25 g, 0.70 mmol), EDC · HCl (0.15 g, 0.78 mmol), HOBt · H_2O (0.072 g, 0.47 mmol), **DOPA(16)** (0.30 g, 0.35 mmol), DPTS (0.15 g, 0.51 mmol), triethylamine (0.15 mL, 1.1 mmol), CH_2Cl_2 (50 mL).

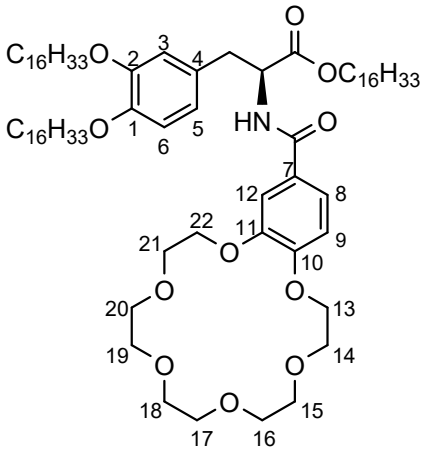

c-DOPA(16)
$C_{74}H_{129}NO_{11}$
(1208.84)

Off-white solid (56 %, 0.23 g, 0.19 mmol).

^{1}H-NMR (700 MHz, $CDCl_3$): δ = 0.88 (t, *J* = 7.0 Hz, 9H, CH_3), 1.18 – 1.37 (m, 76H, CH_2), 1.37 – 1.49 (m, 4H, C*H*$_2$$CH_2CH_2$OAr), 1.59 – 1.65 (m, 2H, C*H*$_2$$CH_2$O(C=O)), 1.71 – 1.82 (m, 4H, C*H*$_2$$CH_2$OAr), 3.13 – 3.18 (m, 2H, HNCHC*H*$_2$), 3.68 (s, 4H, 15-H, 20-H), 3.70 – 3.79 (m, 8H, 16-H, 17-H, 18-H, 19-H), 3.82 – 3.97 (m, 8H, 13-H, 14-H, 21-H, 22-H), 4.07 – 4.22 (m, 4H, CH_2OAr, CH_2O(C=O)), 4.96 – 5.01 (m, 1H, HNC*H*), 6.49 (d, *J* = 7.5 Hz, 1H, NH), 6.59 – 6.66

(m, 2H, 3-H, 6-H), 6.77 (d, *J* = 8.0 Hz, 1H, 5-H), 6.81 (d, *J* = 8.3 Hz, 1H, 9-H), 7.19 (dd, *J* = 1.5 Hz, 8.3 Hz, 1H, 8-H), 7.36 (d, *J* = 1.5 Hz, 1H, 12-H) ppm.

^{13}C-NMR (176 MHz, $CDCl_3$): δ = 14.27 (CH_3), 22.83 ($CH_3C\mathit{H}_2$), 26.05, 26.22 28.68, 29.42, 29.48, 29.53, 29.64, 29.69, 29.78, 29.84, 29.89, 29.91, 32.04 (CH_2), 37.64 (HNCH$\mathit{C}H_2$), 53.75 (HNCH), 65.88 ($\mathit{C}H_2O$(C=O)), 69.01, 69.11 (CH_2OAr), 69.33, 69.41, 69.51, 69.58 (C-13, C-14, C-21, C-22), 70.74, 70.80, 70.86, 70.93, 71.02, 71.05, (C-15, C-16, C-17, C-18, C-19, C-20), 112.40 (C-9), 112.88 (C-3), 113.91 (C-12), 115.12 (C-6), 120.01 (C-5), 121.77 (C-8), 126.88 (C-7), 128.52 (C-4), 148.41 (C-1), 148.85 (C-11), 149.20 (C-2), 152.03 (C-10), 166.39 (N(C=O)), 172.02 (C=O) ppm.

FT-IR (ATR): ν = 3272 (w), 2916 (vs), 2849 (vs), 1749 (w), 1630 (m), 1602 (w), 1582 (w), 1511 (m), 1467 (m), 1430 (m), 1392 (w), 1352 (m), 1309 (w), 1267 (s), 1227 (m), 1208 (m), 1171 (m), 1134 (vs), 1055 (m), 994 (w), 946 (w), 872 (w), 812 (w), 786 (w), 759 (w), 721 (m) cm^{-1}.

MS (ESI): *m/z* ($C_{74}H_{129}NO_{11}$) calcd. 1230.9458 $[M + Na]^+$, found: 1230.94.

HRMS (ESI): *m/z* ($C_{74}H_{129}NO_{11}$) calcd. 1225.9458 $[M + Na]^+$, found: 1230.9430.

DSC: Cr 108 [-47.3 kJ mol^{-1}] I (1st heating), I 100 [49.1 kJ mol^{-1}] Cr (1st cooling).

c-THIQ(14)

According to GP4: **[18]c-6-OH** (0.43 g, 1.2 mmol), EDC · HCl (0.38 g, 2.0 mmol), HOBt · H_2O (0.20 g, 1.3 mmol), **THIQ(14)** (0.61 g, 0.76 mmol), DPTS (0.23 g, 0.78 mmol), triethylamine (0.45 mL, 3.2 mmol), CH_2Cl_2 (100 mL).

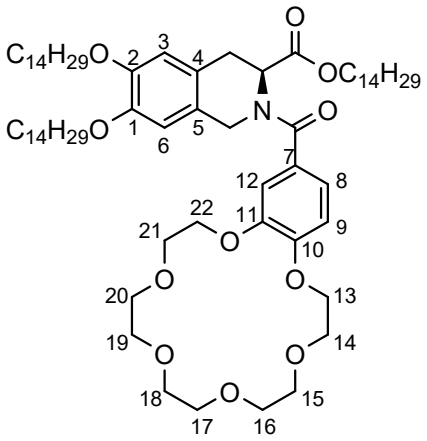

c-THIQ(14)
$C_{69}H_{117}NO_{11}$
(1136.69)

Colourless solid (18 %, 162 mg, 143 µmol).

^{1}H-NMR (400 MHz, $CDCl_3$): δ = 0.88 (t, *J* = 6.7 Hz, 9H, CH_3), 1.06 – 1.60 (m, 66H, CH_2), 1.60 – 1.86 (m, 6H, CH_2CH_2OAr, CH_2CH_2O(C=O)), 2.97 – 3.24 (m, 2H, NCHCH_2), 3.63 – 3.84 (m, 12H, 15-H, 16-H, 17-H, 18-H, 19-H, 20-H), 3.84 – 4.31 (m, 14H, CH_2OAr, CH_2O(C=O), 13-H,

14-H, 21-H, 22-H), 4.37 – 5.62 (m, 3H, NCH, NCH_2), 6.37 – 6.69 (m, 2H, 3-H, 6-H), 6.78 – 7.15 (m, 3H, 8-H, 9-H,12-H) ppm.

^{13}C-NMR (176 MHz, $CDCl_3$): δ = 14.28 (CH_3), 22.83 (CH_3CH_2), 25.88, 25.98, 26.20, 28.73, 29.39, 29.44, 29.54, 29.63, 29.70, 29.82, 29.84, 29.89 (CH_2), 32.12 (NCHCH_2), 48.06 (NCH_2), 52.14 (NCH), 65.56 (CH_2O(C=O)), 65.84, 69.23, 69.45, 69.54, 69.66, (CH_2OAr, C-13, C-14, C-21, C-22), 70.83, 70.90, 70.92, 70.97, 71.11 (C-15, C-16, C-17, C-18, C-19, C-20), 111.14 (C-12), 111.75 (C-3), 113.23 (C8), 113.82 (C-6), 120.03 (C-9), 120.88 (C-4), 124.97 (C-5), 128.60 (C-7), 148.04 (C-11), 148.28 (C-2), 150.44 (C-10), 171.16 (C=O) ppm.

The quaternary C signal of C-10 as well as the amide carbon signal could not be detected.

FT-IR (ATR): ν = 2955 (m), 2917 (vs), 2849 (vs), 1733 (m), 1636 (m), 1581 (w), 1516 (s), 1467 (m), 1430 (s), 1398 (m), 1332 (m), 1265 (s), 1206 (s), 1131 (vs), 1053 (m), 947 (m), 867 (m), 758 (w), 722 (m) cm^{-1}.

MS (ESI): *m/z* ($C_{69}H_{117}NO_{11}$) calcd. 1040.7761 $[M + H]^+$, found: 1136.87; calcd. 1158.8519 $[M + Na]^+$, found: 1158.85.

HRMS (ESI): *m/z* ($C_{69}H_{117}NO_{11}$) calcd. 1136.8699 $[M + H]^+$, found: 1136.8682.

DSC: Cr 39 [-56.7 kJ mol^{-1}] I (1st heating), I 33 [35.0 kJ mol^{-1}] Cr (1st cooling).

c-THIQ(16)

According to GP4: **[18]c-6-OH** (0.52 g, 1.5 mmol), EDC · HCl (0.32 g, 1.7 mmol), HOBt · H_2O (0.19 g, 1.2 mmol), **THIQ(16)** (0.39 g, 0.44 mmol), DPTS (0.22 g, 0.75 mmol), triethylamine (0.45 mL, 3.2 mmol), CH_2Cl_2 (100 mL).

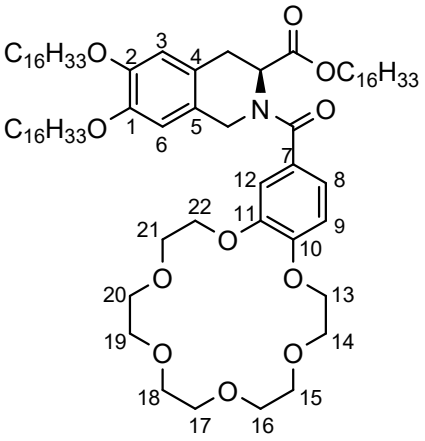

c-THIQ(16)
$C_{75}H_{129}NO_{11}$
(1220.85)

Off-white solid (84 %, 0.45 g, 0.37 mmol).

^{1}H-NMR (400 MHz, $CDCl_3$): δ = 0.88 (t, *J* = 6.7 Hz, 9H, CH_3), 0.98 – 1.50 (m, 72H, CH_2), 1.52 – 1.94 (m, 6H, CH_2CH_2OAr, CH_2CH_2O(C=O)), 2.98 – 3.27 (m, 2H, NCHCH_2), 3.66 – 3.81 (m,

12H, 15-H, 16-H, 17-H, 18-H, 19-H, 20-H), 3.82 – 4.31 (m, 14H, CH_2OAr, $CH_2O(C=O)$, 13-H, 14-H, 21-H, 22-H), 4.39 – 5.58 (m, 3H, NCH, NCH_2), 6.39 – 6.67 (m, 2H, 3-H, 6-H), 6.73 – 7.12 (m, 3H, 8-H, 9-H,12-H) ppm.

^{13}C-NMR (176 MHz, $CDCl_3$): δ = 14.28 (CH_3), 22.84 (CH_3CH_2), 25.88, 25.98, 26.20, 28.73, 29.39, 29.45, 29.54, 29.63, 29.70, 29.82, 29.84, 29.89 (CH_2), 32.08 ($NCHCH_2$), 48.08 (NCH_2), 52.16 (NCH), 65.57 ($CH_2O(C=O)$), 65.84, 69.05, 69.44, 69.54, 69.59, (CH_2OAr, C-13, C-14, C-21, C-22), 70.74, 70.80, 70.85, 70.89, 71.02 (C-15, C-16, C-17, C-18, C-19, C-20), 111.12 (C-12), 111.74 (C-3), 112.95 (C8), 113.85 (C-6), 119.91 (C-9), 120.80 (C-4), 124.49 (C-5), 128.43 (C-7), 148.34 (C-2), 171.16 (C=O) ppm.

The quaternary C signals of C-1, C-11, C-10 as well as the amide carbon signal could not be detected.

FT-IR (ATR): ν = 2917 (vs), 2850 (vs), 1736 (w), 1636 (m), 1581 (w), 1516 (m), 1467 (m), 1431 (m), 1399 (w), 1333 (w), 1266 (s), 1205 (m), 1132 (s), 1056 (w), 951 (w), 910 (w), 864 (m), 731 (m) cm^{-1}.

MS (ESI): *m/z* ($C_{75}H_{129}NO_{11}$) calcd. 1220.9639 $[M + H]^+$, found: 1220.97; calcd. 1242.9458 $[M + Na]^+$, found: 1242.95.

HRMS (ESI): *m/z* ($C_{75}H_{129}NO_{11}$) calcd. 1220.9639 $[M + H]^+$, found: 1220.9647.

DSC: Cr 49 [-75.6 kJ mol^{-1}] I (1st heating), I 49 [62.6 kJ mol^{-1}] Cr (1st cooling).

GP5: Complexation of the crown ether substituted amine[13]

The respective hybrid material of the type **c-DOPA(n)** (n = 12, 14, 16) or **c-THIQ(n)** (n = 14, 16) (51 µmol was dissolved in CH_2Cl_2 (10 mL) and mixed for 24 h with a solution of the corresponding salt (98 µmol) in methanol (10 mL) at room temperature. The solvent was removed, the residue was solved with CH_2Cl_2 and filtered through a syringe filter to obtain the complexed product as colourless solid.

c-DOPA(12) • KSCN

According to GP5: **c-DOPA(12)** (52 mg, 50 µmol), potassium thiocyanate (14 mg, 0.14 mmol), CH_2Cl_2 (10 mL), methanol (10 mL).

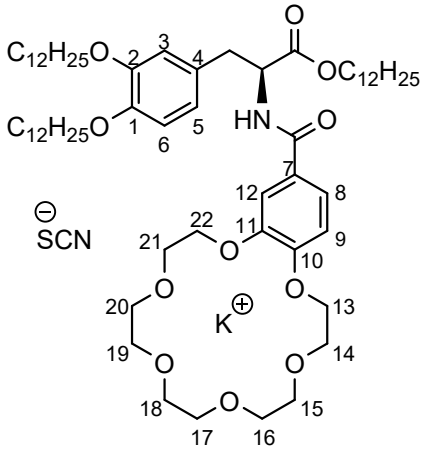

c-DOPA(12) • KSCN
$C_{63}H_{105}KN_2O_{11}S$
(1137.69)

Off-white solid (95 %, 54 mg, 47 µmol).

^{1}H-NMR (700 MHz, $CDCl_3$): δ = 0.86 (t, *J* = 7.0 Hz, 9H, CH_3), 1.10 – 1.48 (m, 54H, CH_2), 1.54 – 1.63 (m, 2H, C*H*$_2$CH$_2$O(C=O)), 1.69 – 1.80 (m, 4H, C*H*$_2$CH$_2$OAr), 3.11 – 3.20 (m, 2H, HNCHC*H*$_2$), 3.60 – 3.81 (m, 12H, 15-H, 16-H, 17-H, 18-H, 19-H, 20-H), 3.84 – 3.98 (m, 8H, CH_2OAr, 14-H, 21-H), 4.08 (t, *J* = 6.8 Hz, 2H, CH_2O(C=O)), 4.11 – 4.28 (m, 4H, 13-H, 22-H), 4.88 – 4.95 (m, 1H, HNC*H*), 6.68 (d, *J* = 8.1 Hz, 1H, NH), 6.74 – 6.79 (m, 2H, 3-H, 5-H, 6-H), 7.11 – 7.20 (m, 1H, 9-H), 7.26 (d, *J* = 7.0 Hz, 1H, 8-H), 7.37 (s, 1H, 12-H) ppm.

^{13}C-NMR (176 MHz, $CDCl_3$): δ = 14.21 (CH_3), 22.77 (CH_3*C*H$_2$), 25.99, 26.15, 26.18, 28.60, 29.37, 29.45, 29.46, 29.57, 29.58, 29.62, 29.72, 29.74, 29.76, 29.79, 29.82, 32.00 (CH_2), 37.40 (HNCH*C*H$_2$), 54.26 (HNCH), 65.74 (*C*H$_2$O(C=O)), 67.44, 67.53 (C-13, C-14, C-21, C-22), 68.55, 68.74 (CH_2OAr), 69.35, 69.38, 69.96, 69.97, 70.02, 70.10 (C-15, C-16, C-17, C-18, C-19, C-20), 110.80 (C-9), 110.94 (C-3), 113.94 (C-12), 115.15 (C-6), 120.62 (C-5), 121.71 (C-8), 126.99 (C-7), 129.03 (C-4), 132.19 (SCN), 146.72 (C-1), 148.21 (C-11), 149.12 (C-2), 149.61 (C-10), 166.28 (N(C=O)), 172.34 (C=O) ppm.

FT-IR (ATR): ν = 3273 (w), 2922 (vs), 2853 (s), 2055 (m), 1735 (m), 1641 (w), 1605 (w), 1585 (w), 1505 (s), 1467 (m), 1344 (m), 1263 (s), 1206 (s), 1118 (vs), 1050 (m), 957 (m), 908 (s), 807 (w), 762 (w), 730 (vs), 645 (w), 516 (w) cm^{-1}.

MS (ESI, pos.): *m/z* for $C_{62}H_{105}NO_{11}$ calcd. 1078.7320 $[M+K]^+$, found: 1078.73.

MS (ESI, neg.): *m/z* for $C_{62}H_{105}NO_{11}$ calcd. 57.9757 $[SCN]^-$, found: 57.98.

HRMS (ESI, pos.): *m/z* for $C_{62}H_{105}NO_{11}$ calcd. 1078.7320 $[M+K]^+$, found: 1078.7276.

HRMS (ESI, neg.): *m/z* for $C_{62}H_{105}NO_{11}$ calcd. 57.9757 $[SCN]^-$, found: 57.9750.

DSC: G 75 [13.1 kJ mol^{-1}] Cr 107 [-24.0 kJ mol^{-1}] I (3rd heating), I 91 [1.6 kJ mol^{-1}] SmA_d 61 G (3rd cooling).

c-DOPA(12) • NaI

According to GP5: **c-DOPA(12)** (8 mg, 8 µmol), sodium iodide (23 mg, 0.15 mmol), CH_2Cl_2 (10 mL), methanol (10 mL).

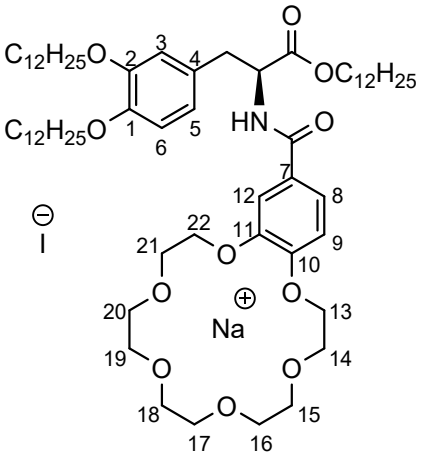

c-DOPA(12) • NaI
$C_{62}H_{105}INNaO_{11}$
(1190.41)

Colourless solid (98 %, 9 mg, 8 µmol).

^{1}H-NMR (700 MHz, $CDCl_3$): δ = 0.85 (t, *J* = 7.0 Hz, 9H, CH_3), 1.13 – 1.35 (m, 50H, CH_2), 1.35 – 1.47 (m, 4H, C*H*$_2$CH$_2$CH$_2$OAr), 1.54 – 1.62 (m, 2H, C*H*$_2$CH$_2$O(C=O)), 1.69 – 1.79 (m, 4H, C*H*$_2$CH$_2$OAr), 3.08 – 3.30 (m, 2H, HNCHC*H*$_2$), 3.55 – 3.82 (m, 12H, 15-H, 16-H, 17-H, 18-H, 19-H, 20-H), 3.82 – 4.02 (m, 8H, CH_2OAr, 14-H, 21-H), 4.02 – 4.28 (m, 6H, CH_2O(C=O), 13-H, 22-H), 4.89 – 4.96 (m, 1H, HNC*H*), 6.67 – 6.79 (m, 4H, NH, 3-H, 5-H, 6-H), 6.99 – 7.06 (m, 1H, 9-H), 7.21 – 7.25 (m, 1H, 8-H), 7.27 – 7.31 (m, 1H, 12-H) ppm.

^{13}C-NMR (176 MHz, $CDCl_3$): δ = 14.19 (CH_3), 22.75 (CH_3*C*H$_2$), 25.98, 26.15, 26.18, 28.59, 29.36, 29.44, 29.51, 29.56, 29.57, 29.62, 29.67, 29.73, 29.75, 29.78, 29.80, 31.48, 31.99 (CH_2), 37.37 (HNCH*C*H$_2$), 54.30 (HNCH), 65.80 (*C*H$_2$O(C=O)), 67.20, 67.23 (C-13, C-14, C-21, C-22), 68.70, 68.75 (CH_2OAr), 69.26, 69.41, 69.45, 69.48, 69.76, 69.78 (C-15, C-16, C-17, C-18, C-19, C-20), 111.02 (C-9), 111.17 (C-3), 113.93 (C-12), 115.30 (C-6), 120.61 (C-5), 121.81 (C-8), 126.72 (C-7), 129.04 (C-4), 146.97 (C-1), 148.28 (C-11), 149.11 (C-2), 150.05 (C-10), 166.57 (N(C=O)), 172.36 (C=O) ppm.

FT-IR (ATR): ν = 3426 (w), 2921 (vs), 2852 (vs), 1735 (m), 1649 (m), 1587 (m), 1504 (vs), 1467 (s), 1345 (m), 1266 (vs), 1213 (s), 1120 (vs), 956 (m), 920 (w), 831 (w), 762 (m), 723 (m), 520 (w) cm^{-1}.

MS (ESI, pos.): *m/z* ($C_{62}H_{105}NO_{11}$) calcd. 1062.7580 $[M + Na]^+$, found: 1062.76.

MS (ESI, neg.): *m/z* ($C_{62}H_{105}NO_{11}$) calcd. 126.9050 $[I]^-$, found: 126.90.

HRMS (ESI, pos.): *m/z* ($C_{62}H_{105}NO_{11}$) calcd. 1062.7580 $[M + Na]^+$, found: 1062.7586.

HRMS (ESI, neg.): *m/z* ($C_{62}H_{105}NO_{11}$) calcd. 126.9050 $[I]^-$, found: 126.9048.

DSC: G 64 SmA_d 85 [-0.9 kJ mol^{-1}] I (3^{rd} heating), I 83 [1.0 kJ mol^{-1}] SmA_d 81 G (3^{rd} cooling).

c-DOPA(12) • KI

According to GP5: **c-DOPA(12)** (10 mg, 9.6 µmol), potassium iodide (15 mg, 90 µmol), CH_2Cl_2 (10 mL), methanol (10 mL).

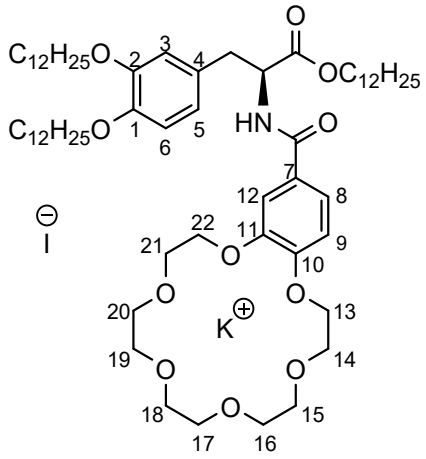

c-DOPA(12) • KI
$C_{62}H_{105}IKNO_{11}$
(1206.52)

Colourless solid (95 %, 11 mg, 9.1 µmol).

^{1}H-NMR (400 MHz, $CDCl_3$): δ = 0.88 (t, *J* = 6.8 Hz, 9H, CH_3), 1.16 – 1.51 (m, 54H, CH_2), 1.51 – 1.69 (m, 2H, C*H*$_2$CH$_2$O(C=O)), 1.70 – 1.86 (m, 4H, C*H*$_2$CH$_2$OAr), 3.16 (d, *J* = 5.6 Hz, 2H, HNCHC*H*$_2$), 3.67 – 3.77 (m, 8H, 16-H, 17-H, 18-H, 19-H), 3.77 – 4.07 (m, 12H, 14-H, 15-H, 20-H, 21-H, CH_2OAr), 4.07 – 4.29 (m, 6H, 13-H, 22-H, CH_2O(C=O)), 4.94 – 5.02 (m, 1H, HNC*H*), 6.48 – 6.55 (m, 1H, 3-H), 6.60 – 6.67 (m, 2H, NH, 6-H) 6.74 – 6.86 (m, 2H, 5-H, 9-H), 7.20 (dd, *J* = 2.0 Hz, 8.3 Hz, 1H, 8-H), 7.38 (d, *J* = 2.0 Hz, 1H, 12-H) ppm.

^{13}C-NMR (176 MHz, $CDCl_3$): δ = 14.21 (CH_3), 22.77 (CH_3*C*H_2), 25.99, 26.15, 26.18, 28.60, 29.35, 29.45, 29.46, 29.56, 29.62, 29.70, 29.74, 29.76, 29.79, 29.82, 32.00 (CH_2), 37.45 (HNCH*C*H_2), 54.00 (HNCH), 65.84 (*C*H_2O(C=O)), 67.55, 67.70, 68.58, 68.71 (C-13, C-14, C-21, C-22), 69.36 (CH_2OAr), 69.95, 69.99, 70.02, 70.10 (C-15, C-16, C-17, C-18, C-19, C-20), 110.85 (C-9), 111.04 (C-3), 113.90 (C-12), 115.14 (C-6), 120.27 (C-5), 121.76 (C-8), 127.08 (C-7), 128.67 (C-4), 146.96 (C-1), 148.33 (C-11), 149.14 (C-2), 149.82 (C-10), 166.08 (N(C=O)), 172.13 (C=O) ppm.

FT-IR (ATR): ν = 3280 (w), 2922 (vs), 2853 (s), 1736 (m), 1644 (w), 1604 (w), 1585 (w), 1501 (s), 1467 (m), 1343 (m), 1263 (s), 1206 (s), 1118 (vs), 1049 (m), 957 (m), 909 (s), 833 (w), 761 (w), 729 (vs), 643 (w), 517 (w) cm^{-1}.

MS (ESI, pos.): *m/z* ($C_{62}H_{105}NO_{11}$) calcd. 1078.7320 $[M + K]^+$, found: 1078.73.

MS (ESI, neg.): *m/z* ($C_{62}H_{105}NO_{11}$) calcd. 126.9050 $[I]^-$, found: 126.91.

HRMS (ESI, pos.): *m/z* ($C_{62}H_{105}NO_{11}$) calcd. 1078.7320 $[M + K]^+$, found: 1078.7299.

HRMS (ESI, neg.): *m/z* ($C_{62}H_{105}NO_{11}$) calcd. 126.9050 $[I]^-$, found: 126.9050.

DSC: G 105 [9.8 kJ/mol] Cr 120 (-8.5 kJ/mol) I (3rd heating), I 77 (1.2 kJ/mol) SmA_d 63 G.

c-DOPA(12) • $NaBF_4$

According to GP5: **c-DOPA(12)** (23 mg, 22 µmol), sodium tetrafluoroborate (35 mg, 0.32 mmol), CH_2Cl_2 (5 mL), methanol (5 mL).

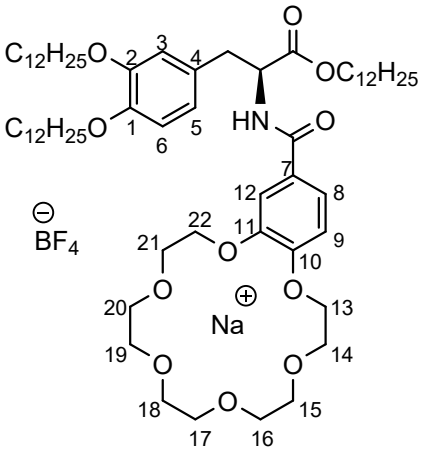

c-DOPA(12) • $NaBF_4$
$C_{62}H_{105}BF_4NNaO_{11}$
(1150.31)

Off-white solid (98 %, 25 mg, 22 µmol).

^{1}H-NMR (400 MHz, $CDCl_3$δ = 0.88 (t, *J* = 6.8 Hz, 9H, CH_3), 1.16 – 1.51 (m, 54H, CH_2), 1.51 – 1.70 (m, 2H, C*H*$_2$CH$_2$O(C=O)), 1.69 – 1.87 (m, 4H, C*H*$_2$CH$_2$OAr), 3.09 – 3.29 (m, 2H, HNCHC*H*$_2$), 3.64 – 3.82 (m, 12H, 15-H, 16-H, 17-H, 18-H, 19-H, 20-H), 3.82 – 4.07 (m, 8H, CH_2OAr, 14-H, 21-H), 4.06 – 4.26 (m, 6H, 13-H, 22-H; CH_2O(C=O)) 4.95 – 5.03 (m, 1H, HNC*H*), 6.48 (d, *J* = 7.6 Hz, 1H, NH), 6.59 – 6.65 (m, 2H, 3-H, 6-H), 6.73 – 6.87 (m, 2H, 5-H, 9-H), 7.20 (dd, *J* = 2.0 Hz, 8.4 Hz, 1H, 8-H), 7.37 (d, *J* = 2.0 Hz, 1H, 12-H) ppm.

^{13}C-NMR (176 MHz, $CDCl_3$): δ = 14.28 (CH_3), 22.84 (CH_3CH_2), 26.00, 26.06, 26.15, 26.18, 26.23, 25.24, 28.59, 28.69, 29.30, 29.42, 29.48, 29.54, 29.55, 29.60, 29.64, 29.70, 29.78, 29.83, 29.85, 29.88, 29.91, 32.08 (CH_2), 37.64 (HNCH*C*H$_2$), 53.77 (HNCH), 65.91 (*C*H$_2$O(C=O)), 69.37, 69.43 (CH_2OAr, C-13 – C-22), 113.94 (C-3, C-9, C-12), 115.16 (C-6), 120.02 (C-5), 121.80 (C-8), 124.97 (C-7), 128.50 (C-4), 148.45 (C-1), 149.23 (C-2), 172.01 ((C=O)) ppm.

The quaternary C signals of C-10 and C-11 as well as the amide carbon could not be detected.

^{19}F-NMR (376 MHz, $CDCl_3$): δ = -155.50 ppm.

FT-IR (ATR): ν = 3291 (w), 2922 (vs), 2853 (s), 1740 (w), 1631 (w), 1603 (w), 1509 (m), 1467 (m), 1355 (w), 1269 (m), 1217 (m), 1133 (m), 1057 (m), 954 (w) cm^{-1}.

MS (ESI, pos.): *m/z* ($C_{62}H_{105}NO_{11}$) calcd. 1062.7580 $[M+Na]^+$, found: 1062.76.

MS (ESI, neg.): *m/z* ($C_{62}H_{105}NO_{11}$) calcd. 87.0034 $[BF_4]^-$, found: 87.00.

HRMS (ESI, pos.): *m/z* ($C_{62}H_{105}NO_{11}$) calcd. 1062.7580 $[M+Na]^+$, found: 1062.7558.

HRMS (ESI, neg.): *m/z* ($C_{62}H_{105}NO_{11}$) calcd. 87.0034 $[BF_4]^-$, found: 87.0029.

DSC: G 57 (5.2) Cr 80 [-6.3 kJ mol^{-1}] I (6^{th} heating), I 115 [0.1 kJ mol^{-1}] SmA_d 32 G -19 [2.6 kJ mol^{-1}] Cr (6^{th} cooling).

c-DOPA(12) • KBF_4

According to GP5: **c-DOPA(12)** (49 mg, 47 µmol), potassium tetrafluoroborate (17 mg, 0.14 mmol), CH_2Cl_2 (10 mL), methanol (10 mL).

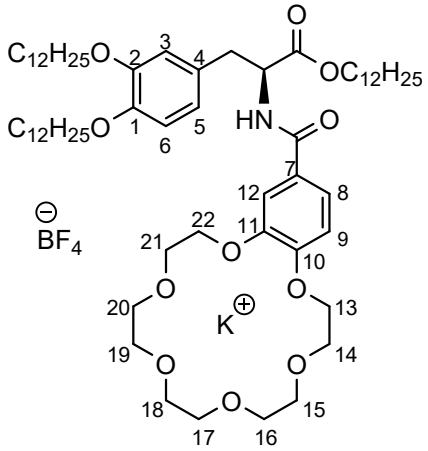

c-DOPA(12) • KBF_4
$C_{62}H_{105}BF_4KNO_{11}$
(1166.42)

Off-white solid (95 %, 52 mg, 45 µmol).

^{1}H-NMR (700 MHz, $CDCl_3$): δ = 0.87 (t, *J* = 7.0 Hz, 9H, CH_3), 1.16 – 1.47 (m, 54H, CH_2), 1.59 – 1.65 (m, 2H, C*H*$_2$CH$_2$O(C=O)), 1.71 – 1.81 (m, 4H, C*H*$_2$CH$_2$OAr), 3.12 – 3.17 (m, 2H, HNCHC*H*$_2$), 3.64 – 3.78 (m, 12H, 15-H, 16-H, 17-H, 18-H, 19-H, 20-H), 3.80 – 3.96 (m, 8H, CH_2OAr, 14-H, 21-H), 4.06 – 4.15 (m, 2H, CH_2O(C=O)), 4.15 – 4.20 (m, 4H, 13-H, 22-H) 4.95 – 5.00 (m, 1H, HNC*H*), 6.49 – 6.54 (m, 1H, NH), 6.59 – 6.64 (m, 2H, 3-H, 6-H), 6.74 – 6.78 (m, 1H, 5-H), 6.78 – 6.82 (m, 1H, 9-H), 7.17 – 7.21 (m, 1H, 8-H), 7.35 (s, 1H, 12-H) ppm.

^{13}C-NMR (176 MHz, $CDCl_3$): δ = 14.23 (CH_3), 22.80 (CH_3*C*H_2), 26.01, 26.18, 28.63, 29.37, 29.43, 29.48, 29.50, 29.55, 29.58, 29.64, 29.72, 29.76, 29.78, 29.82, 29.85, 32.03 (CH_2), 37.58 (HNCH*C*H_2), 53.74 (HNCH), 65.85 (*C*H_2O(C=O)), 68.76, 68.82 (C-13, C-22), 69.30, 69.32, 69.37, 69.40 (CH_2OAr, C-14, C-21), 70.58, 70.64, 70.69, 70.74, 70.81, 70.84 (C-15, C-16, C-17, C-18, C-19, C-20), 112.12 (C-9), 112.58 (C-3), 113.87 (C-12), 115.09 (C-6), 119.98 (C-5), 121.73 (C-8), 126.86 (C-7), 128.51 (C-4), 148.37 (C-1), 148.60 (C-11), 149.18 (C-2), 151.75 (C-10), 166.32 (N(C=O)), 172.00 ((C=O)) ppm.

^{19}F-NMR (376 MHz, $CDCl_3$): δ = -153.27 ppm.

FT-IR (ATR): ν = 3279 (w), 2919 (vs), 2850 (s), 1751 (m), 1629 (s), 1582 (w), 1511 (s), 1466 (m), 1430 (m), 1392 (w), 1351 (m), 1265 (s), 1227 (s), 1207 (s), 1172 (s), 1134 (vs), 1097 (s), 1055 (s), 995 (m), 947 (m), 871 (m), 812 (m), 786 (w), 761 (w), 721 (m), 683 (w), 650 (w), 628 (w), 566 (w) cm^{-1}.

MS (ESI, pos.): *m/z* ($C_{62}H_{105}NO_{11}$) calcd. 1078.7320 $[M+K]^+$, found: 1078.73.

MS (ESI, neg.): *m/z* ($C_{62}H_{105}NO_{11}$) calcd. 87.0034 $[BF_4]^-$, found: 87.00.

HRMS (ESI, pos.): *m/z* ($C_{62}H_{105}NO_{11}$) calcd. 1078.7320 $[M+K]^+$, found: 1078.7286.

HRMS (ESI, neg.): *m/z* ($C_{62}H_{105}NO_{11}$) calcd. 87.0034 $[BF_4]^-$, found: 87.0031.

DSC: Cr 112 [-42.5 kJ mol^{-1}] I (1st heating), I 97 [61.1 kJ mol^{-1}] Cr (1st cooling).

c-DOPA(12) • KPF_6

According to GP5: **c-DOPA(12)** (53 mg, 51 µmol), potassium hexafluorophosphate (18 mg, 98 µmol), CH_2Cl_2 (10 mL), methanol (10 mL).

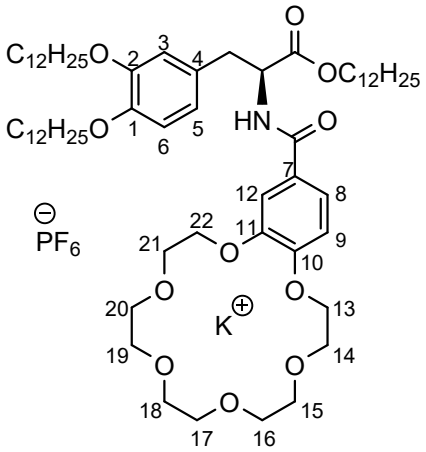

c-DOPA(12) • KPF_6
$C_{62}H_{105}F_6KNO_{11}P$
(1224.58)

Off-white solid (93 %, 58 mg, 47 µmol).

^{1}H-NMR (700 MHz, $CDCl_3$): δ = 0.84 – 0.89 (m, 9H, CH_3), 1.13 – 1.48 (m, 54H, CH_2), 1.58 – 1.64 (m, 2H, C*H*$_2$CH$_2$O(C=O)), 1.73 – 1.81 (m, 4H, C*H*$_2$CH$_2$OAr), 3.12 – 3.18 (m, 2H, HNCHC*H*$_2$), 3.61 – 3.72 (m, 12H, 15-H, 16-H, 17-H, 18-H, 19-H, 20-H), 3.81 – 3.90 (m, 6H, CH_2OAr, 14-H, 21-H), 3.93 (t, *J* = 6.7 Hz, 2H, CH_2OAr), 4.07 – 4.16 (m, 2H, CH_2O(C=O)), 4.17 – 4.23 (m, 4H, 13-H, 22-H), 4.93 – 4.98 (m, 1H, HNC*H*), 6.63 – 6.68 (m, 2H, 3-H, 6-H), 6.68 – 6.72 (m, 1H, NH), 6.76 – 6.82 (m, 2H, 5-H, 9-H), 7.19 (dd, *J* = 2.0 Hz, 8.4 Hz, 1H, 8-H), 7.30 – 7.32 (m, 1H, 12-H) ppm.

^{13}C-NMR (176 MHz, $CDCl_3$): δ = 14.24 (CH_3), 22.80 (CH_3CH_2), 26.02, 26.19, 26.21, 28.64, 29.38, 29.46, 29.48, 29.50, 29.60, 29.65, 29.71, 29.74, 29.77, 29.79, 29.83, 29.85, 32.04 (CH_2), 37.52 (HNCHCH_2), 53.95 (HNCH), 65.88 (CH_2O(C=O)), 67.25, 67.51, 68.33, 68.48 (C-13, C-14, C-21, C-22), 69.37 (CH_2OAr), 69.89, 69.94, 69.96 (C-15, C-16, C-17, C-18, C-19, C-20), 110.80 (C-9), 110.84 (C-3), 113.92 (C-12), 115.10 (C-6), 120.12 (C-5), 121.78 (C-8), 127.07 (C-7), 128.58 (C-4), 146.93 (C-1), 148.42 (C-11), 149.20 (C-2), 149.81 (C-10), 166.13 (N(C=O)), 172.19 (C=O) ppm.

^{19}F-NMR (376 MHz, $CDCl_3$): δ = -73.60, -71.69 ppm.

FT-IR (ATR): ν = 2923 (s), 2853 (m), 1736 (w), 1647 (w), 1605 (w), 1587 (w), 1505 (m), 1467 (m), 1355 (w), 1263 (m), 1207 (m), 1120 (s), 1052 (w), 959 (m), 908 (s), 841 (vs), 731 (vs), 648 (w), 558 (m) cm^{-1}.

MS (ESI, pos.): *m/z* ($C_{62}H_{105}NO_{11}$) calcd. 1078.7320 $[M + K]^+$, found: 1078.73.

MS (ESI, neg.): *m/z* ($C_{62}H_{105}NO_{11}$) calcd. 144.9647 $[PF_6]^-$, found: 144.96.

HRMS (ESI, pos.): *m/z* ($C_{62}H_{105}NO_{11}$) calcd. 1078.7320 $[M + K]^+$, found: 1078.7312.

HRMS (ESI, neg.): *m/z* ($C_{62}H_{105}NO_{11}$) calcd. 144.9647 $[PF_6]^-$, found: 144.9647.

DSC: Cr 56 [-1.9 kJ mol^{-1}] SmA_d 105 [-0.6 kJ mol^{-1}] I (3rd heating), I 101 [0.4 kJ mol^{-1}] SmA_d 69 G (3rd cooling).

c-DOPA(14) • KSCN

According to GP5: **c-DOPA(14)** (9 mg, 8 µmol), potassium thiocyanate (38 mg, 0.39 mmol), CH_2Cl_2 (5 mL), methanol (5 mL).

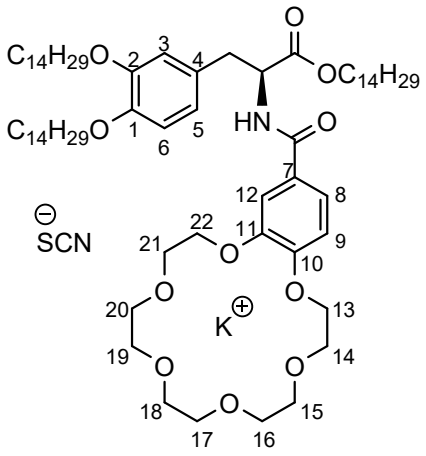

c-DOPA(14) • KSCN
$C_{69}H_{117}KN_2O_{11}S$
(1221.86)

Off-white solid (92 %, 9 mg, 7 µmol).

^{1}H-NMR (700 MHz, $CDCl_3$): δ = 0.84 – 0.88 (m, 9H, CH_3), 1.04 – 1.47 (m, 66H, CH_2), 1.54 – 1.65 (m, 2H, C*H*$_2$CH$_2$O(C=O)), 1.70 – 1.80 (m, 4H, C*H*$_2$CH$_2$OAr), 3.12 – 3.21 (m, 2H, HNCHC*H*$_2$), 3.59 – 3.81 (m, 12H, 15-H, 16-H, 17-H, 18-H, 19-H, 20-H), 3.84 – 3.99 (m, 8H, CH_2OAr, 14-H, 21-H), 4.03 – 4.12 (m, 2H, CH_2O(C=O)), 4.12 – 4.29 (m, 4H, 13-H, 22-H), 4.89 – 4.96 (m, 1H, HNC*H*), 6.64 – 6.72 (m, 2H, 3-H, 6-H), 6.74 – 6.80 (m, 2H, 5-H, 9-H), 6.97 – 7.12 (m, 1H, NH), 7.22 – 7.25 (m, 1H, 8-H), 7.38 (s, 1H, 12-H) ppm.

^{13}C-NMR (176 MHz, $CDCl_3$): δ = 14.23 (CH_3), 22.79 (CH_3*C*H$_2$), 26.01, 26.18, 26.21, 28.62, 29.39, 29.48, 29.60, 29.65, 29.70, 29.74, 29.77, 29.79, 29.82, 29.84, 32.03 (CH_2), 37.46 (HNCH*C*H$_2$), 54.19 (HNCH), 65.79 (*C*H$_2$O(C=O)), 67.44, 67.56, 68.57, 68.76, 69.37, 69.40 (CH_2OAr, C-13, C-14, C-21, C-22), 69.98, 70.00, 70.13 (C-15, C-16, C-17, C-18, C-19, C-20), 110.81 (C-9), 111.01 (C-3), 113.94 (C-12), 115.16 (C-6), 120.50 (C-5), 121.75 (C-8), 127.11 (C-7), 128.92 (C-4), 132.26 (SCN), 146.82 (C-1), 148.27 (C-11), 149.15 (C-2), 149.69 (C-10), 166.26 (N(C=O)), 172.28 (C=O) ppm.

FT-IR (ATR): ν = 3261 (w), 2921 (vs), 2852 (s), 2055 (m), 1736 (m), 1640 (w), 1605 (w), 1585 (w), 1505 (s), 1467 (m), 1344 (m), 1264 (vs), 1206 (s), 1119 (vs), 1050 (m), 957 (m), 908 (s), 834 (w), 788 (w), 762 (w), 730 (vs), 645 (m), 516 (w) cm^{-1}.

MS (ESI, pos.): *m/z* ($C_{68}H_{117}NO_{11}$) calcd. 1162.8259 $[M + K]^+$, found: 1162.82.

MS (ESI, neg.): *m/z* ($C_{68}H_{117}NO_{11}$) calcd. 57.9757 $[SCN]^-$, found: 57.98.

HRMS (ESI, pos.): *m/z* ($C_{68}H_{117}NO_{11}$) calcd. 1162.8238 $[M+K]^+$, found: 1162.8238.

HRMS (ESI, neg.): *m/z* ($C_{68}H_{117}NO_{11}$) calcd. 57.9757 $[SCN]^-$, found: 57.9750.

DSC: G 78 [17.6 kJ mol^{-1}] Cr 101 [-18.7 kJ mol^{-1}] I (3rd heating), I 88 [1.2 kJ mol^{-1}] SmA_d 61 G (3rd cooling).

c-DOPA(14) • NaI

According to GP5: **c-DOPA(14)** (43 mg, 38 µmol), sodium iodide (38 mg, 0.25 mmol), CH_2Cl_2 (10 mL), methanol (10 mL).

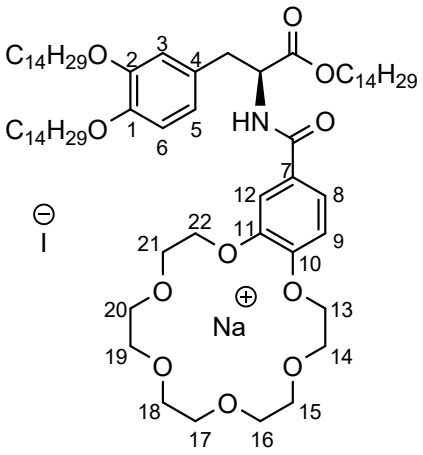

c-DOPA(14) • NaI
$C_{68}H_{117}INNaO_{11}$
(1274.57)

Off-white solid (90 %, 44 mg, 35 µmol).

^{1}H-NMR (400 MHz, $CDCl_3$): δ = 0.84 – 0.91 (m, 9H, CH_3), 1.16 – 1.52 (m, 66H, CH_2), 1.53 – 1.70 (m, 2H, C*H*$_2$CH$_2$O(C=O)), 1.70 – 1.84 (m, 4H, CH$_2$C*H*$_2$OAr), 3.17 (d, *J* = 5.7 Hz, 2H, HNCHC*H*$_2$), 3.67 – 3.85 (m, 12H, 15-H, 16-H, 17-H, 18-H, 19-H, 20-H), 3.85 – 4.05 (m, 8H, 14-H – 21-H, CH_2OAr), 4.06 – 4.32 (m, 6H, 13-H, 22-H, CH_2O(C=O)), 4.94 – 5.02 (m, 1H, HNC*H*), 6.54 (d, *J* = 7.4 Hz, 6-H), 6.62 – 6.68 (d, *J* = 6.9 Hz, 2H, 3-H, NH), 6.75 – 6.88 (m, 2H, 5-H, 9-H), 7.21 (dd, *J* = 2.0 Hz, 8.4 Hz, 1H, 8-H), 7.33 (d, *J* = 2.0 Hz, 1H, 12-H) ppm.

^{13}C-NMR (176 MHz, $CDCl_3$): δ = 14.22 (CH_3), 22.78 ($CH_3C H_2$), 26.01, 26.18, 26.21, 28.62, 29.39, 29.47, 29.60, 29.65, 29.76, 29.81, 32.02 (CH_2), 37.39 (HNCH*C*H$_2$), 54.35 (HNCH), 65.83 (*C*H$_2$O(C=O)), 67.10, 67.13 (C-13, C-14, C-21, C-22), 68.68, 68.71, 69.12, 69.35, 69.39, 69.43, 69.47, 69.74 (CH_2OAr, C-15, C-16, C-17, C-18, C-19, C-20), 110.96 (C-9), 111.14 (C-3), 113.95 (C-12), 115.33 (C-6), 120.62 (C-5), 121.84 (C-8), 126.77 (C-7), 129.05 (C-4), 146.88 (C-1), 148.31 (C-11), 149.14 (C-2), 149.95 (C-10), 166.57 (N(C=O)), 172.40 (C=O) ppm.

FT-IR (ATR): ν = 3294 (w), 2921 (vs), 2852 (vs), 1733 (m), 1632 (m), 1603 (w), 1586 (m), 1495 (s), 1467 (m), 1344 (m), 1268 (vs), 1211 (s), 1119 (vs), 1096 (s), 1052 (m), 952 (m), 920 (m), 828 (w), 764 (m), 726 (s), 641 (w), 520 (w) cm^{-1}.

MS (ESI, pos.): *m/z* ($C_{68}H_{117}NO_{11}$) calcd. 1146.8519 $[M + Na]^+$, found: 1146.85.

MS (ESI, neg.): *m/z* ($C_{68}H_{117}NO_{11}$) calcd. 126.9050 $[I]^-$, found: 126.91.

HRMS (ESI, pos.): *m/z* ($C_{68}H_{117}NO_{11}$) calcd. 1146.8519 $[M + Na]^+$, found: 1146.8495.

HRMS (ESI, neg.): *m/z* ($C_{68}H_{117}NO_{11}$) calcd. 126.9050 $[I]^-$, found: 126.9051.

DSC: G 59 SmA_d 87 [-0.8 kJ mol^{-1}] I (3rd heating), I 83 [1.0 kJ mol^{-1}] SmA_d 81 G (3rd cooling).

c-DOPA(14) • KI

According to GP5: **CEDOPA(14)** (42 mg, 37 µmol), potassium iodide (53 mg, 0.32 mmol), CH_2Cl_2 (10 mL), methanol (10 mL).

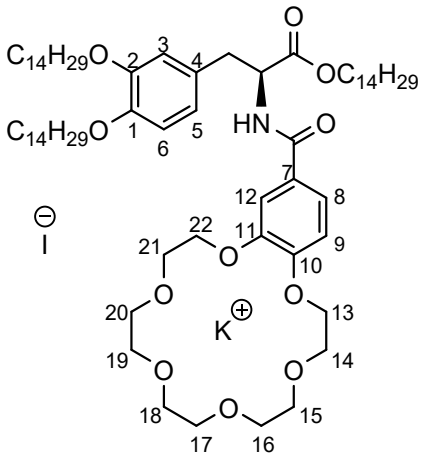

c-DOPA(14) • KI
$C_{68}H_{117}IKNO_{11}$
(1290.68)

Off-white solid (98 %, 47 mg, 36 µmol).

^{1}H-NMR (700 MHz, $CDCl_3$): δ = 0.84 – 0.89 (m, 9H, CH_3), 1.07 – 1.47 (m, 66H, CH_2), 1.58 – 1.65 (m, 2H, C*H*$_2$CH$_2$O(C=O)), 1.71 – 1.79 (m, 4H, CH$_2$C*H*$_2$OAr), 3.10 – 3.23 (m, 2H, HNCHC*H*$_2$), 3.64 – 3.85 (m, 12H, 15-H, 16-H, 17-H, 18-H, 19-H, 20-H), 3.85 – 3.90 (m, 2H, CH_2OAr), 3.93 (t, *J* = 6.6 Hz, 2H, CH_2OAr), 3.96 – 4.07 (m, 4H, 14-H, 21-H), 4.07 – 4.15 (m, 2H, CH_2O(C=O)), 4.19 – 4.28 (m, 4H, 13-H, 22-H), 4.91 – 4.99 (m, 1H, HNC*H*), 6.61 – 6.68 (m, 2H, 3-H, 6-H), 6.67 – 6.75 (m, 1H, NH), 6.75 – 6.78 (m, 1H, 5-H), 6.78 – 6.82 (m, 1H, 9-H), 7.19 – 7.24 (m, 1H, 8-H), 7.37 (d, *J* = 2.0 Hz, 1H, 12-H) ppm.

^{13}C-NMR (176 MHz, $CDCl_3$): δ = 14.23 (CH_3), 22.80 (CH_3*C*H$_2$), 26.01, 26.19, 26.21, 28.63, 29.38, 29.46, 29.48, 29.59, 29.65, 29.74, 29.77, 29.79, 29.83, 29.85, 32.03 (CH_2), 37.51 (HNCH*C*H$_2$), 53.94 (HNCH), 65.89 (*C*H$_2$O(C=O)), 67.59, 67.74, 68.63, 68.76 (C-13, C-14, C-21, C-22), 69.38, 69.39 (CH_2OAr), 70.00, 70.06, 70.10, 70.18 (C-15, C-16, C-17, C-18, C-19, C-20), 110.88 (C-9), 111.13 (C-3), 113.91 (C-12), 115.15 (C-6), 120.19 (C-5), 121.79 (C-8), 127.15 (C-7), 128.61 (C-4), 147.07 (C-1), 148.38 (C-11), 149.17 (C-2), 149.93 (C-10), 166.08 (N(C=O)), 172.11 (C=O) ppm.

FT-IR (ATR): ν = 3282 (w), 2921 (vs), 2852 (s), 1736 (m), 1642 (m), 1603 (w), 1585 (w), 1500 (s), 1467 (m), 1343 (m), 1264 (s), 1206 (s), 1118 (vs), 1049 (m), 957 (m), 908 (s), 833 (w), 788 (w), 761 (w), 729 (vs), 642 (w), 517 (w) cm^{-1}.

MS (ESI, pos.): *m/z* ($C_{68}H_{117}NO_{11}$) calcd. 1162.8259 $[M + K]^+$, found: 1162.82.

MS (ESI, neg.): *m/z* ($C_{68}H_{117}NO_{11}$) calcd. 126.9050 $[I]^-$, found: 126.91.

HRMS (ESI, pos.): *m/z* ($C_{68}H_{117}NO_{11}$) calcd. 1162.8259 $[M+K]^+$, found: 1162.8243.

HRMS (ESI, neg.): *m/z* ($C_{68}H_{117}NO_{11}$) calcd. 126.9050 $[I]^-$, found: 126.9051.

DSC: G 105 [8.3 kJ mol^{-1}] Cr 121 [-7.0 kJ mol^{-1}] I (3rd heating), I 98 [0.4 kJ mol^{-1}] SmA_d 57 G (3rd cooling).

c-DOPA(14) • $NaBF_4$

According to GP5: **c-DOPA(14)** (26 mg, 23 µmol), sodium tetrafluoroborate (20 mg, 0.18 mmol), CH_2Cl_2 (5 mL), methanol (5 mL).

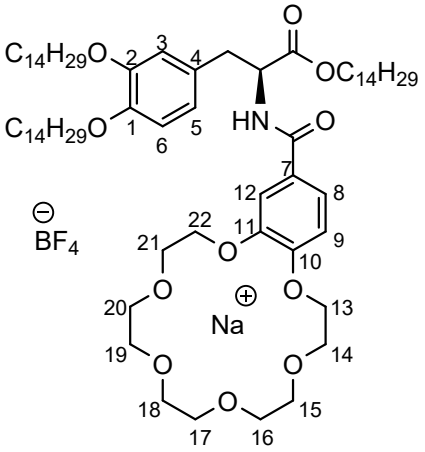

c-DOPA(14) • $NaBF_4$
$C_{68}H_{117}BF_4NNaO_{11}$
(1234.47)

Off-white solid (88 %, 25 mg, 20 µmol).

^{1}H-NMR (400 MHz, $CDCl_3$): δ = 0.84 – 0.91 (m, 9H, CH_3), 1.20 – 1.49 (m, 64H, CH_2), 1.54 – 1.86 (m, 6H, C*H*$_2$CH$_2$Oar, C*H*$_2$CH$_2$O(C=O)), 3.16 (d, *J* = 5.5 Hz, 2H, HNCHC*H*$_2$), 3.62 – 3.82 (m, 12H, 15-H, 16-H, 17-H, 18-H, 19-H, 20-H), 3.82 – 4.04 (m, 8H, CH_2OAr, 14-H, 21-H), 4.06 – 4.26 (m, 6H, 13-H, 22-H, CH_2O(C=O)), 4.94 – 5.03 (m, 1H, HNC*H*), 6.50 (d, *J* = 7.5 Hz, 1H, NH), 6.59 – 6.67 (m, 2H, 3-H, 6-H), 6.74 – 6.84 (m, 2H, 5-H, 9-H), 7.20 (dd, *J* = 2.0 Hz, 8.4 Hz, 1H, 8-H), 7.37 (d, *J* = 2.0 Hz, 1H, 12-H) ppm.

^{13}C-NMR (176 MHz, $CDCl_3$): δ = 14.28 (CH_3), 22.85 (CH_3*C*H_2), 26.00, 26.06, 26.15, 26.23, 26.24, 28.69, 29.43, 29.49, 29.52, 29.54, 29.65, 29.70, 29.79, 29.84, 29.85, 29.89, 29.91, 32.09 (CH_2), 37.64 (HNCH*C*H$_2$), 53.78 (HNCH), 65.91 (*C*H$_2$O(C=O)), 69.37, 69.43, (C-13 – C-22, CH_2OAr), 113.94 (C-3, C-9, C-12), 115.15 (C-6), 120.02 (C-5), 121.80 (C-8), 127.08 (C-7), 128.50 (C-4), 148.45 (C-1), 149.23 (C-2), 166.24 (N(C=O)), 172.02 (C=O) ppm.

The quaternary C signals of C-10 and C-11 could not be detected.

^{19}F-NMR (376 MHz, $CDCl_3$): δ = -155.43 ppm.

FT-IR (ATR): ν = 3332 (w), 2918 (vs), 2850 (vs), 1738 (m), 1639 (m), 1603 (w), 1586 (w), 1506 (s), 1468 (m), 1428 (w), 1357 (m), 1268 (s), 1219 (m), 1129 (s), 1054 (s), 957 (w), 761 (w), 722 (w) cm^{-1}.

MS (ESI, pos.): *m/z* ($C_{68}H_{117}NO_{11}$) calcd. 1146.8519 $[M + Na]^+$, found: 1146.85.

MS (ESI, neg.): *m/z* ($C_{68}H_{117}NO_{11}$) calcd. 87.0035 $[BF_4]^-$, found: 87.00.

HRMS (ESI, pos.): *m/z* ($C_{68}H_{117}NO_{11}$) calcd. 1146.8519 $[M + Na]^+$, found: 1146.8491.

HRMS (ESI, neg.): *m/z* ($C_{68}H_{117}NO_{11}$) calcd. 87.0034 $[BF_4]^-$, found: 87.0029.

DSC: Cr 2 [-2.3 kJ mol^{-1}] G 60 [6.8 kJ mol^{-1}] Cr 86 [-11.1 kJ mol^{-1}] SmA_d 107 [-0.7 kJ mol^{-1}] I (3rd heating), I 112 [0.5 kJ mol^{-1}] SmA_d 58 G 12 [2.2 kJ mol^{-1}] Cr (3rd cooling).

c-DOPA(14) • KBF_4

According to GP5: **c-DOPA(14)** (44 mg, 39 µmol), potassium tetrafluoroborate (69 mg, 0.55 mmol), CH_2Cl_2 (10 mL), methanol (10 mL).

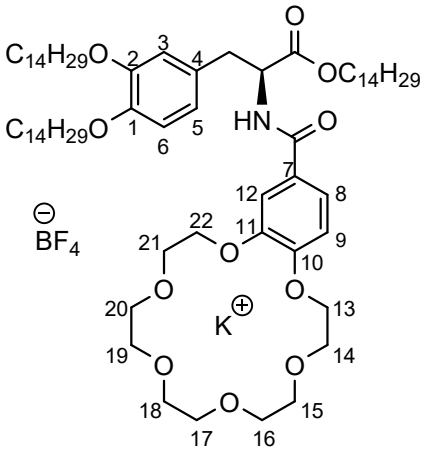

c-DOPA(14) • KBF_4
$C_{68}H_{117}BF_4KNO_{11}$
(1250.58)

Off-white solid (92 %, 45 mg, 36 µmol).

^{1}H-NMR (700 MHz, $CDCl_3$): δ = 0.85 – 0.89 (m, 9H, CH_3), 1.11 – 1.48 (m, 64H, CH_2), 1.59 – 1.66 (m, 2H, C*H*$_2$CH$_2$O(C=O)), 1.70 – 1.83 (m, 4H, C*H*$_2$CH$_2$OAr), 3.10 – 3.19 (m, 2H, HNCHC*H*$_2$), 3.63 – 3.78 (m, 12H, 15-H, 16-H, 17-H, 18-H, 19-H, 20-H), 3.81 – 3.88 (m, 2H, CH_2OAr), 3.88 – 3.96 (m, 6H, CH_2OAr, 14-H, 21-H), 4.07 – 4.15 (m, 2H, CH_2O(C=O)), 4.15 – 4.20 (m, 4H, 13-H, 22-H), 4.95 – 5.01 (m, 1H, HNC*H*), 6.48 – 6.53 (m, 1H, NH), 6.59 – 6.64 (m, 2H, 3-H, 6-H), 6.76 (d, *J* = 8.1 Hz, 1H, 5-H), 6.80 (d, *J* = 8.3 Hz, 1H, 9-H), 7.19 (dd, *J* = 2.1 Hz, 8.3 Hz, 1H, 8-H), 7.35 (d, *J* = 2.0 Hz, 1H, 12-H) ppm.

^{13}C-NMR (176 MHz, $CDCl_3$): δ = 14.24 (CH_3), 22.81 (CH_3CH_2), 26.02, 26.20, 28.64, 29.38, 29.44, 29.49, 29.60, 29.65, 29.74, 29.78, 29.80, 29.84, 29.86, 32.05 (CH_2), 37.59 (HNCH*C*H$_2$), 53.74 (HNCH), 65.86 (*C*H$_2$O(C=O)), 68.81, 68.88, 69.30, 69.36, 69.38, 69.44 (CH_2OAr, C-13, C-14, C-21, C-22), 70.62, 70.67, 70.73, 70.79, 70.86, 70.89 (C-15, C-16, C-17, C-18, C-19, C-20), 112.17 (C-9), 112.63 (C-3), 113.87 (C-12), 115.10 (C-6), 119.98 (C-5), 121.74 (C-8), 126.86 (C-7), 128.51 (C-4), 148.38 (C-1), 148.65 (C-11), 149.19 (C-2), 151.80 (C-10), 166.35 (N(C=O)), 172.00 (C=O) ppm.

^{19}F-NMR (376 MHz, $CDCl_3$): δ = -153.11 ppm.

FT-IR (ATR): ν = 3272 (w), 2918 (vs), 2849 (vs), 1751 (m), 1629 (s), 1582 (w), 1511 (s), 1466 (m), 1430 (m), 1392 (w), 1352 (m), 1266 (s), 1227 (s), 1208 (m), 1173 (s), 1134 (vs), 1097 (s), 1054 (s), 989 (m), 945 (m), 871 (m), 812 (m), 786 (w), 760 (w), 721 (m), 649 (w), 628 (w) cm^{-1}.

MS (ESI, pos.): *m/z* ($C_{68}H_{117}NO_{11}$) calcd. 1162.8259 $[M + K]^+$, found: 1162.82.

MS (ESI, neg.): *m/z* ($C_{68}H_{117}NO_{11}$) calcd. 87.0035 $[BF_4]^-$, found: 87.00.

HRMS (ESI, pos.): *m/z* ($C_{68}H_{117}NO_{11}$) calcd. 1162.8259 $[M + K]^+$, found: 1162.8240.

HRMS (ESI, neg.): *m/z* ($C_{68}H_{117}NO_{11}$) calcd. 87.0034 $[BF_4]^-$, found: 87.0031.

DSC: Cr 109 [-47.4 kJ mol^{-1}] I (1st heating), I 99 [69.1 kJ mol^{-1}] Cr (1st cooling).

c-DOPA(14) • KPF_6

According to GP5: **c-DOPA(14)** (57 mg, 51 µmol), potassium hexafluorophosphate (56 mg, 0.30 µmol), CH_2Cl_2 (10 mL), methanol (10 mL).

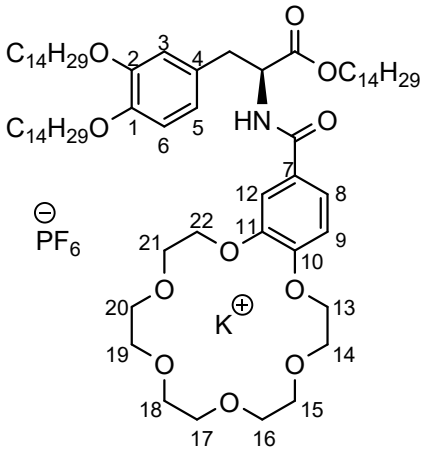

c-DOPA(14) • KPF_6
$C_{63}H_{117}F_6KNO_{11}P$
(1308.74)

Off-white solid (83 %, 55 mg, 42 µmol).

^{1}H-NMR (700 MHz, $CDCl_3$): δ = 0.84 – 0.89 (m, 9H, CH_3), 1.09 – 1.48 (m, 66H, CH_2), 1.57 – 1.66 (m, 2H, C*H*$_2$CH$_2$O(C=O)), 1.69 – 1.82 (m, 4H, C*H*$_2$CH$_2$OAr), 3.09 – 3.19 (m, 2H, HNCHC*H*$_2$), 3.54 – 3.76 (m, 12H, 15-H, 16-H, 17-H, 18-H, 19-H, 20-H), 3.81 – 3.90 (m, 6H, CH_2OAr, 14-H, 21-H), 3.93 (t, *J* = 6.6 Hz, 2H, CH_2OAr), 4.06 – 4.16 (m, 2H, CH_2O(C=O)), 4.16 – 4.25 (m, 4H, 13-H, 22-H), 4.93 – 4.98 (m, 1H, HNC*H*), 6.62 – 6.67 (m, 2H, 3-H, 6-H), 6.67 – 6.71 (m, 1H, NH), 6.75 – 6.82 (m, 2H, 5-H, 9-H), 7.19 (dd, *J* = 2.0 Hz, 8.6 Hz, 1H, 8-H), 7.30 – 7.33 (m, 1H, 12-H) ppm.

^{13}C-NMR (176 MHz, $CDCl_3$): δ = 14.25 (CH_3), 22.81 (CH_3CH_2), 26.03, 26.20, 26.22, 28.64, 29.40, 29.47, 29.49, 29.56, 29.61, 29.66, 29.76, 29.79, 29.81, 29.84, 29.86, 32.05 (CH_2), 37.53 (HNCHCH_2), 53.94 (HNCH), 65.90 (CH_2O(C=O)), 67.26, 67.51, 68.34, 68.49, 69.38 (CH_2OAr, C-13, C-14, C-21, C-22), 69.89, 69.94, 69.96 (C-15, C-16, C-17, C-18, C-19, C-20), 110.79 (C-9), 110.86 (C-3), 113.92 (C-12), 115.10 (C-6), 120.11 (C-5), 121.79 (C-8), 127.08 (C-7), 128.57 (C-4), 146.95 (C-1), 148.43 (C-11), 149.20 (C-2), 149.82 (C-10), 166.13 (N(C=O)), 172.18 (C=O) ppm.

^{19}F-NMR (376 MHz, $CDCl_3$): δ = -73.57, -71.67 ppm.

FT-IR (ATR): ν = 2920 (s), 2852 (m), 1737 (w), 1647 (w), 1605 (w), 1587 (w), 1505 (m), 1467 (m), 1355 (w), 1263 (s), 1207 (m), 1120 (s), 1052 (m), 959 (m), 838 (vs), 759 (w), 740 (w), 721 (w), 558 (s) cm^{-1}.

MS (ESI, pos.): *m/z* ($C_{68}H_{117}NO_{11}$) calcd. 1162.8259 $[M + K]^+$, found: 1162.82.

MS (ESI, neg.): *m/z* ($C_{68}H_{117}NO_{11}$) calcd. 144.9647 $[PF_6]^-$, found: 144.96.

HRMS (ESI, pos.): *m/z* ($C_{68}H_{117}NO_{11}$) calcd. 1162.8259 $[M + K]^+$, found: 1162.8244.

HRMS (ESI, neg.): *m/z* ($C_{68}H_{117}NO_{11}$) calcd. 144.9647 $[PF_6]^-$, found: 144.9648.

DSC: G 52 Col_h 134 [-0.8 kJ mol^{-1}] I (3rd heating), I 134 [0.8 kJ mol^{-1}] Col_h 57 G (3rd cooling).

c-DOPA(16) • KSCN

According to GP5: **c-DOPA(16)** (20 mg, 17 µmol), potassium thiocyanate (3 mg, 31 µmol), CH_2Cl_2 (5 mL), methanol (5 mL).

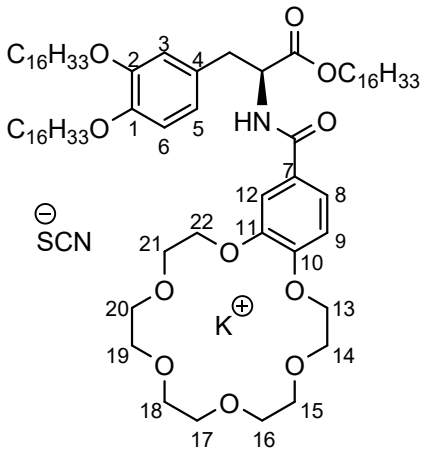

c-DOPA(16) • KSCN
$C_{75}H_{129}KN_2O_{11}S$
(1306.02)

Off-white solid (88 %, 19 mg, 15 µmol).

^{1}H-NMR (400 MHz, $CDCl_3$): δ = 0.87 (t, *J* = 6.8 Hz, 9H, CH_3), 1.15 – 1.53 (m, 78H, CH_2), 1.57 – 1.70 (m, 2H, C$H_2$$CH_2$O(C=O)), 1.70 – 1.84 (m, 4H, C$H_2$$CH_2$OAr), 3.17 (d, *J* = 5.8 Hz, 2H,

HNCHCH_2), 3.64 – 3.84 (m, 12H, 15-H, 16-H, 17-H, 18-H, 19-H, 20-H), 3.84 – 4.05 (m, 8H, CH_2OAr, 14-H, 21-H), 4.06 – 4.31 (m, 6H, 13-H, 22-H, CH_2O(C=O)), 4.92 – 5.00 (m, 1H, HNC*H*), 6.60 – 6.84 (m, 5H, NH, 3-H, 5-H, 6-H, 9-H), 7.22 (dd, *J* = 1.8 Hz, 8.4 Hz, 1H, 8-H), 7.39 (d, *J* = 1.8 Hz, 1H, 12-H) ppm.

^{13}C-NMR (176 MHz, $CDCl_3$): δ = 14.27 (CH_3), 22.84 (CH_3CH_2), 26.05, 26.23, 26.25, 28.68, 29.42, 29.49, 29.51, 29.64, 29.69, 29.78, 29.81, 29.84, 29.86, 29.91, 32.08 (CH_2), 37.57 (HNCHCH_2), 53.95 (HNCH), 65.91 (CH_2O(C=O)), 67.64, 67.78, 68.69, 68.85, 69.39, 69.43 (CH_2OAr, C-13, C-14, C-21, C-22), 70.11, 70.16, 70.18, 70.25, 70.33 (C-15, C-16, C-17, C-18, C-19, C-20), 110.97 (C-9), 111.35 (C-3), 113.94 (C-12), 115.17 (C-6), 120.18 (C-5), 121.81 (C-8), 127.27 (C-7), 128.67 (C-4), 132.20 (SCN), 147.22 (C-1), 148.40 (C-11), 149.22 (C-2), 150.06 (C-10), 166.14 (N(C=O)), 172.12 (C=O) ppm.

FT-IR (ATR): ν = 3272 (w), 2916 (vs), 2849 (vs), 2055 (m), 1737 (m), 1644 (m), 1605 (w), 1585 (w), 1541 (w), 1505 (s), 1467 (s), 1428 (m), 1344 (m), 1265 (vs), 1204 (s), 1120 (vs), 1065 (m), 957 (m), 915 (m), 833 (w), 788 (w), 762 (w), 727 (s), 645 (w) cm^{-1}.

MS (ESI, pos.): *m/z* ($C_{74}H_{129}NO_{11}$) calcd. 1246.9198 $[M + K]^+$, found: 1246.92.

MS (ESI, neg.): *m/z* ($C_{74}H_{129}NO_{11}$) calcd. 57.9757 $[SCN]^-$, found: 57.97.

HRMS (ESI, pos.): *m/z* ($C_{74}H_{129}NO_{11}$) calcd. 1246.9198 $[M+K]^+$, found: 1246.9182.

HRMS (ESI, neg.): *m/z* ($C_{74}H_{129}NO_{11}$) calcd. 57.9757 $[SCN]^-$, found: 57.9749.

DSC: Cr 57 [-24.0 kJ mol^{-1}] Col_h 106 [-0.6 kJ mol^{-1}] I (3^{rd} heating), I 106 [0.6 kJ mol^{-1}] Col_h 53 [17.3 kJ mol^{-1}] Cr (3^{rd} cooling).

c-DOPA(16) • NaI

According to GP5: **c-DOPA(16)** (52 mg, 43 µmol), sodium iodide (46 mg, 0.31 mmol), CH_2Cl_2 (10 mL), methanol (10 mL).

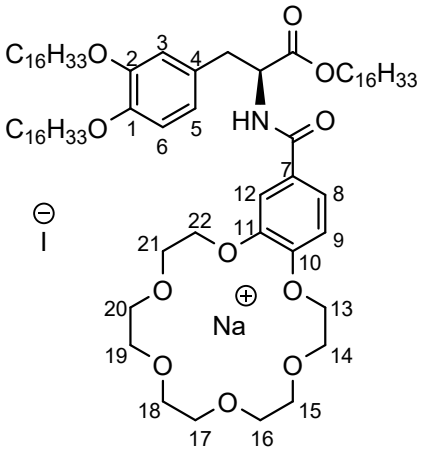

c-DOPA(16) • NaI
$C_{74}H_{129}INNaO_{11}$
(1358.74)

Off-white solid (91 %, 53 mg, 39 µmol).

^{1}H-NMR (400 MHz, $CDCl_3$): δ = 0.83 – 0.92 (t, *J* = 6.8 Hz, 9H, CH_3), 1.19 – 1.48 (m, 78H, CH_2), 1.52 – 1.84 (m, 6H, C*H*$_2$CH$_2$OAr, C*H*$_2$CH$_2$O(C=O)), 3.10 – 3.26 (m, 2H, HNCHC*H*$_2$), 3.65 – 4.00 (m, 16H, CH_2OAr, 15-H, 16-H, 17-H, 18-H, 19-H, 20-H), 4.00 – 4.29 (m, 10H, 13-H, 14-H, 21-H, 22-H, CH_2O(C=O)), 4.90 – 5.02 (m, 1H, HNC*H*), 6.63 – 6.70 (m, 3H, NH, 3-H, 6-H), 6.75 – 6.84 (m, 2H, 5-H, 9-H), 7.22 (dd, *J* = 2.0 Hz, 8.4 Hz, 1H, 8-H), 7.34 (d, *J* = 2.0 Hz, 1H, 12-H) ppm.

^{13}C-NMR (176 MHz, $CDCl_3$): δ = 14.27 (CH_3), 22.84 (CH_3*C*H_2), 26.06, 26.23, 26.26, 28.68, 29.44, 29.53, 29.65, 29.70, 29.79, 29.81, 29.84, 29.86, 29.91, 32.07 (CH_2), 37.55 (HNCH*C*H_2), 54.08 (HNCH), 65.91 (*C*H_2O(C=O)), 67.49, 68.84, 68.89, 69.45, 69.66, 69.73, 69.99, 70.04 (CH_2OAr, C-13 – C-22), 111.32 (C-9), 111.58 (C-3), 113.96 (C-12), 115.26 (C-6), 120.30 (C-5), 121.86 (C-8), 127.03 (C-7), 128.70 (C-4), 147.50 (C-1), 148.44 (C-11), 149.21 (C-2), 150.47 (C-10), 166.37 (N(C=O)), 172.20 (C=O) ppm.

FT-IR (ATR): ν = 3439 (w), 2918 (vs), 2850 (vs), 1733 (m), 1630 (m), 1602 (m), 1586 (m), 1532 (m), 1494 (s), 1467 (s), 1456 (m), 1437 (m), 1345 (m), 1270 (vs), 1212 (vs), 1118 (vs), 1095 (vs), 1051 (s), 952 (s), 920 (m), 828 (m), 766 (m), 723 (s), 641 (w), 589 (w), 527 (w) cm^{-1}.

MS (ESI, pos.): *m/z* ($C_{74}H_{129}NO_{11}$) calcd. 1230.9458 $[M + Na]^+$, found: 1230.94.

MS (ESI, neg.): *m/z* ($C_{74}H_{129}NO_{11}$) calcd. 126.9050 $[I]^-$, found: 126.90.

HRMS (ESI, pos.): *m/z* ($C_{74}H_{129}NO_{11}$) calcd. 1230.9458 $[M+Na]^+$, found: 1230.9446.

HRMS (ESI, neg.): *m/z* ($C_{74}H_{129}NO_{11}$) calcd. 126.9050 $[I]^-$, found: 126.9049.

DSC: Cr 6 [-13.0 kJ mol^{-1}] G 60 Col$_h$ 139 [-0.4 kJ mol^{-1}] I (3rd heating), I 137 [0.2 kJ mol^{-1}] Col$_h$ 75 G 22 [13.8 kJ mol^{-1}] Cr (3rd cooling).

c-DOPA(16) • KI

According to GP5: **c-DOPA(16)** (20 mg, 17 µmol), potassium iodide (14 mg, 84 µmol), CH_2Cl_2 (5 mL), methanol (5 mL).

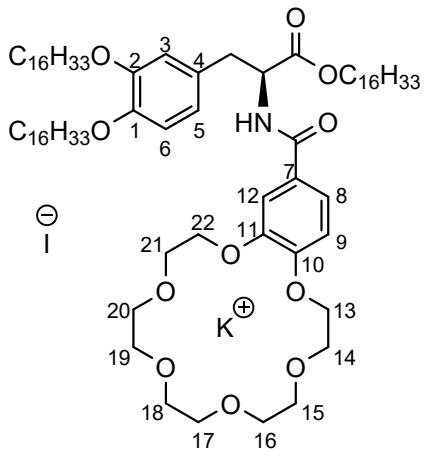

c-DOPA(16) • KI
$C_{74}H_{129}IKNO_{11}$
(1374.84)

Off-white solid (88 %, 20 mg, 15 µmol).

^{1}H-NMR (400 MHz, $CDCl_3$): δ = 0.83 – 0.91 (t, *J* = 6.8 Hz, 9H, CH_3), 1.05 – 1.50 (m, 78H, CH_2), 1.55 – 1.68 (m, 2H, C*H*$_2$CH$_2$O(C=O)), 1.68 – 1.88 (m, 4H, C*H*$_2$CH$_2$OAr), 3.10 – 3.23 (m, 2H, HNCHC*H*$_2$), 3.63 – 3.77 (m, 8H, 16-H, 17-H, 18-H, 19-H), 3.77 – 3.96 (m, 8H, CH_2OAr, 15-H, 20-H), 3.97 – 4.31 (m, 10H, 13-H, 14-H, 21-H, 22-H, CH_2O(C=O)), 4.91 – 5.02 (m, 1H, HNC*H*), 6.57 – 6.70 (m, 3H, NH, 3-H, 6-H), 6.74 – 6.85 (m, 2H, 5-H, 9-H), 7.21 (dd, *J* = 2.0 Hz, 8.4 Hz, 1H, 8-H), 7.38 (d, *J* = 2.0 Hz, 1H, 12-H) ppm.

^{13}C-NMR (176 MHz, $CDCl_3$): δ = 14.25 (CH_3), 22.82 (CH_3*C*H$_2$), 26.04, 26.21, 26.23, 28.65, 29.40, 29.47, 29.49, 29.51, 29.61, 29.67, 29.76, 29.79, 29.82, 29.84, 29.89, 32.06 (CH_2), 37.55 (HNCH*C*H$_2$), 53.91 (HNCH), 65.89 (*C*H$_2$O(C=O)), 67.71, 67.86, 68.73, 68.85, 69.39, 69.41 (CH_2OAr, C-13, C-14, C-21, C-22), 70.09, 70.10, 70.16, 70.22, 70.30 (C-15, C-16, C-17, C-18, C-19, C-20), 111.01 (C-9), 111.30 (C-3), 113.92 (C-12), 115.16 (C-6), 120.14 (C-5), 121.81 (C-8), 127.21 (C-7), 128.57 (C-4), 147.24 (C-1), 148.42 (C-11), 149.20 (C-2), 150.09 (C-10), 166.06 (N(C=O)), 172.05 (C=O) ppm.

FT-IR (ATR): ν = 2923 (m), 2853 (m), 1734 (w), 1646 (w), 1604 (w), 1587 (w), 1504 (m), 1467 (w), 1354 (w), 1265 (m), 1208 (m), 1119 (m), 1051 (w), 957 (w), 906 (vs), 834 (w), 726 (vs), 644 (m) cm^{-1}.

MS (ESI, pos.): *m/z* ($C_{74}H_{129}NO_{11}$) calcd. 1246.9198 $[M + K]^+$, found: 1246.92.

MS (ESI, neg.): *m/z* ($C_{74}H_{129}NO_{11}$) calcd. 126.9050 $[I]^-$, found: 126.90.

HRMS (ESI, pos.): *m/z* ($C_{74}H_{129}NO_{11}$) calcd. 1246.9198 $[M+K]^+$, found: 1246.9195.

HRMS (ESI, neg.): *m/z* ($C_{74}H_{129}NO_{11}$) calcd. 126.9050 $[I]^-$, found: 126.9049.

DSC: Cr 10 [-16.7 kJ mol^{-1}] G 47 Col_h 114 [-0.4 kJ mol^{-1}] I (3rd heating), I 116 [0.4 kJ mol^{-1}] Col_h 54 G 30 [17.5 kJ mol^{-1}] Cr (3rd cooling).

c-DOPA(16) • $NaBF_4$

According to GP5: **c-DOPA(16)** (20 mg, 17 µmol), sodium tetrafluoroborate (4 mg, 36 µmol), CH_2Cl_2 (5 mL), methanol (5 mL).

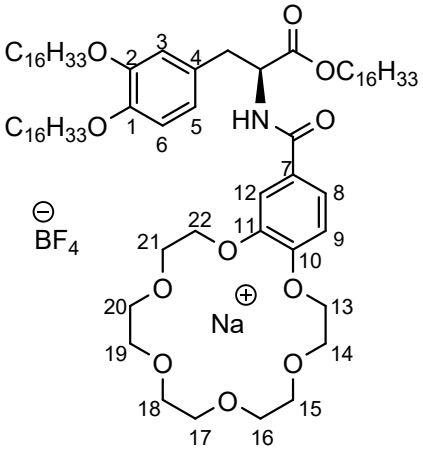

c-DOPA(16) • $NaBF_4$
$C_{74}H_{129}BF_4NNaO_{11}$
(1318.64)

Off-white solid (92 %, 20 mg, 15 µmol).

^{1}H-NMR (400 MHz, $CDCl_3$): δ = 0.84 – 0.93 (m, 9H, CH_3), 1.15 – 1.53 (m, 78H, CH_2), 1.57 – 1.70 (m, 2H, C*H*$_2$CH$_2$O(C=O)), 1.70 – 1.86 (m, 4H, C*H*$_2$CH$_2$OAr), 3.16 (d, *J* = 5.6 Hz, 2H, HNCHC*H*$_2$), 3.63 – 3.83 (m, 12H, 15-H, 16-H, 17-H, 18-H, 19-H, 20-H), 3.83 – 4.06 (m, 8H, CH_2OAr, 14-H, 21-H), 4.06 – 4.26 (m, 6H, 13-H, 22-H, CH_2O(C=O)), 4.93 – 5.03 (m, 1H, HNC*H*), 6.50 (d, *J* = 7.5 Hz, 1H, NH), 6.60 – 6.66 (m, 2H, 3-H, 6-H), 6.75 – 6.84 (m, 2H, 5-H, 9-H), 7.20 (dd, *J* = 2.0 Hz, 8.4 Hz, 1H, 8-H), 7.36 – 7.38 (m, 1H, 12-H) ppm.

^{13}C-NMR (176 MHz, $CDCl_3$): δ = 14.28 (CH_3), 22.85 (CH_3CH_2), 26.07, 26.16, 26.24, 26.25, 28.59, 28.70, 29.44, 29.50, 29.54, 29.57, 29.66, 29.71, 29.80, 29.85, 29.86, 29.90, 29.92, 32.09 (CH_2), 37.65 (HNCH*C*H$_2$), 53.79 (HNCH), 65.93 (*C*H$_2$O(C=O)), 69.38, 69.43, (C-13 – C-22, CH_2OAr), 113.94 (C-3, C-9, C-12), 115.15 (C-6), 120.00 (C-5), 121.81 (C-8), 124.97 (C-7), 128.48 (C-4), 148.46 (C-1), 149.23 (C-2), 172.01 (C=O) ppm.

The quaternary C signals of C-10 and C-11 as well as the amide carbon could not be detected.

^{19}F-NMR (376 MHz, $CDCl_3$): δ = -155.44 ppm.

FT-IR (ATR): ν = 3369 (w), 2917 (vs), 2850 (vs), 1739 (w), 1643 (w), 1604 (w), 1587 (w), 1507 (m), 1468 (w), 1356 (w), 1268 (m), 1219 (w), 1129 (m), 955 (w), 763 (w), 722 (w) cm^{-1}.

MS (ESI, pos.): *m/z* ($C_{74}H_{129}NO_{11}$) calcd. 1230.9458 $[M + Na]^+$, found: 1230.94.

MS (ESI, neg.): *m/z* ($C_{74}H_{129}NO_{11}$) calcd. 87.0035 $[BF_4]^-$, found: 87.00.

HRMS (ESI, pos.): *m/z* ($C_{74}H_{129}NO_{11}$) calcd. 1230.9458 $[M + Na]^+$, found: 1230.9446.

HRMS (ESI, neg.): *m/z* ($C_{74}H_{129}NO_{11}$) calcd. 87.0034 $[BF_4]^-$, found: 87.0029.

DSC: Cr 25 [-12.6 kJ mol^{-1}] G 64 [4.6 kJ mol^{-1}] Cr 82 [-8.0 kJ mol^{-1}] I (3rd heating), I 122 [0.4 kJ mol^{-1}] Col_h 50 G 34 [28.1 kJ mol^{-1}] Cr (3rd cooling).

c-DOPA(16) • KPF_6

According to GP5: **c-DOPA(16)** (55 mg, 46 µmol), potassium hexafluorophosphate (54 mg, 0.29 mmol), CH_2Cl_2 (10 mL), methanol (10 mL).

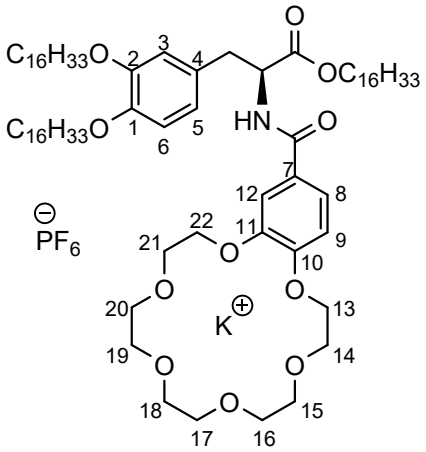

c-DOPA(16) • KPF_6
$C_{74}H_{129}F_6KNO_{11}P$
(1392.90)

Colourless solid (90 %, 57 mg, 41 µmol).

^{1}H-NMR (400 MHz, $CDCl_3$): δ = 0.79 – 0.95 (m, 9H, CH_3), 1.17 – 1.53 (m, 78H, CH_2), 1.55 – 1.84 (m, 6H, C*H*$_2$CH$_2$OAr, C*H*$_2$CH$_2$O(C=O)), 3.16 (d, *J* = 5.7 Hz, 2H, HNCHC*H*$_2$), 3.59 – 3.79 (m, 12H, 15-H, 16-H, 17-H, 18-H, 19-H, 20-H), 3.81 – 4.01 (m, 8H, CH_2OAr, 14-H, 21-H), 4.04 – 4.29 (m, 6H, 13-H, 22-H, CH_2O(C=O)), 4.93 – 5.02 (m, 1H, HNC*H*), 6.56 (d, *J* = 7.6 Hz, 1H, NH), 6.60 – 6.67 (m, 2H, 3-H, 6-H), 6.75 – 6.84 (m, 2H, 5-H, 9-H), 7.19 (dd, *J* = 2.0 Hz, 8.4 Hz, 1H, 8-H), 7.36 (d, *J* = 2.0 Hz, 1H, 12-H) ppm.

^{13}C-NMR (176 MHz, $CDCl_3$): δ = 14.28 (CH_3), 22.85 (CH_3*C*H$_2$), 26.06, 26.23, 26.25, 28.68, 29.43, 29.49, 29.53, 29.63, 29.65, 29.70, 29.79, 29.83, 29.85, 29.89, 29.91, 32.08 (CH_2), 37.58 (HNCH*C*H$_2$), 53.87 (HNCH), 65.95 (*C*H$_2$O(C=O)), 67.35, 67.56, 68.40, 68.55, 69.41 (CH_2OAr, C-13, C-14, C-21, C-22), 69.97, 69.99, 70.04 (C-15, C-16, C-17, C-18, C-19, C-20), 110.80 (C-9), 111.06, (C-3), 113.93 (C-12), 115.14 (C-6), 120.00 (C-5), 121.83 (C-8), 127.22 (C-7), 128.44 (C-4), 147.11 (C-1), 148.47 (C-11), 149.22 (C-2), 149.92 (C-10), 166.12 (N(C=O)), 172.01 (C=O) ppm.

^{19}F-NMR (376 MHz, $CDCl_3$): δ = -73.69, -71.80 ppm.

FT-IR (ATR): ν = 3269 (w), 2954 (m), 2916 (vs), 2849 (vs), 1737 (m), 1631 (m), 1604 (w), 1585 (w), 1508 (s), 1467 (m), 1429 (w), 1392 (w), 1355 (m), 1265 (vs), 1213 (s), 1127 (vs), 1065 (m), 956 (m), 841 (vs), 759 (m), 722 (s), 558 (m), 494 (m) cm^{-1}.

MS (ESI, pos.): *m/z* ($C_{74}H_{129}NO_{11}$) calcd. 1246.9198 $[M + K]^+$, found: 1246.92.

MS (ESI, neg.): *m/z* ($C_{74}H_{129}NO_{11}$) calcd. 144.9647 $[PF_6]^-$, found: 144.96.

HRMS (ESI, pos.): *m/z* ($C_{74}H_{129}NO_{11}$) calcd. 1246.9198 $[M+K]^+$, found: 1246.9200.

HRMS (ESI, neg.): *m/z* ($C_{74}H_{129}NO_{11}$) calcd. 144.9647 $[PF_6]^-$, found: 144.9647.

DSC: Cr 10 [-17.5 kJ mol^{-1}] G 51 Col_h 133 [-0.4 kJ mol^{-1}] I (3^{rd} heating), I 133 [0.4 kJ mol^{-1}] Col_h 69 G 28 [18.0 kJ mol^{-1}] Cr (3^{rd} cooling).

c-THIQ(14) • KPF_6

According to GP5: **c-THIQ(14)** (40 mg, 35 µmol), potassium hexafluorophosphate (41 mg, 0.22 mmol), CH_2Cl_2 (10 mL), methanol (5 mL).

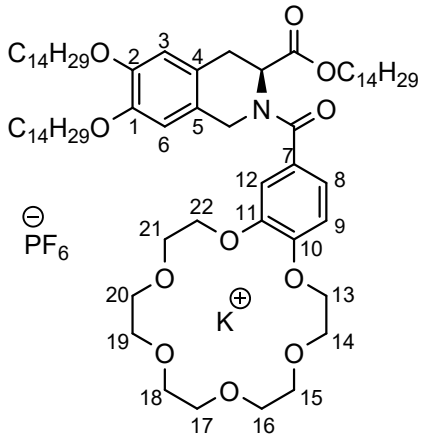

c-THIQ(14) • KPF_6
$C_{69}H_{117}F_6KNO_{11}P$
(1320.75)

Colourless solid (99 %, 46 mg, 35 µmol).

^{1}H-NMR (400 MHz, $CDCl_3$): δ = 0.88 (t, *J* = 6.8 Hz, 9H, CH_3), 0.99 – 1.52 (m, 66H, CH_2), 1.53 – 1.95 (m, 6H, C*H*$_2$$CH_2$OAr, C*H*$_2$$CH_2$O(C=O)), 2.82 – 3.30 (m, 2H, NCHC*H*$_2$), 3.59 – 3.80 (m, 12H, 15-H, 16-H, 17-H, 18-H, 19-H, 20-H), 3.80 – 4.37 (m, 14H, CH_2OAr, CH_2O(C=O), 13-H, 14-H, 21-H, 22-H), 4.37 – 5.54 (m, 3H, NCH, NCH_2), 6.46 – 6.71 (m, 2H, 3-H, 6-H), 6.75 – 6.84 (m, 3H, 8-H, 9-H,12-H) ppm.

^{13}C-NMR (176 MHz, $CDCl_3$): δ = 14.27 (CH_3), 22.85 (CH_3*C*H_2), 28.61, 28.70, 29.37, 29.45, 29.52, 29.61, 29.68, 29.81, 29.87 (CH_2), 32.08 (NCH*C*H_2), 48.05 (NCH_2), 52.40 (NCH), 65.59 (*C*H_2O(C=O)), 67.22, 67.30, 68.66, 69.28, 69.48, 69.66, (CH_2OAr, C-13, C-14, C-21, C-22), 69.98, 70.03, 70.08 (C-15, C-16, C-17, C-18, C-19, C-20), 110.69 (C-12), 111.15 (C-3), 111.75 (C8), 113.83 (C-6), 120.34 (d, *J* = 151.9 Hz, C-9), 123.82 (C-4), 124.72 (C-5), 129.12 (C-7),

146.93 (C-1), 148.14 (C-11), 148.60 (C-2), 150.79 (C-10), 166.14 (N(C=O)), 171.15 (C=O) ppm.

^{19}F-NMR (376 MHz, $CDCl_3$): δ = -73.84, -71.95 ppm.

FT-IR (ATR): ν = 2920 (s), 2852 (s), 1733 (w), 1634 (w), 1516 (m), 1466 (m), 1431 (m), 1332 (w), 1260 (m), 1209 (m), 1117 (s), 1051 (w), 958 (m), 839 (vs), 757 (w), 722 (w), 558 (m) cm^{-1}.

MS (ESI, pos.): *m/z* ($C_{69}H_{117}NO_{11}$) calcd. 1174.8258 $[M + K]^+$, found: 1174.82.

MS (ESI, neg.): *m/z* ($C_{69}H_{117}NO_{11}$) calcd. 144.9647 $[PF_6]^-$, found: 144.96.

HRMS (ESI, pos.): *m/z* ($C_{69}H_{117}NO_{11}$) calcd. 1174.8258 $[M + K]^+$, found: 1174.8244.

HRMS (ESI, neg.): *m/z* ($C_{69}H_{117}NO_{11}$) calcd. 144.9647 $[PF_6]^-$, found: 144.9645.

DSC: G 47 SmA_d 113 [-0.4 kJ mol^{-1}] I (3rd heating), I 112 [0.4 kJ mol^{-1}] SmA_d 65 G (3rd cooling).

c-THIQ(16) • KPF_6

According to GP5: **c-THIQ(16)** (22 mg, 18 µmol), potassium hexafluorophosphate (43 mg, 0.23 mmol), CH_2Cl_2 (10 mL), methanol (5 mL).

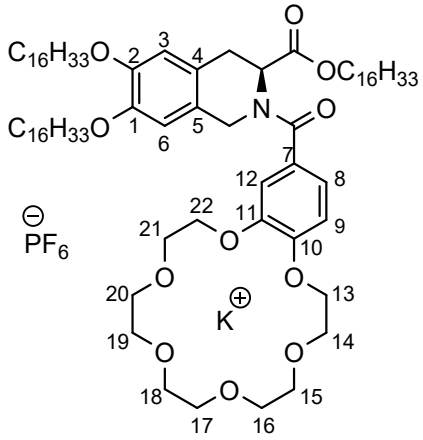

c-THIQ(16) • KPF_6
$C_{75}H_{129}F_6KNO_{11}P$
(1404.92)

Colourless solid (83 %, 21 mg, 15 µmol).

^{1}H-NMR (400 MHz, $CDCl_3$): δ = 0.87 (t, *J* = 6.8 Hz, 9H, CH_3), 1.05 – 1.92 (m, 78H, CH_2), 2.83 – 3.29 (m, 2H, NCHCH_2), 3.55 – 3.81 (m, 12H, 15-H, 16-H, 17-H, 18-H, 19-H, 20-H), 3.80 – 4.31 (m, 14H, CH_2OAr, CH_2O(C=O), 13-H, 14-H, 21-H, 22-H), 4.40 – 5.56 (m, 3H, NCH, NCH_2), 6.39 – 6.70 (m, 2H, 3-H, 6-H), 6.75 – 7.11 (m, 3H, 8-H, 9-H,12-H) ppm.

^{13}C-NMR (176 MHz, $CDCl_3$): δ = 14.26 (CH_3), 22.74, 22.82 (CH_3CH_2), 25.86, 25.96, 26.18, 26.26, 29.37, 29.44, 29.52, 29.61, 29.63, 29.68, 29.70, 29.74, 29.79, 29.83, 29.88 (CH_2), 32.07 (NCHCH_2), 48.08 (NCH_2), 52.22 (NCH), 63.22 (CH_2O(C=O)), 65.57, 65.83, 68.74, 69.43,

69.47, 69.53, (CH_2OAr, C-13, C-14, C-21, C-22), 70.60, 70.65, 70.68, 70.72, 70.83 (C-15, C-16, C-17, C-18, C-19, C-20), 111.11 (C-12), 111.72 (C-3), 112.63 (C8), 113.82 (C-6), 120.32 (d, *J* = 159.8 Hz, C-9), 123.90 (C-4), 124.40 (d, *J* = 48.8 Hz C-5), 128.41 (C-7), 148.05 (C-1), 148.27 (C-11), 148.56 (C-2), 149.99 (C-10), 171.11 (C=O) ppm.

The amide carbon signal could not be detected.

^{19}F-NMR (376 MHz, $CDCl_3$): δ = -73.84, -71.95 ppm.

FT-IR (ATR): ν = 2918 (vs), 2851 (s), 1735 (w), 1637 (w), 1516 (w), 1467 (m), 1262 (m), 1119 (m), 843 (s), 558 (w) cm^{-1}.

MS (ESI, pos.): *m/z* ($C_{75}H_{129}NO_{11}$) calcd. 1258.9198 $[M + K]^+$, found: 1258.92.

MS (ESI, neg.): *m/z* ($C_{75}H_{129}NO_{11}$) calcd. 144.9647 $[PF_6]^-$, found: 144.96.

HRMS (ESI, pos.): *m/z* ($C_{75}H_{129}NO_{11}$) calcd. 1258.9198 $[M + K]^+$, found: 1258.9206.

HRMS (ESI, neg.): *m/z* ($C_{75}H_{129}NO_{11}$) calcd. 144.9647 $[PF_6]^-$, found: 144.9644.

DSC: Cr 52 [-3.4 kJ mol^{-1}] Col_h 132 [-0.4 kJ mol^{-1}] I (3^{rd} heating), I 132 [0.4 kJ mol^{-1}] Col_h 54 G 31 [18.1 kJ mol^{-1}] Cr (3^{rd} cooling).

3 NMR spectra

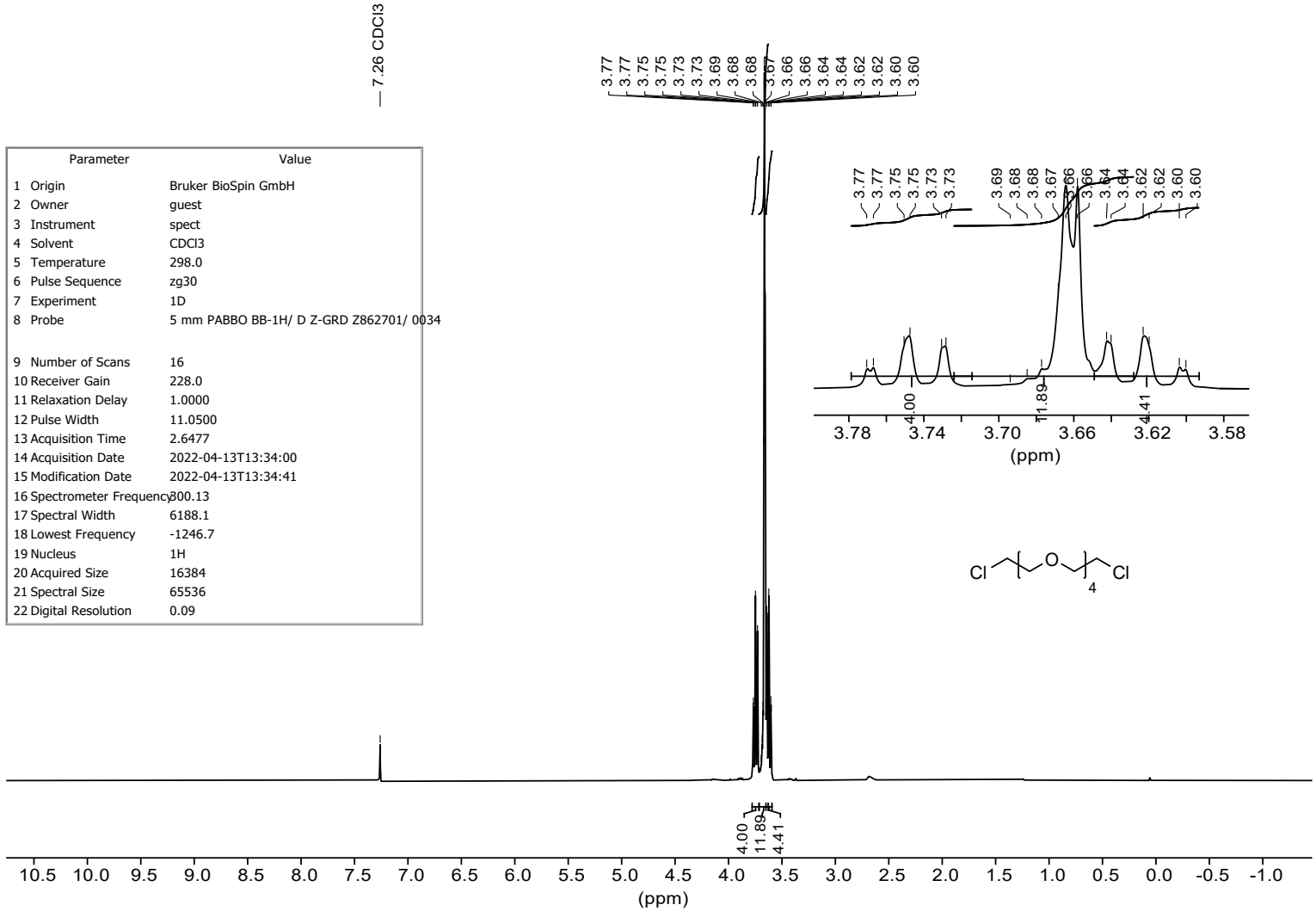

Figure S1: ^{1}H NMR spectrum of dichloride **4** at 300 MHz.

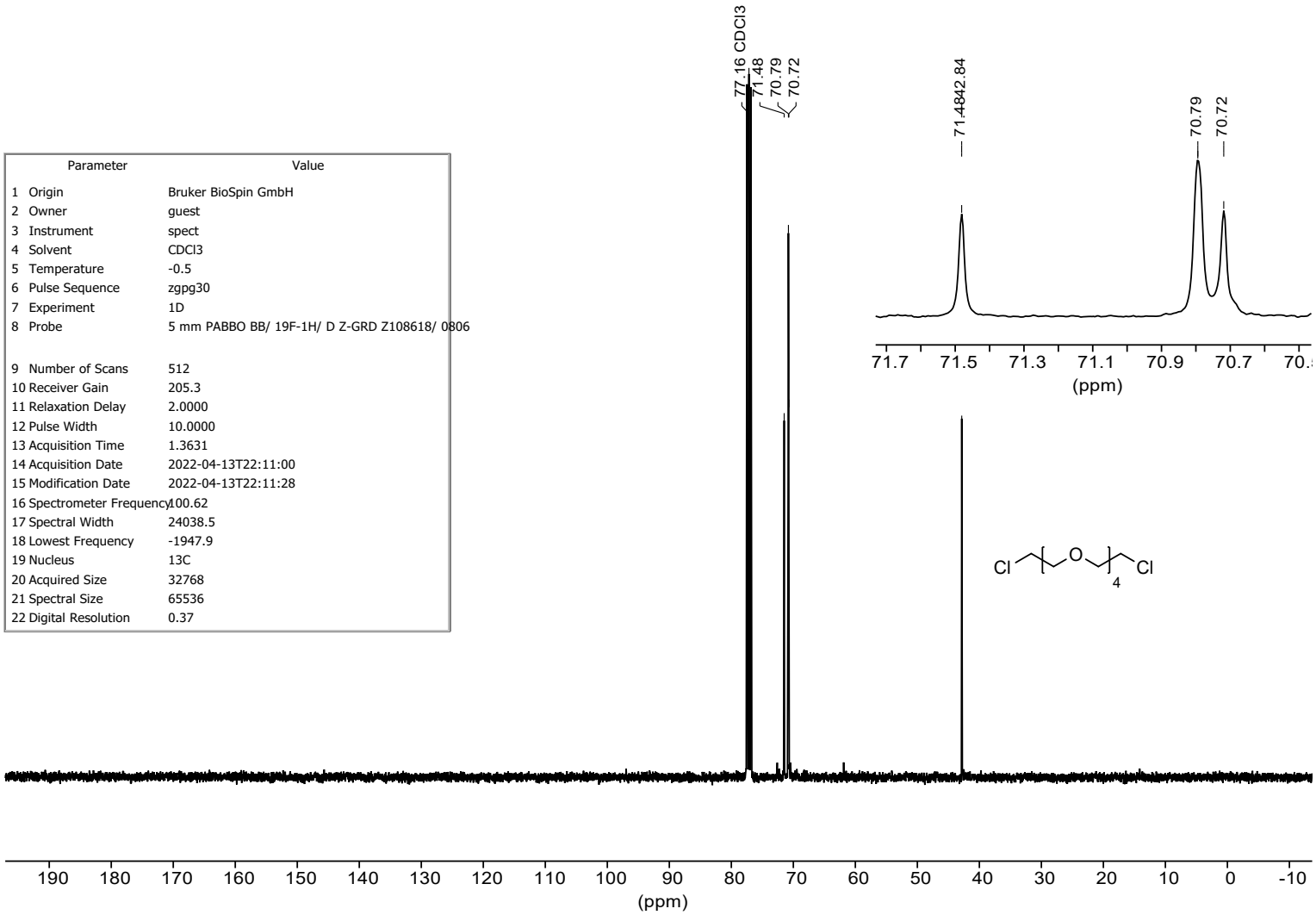

Parameter	Value
1 Origin	Bruker BioSpin GmbH
2 Owner	guest
3 Instrument	spect
4 Solvent	CDCl3
5 Temperature	-0.5
6 Pulse Sequence	zgpg30
7 Experiment	1D
8 Probe	5 mm PABBO BB/ 19F-1H/ D Z-GRD Z108618/ 0806
9 Number of Scans	512
10 Receiver Gain	205.3
11 Relaxation Delay	2.0000
12 Pulse Width	10.0000
13 Acquisition Time	1.3631
14 Acquisition Date	2022-04-13T22:11:00
15 Modification Date	2022-04-13T22:11:28
16 Spectrometer Frequency	100.62
17 Spectral Width	24038.5
18 Lowest Frequency	-1947.9
19 Nucleus	13C
20 Acquired Size	32768
21 Spectral Size	65536
22 Digital Resolution	0.37

Figure S2: ^{13}C NMR spectrum of dichloride **4** at 101 MHz.

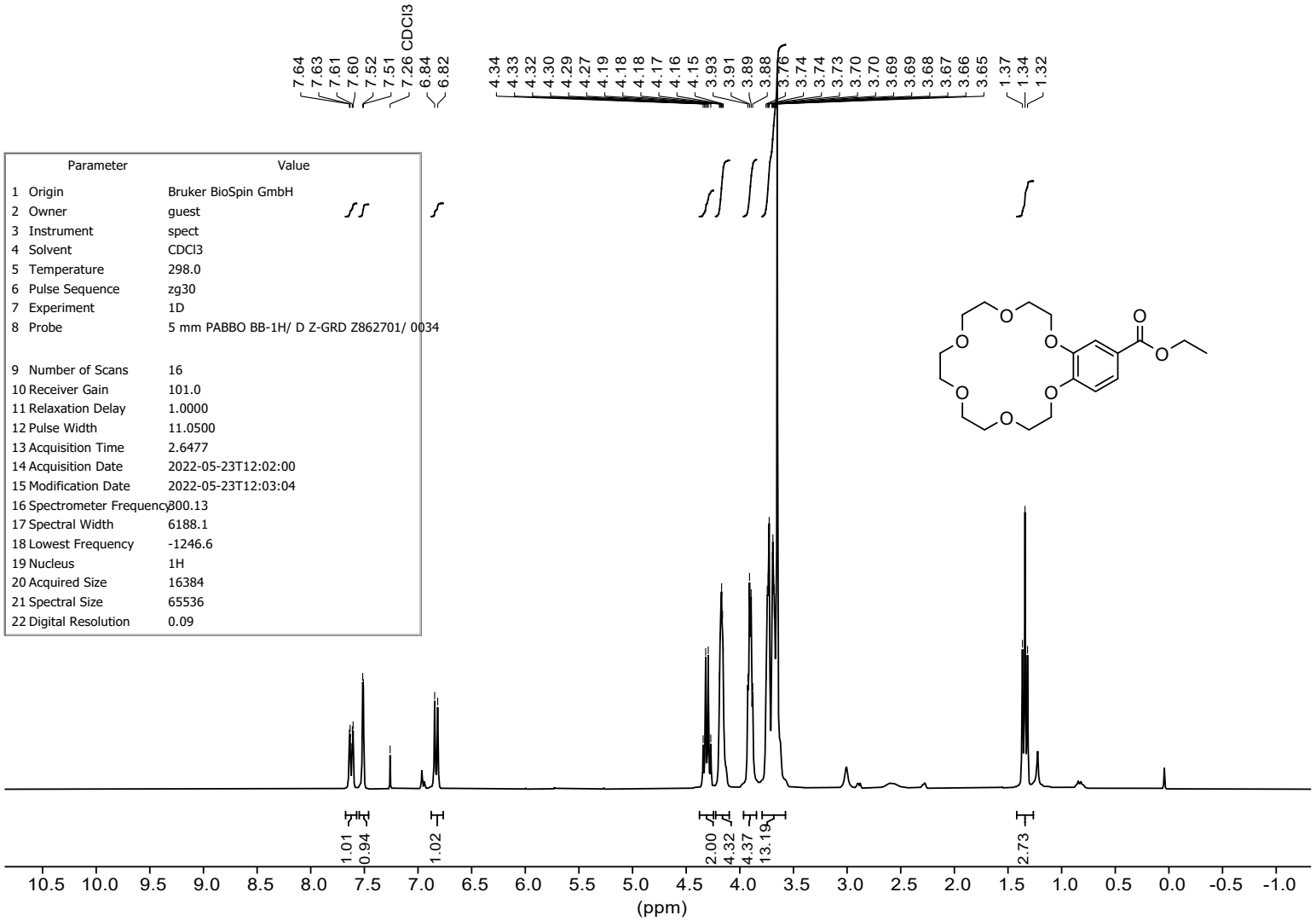

Figure S3: ^{1}H NMR spectrum of crown ether **5** at 300 MHz.

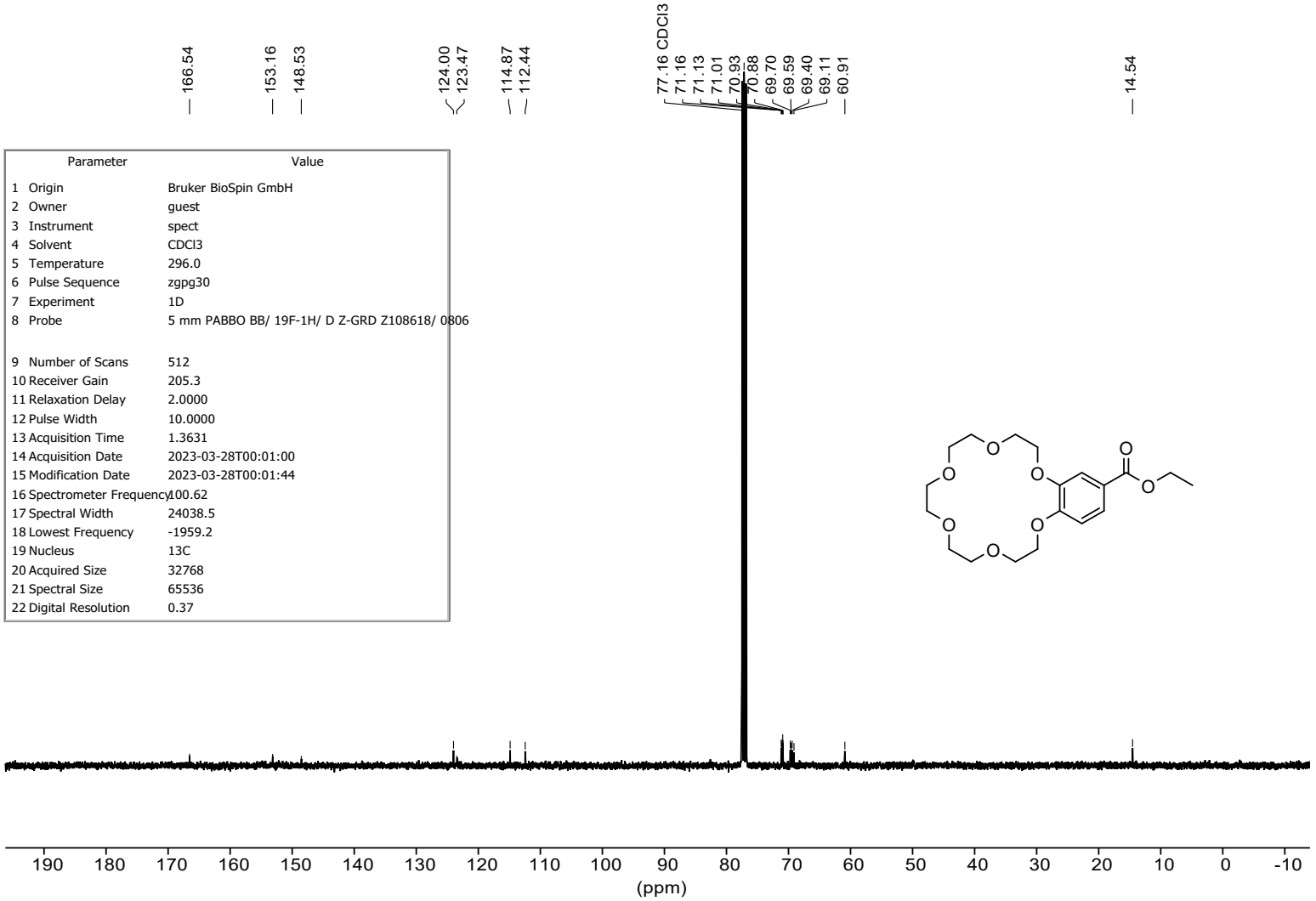

Parameter	Value
1 Origin	Bruker BioSpin GmbH
2 Owner	guest
3 Instrument	spect
4 Solvent	CDCl3
5 Temperature	296.0
6 Pulse Sequence	zgpg30
7 Experiment	1D
8 Probe	5 mm PABBO BB/ 19F-1H/ D Z-GRD Z108618/ 0806
9 Number of Scans	512
10 Receiver Gain	205.3
11 Relaxation Delay	2.0000
12 Pulse Width	10.0000
13 Acquisition Time	1.3631
14 Acquisition Date	2023-03-28T00:01:00
15 Modification Date	2023-03-28T00:01:44
16 Spectrometer Frequency	100.62
17 Spectral Width	24038.5
18 Lowest Frequency	-1959.2
19 Nucleus	13C
20 Acquired Size	32768
21 Spectral Size	65536
22 Digital Resolution	0.37

Figure S4: ^{13}C NMR spectrum of crown ether **5** at 101 MHz.

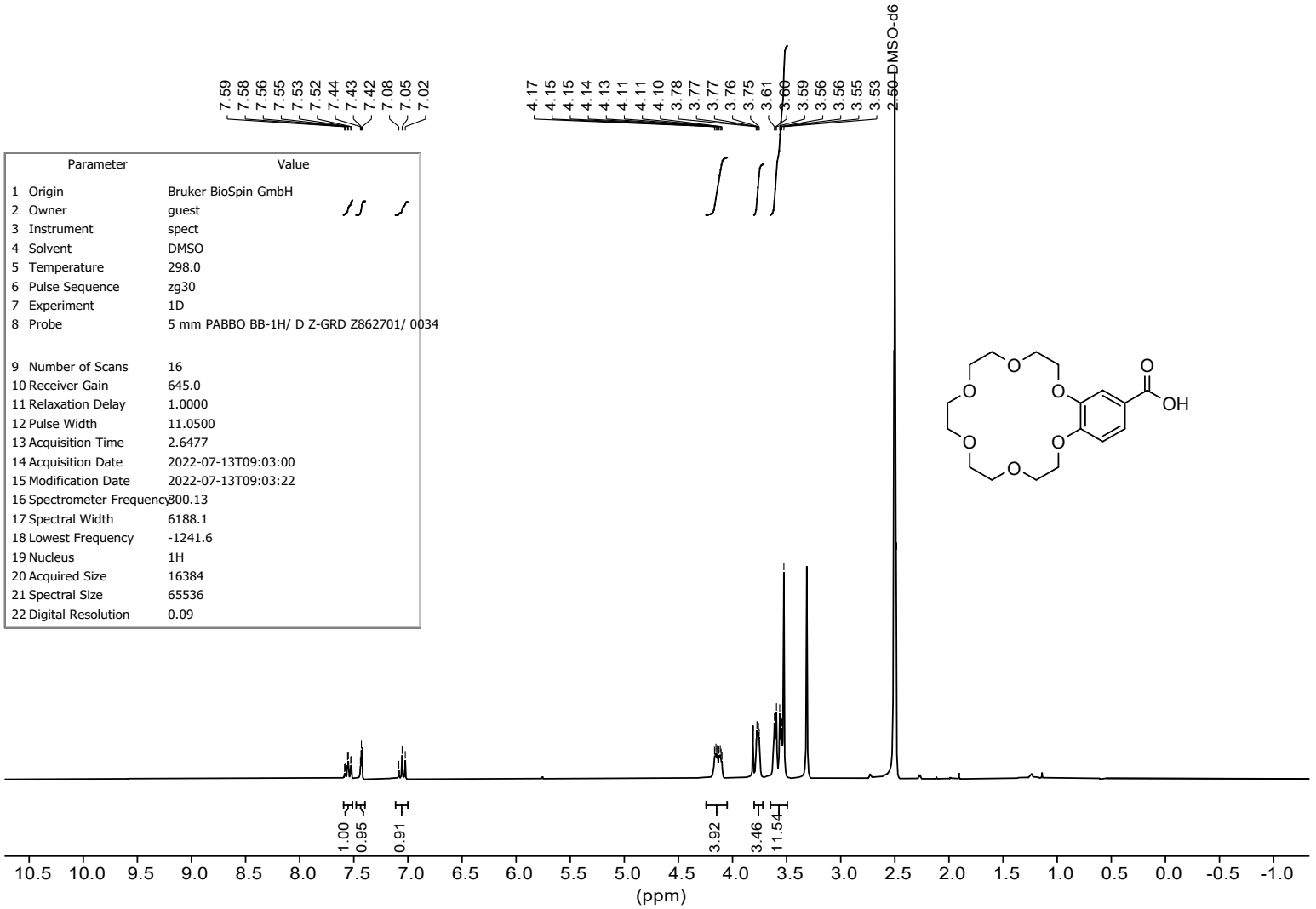

Figure S5: ^{1}H NMR spectrum of crown ether acid **[18]c-6-OH** at 300 MHz.

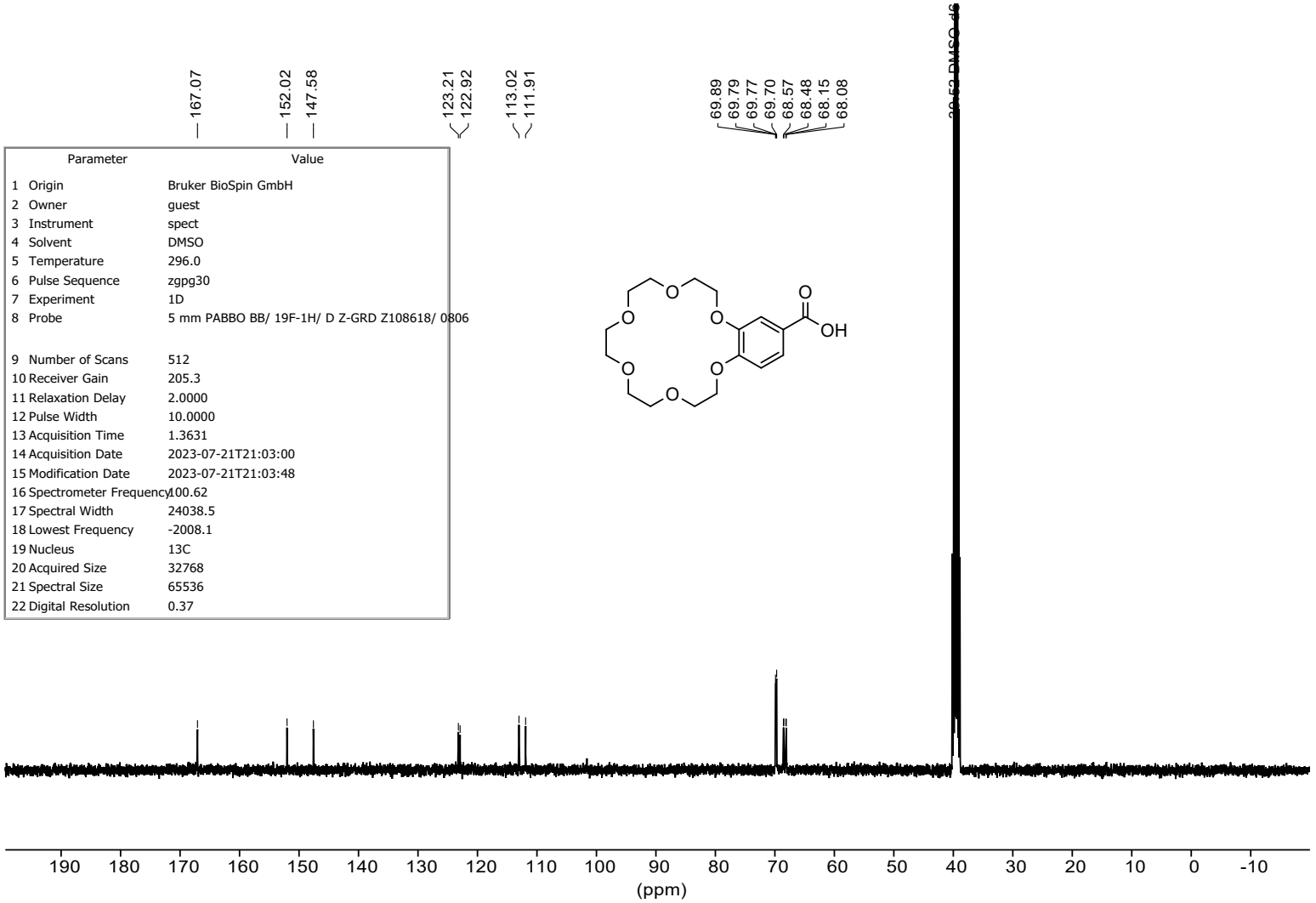

Parameter	Value
1 Origin	Bruker BioSpin GmbH
2 Owner	guest
3 Instrument	spect
4 Solvent	DMSO
5 Temperature	296.0
6 Pulse Sequence	zgpg30
7 Experiment	1D
8 Probe	5 mm PABBO BB/ 19F-1H/ D Z-GRD Z108618/ 0806
9 Number of Scans	512
10 Receiver Gain	205.3
11 Relaxation Delay	2.0000
12 Pulse Width	10.0000
13 Acquisition Time	1.3631
14 Acquisition Date	2023-07-21T21:03:00
15 Modification Date	2023-07-21T21:03:48
16 Spectrometer Frequency	100.62
17 Spectral Width	24038.5
18 Lowest Frequency	-2008.1
19 Nucleus	13C
20 Acquired Size	32768
21 Spectral Size	65536
22 Digital Resolution	0.37

Figure S6: ^{13}C NMR spectrum of crown ether acid **[18]c-6-OH** at 101 MHz.

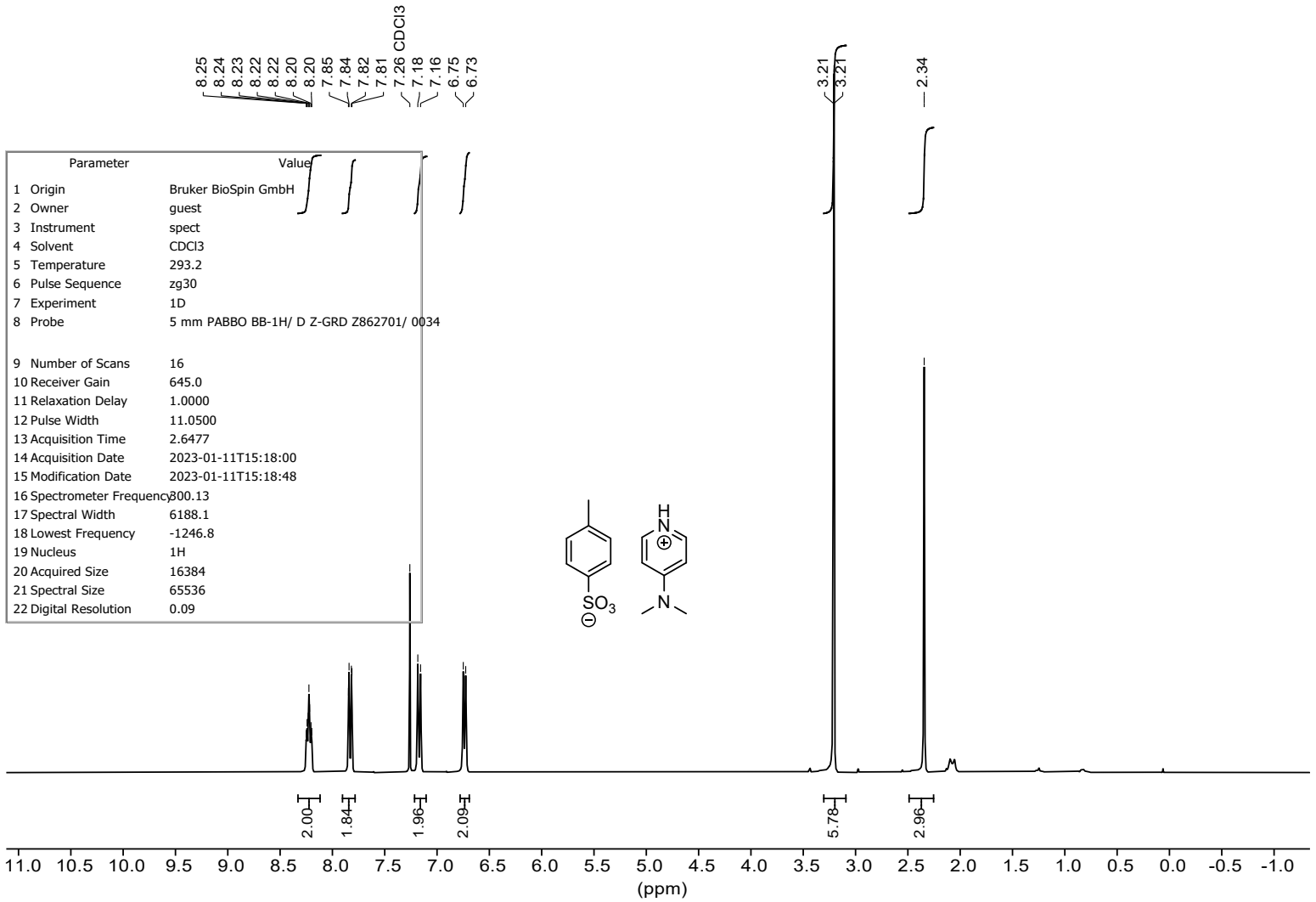

Figure S7:[1]H NMR spectrum of catalyst DPTS at 300 MHz.

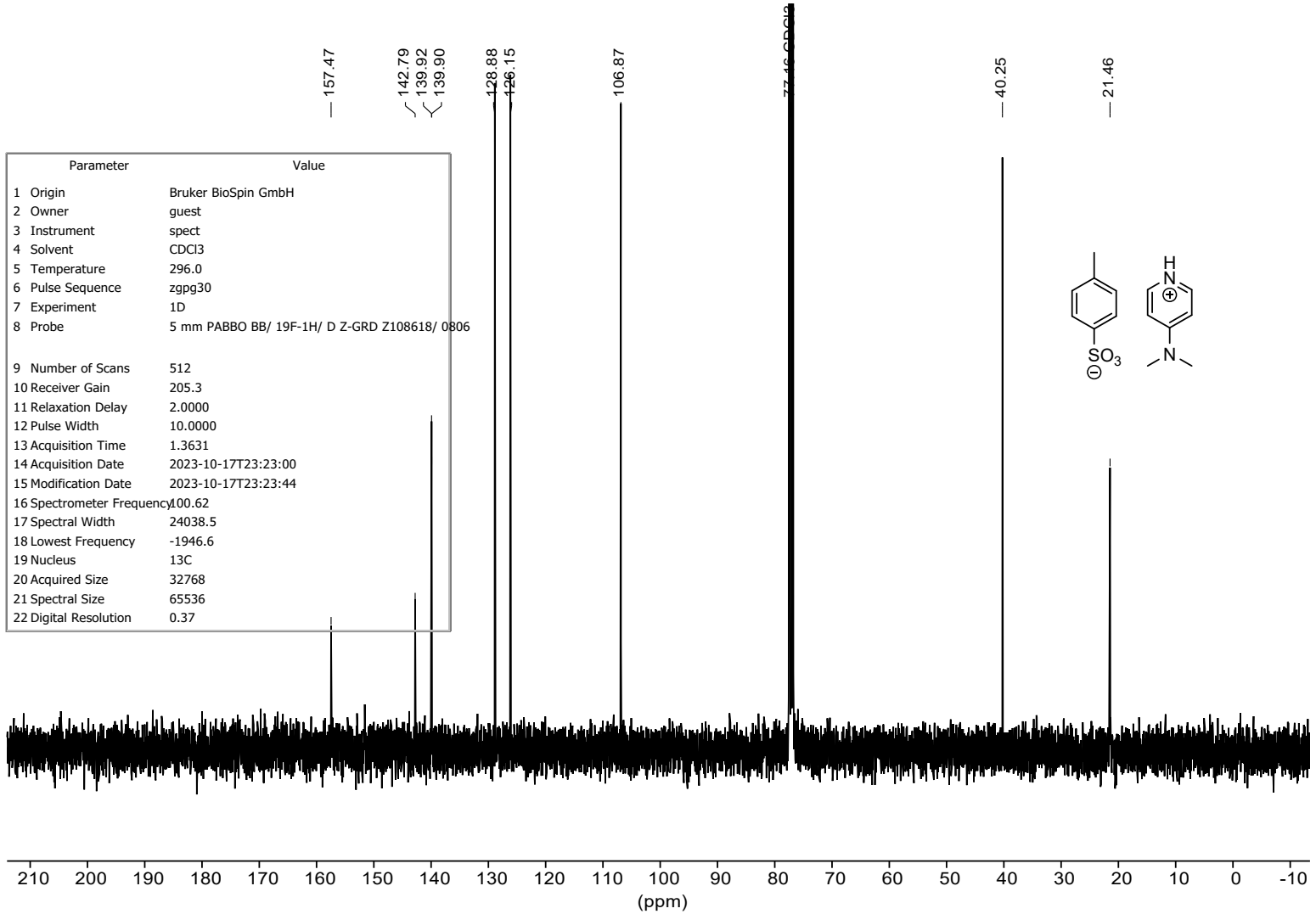

Figure S8: ^{13}C NMR spectrum of catalyst DPTS at 101 MHz.

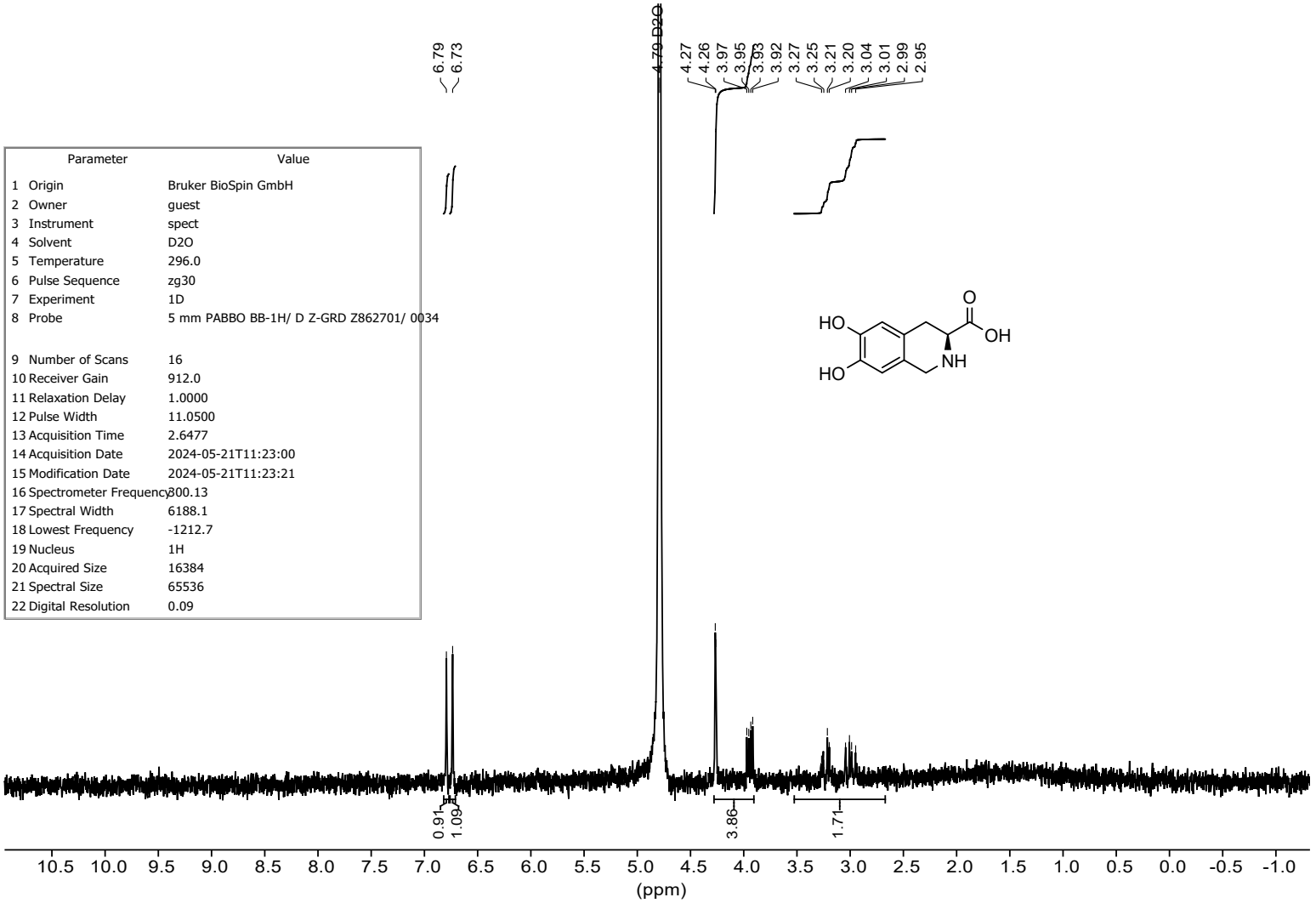

Figure S9: ^{1}H NMR spectrum of **3** at 300 MHz.

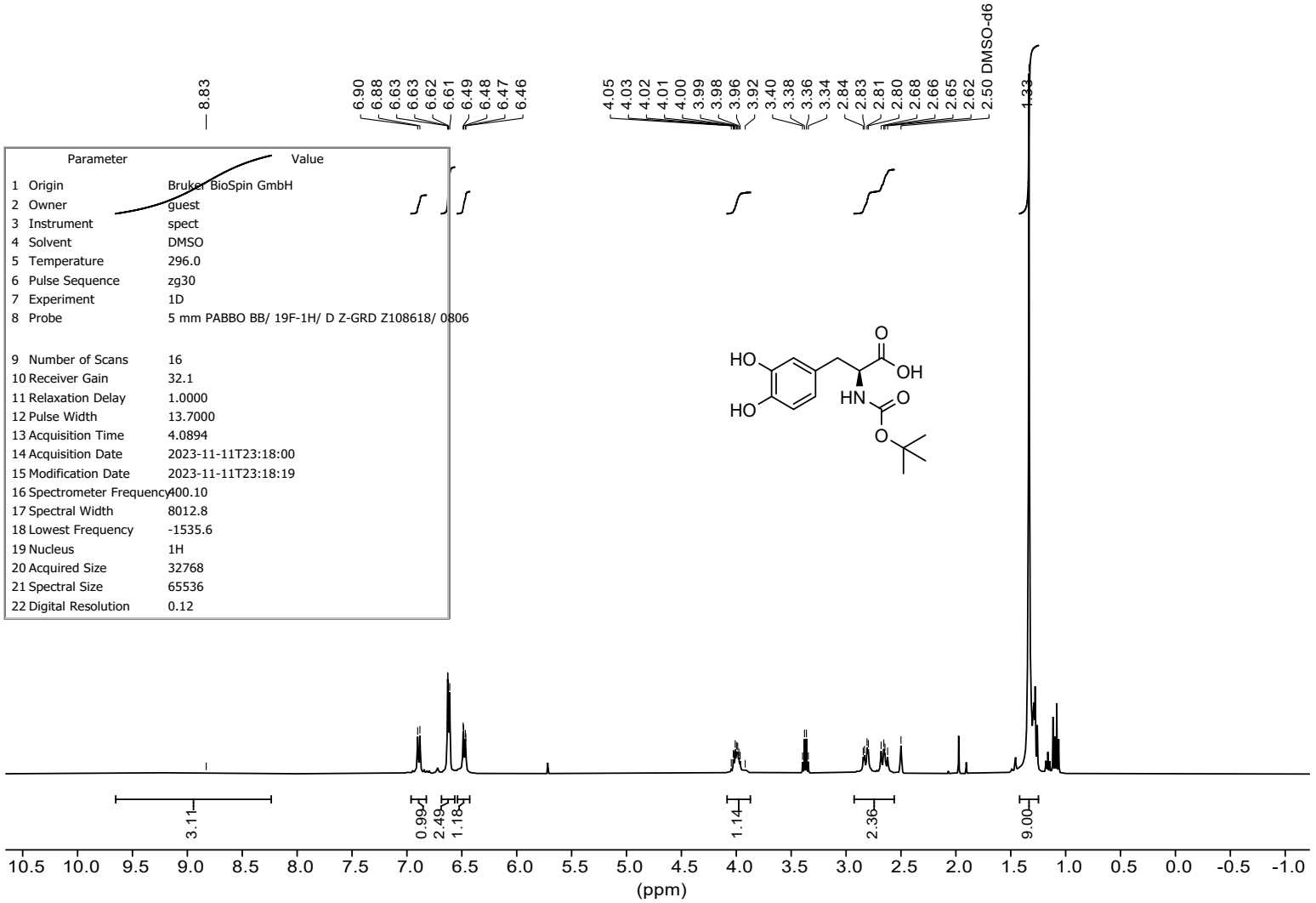

Figure S10: ^{1}H NMR spectrum of **Boc-DOPA** at 400 MHz.

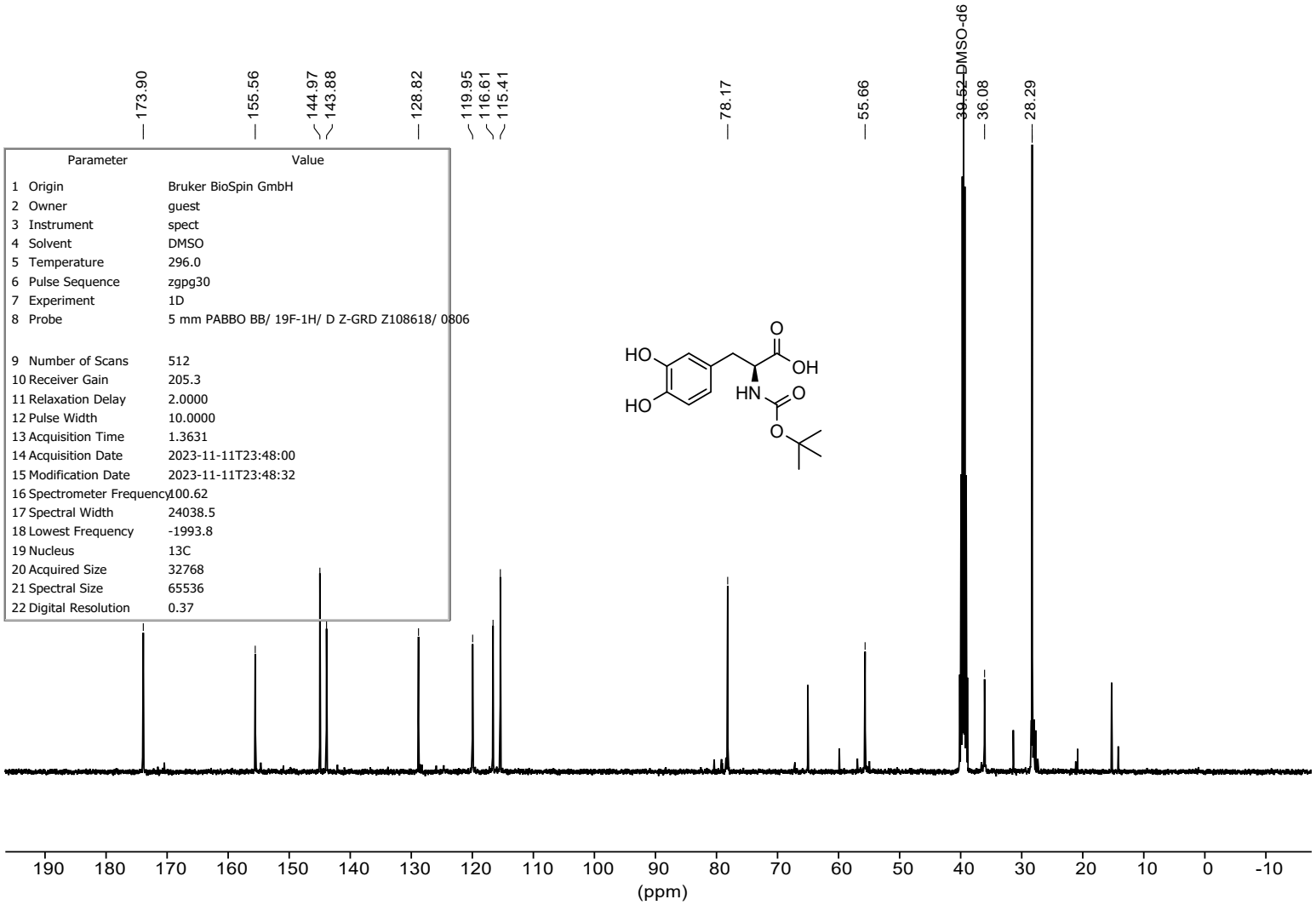

Parameter	Value
1 Origin	Bruker BioSpin GmbH
2 Owner	guest
3 Instrument	spect
4 Solvent	DMSO
5 Temperature	296.0
6 Pulse Sequence	zgpg30
7 Experiment	1D
8 Probe	5 mm PABBO BB/ 19F-1H/ D Z-GRD Z108618/ 0806
9 Number of Scans	512
10 Receiver Gain	205.3
11 Relaxation Delay	2.0000
12 Pulse Width	10.0000
13 Acquisition Time	1.3631
14 Acquisition Date	2023-11-11T23:48:00
15 Modification Date	2023-11-11T23:48:32
16 Spectrometer Frequency	100.62
17 Spectral Width	24038.5
18 Lowest Frequency	-1993.8
19 Nucleus	13C
20 Acquired Size	32768
21 Spectral Size	65536
22 Digital Resolution	0.37

Figure S11: ^{13}C NMR spectrum of **Boc-DOPA** at 101 MHz.

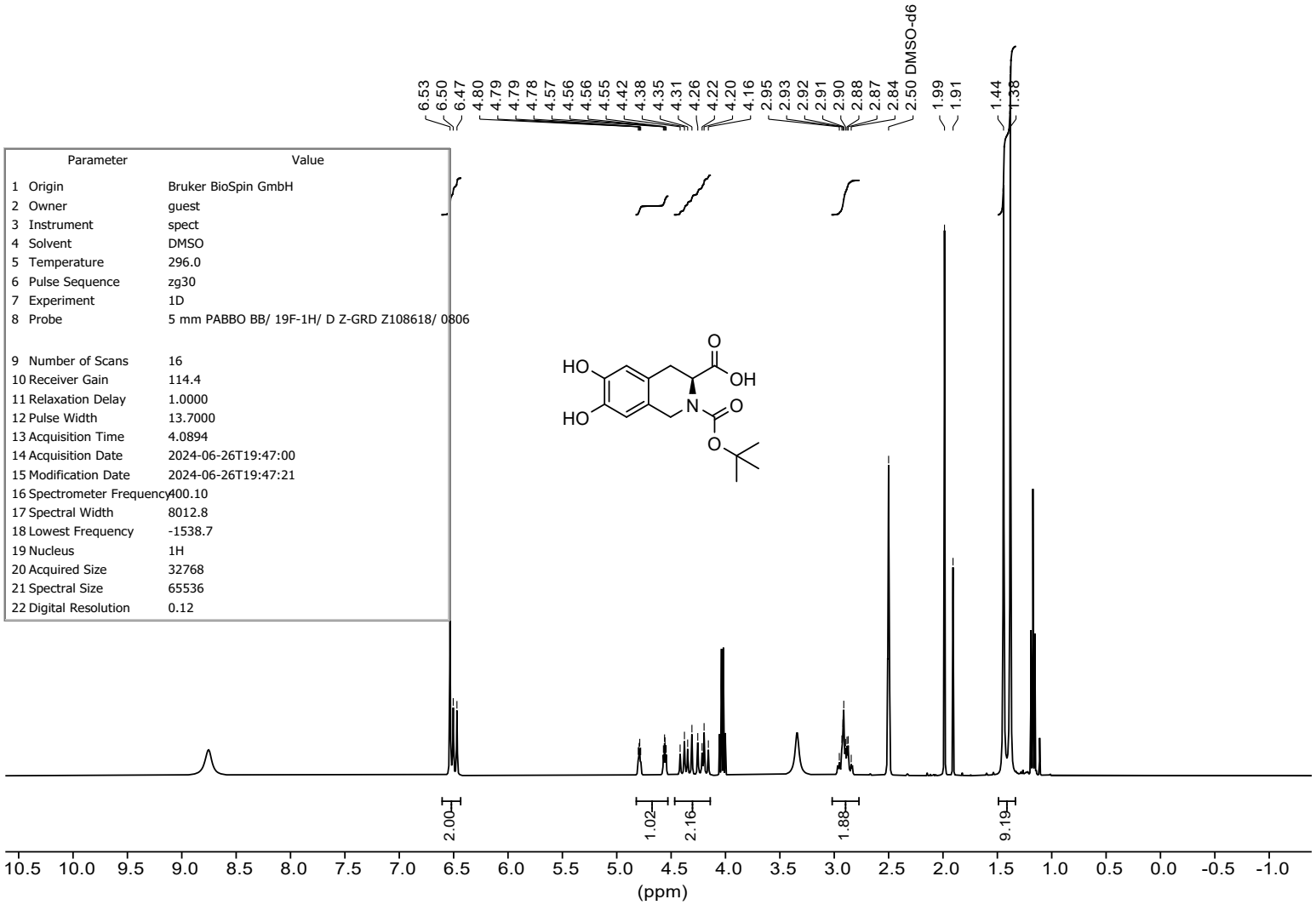

Figure S12: ^{1}H NMR spectrum of **Boc-THIQ** at 400 MHz.

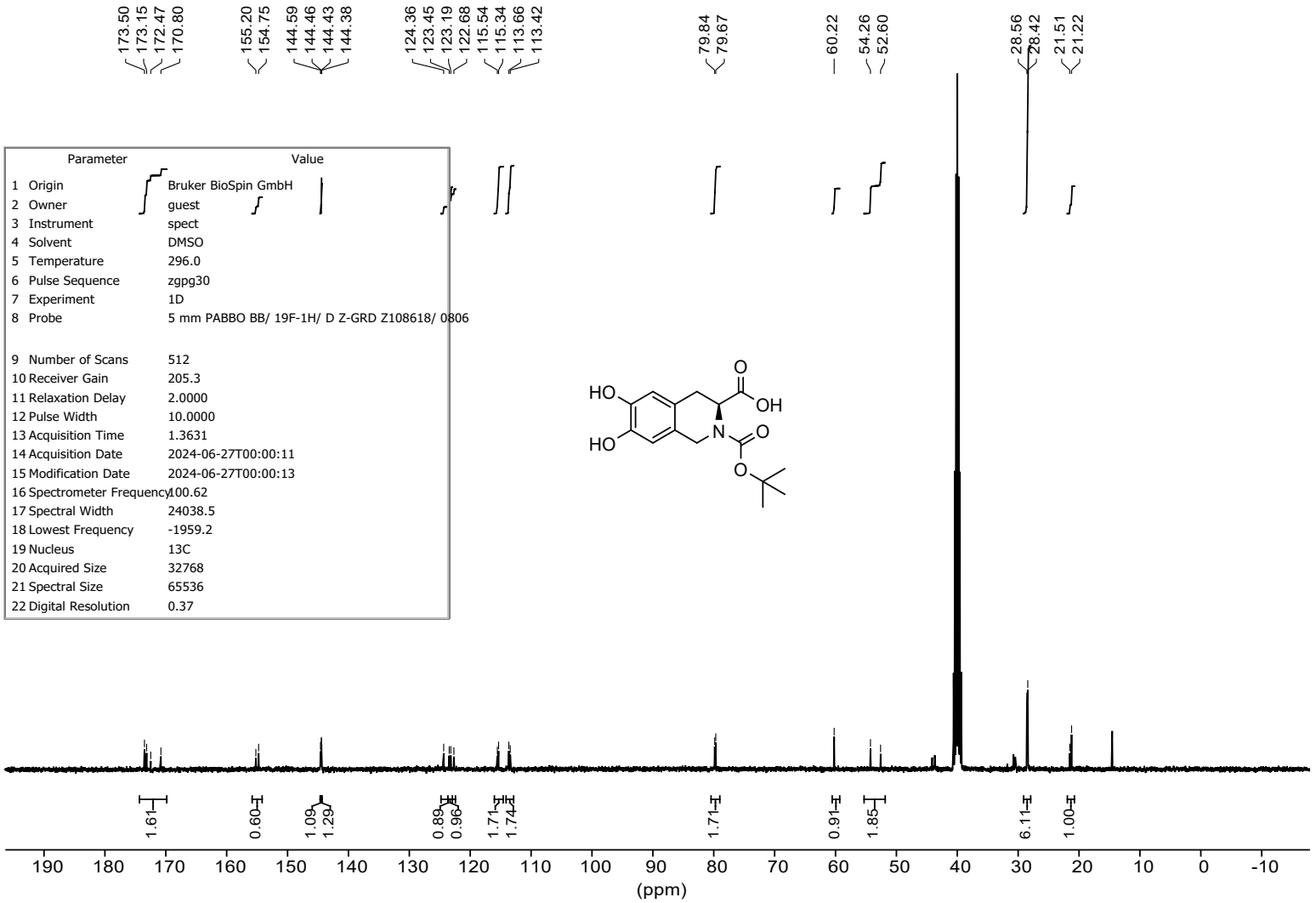

Figure S13: ^{13}C NMR spectrum of **Boc-THIQ** at 101 MHz.

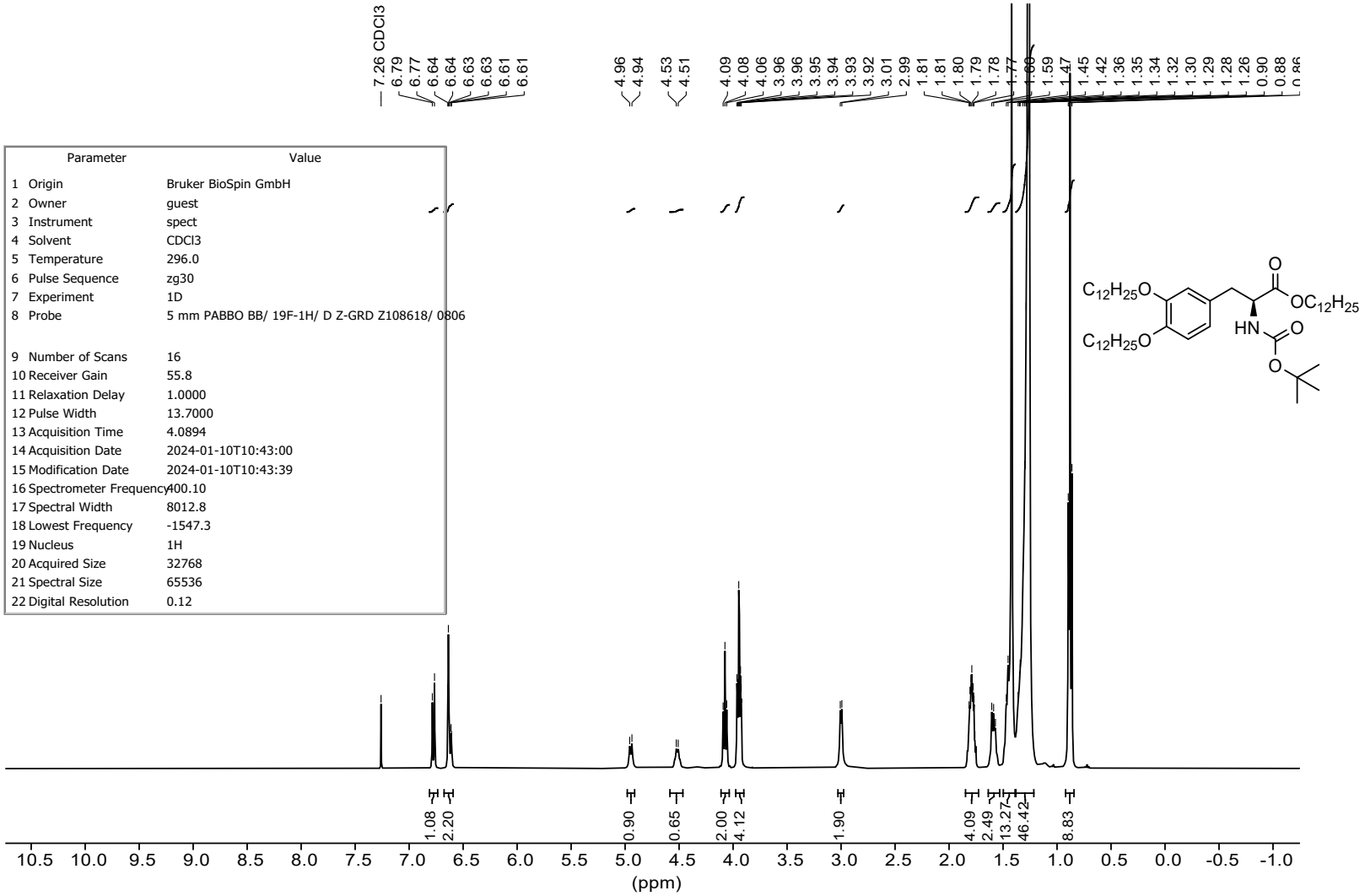

Figure S14: ^{1}H NMR spectrum of **Boc-DOPA(12)** at 400 MHz.

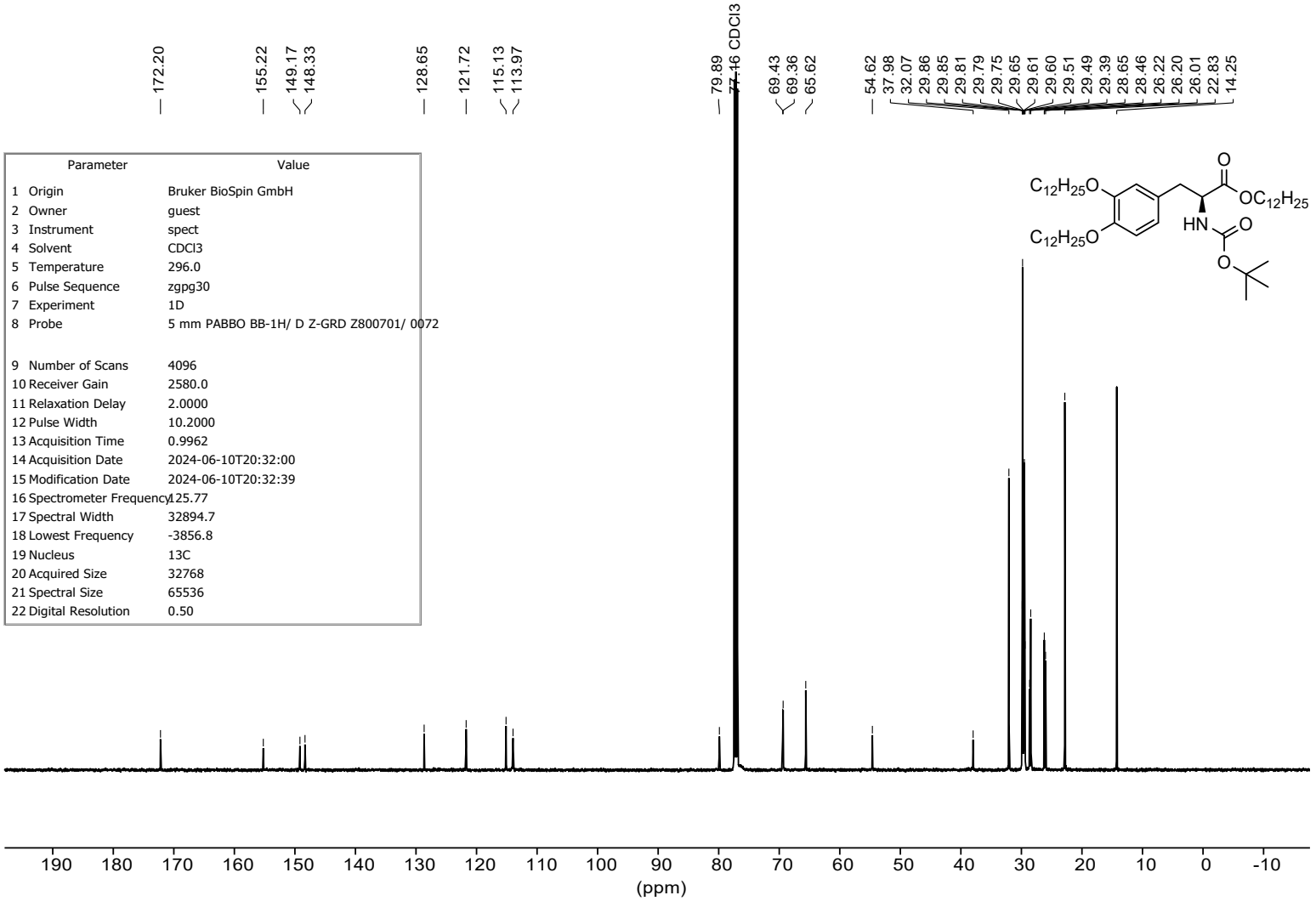

Figure S15: ^{13}C NMR spectrum of **Boc-DOPA(12)** at 126 MHz.

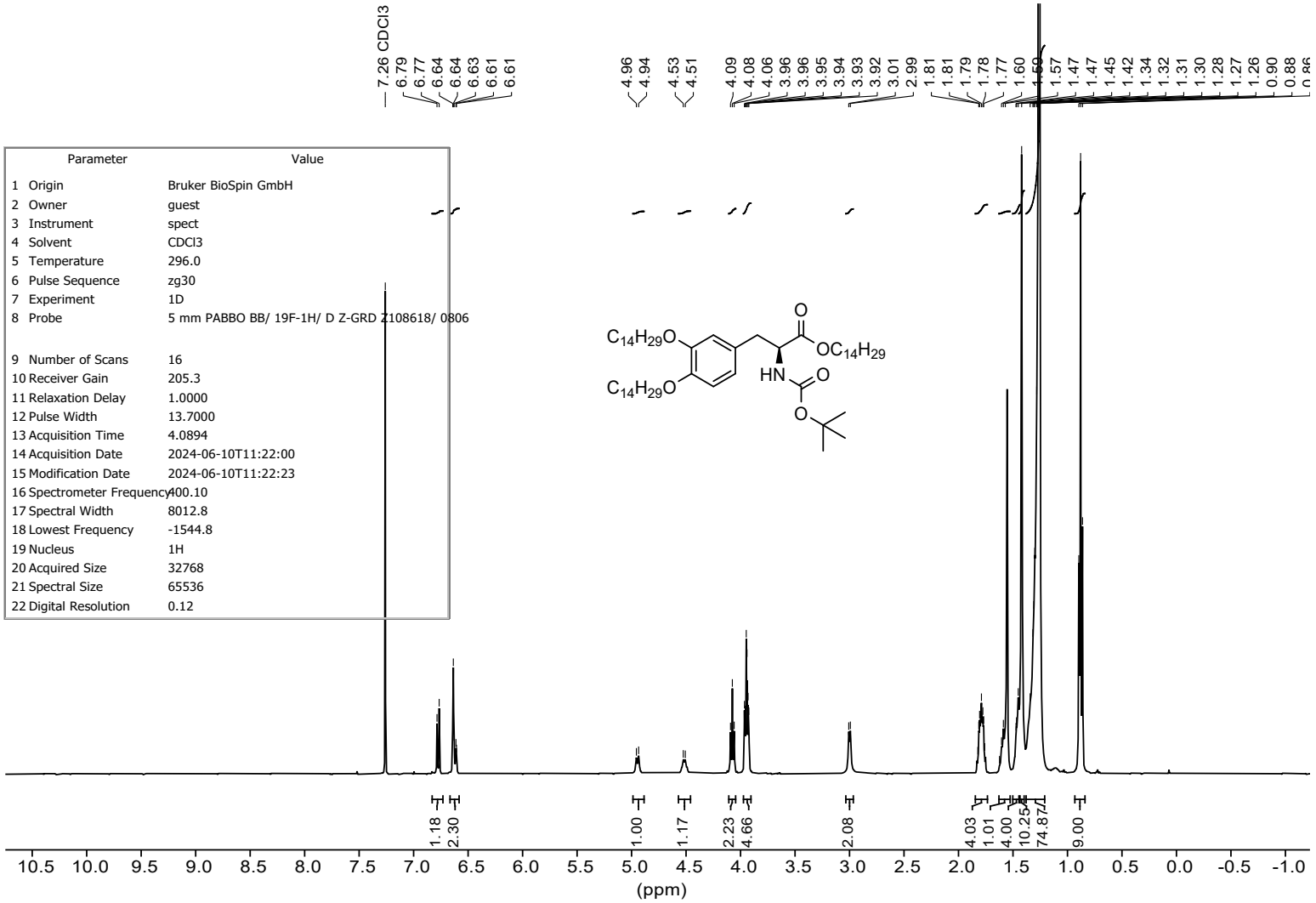

Figure S16: ^{1}H NMR spectrum of **Boc-DOPA(14)** at 400 MHz.

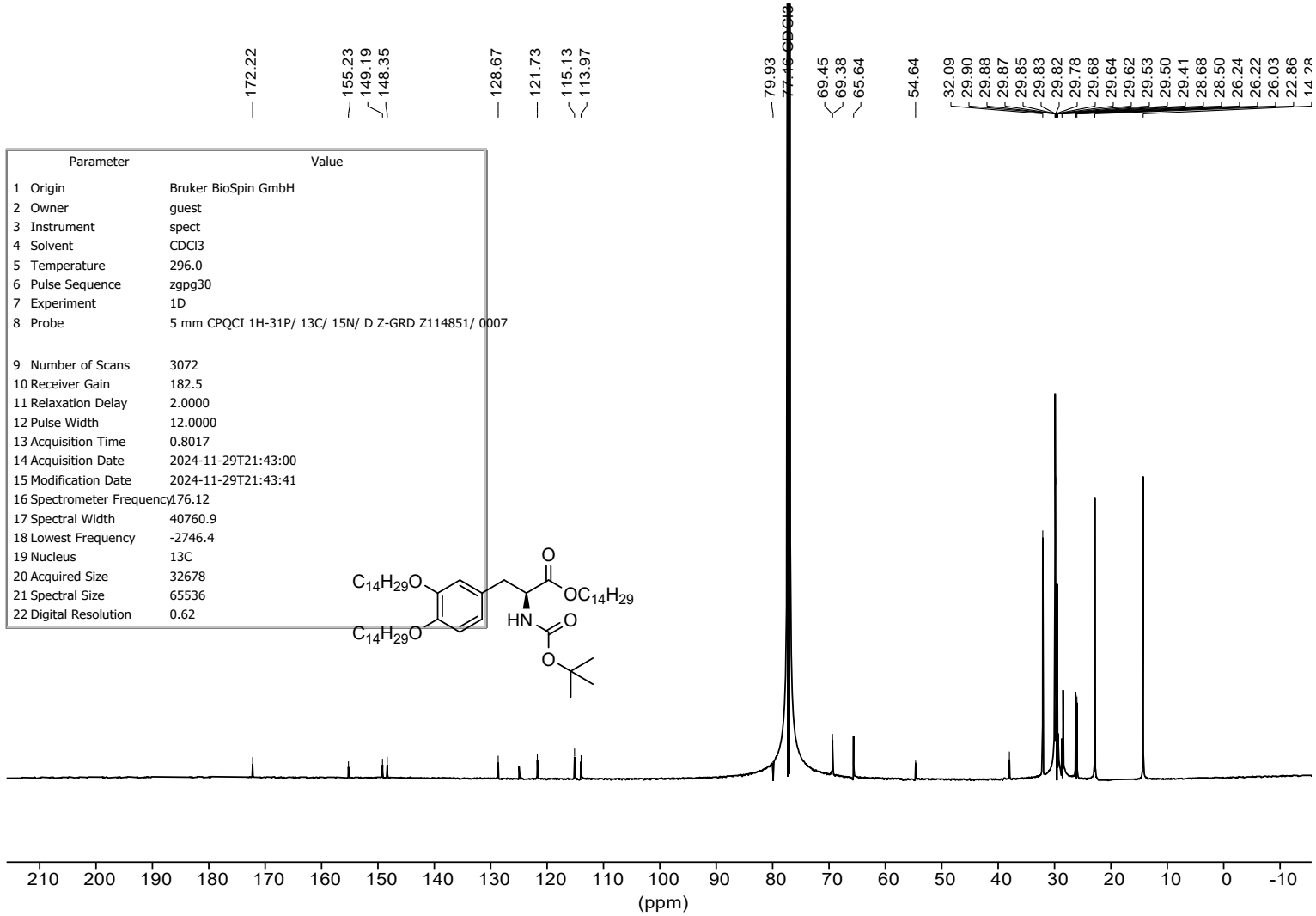

Figure S17: ^{13}C NMR spectrum of **Boc-DOPA(14)** at 101 MHz.

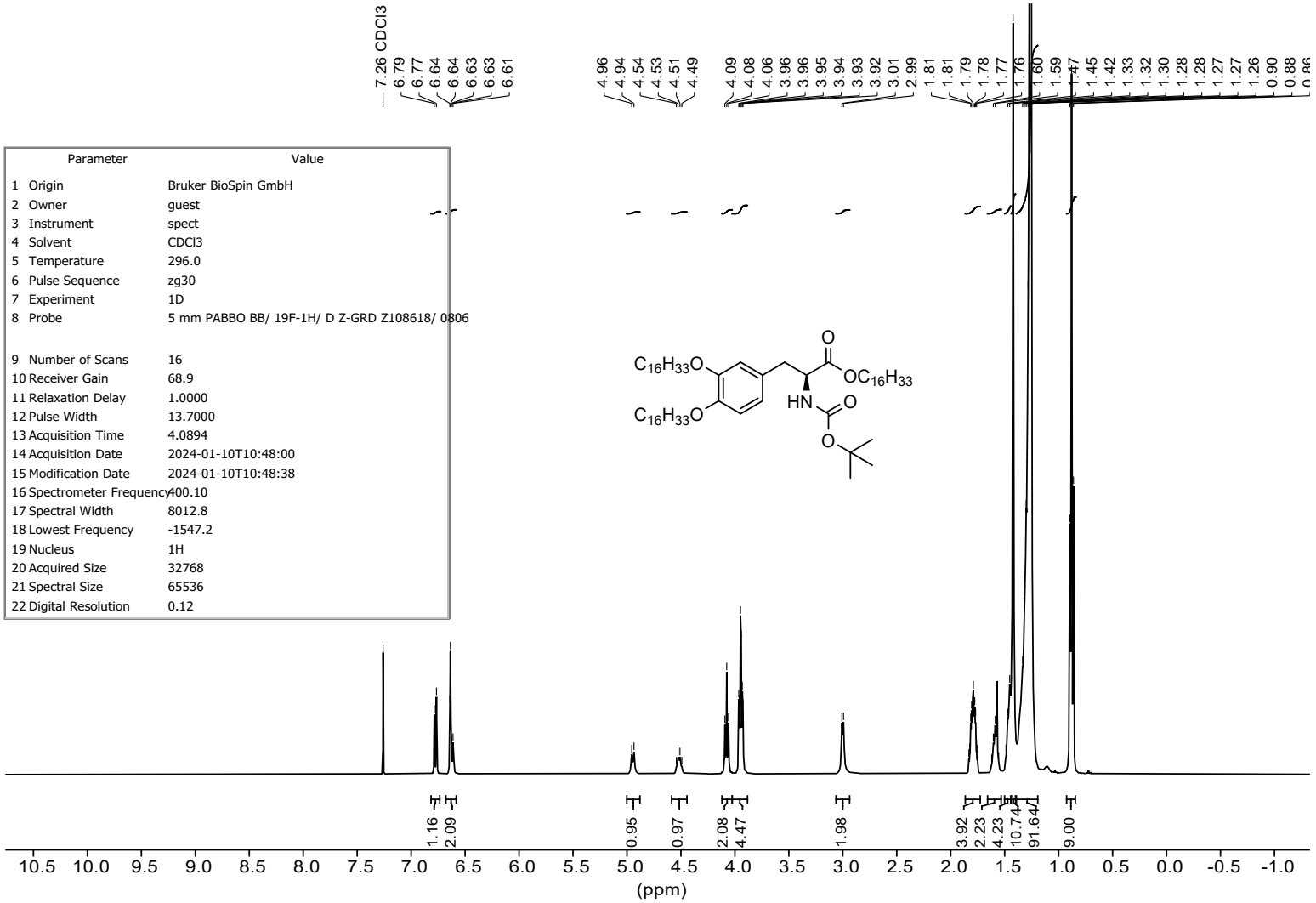

Figure S18: ^{1}H NMR spectrum of **Boc-DOPA(16)** at 400 MHz.

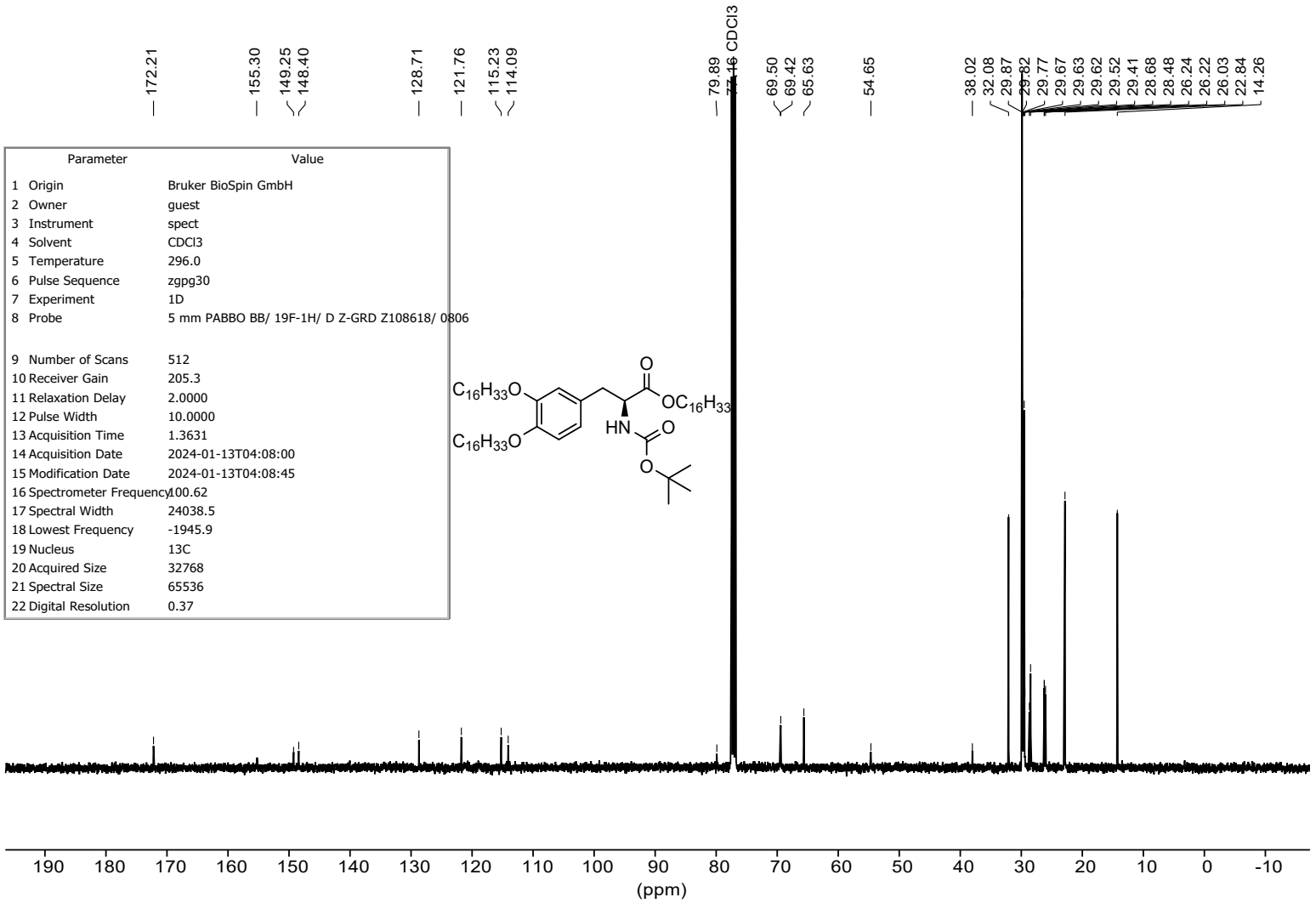

Figure S19: ^{13}C NMR spectrum of **Boc-DOPA(16)** at 101 MHz.

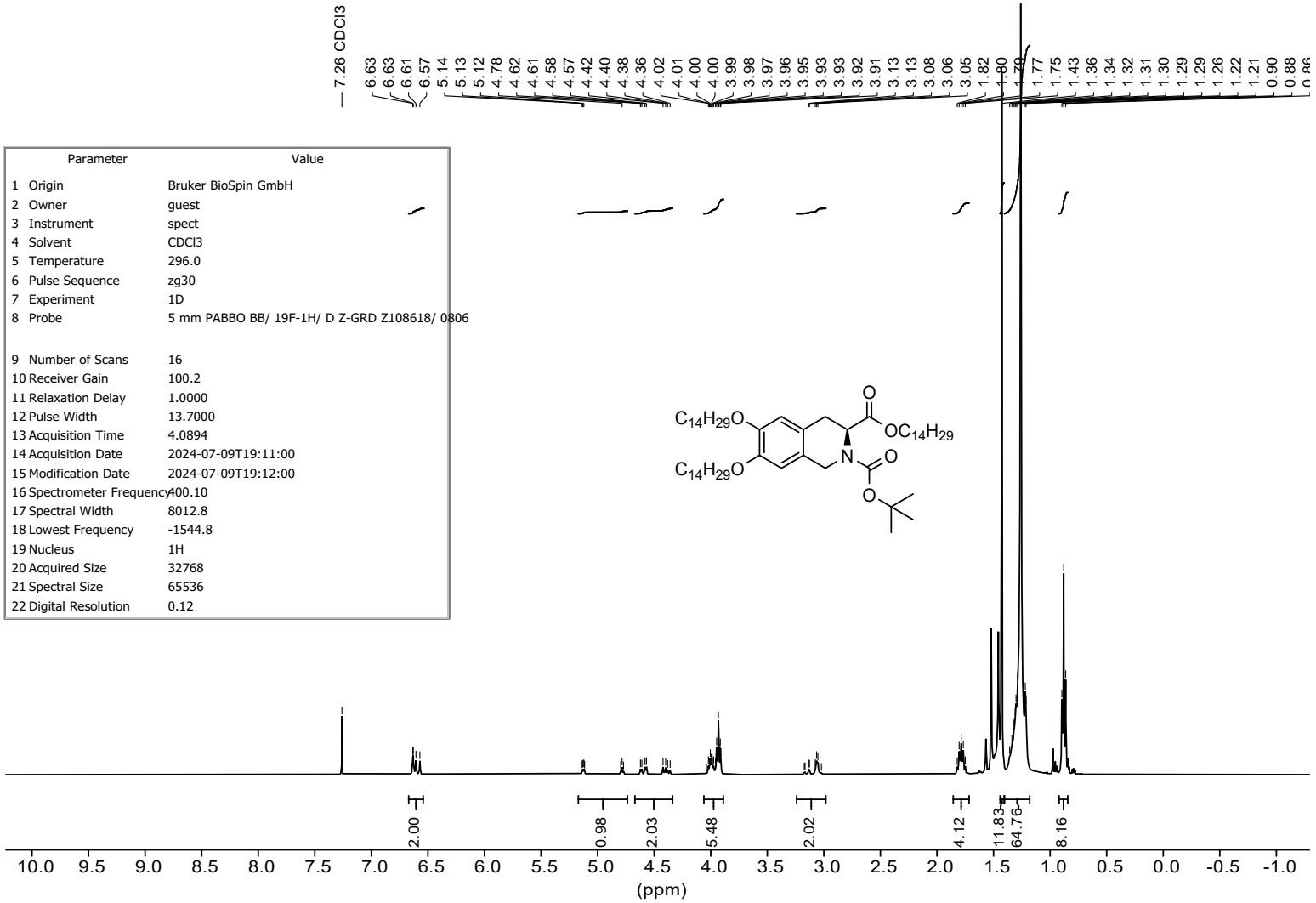

Figure S20: ^{1}H NMR spectrum of **Boc-THIQ(14)** at 400 MHz.

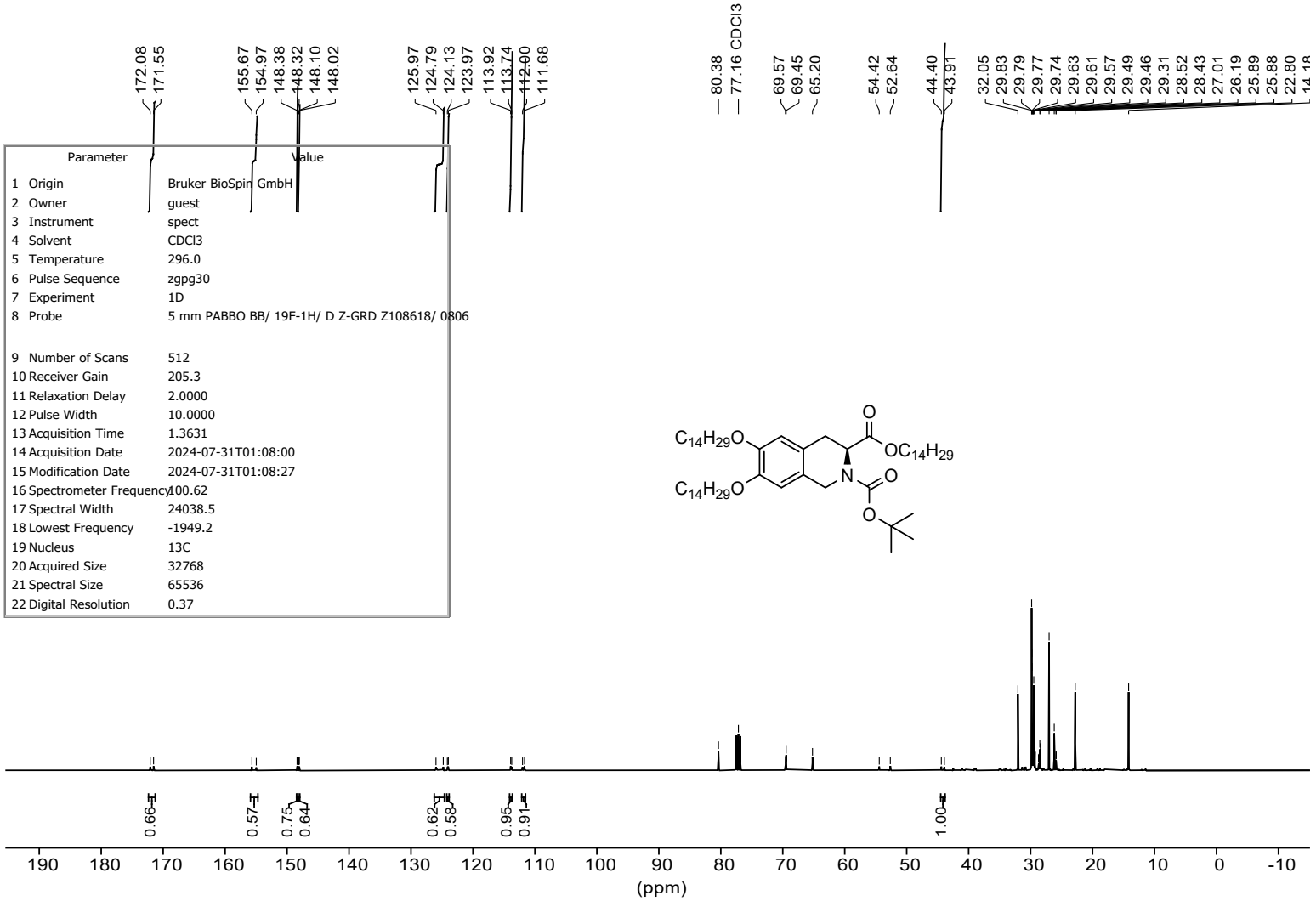

Figure S21: ^{13}C NMR spectrum of **Boc-THIQ(14)** at 101 MHz.

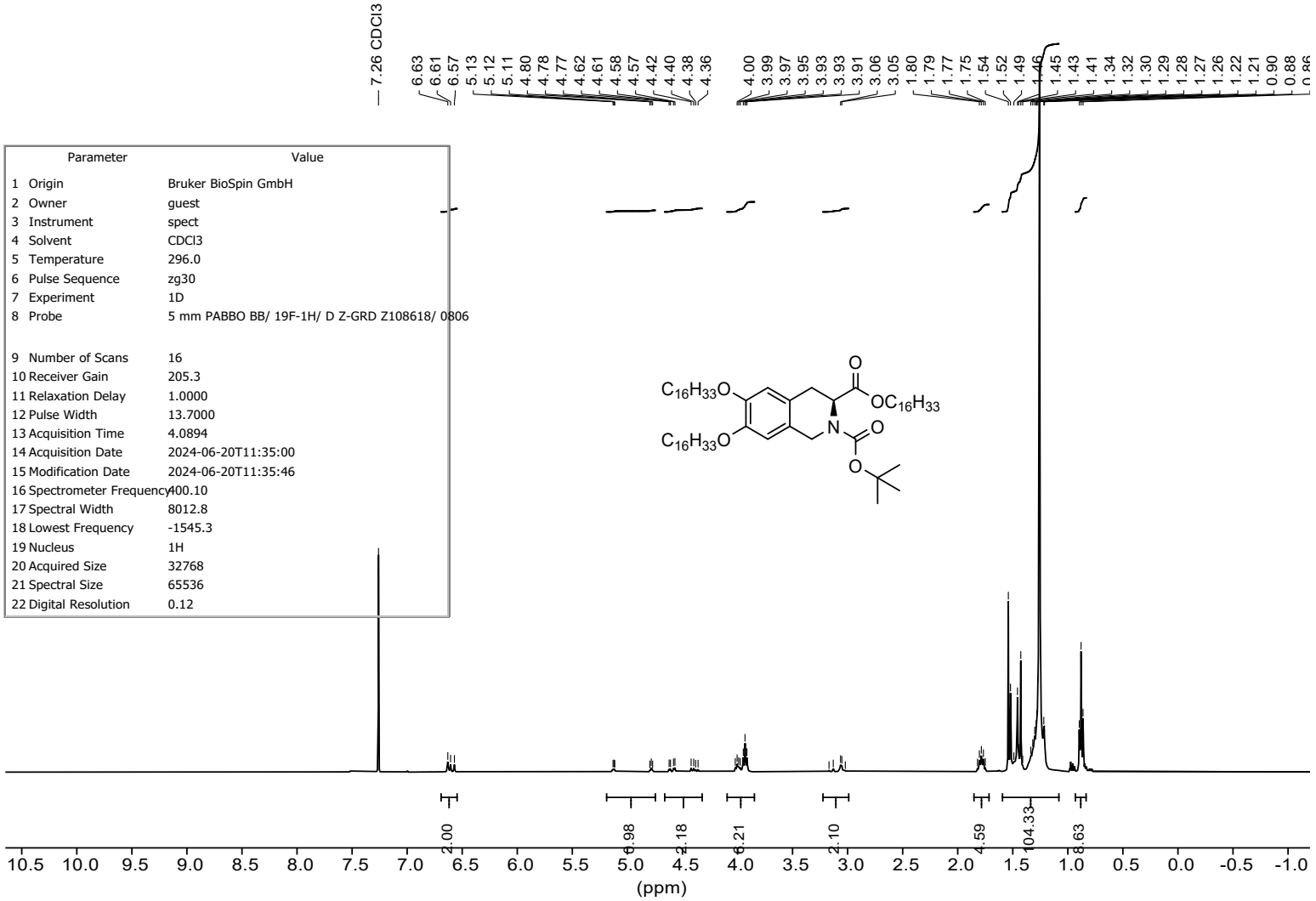

Figure S22: ^{1}H NMR spectrum of **Boc-THIQ(16)** at 400 MHz.

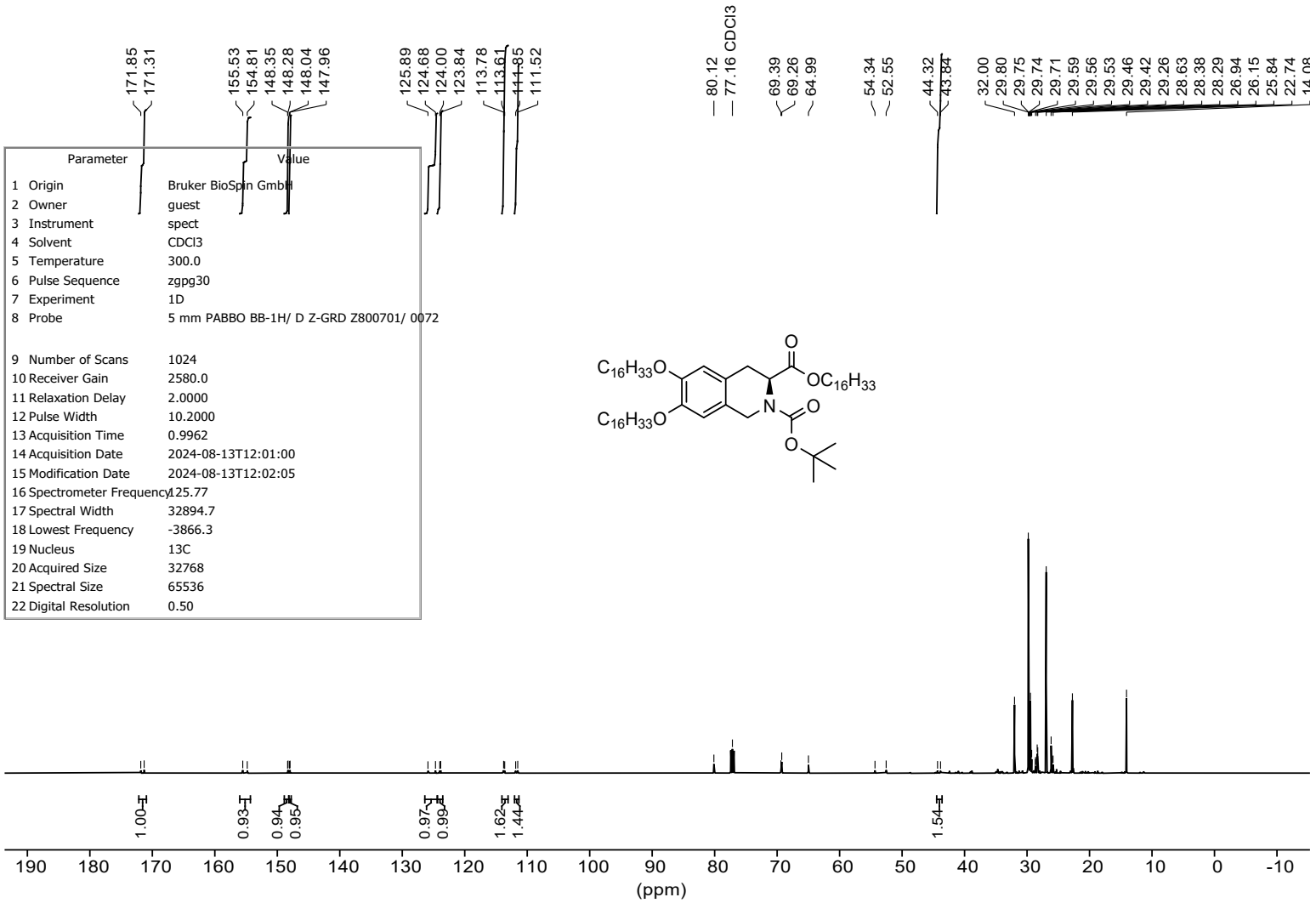

Figure S23: ^{13}C NMR spectrum of **Boc-THIQ(16)** at 126 MHz.

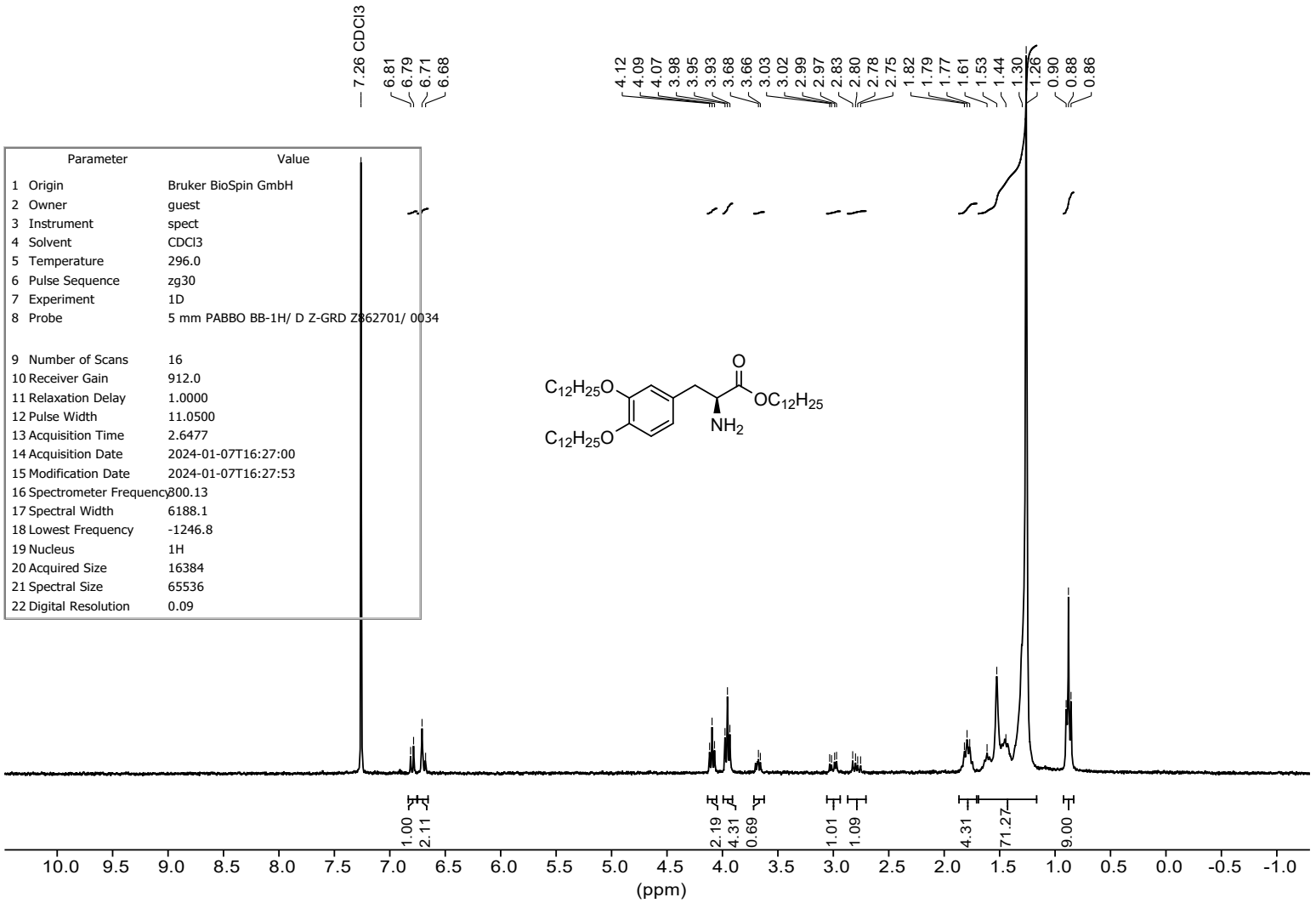

Figure S24: ^{1}H NMR spectrum of **DOPA(12)** at 300 MHz.

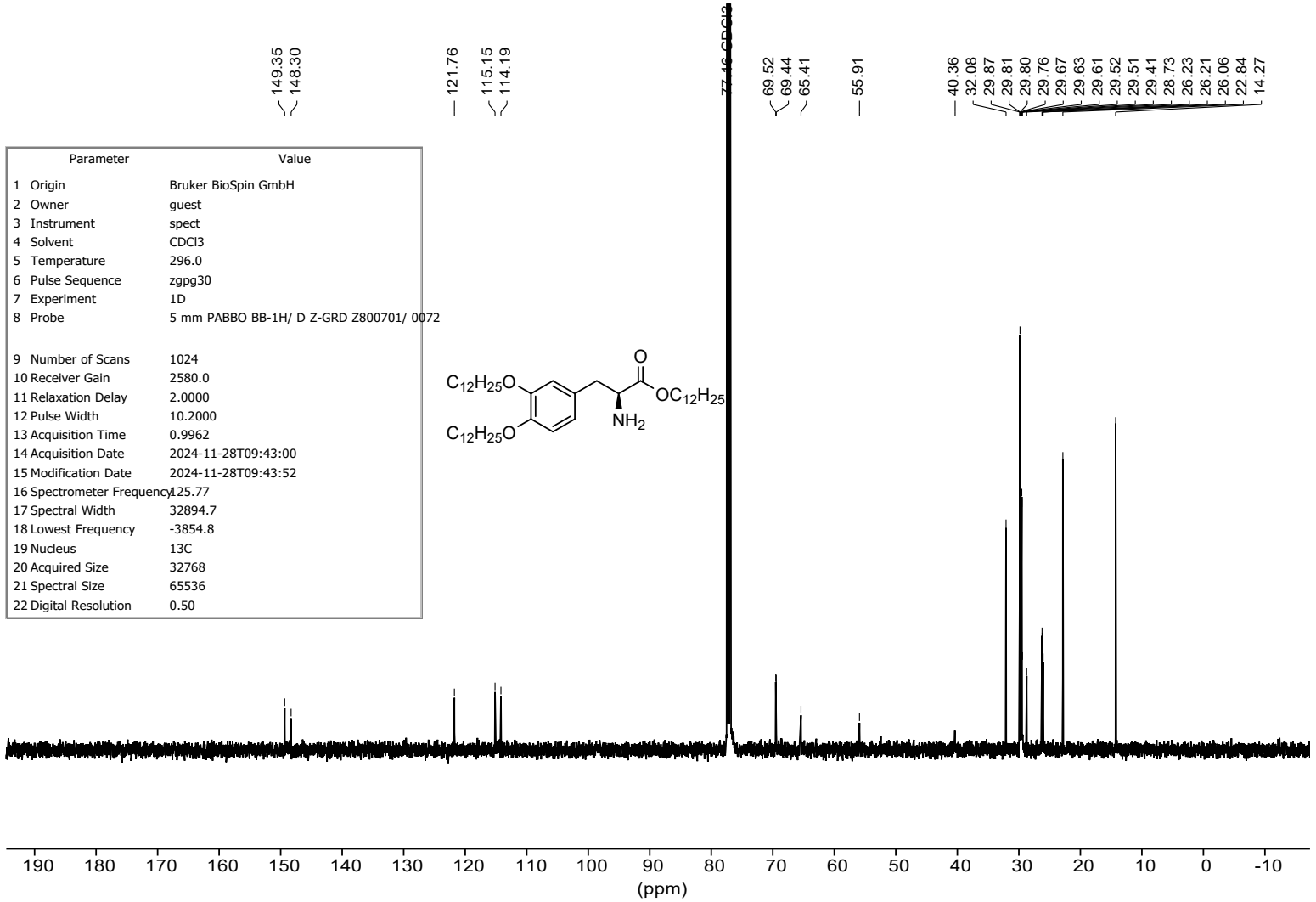

Figure S25: ^{13}C NMR spectrum of **DOPA(12)** at 126 MHz.

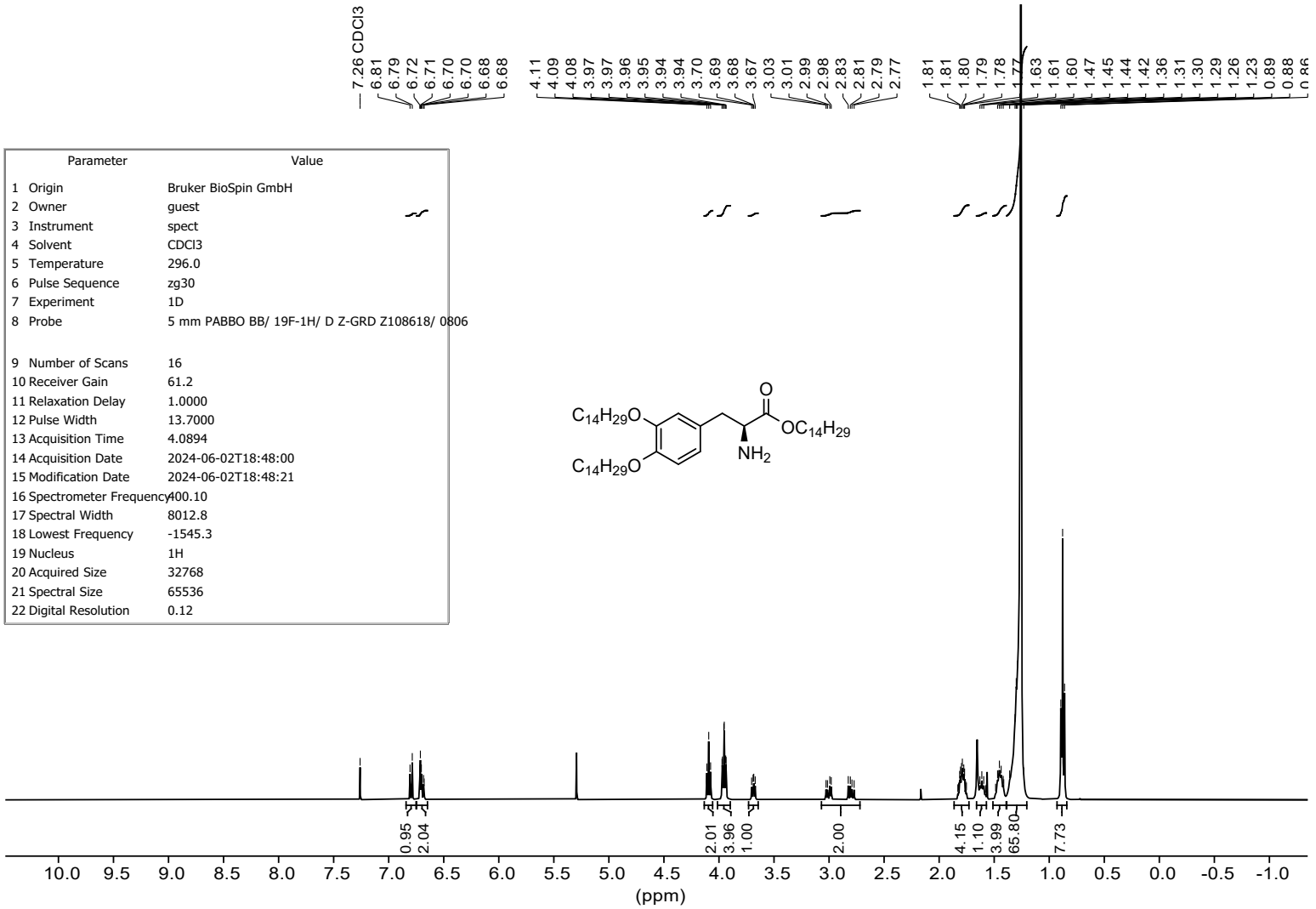

Figure S26: ^{1}H NMR spectrum of **DOPA(14)** at 400 MHz.

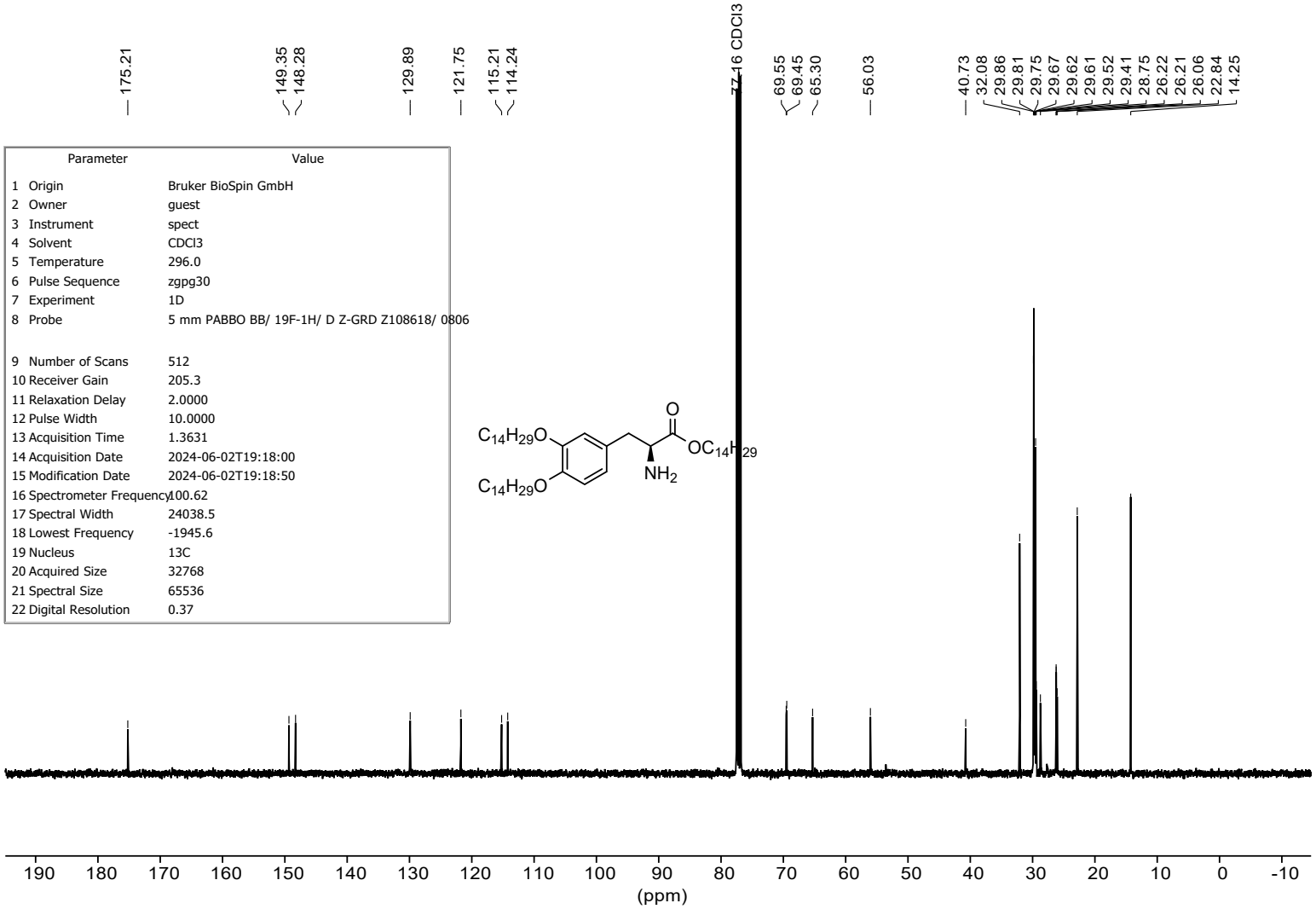

Figure S27: ^{13}C NMR spectrum of **DOPA(14)** at 101 MHz.

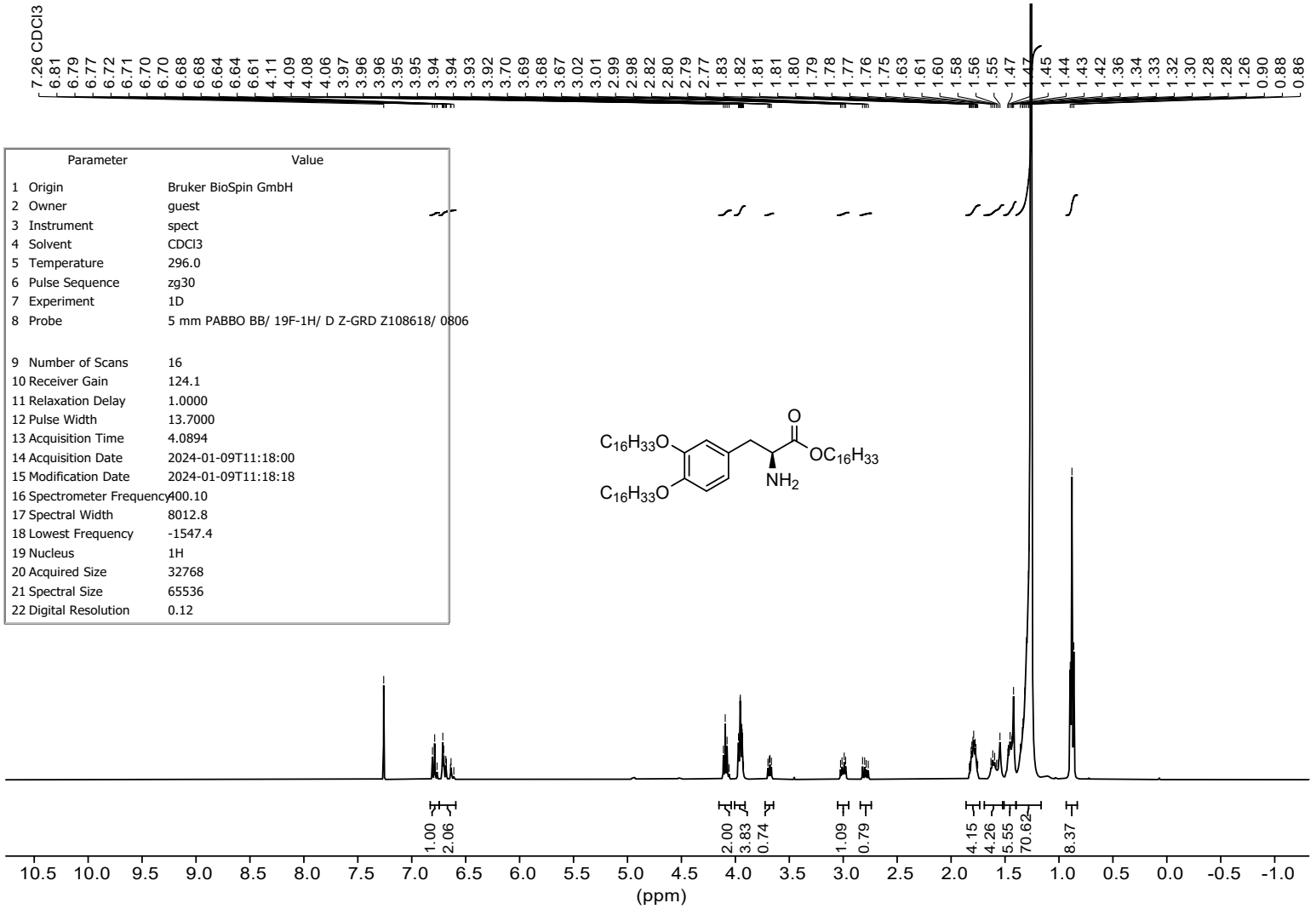

Figure S28: ^{1}H NMR spectrum of **DOPA(16)** at 400 MHz.

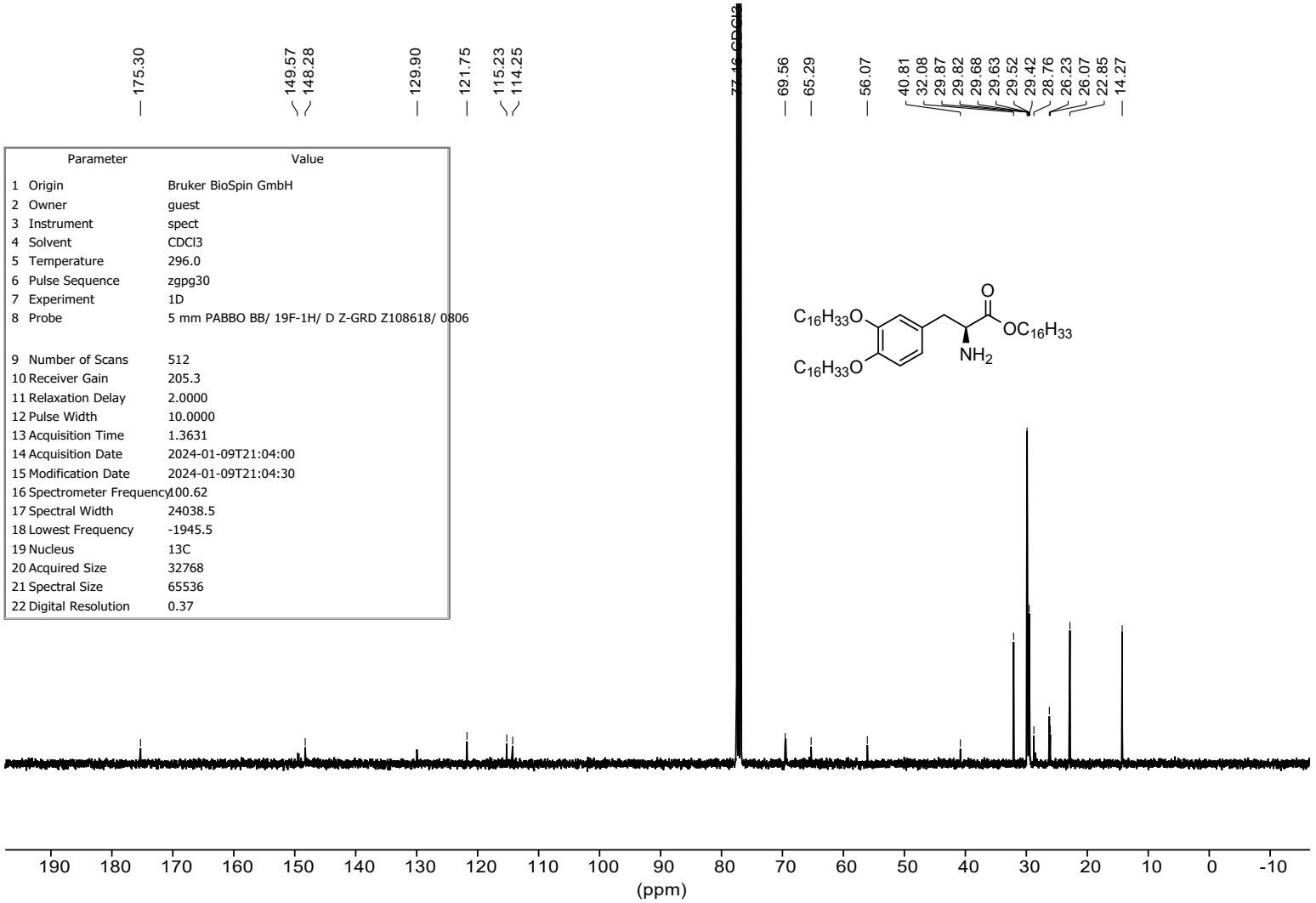

Parameter	Value
1 Origin	Bruker BioSpin GmbH
2 Owner	guest
3 Instrument	spect
4 Solvent	CDCl3
5 Temperature	296.0
6 Pulse Sequence	zgpg30
7 Experiment	1D
8 Probe	5 mm PABBO BB/ 19F-1H/ D Z-GRD Z108618/ 0806
9 Number of Scans	512
10 Receiver Gain	205.3
11 Relaxation Delay	2.0000
12 Pulse Width	10.0000
13 Acquisition Time	1.3631
14 Acquisition Date	2024-01-09T21:04:00
15 Modification Date	2024-01-09T21:04:30
16 Spectrometer Frequency	100.62
17 Spectral Width	24038.5
18 Lowest Frequency	-1945.5
19 Nucleus	13C
20 Acquired Size	32768
21 Spectral Size	65536
22 Digital Resolution	0.37

Figure S29: ^{13}C NMR spectrum of **DOPA(16)** at 101 MHz.

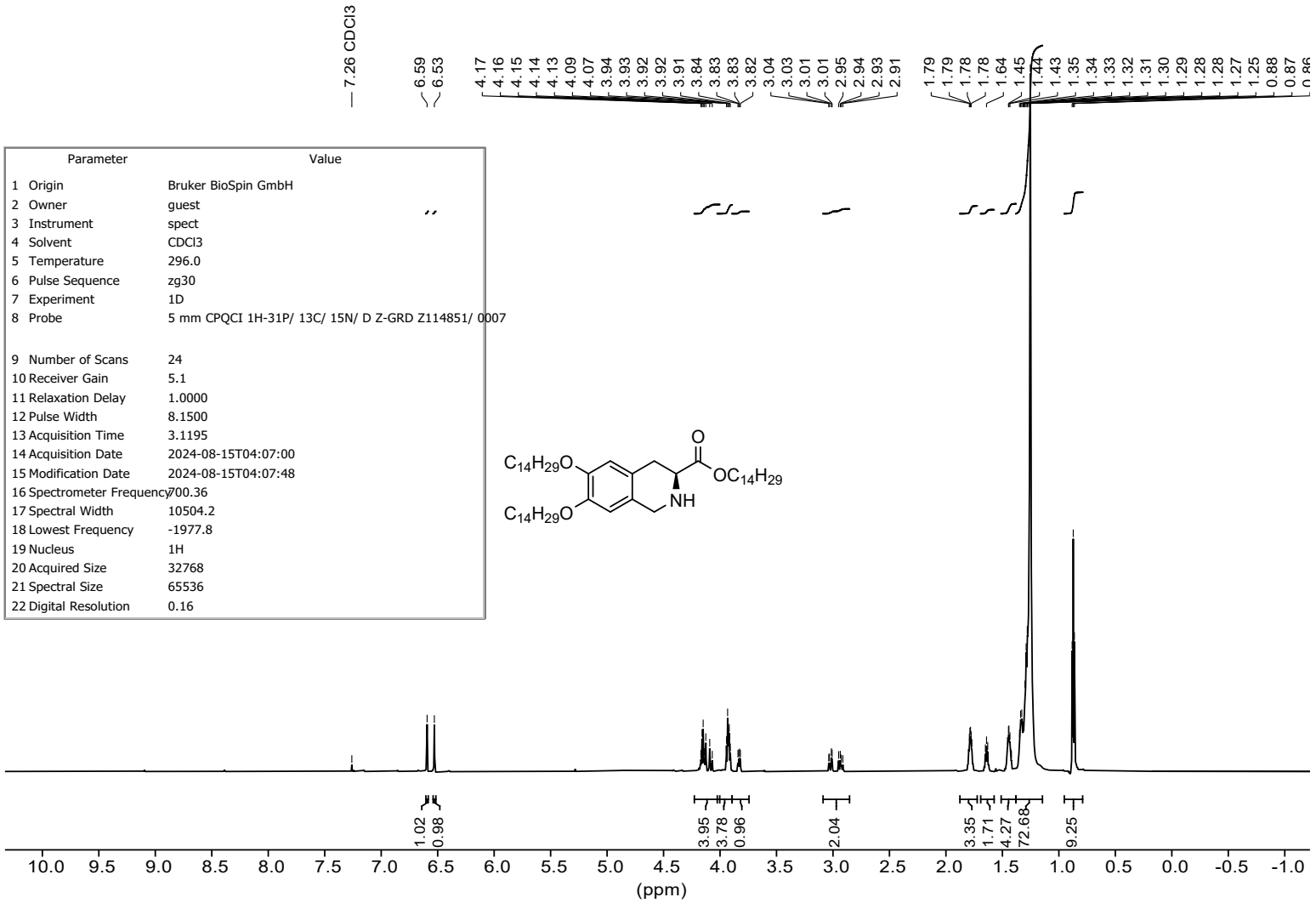

Figure S30: ^{1}H NMR spectrum of **THIQ(14)** at 700 MHz.

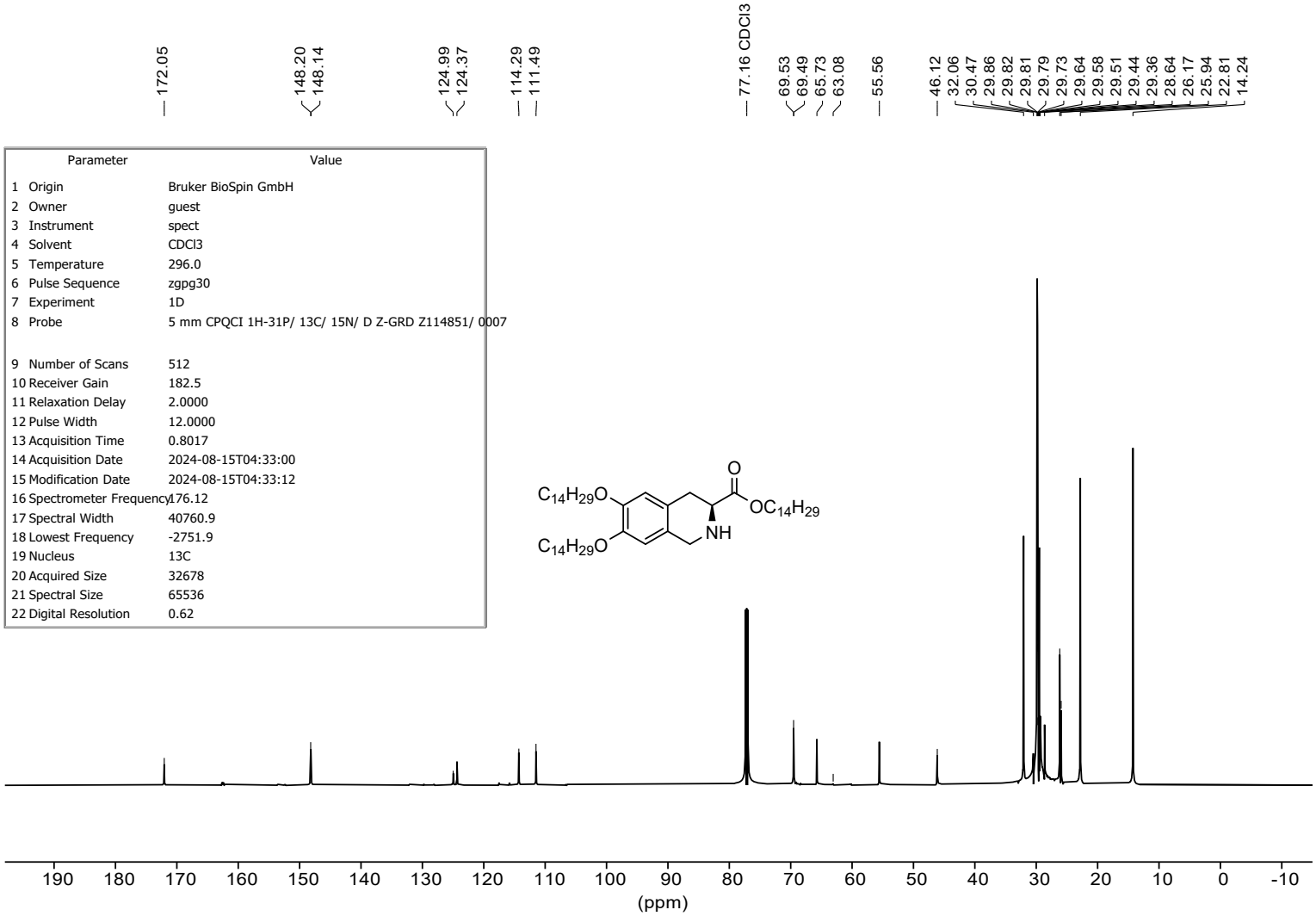

Figure S31: ^{13}C NMR spectrum of **THIQ(14)** at 176 MHz.

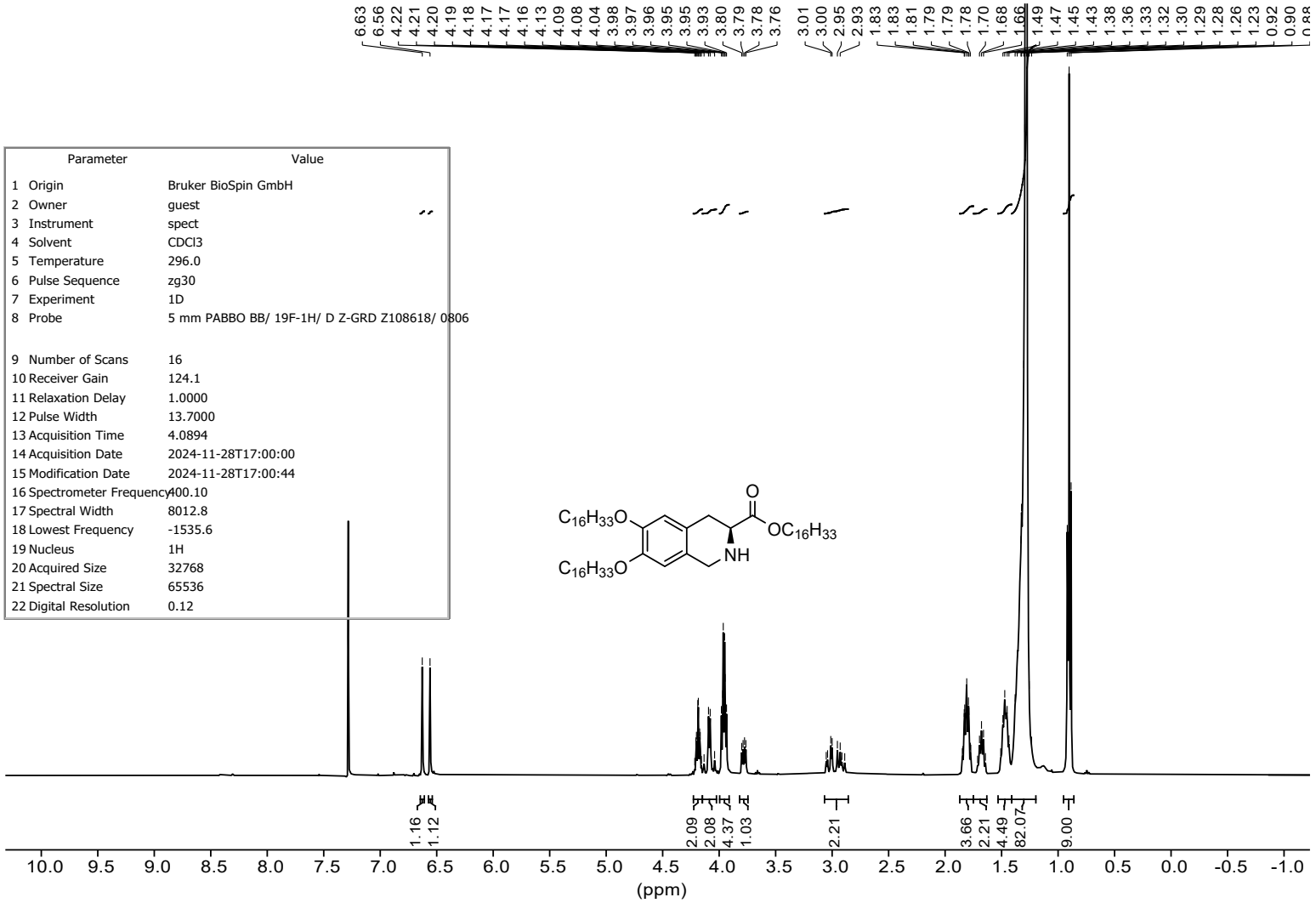

Figure S32: ^{1}H NMR spectrum of **THIQ(16)** at 400 MHz.

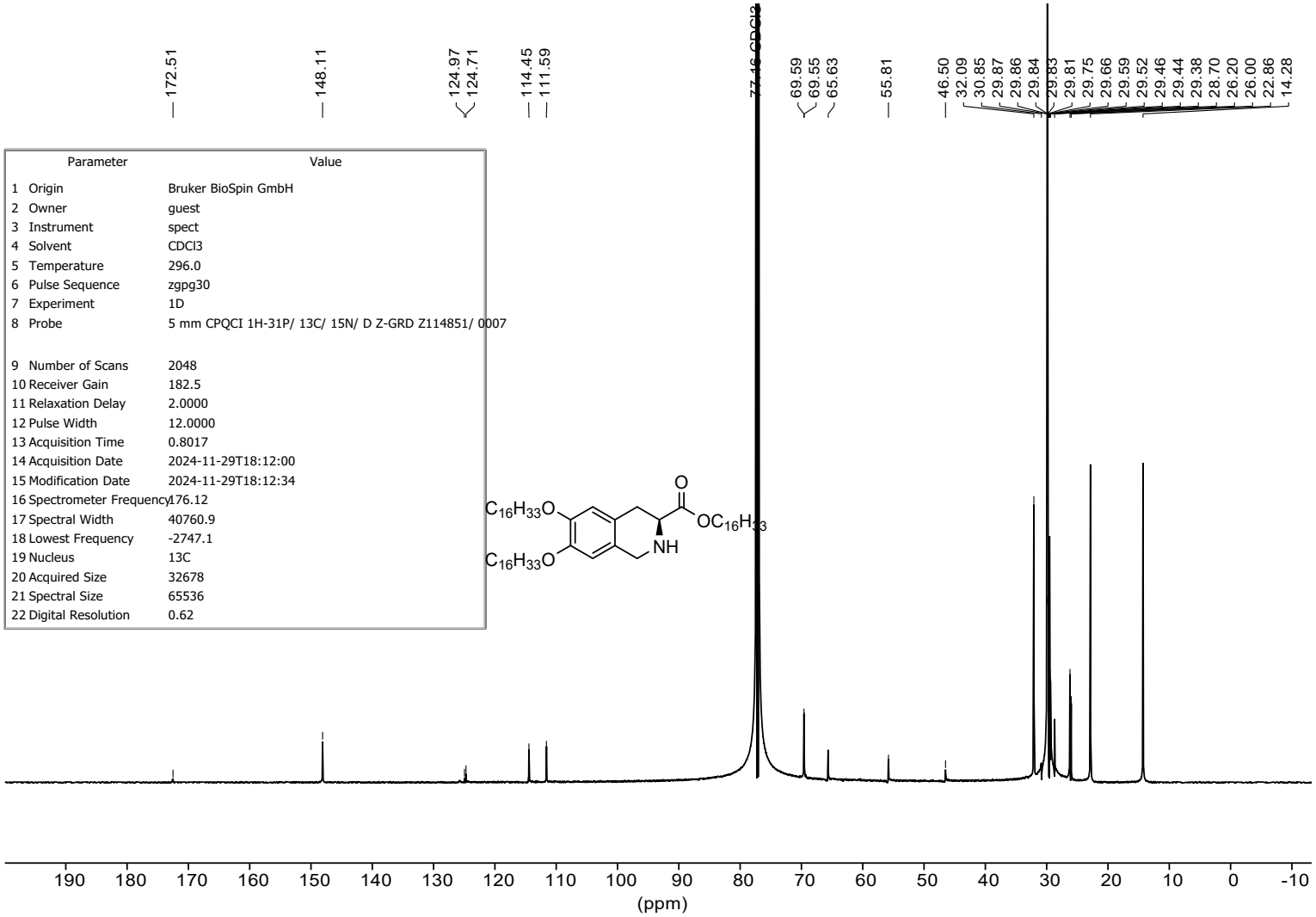

Figure S33: ^{13}C NMR spectrum of **THIQ(16)** at 176 MHz.

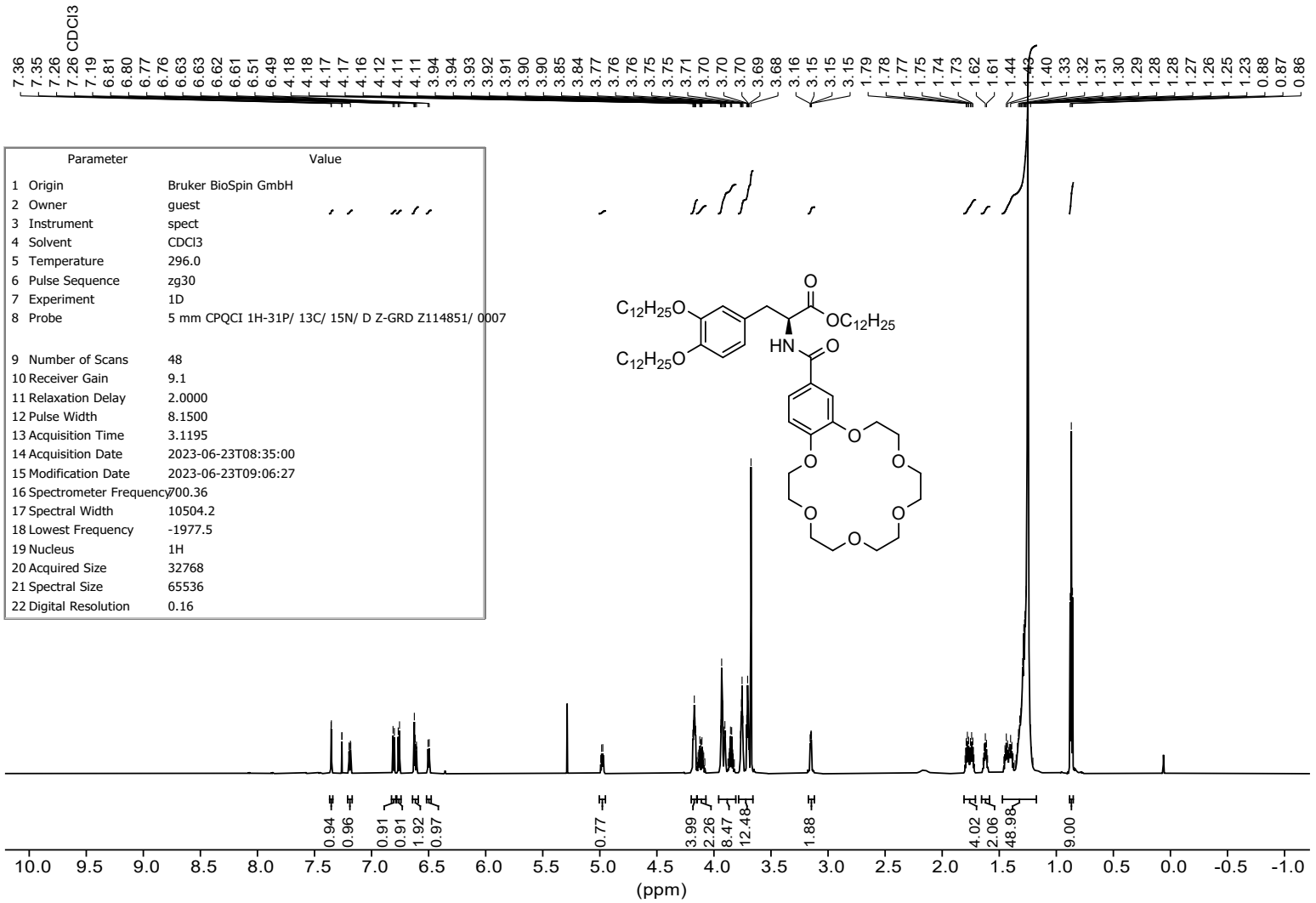

Figure S34: ^{1}H NMR spectrum of **c-DOPA(12)** at 700 MHz.

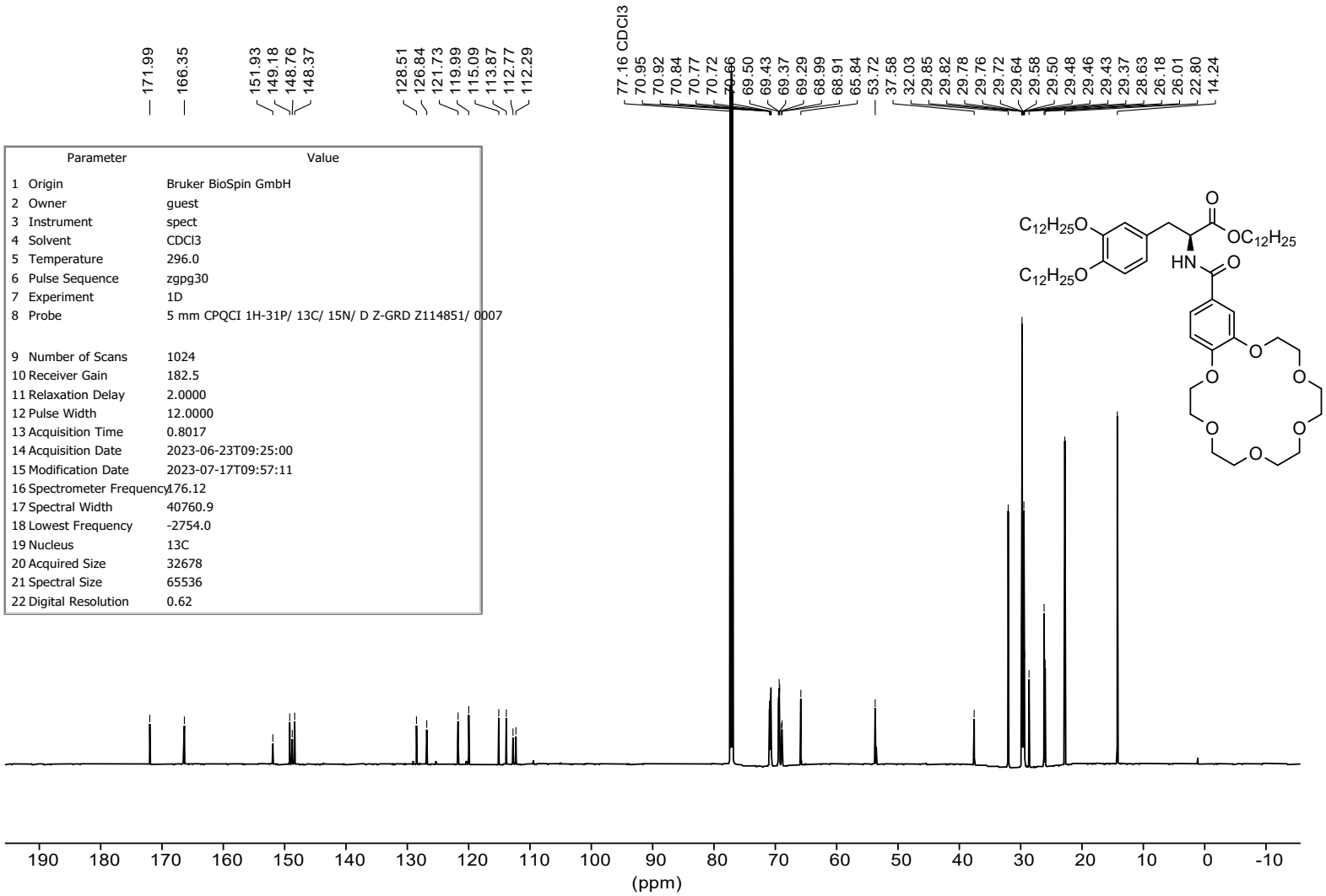

Figure S35: ^{13}C NMR spectrum of **c-DOPA(12)** at 176 MHz.

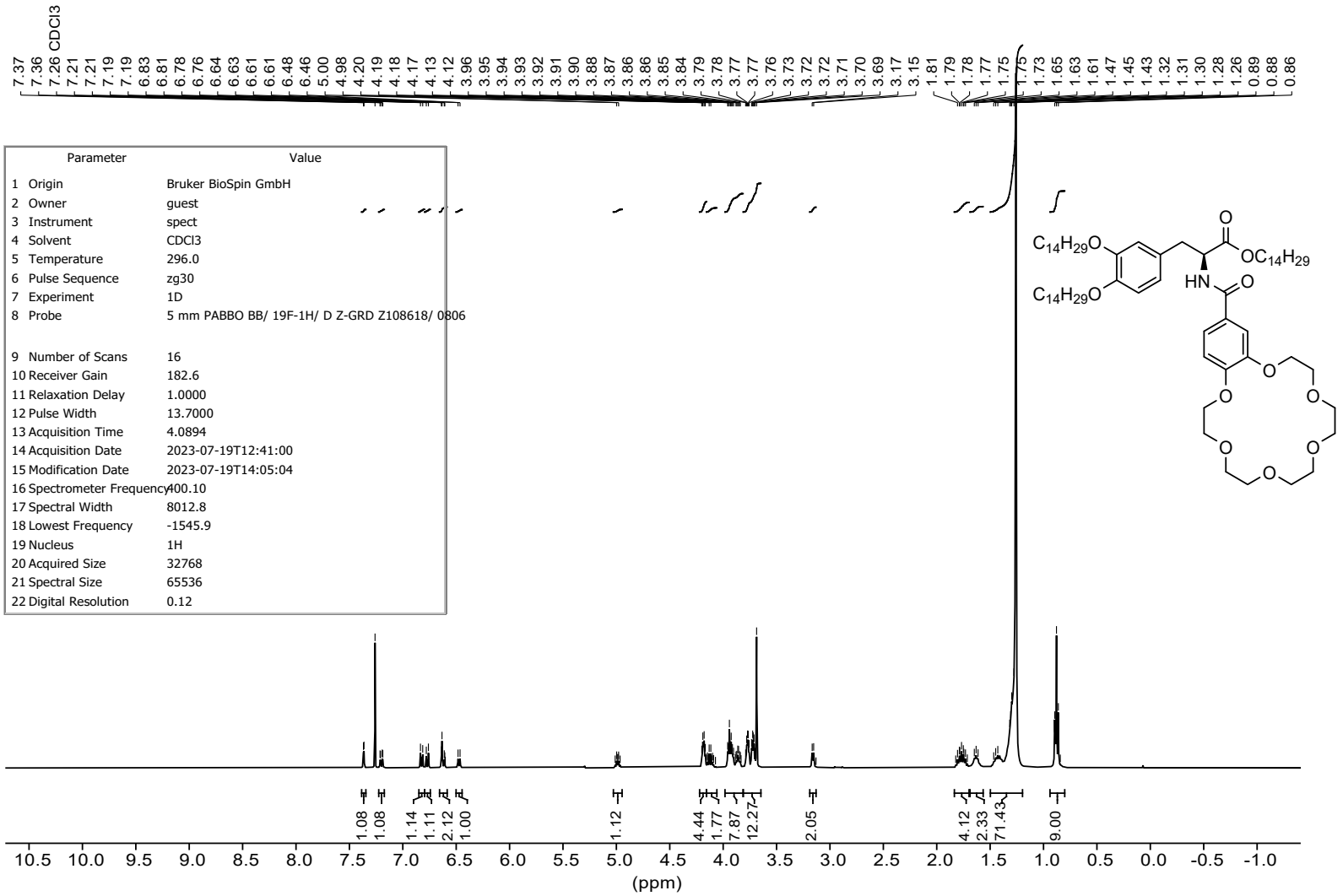

Figure S36: ^{1}H NMR spectrum of **c-DOPA(14)** at 400 MHz.

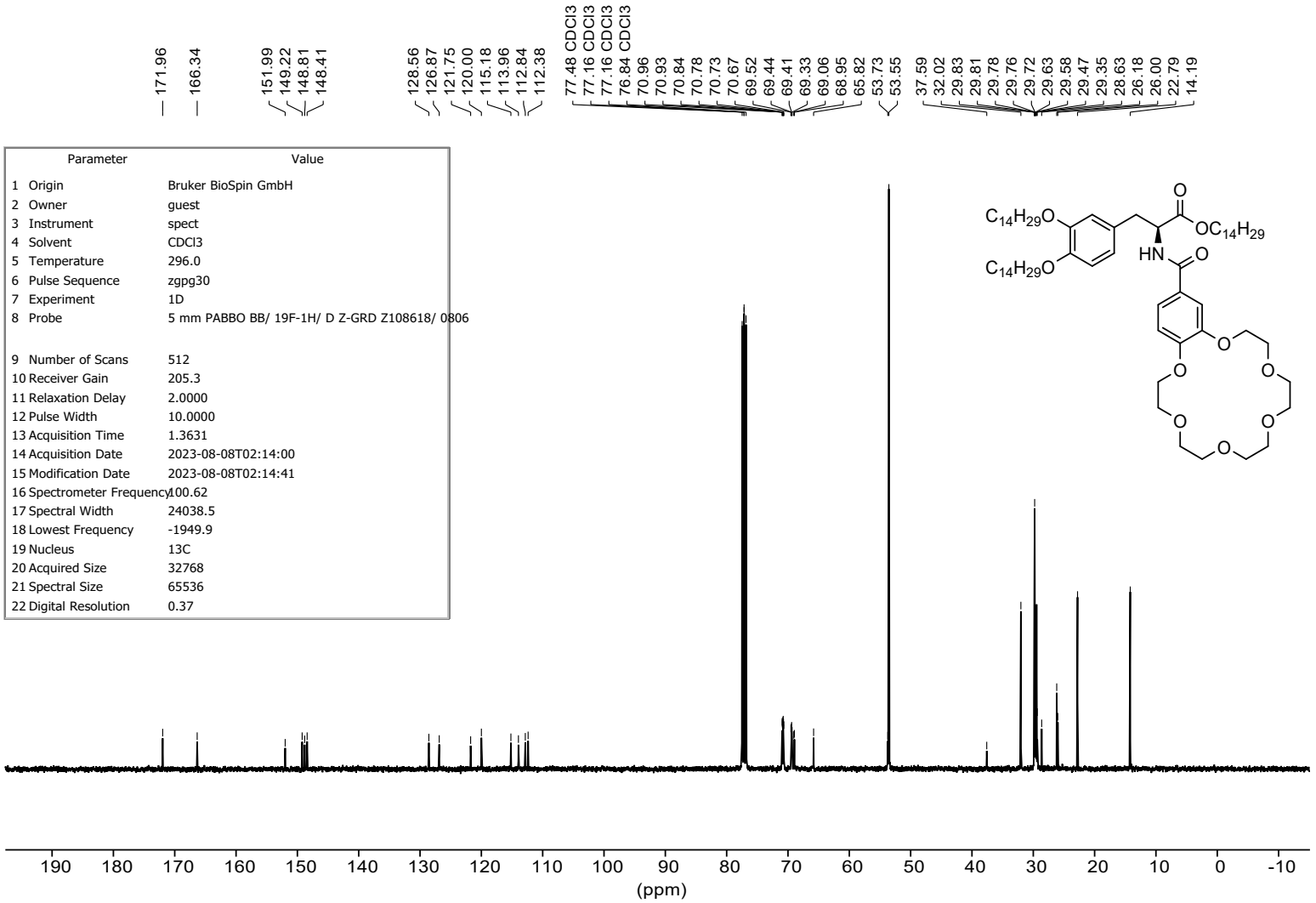

Figure S37: ^{13}C NMR spectrum of **c-DOPA(14)** at 101 MHz.

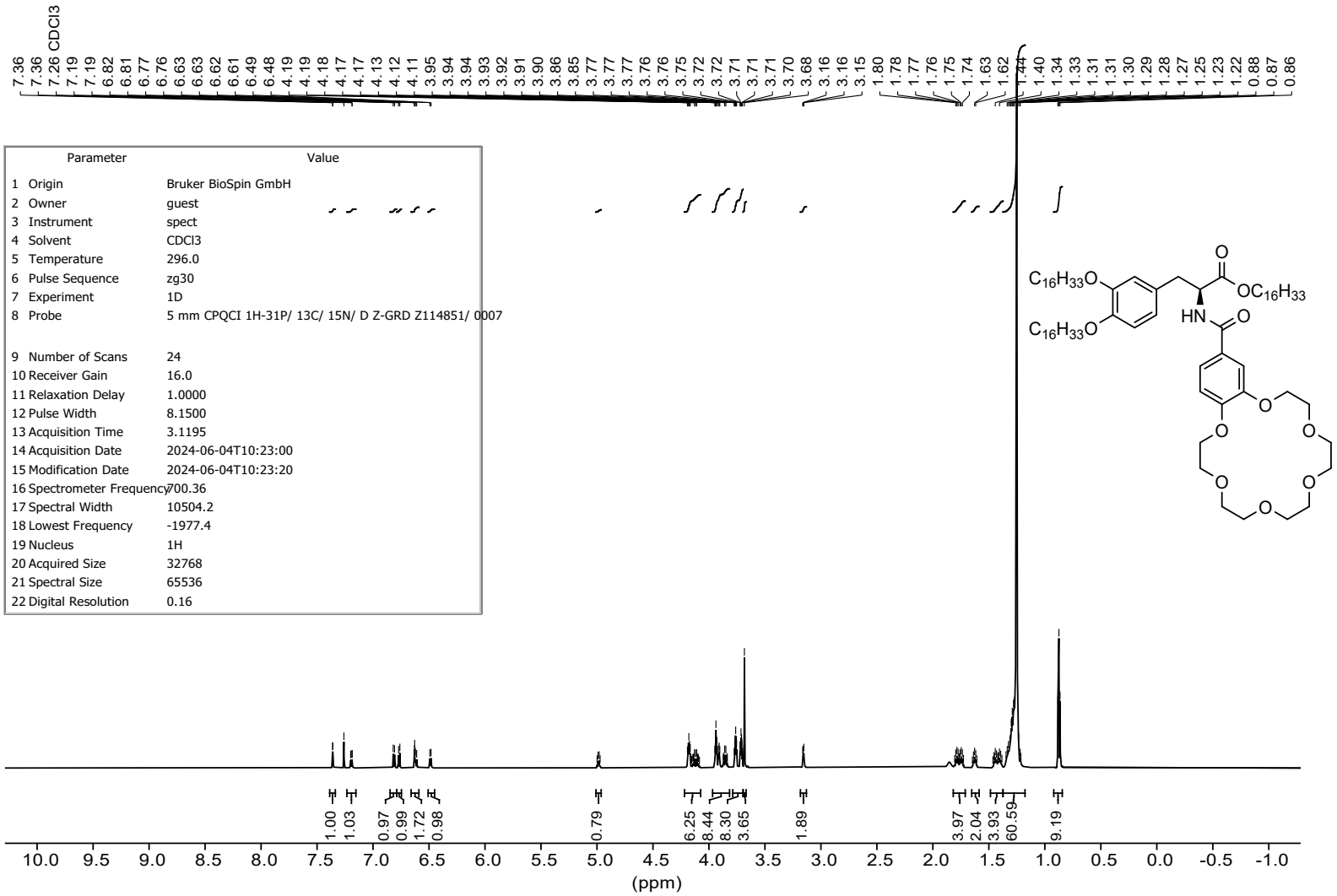

Figure S38: ^{1}H NMR spectrum of **c-DOPA(16)** at 700 MHz.

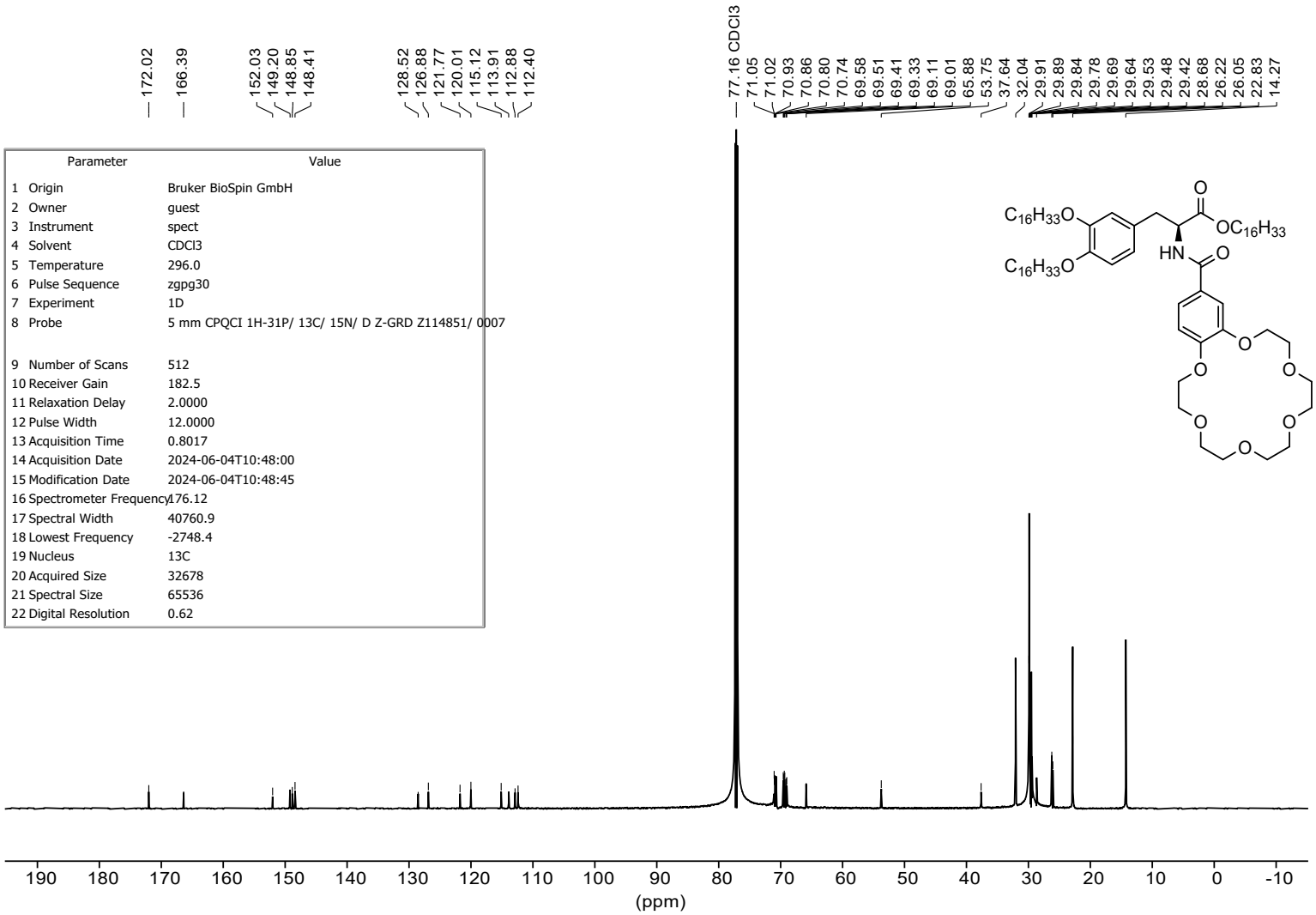

Figure S39: ^{13}C NMR spectrum of **c-DOPA(16)** at 176 MHz.

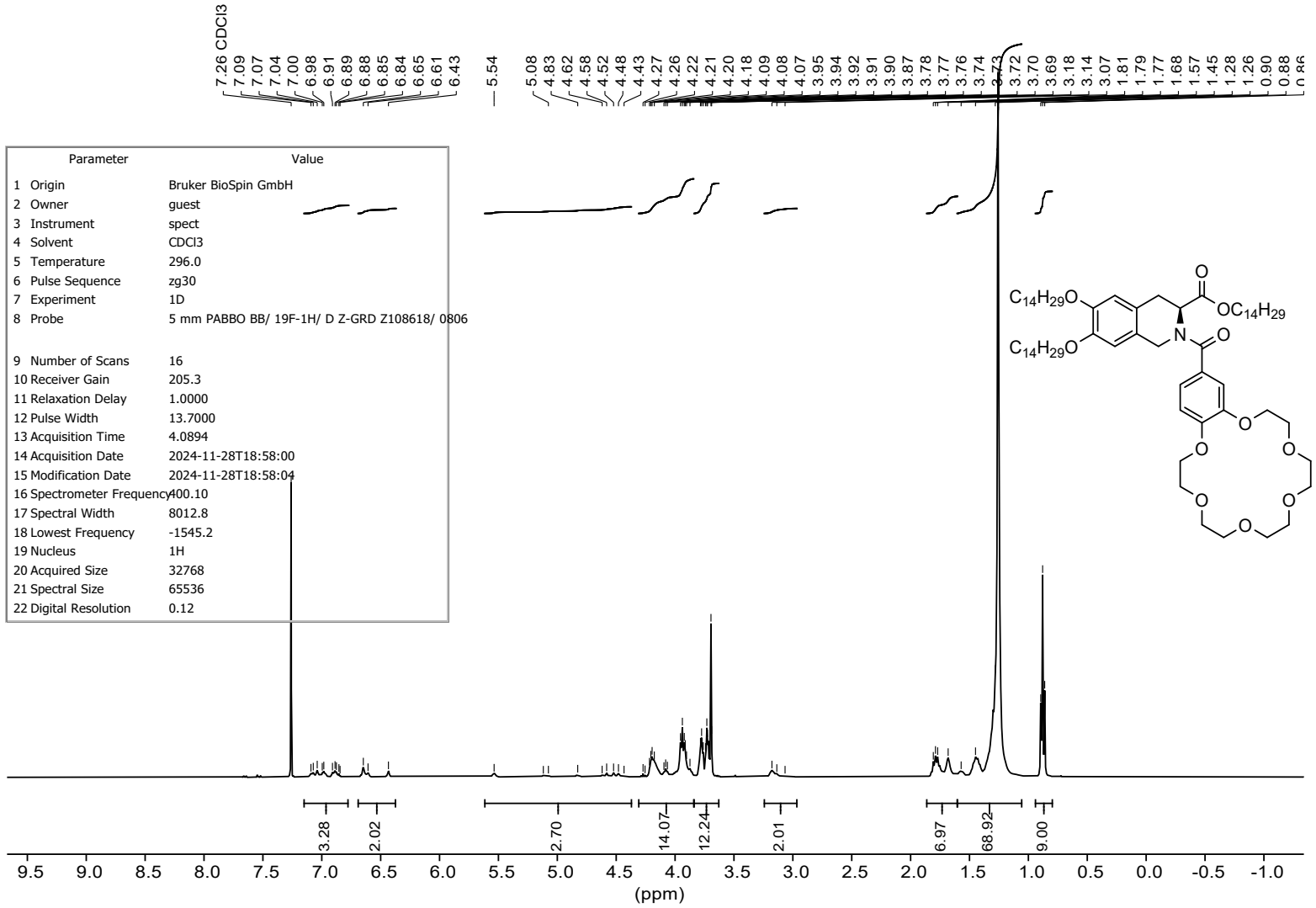

Figure S40: ^{1}H NMR spectrum of **c-THIQ(14)** at 400 MHz.

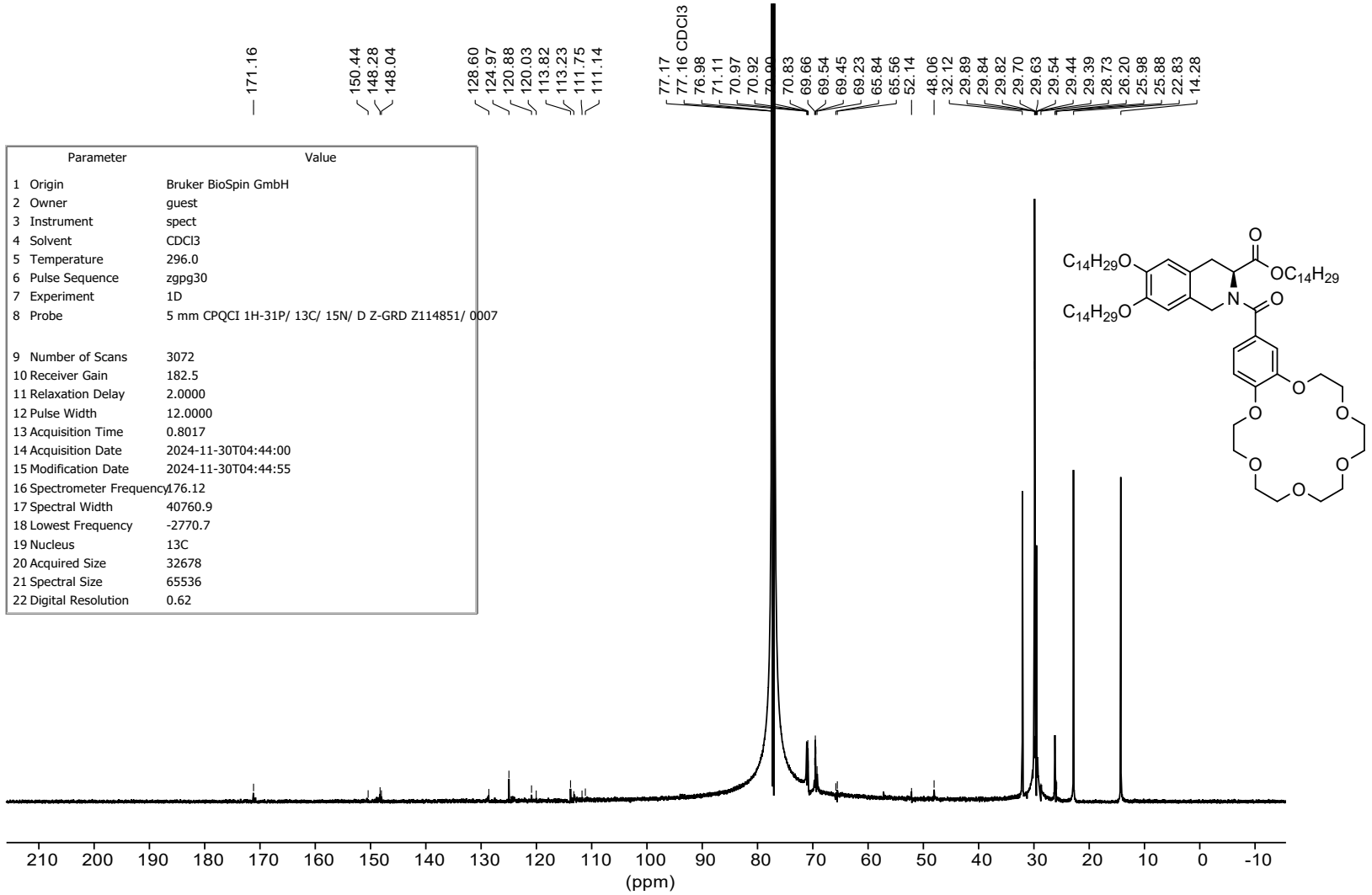

Figure S41: ^{13}C NMR spectrum of **c-THIQ(14)** at 176 MHz.

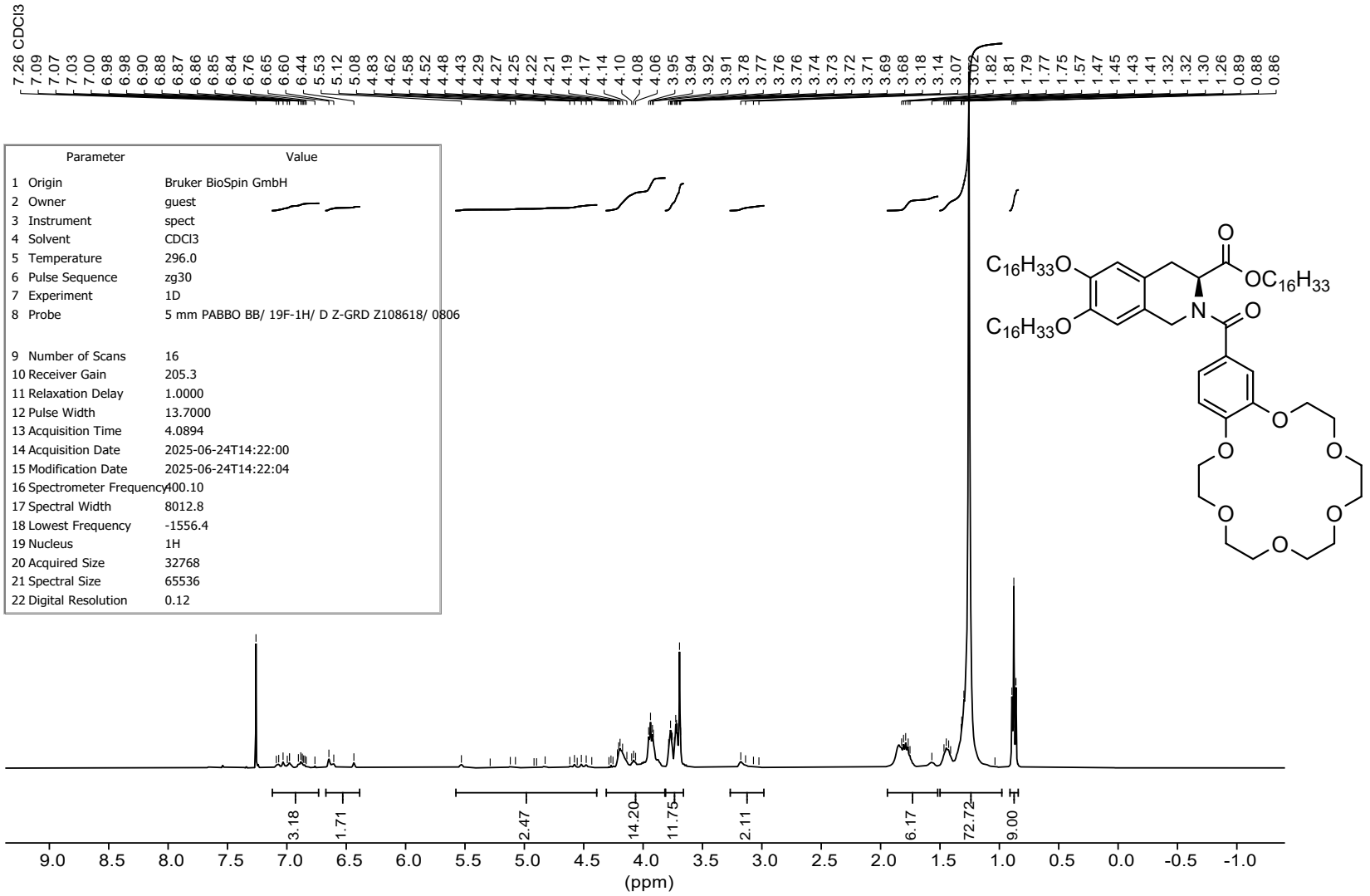

Figure S42: ^{1}H NMR spectrum of **c-THIQ(16)** at 400 MHz.

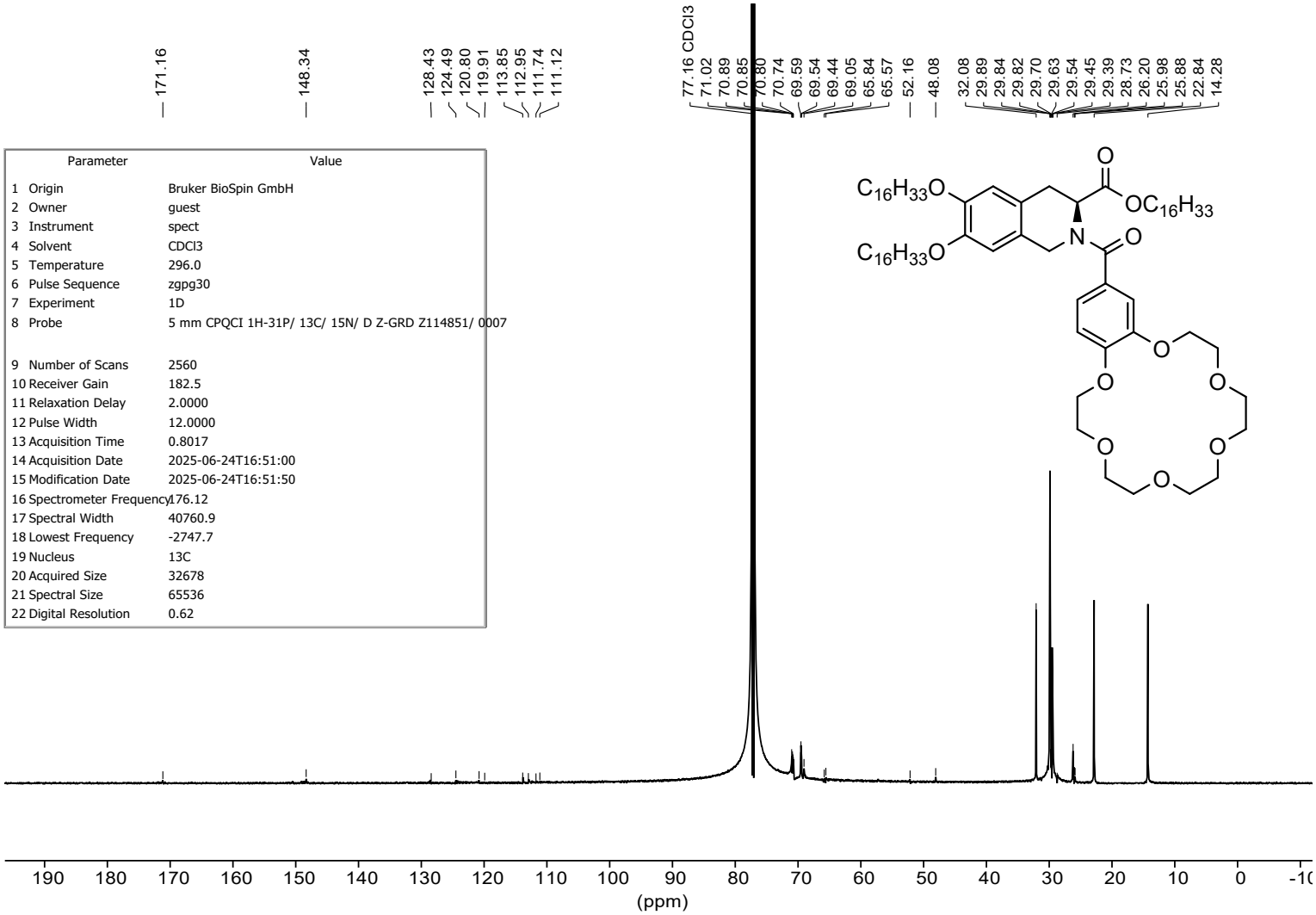

Figure S43: ^{13}C NMR spectrum of **c-THIQ(16)** at 176 MHz.

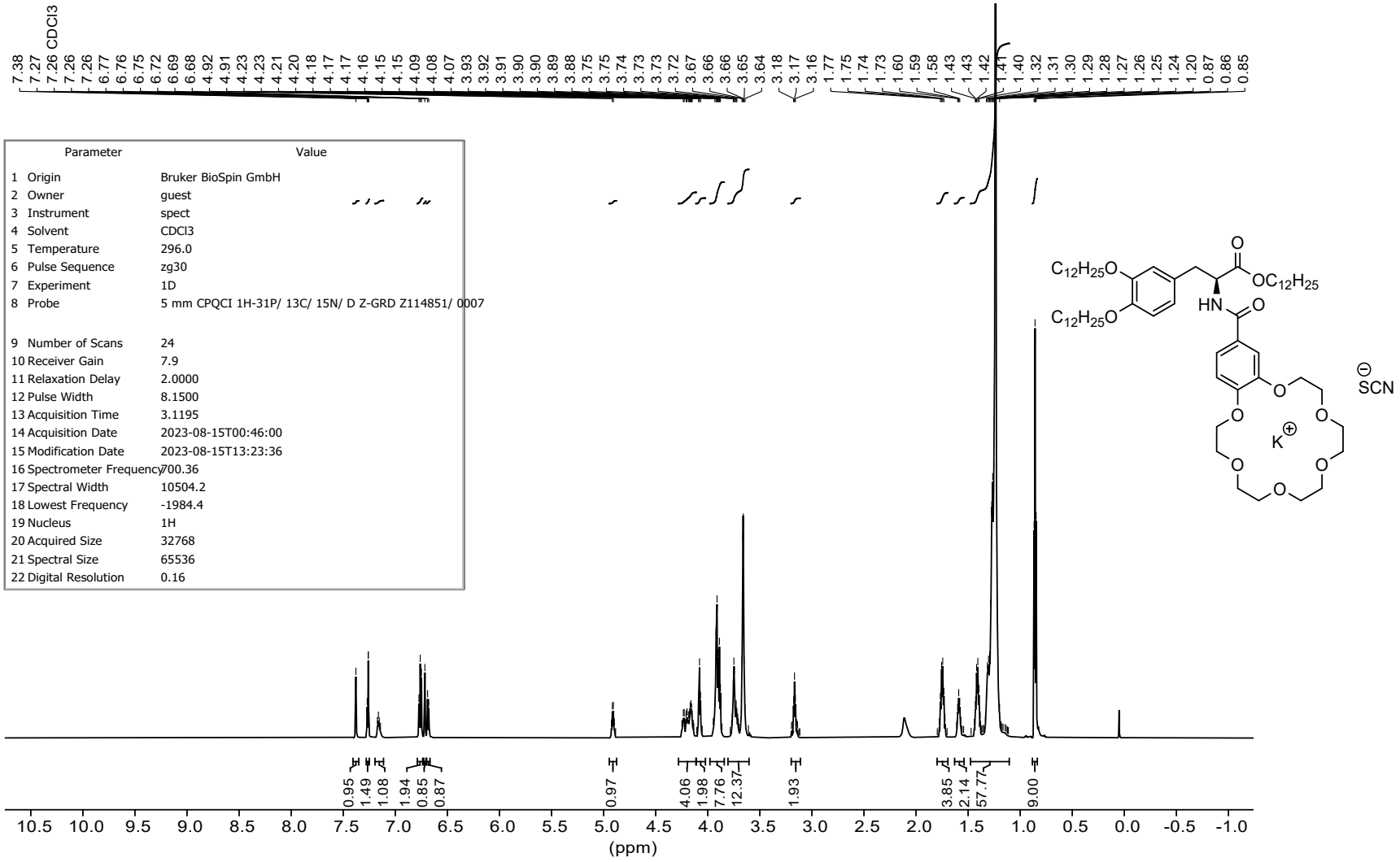

Figure S44: ^{1}H NMR spectrum of **c-DOPA(12) • KSCN** at 700 MHz.

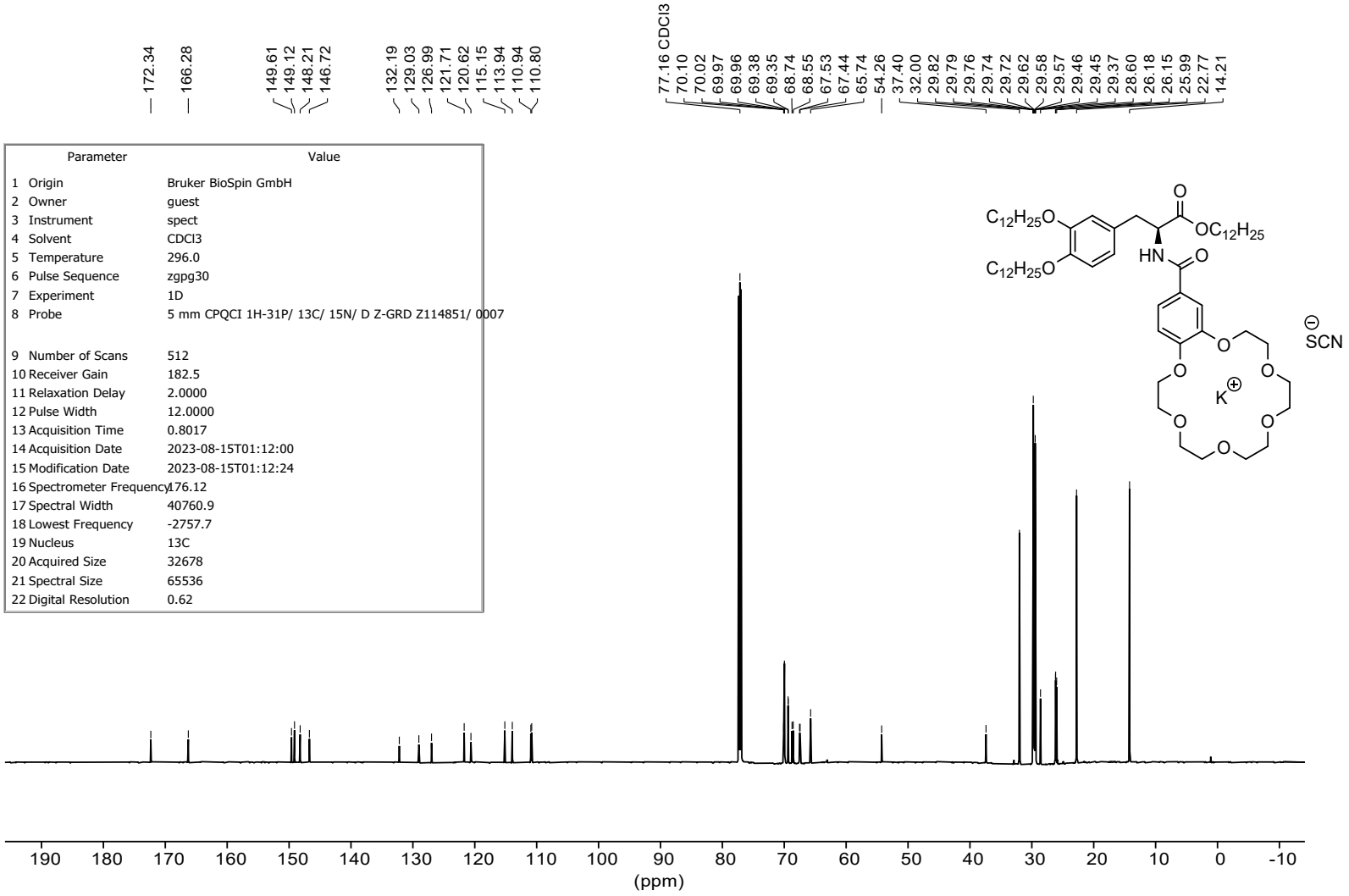

Figure S45: ^{13}C NMR spectrum of **c-DOPA(12) • KSCN** at 176 MHz.

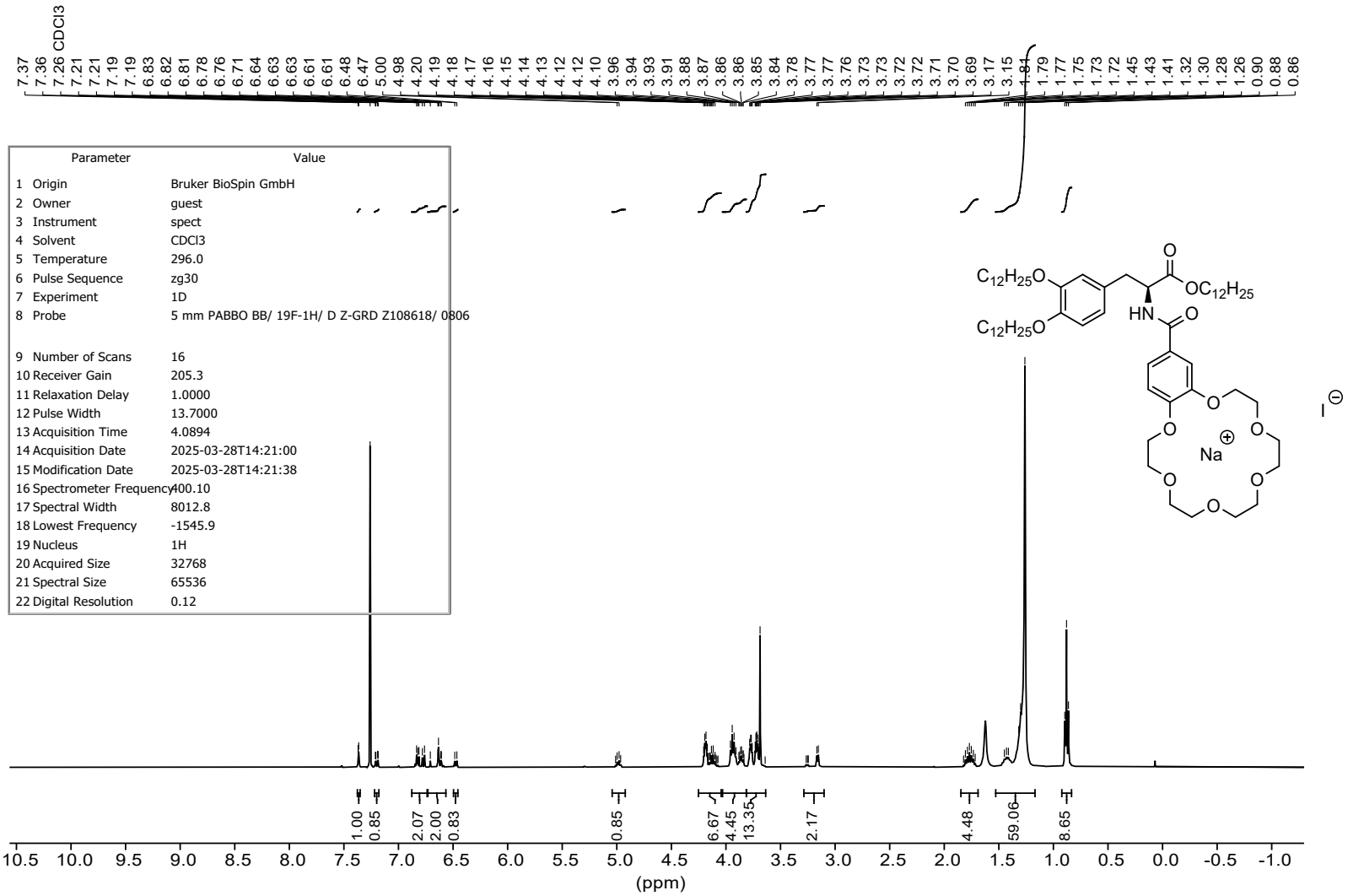

Figure S46: ^{1}H NMR spectrum of **c-DOPA(12) • NaI** at 400 MHz.

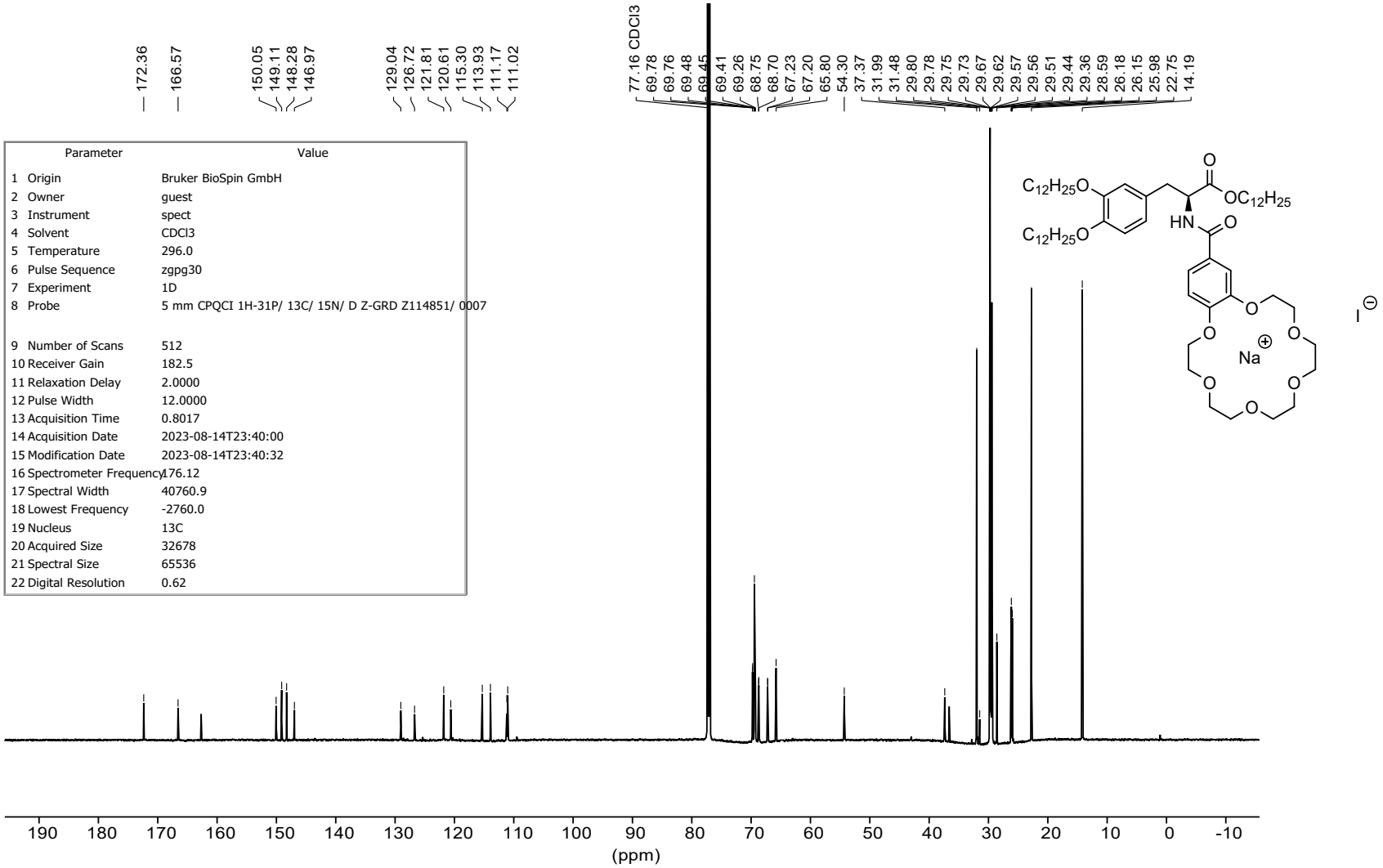

Figure S47: ^{13}C NMR spectrum of **c-DOPA(12) • NaI** at 176 MHz.

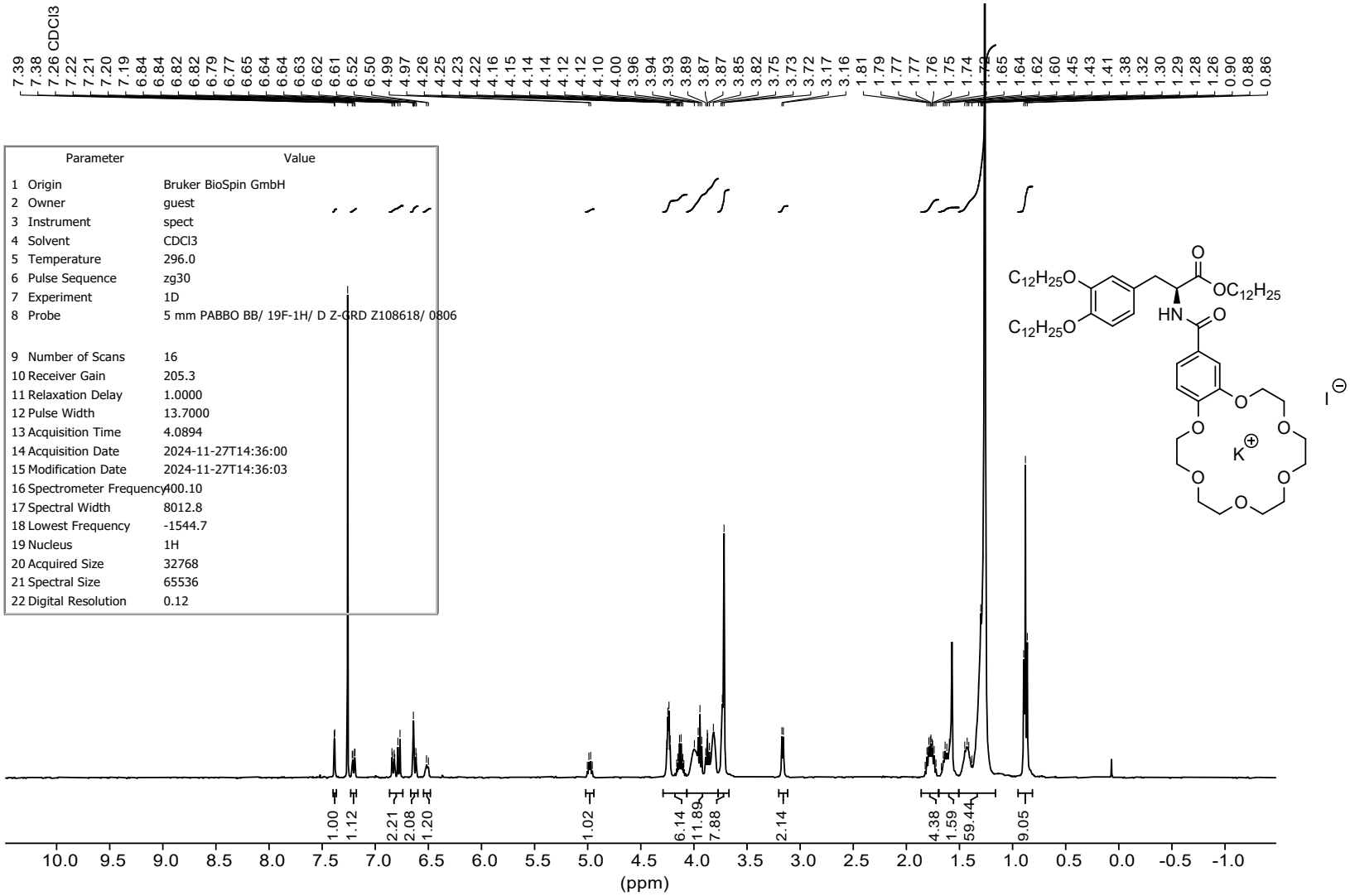

Figure S48: ^{1}H NMR spectrum of **c-DOPA(12) • KI** at 400 MHz.

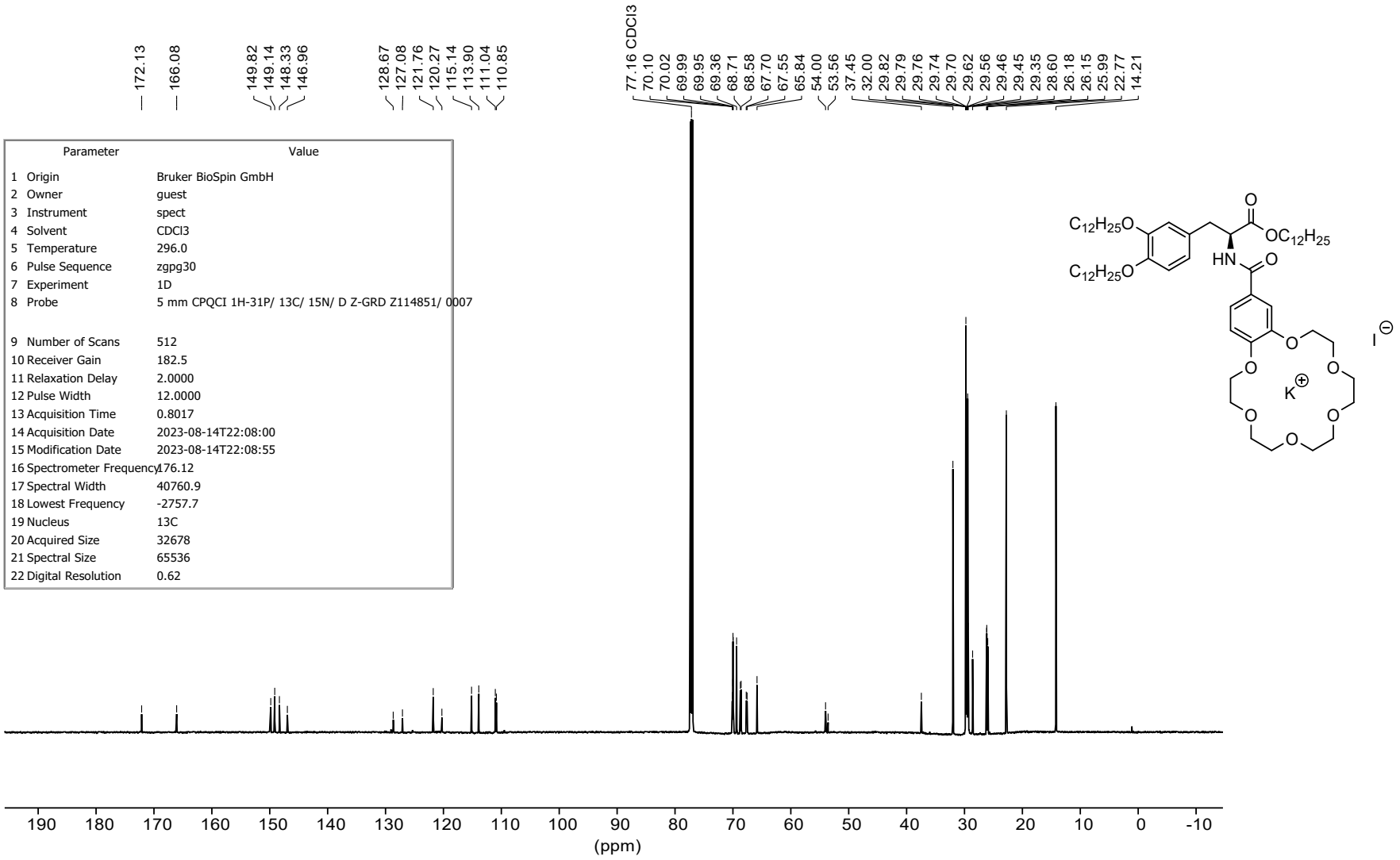

Figure S49: ^{13}C NMR spectrum of **c-DOPA(12) • KI** at 176 MHz.

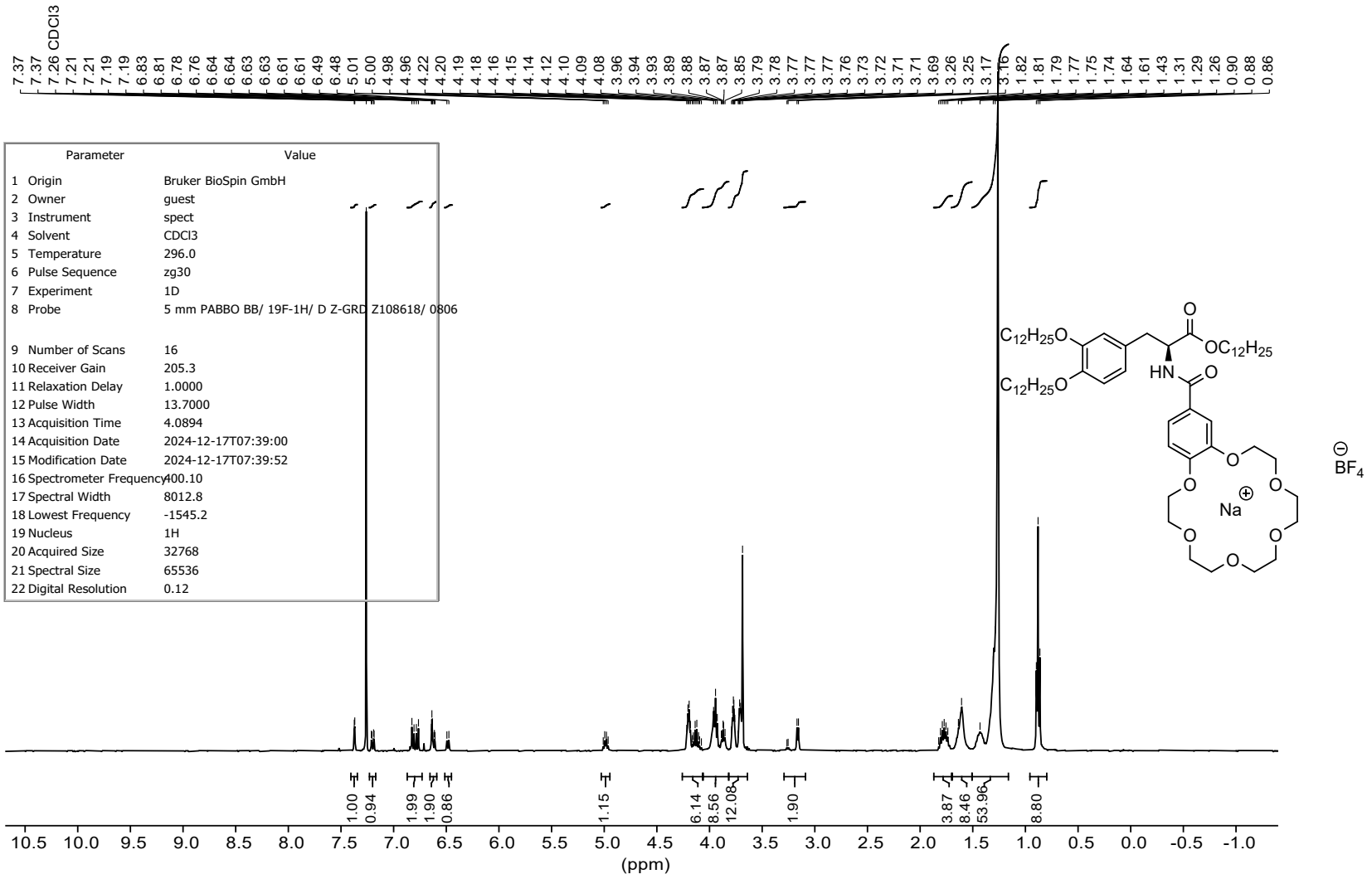

Figure S50: ^{1}H NMR spectrum of **c-DOPA(12) • $NaBF_4$** at 700 MHz.

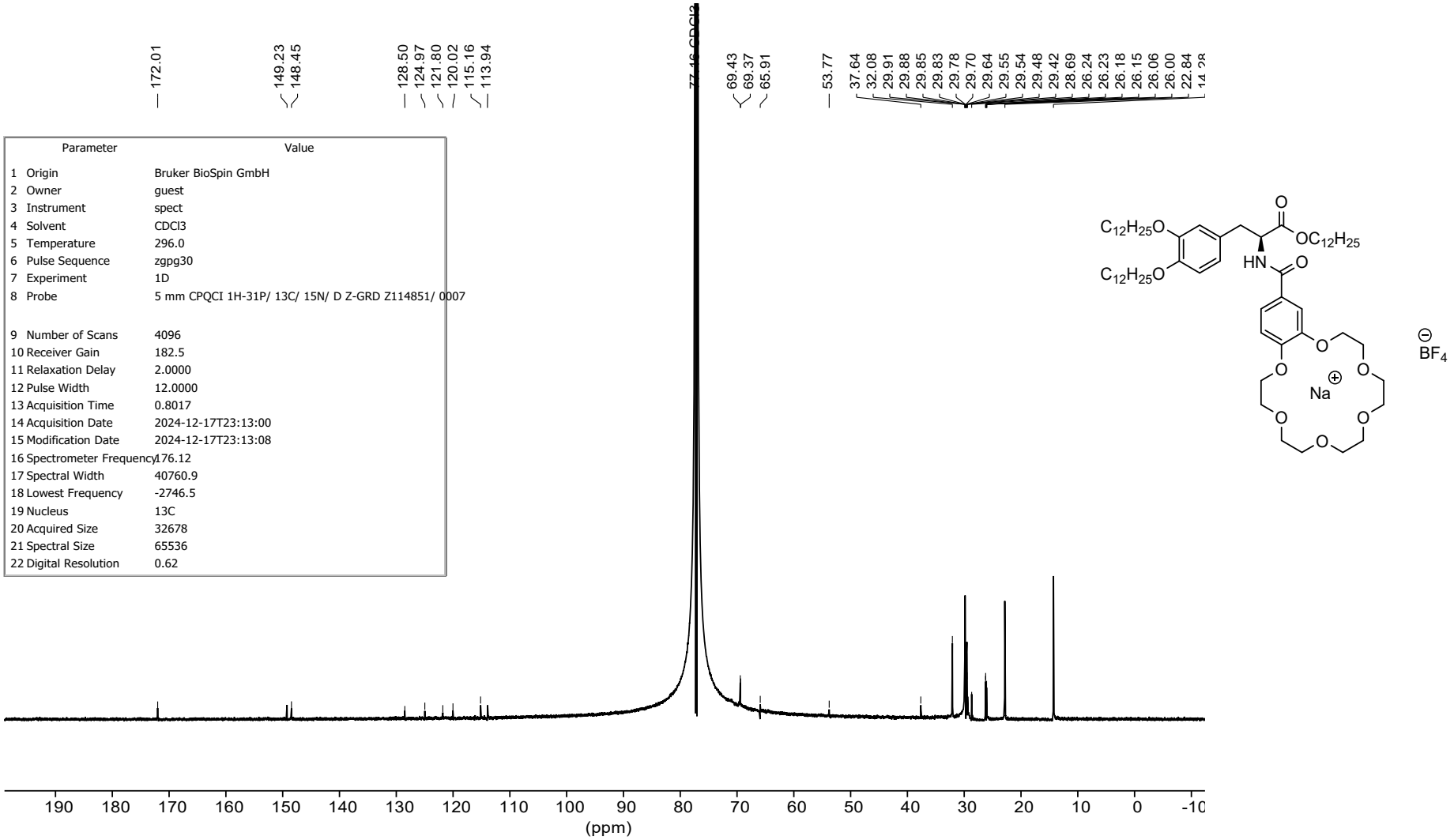

Figure S51: ^{13}C NMR spectrum of **c-DOPA(12) • $NaBF_4$** at 176 MHz.

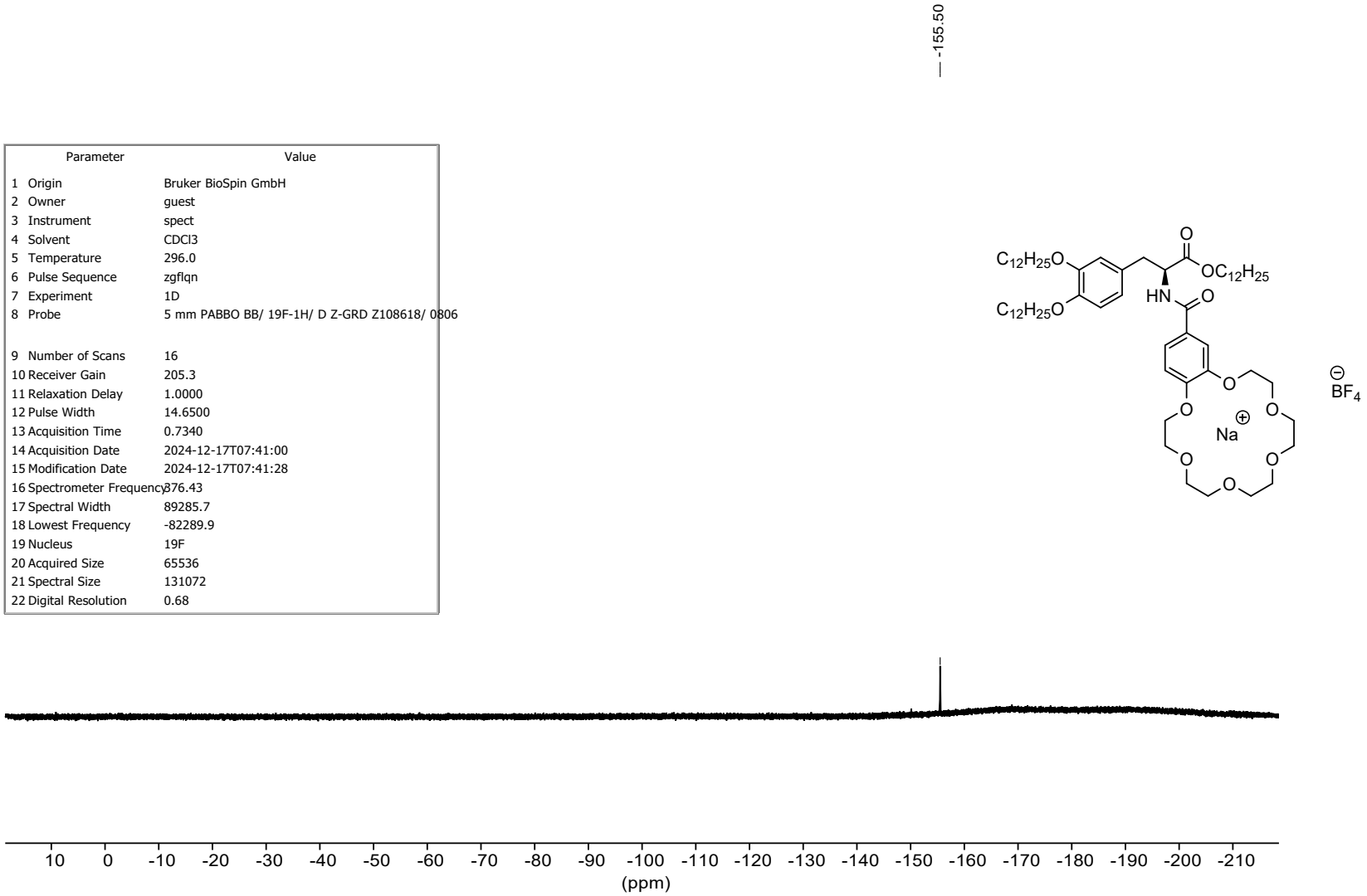

Figure S52: ^{19}F NMR spectrum of **c-DOPA(12) • $NaBF_4$** at 376 MHz.

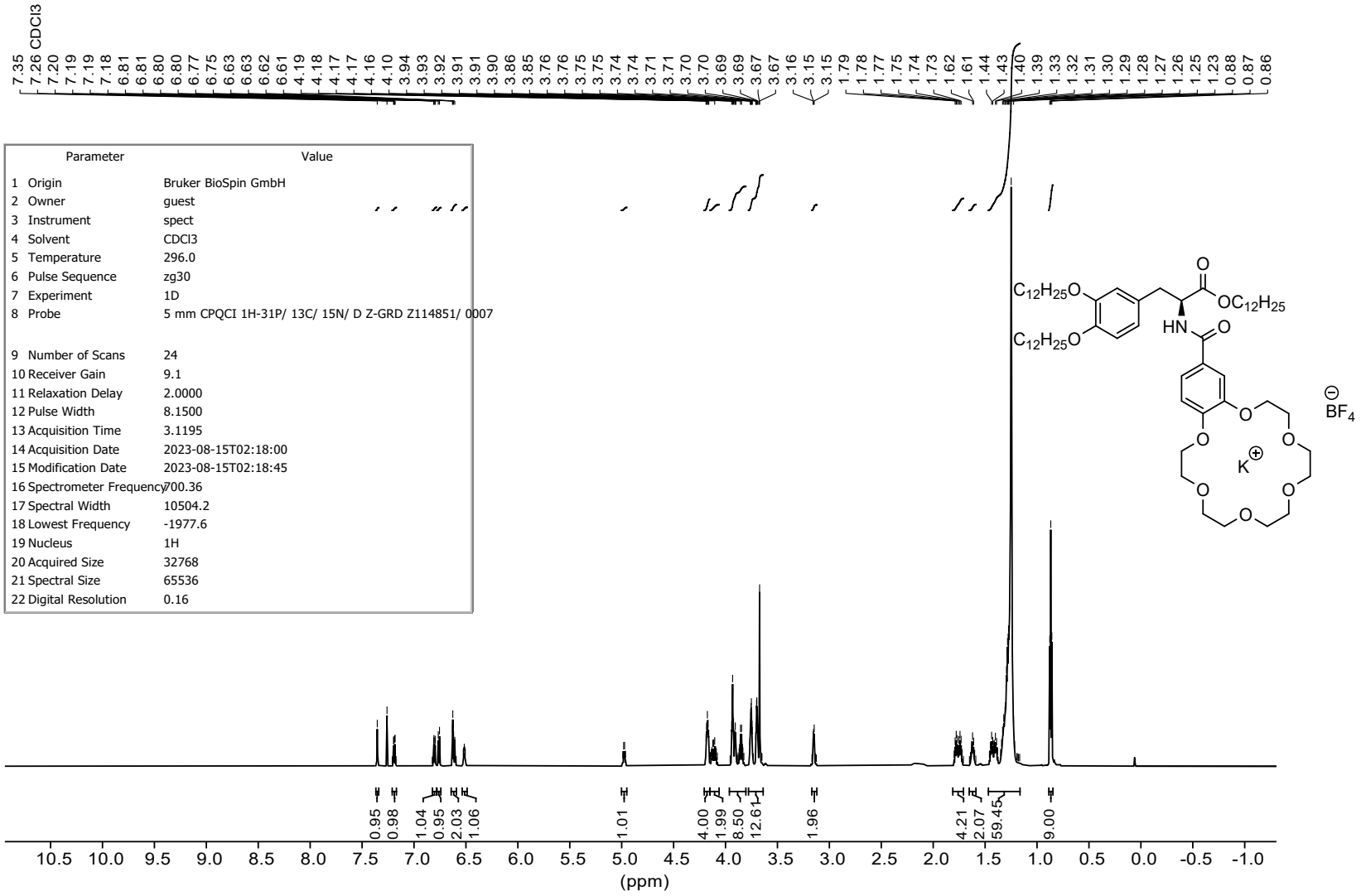

Figure S53: ^{1}H NMR spectrum of **c-DOPA(12) • KBF_4** at 700 MHz.

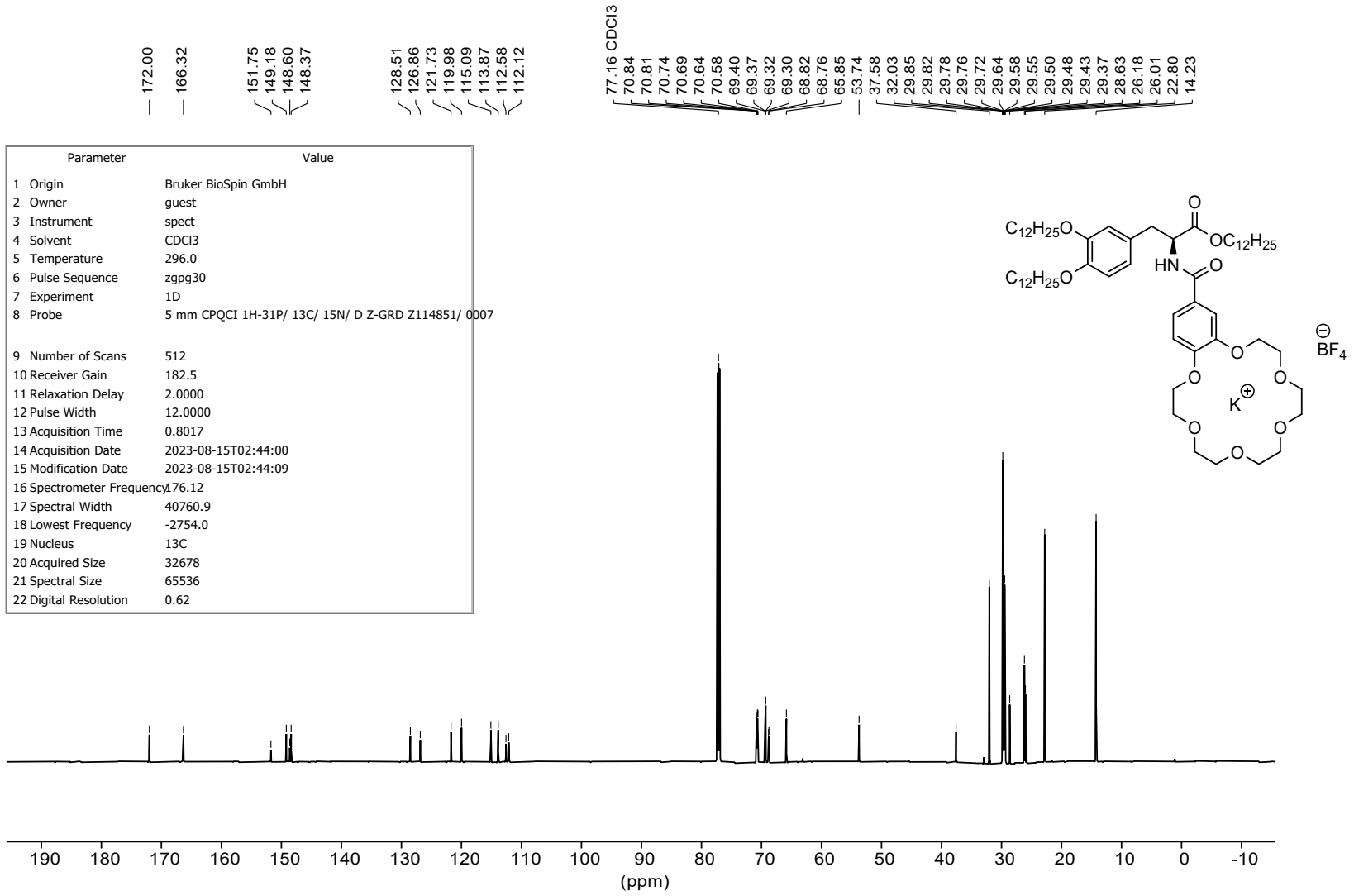

Figure S54: ^{13}C NMR spectrum of **c-DOPA(12) • KBF_4** at 176 MHz.

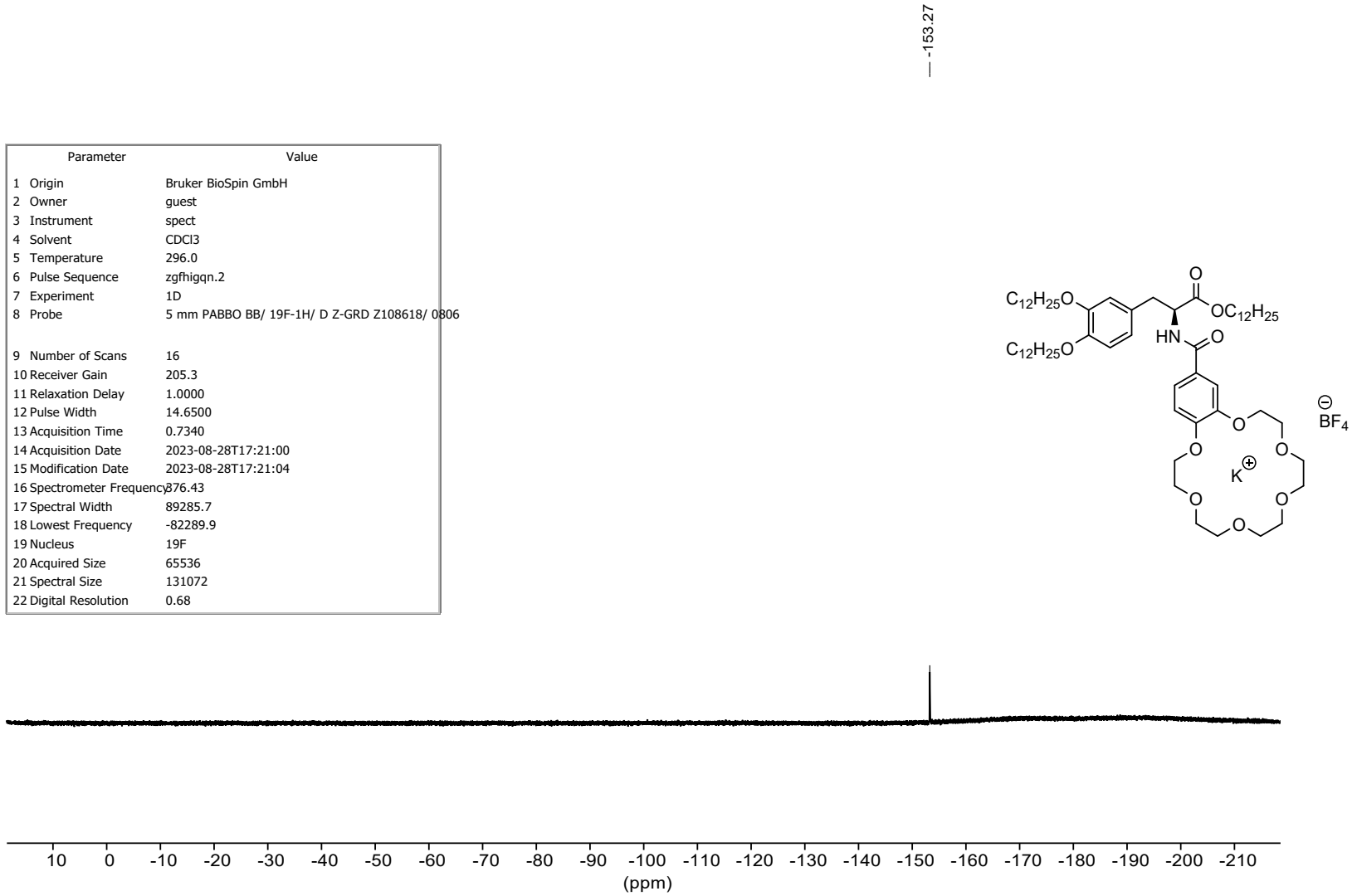

Figure S55: ^{19}F NMR spectrum of **c-DOPA(12) • KBF_4** at 376 MHz.

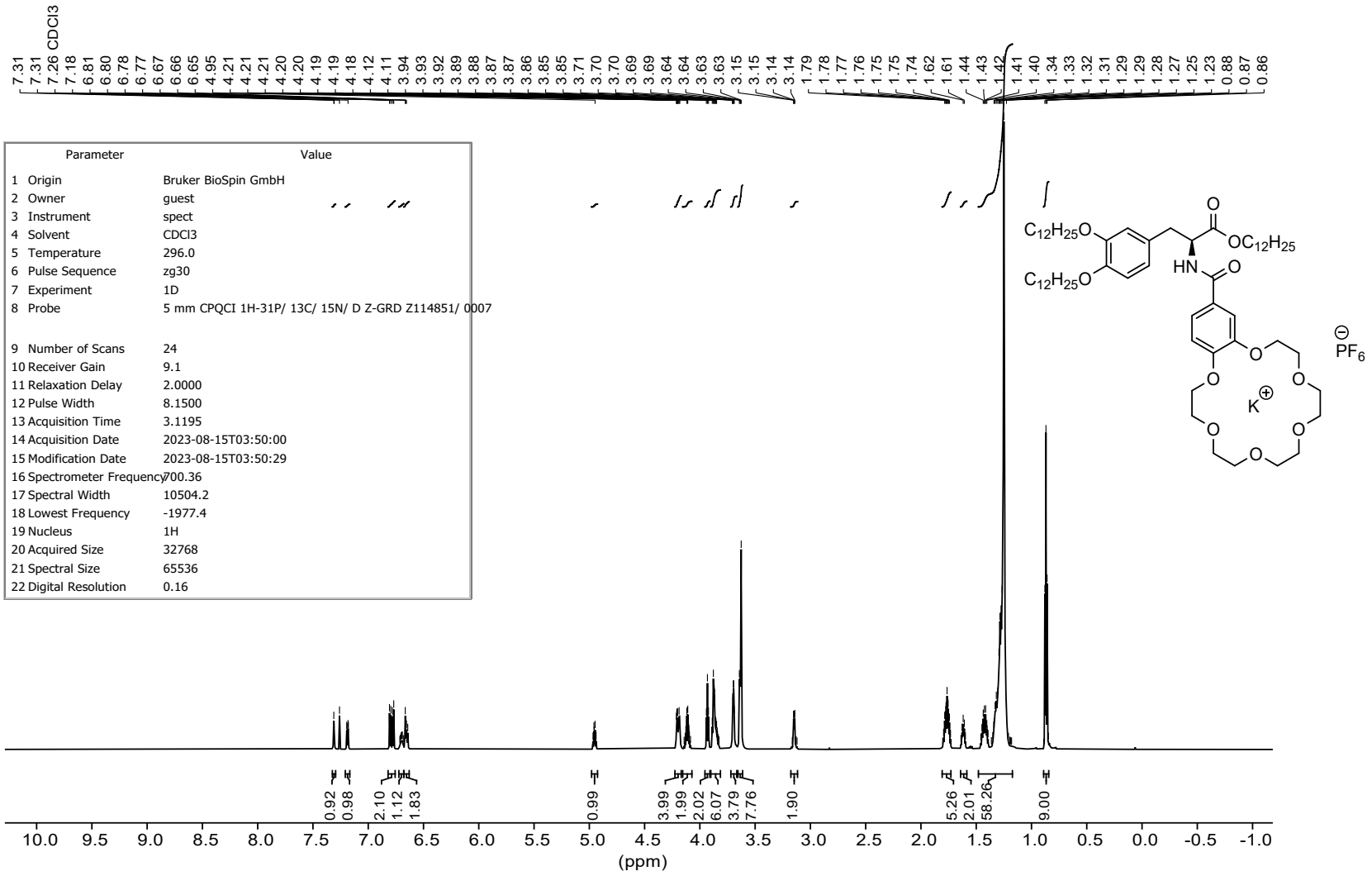

Figure S56: ^{1}H NMR spectrum of **c-DOPA(12) • KPF_6** at 700 MHz.

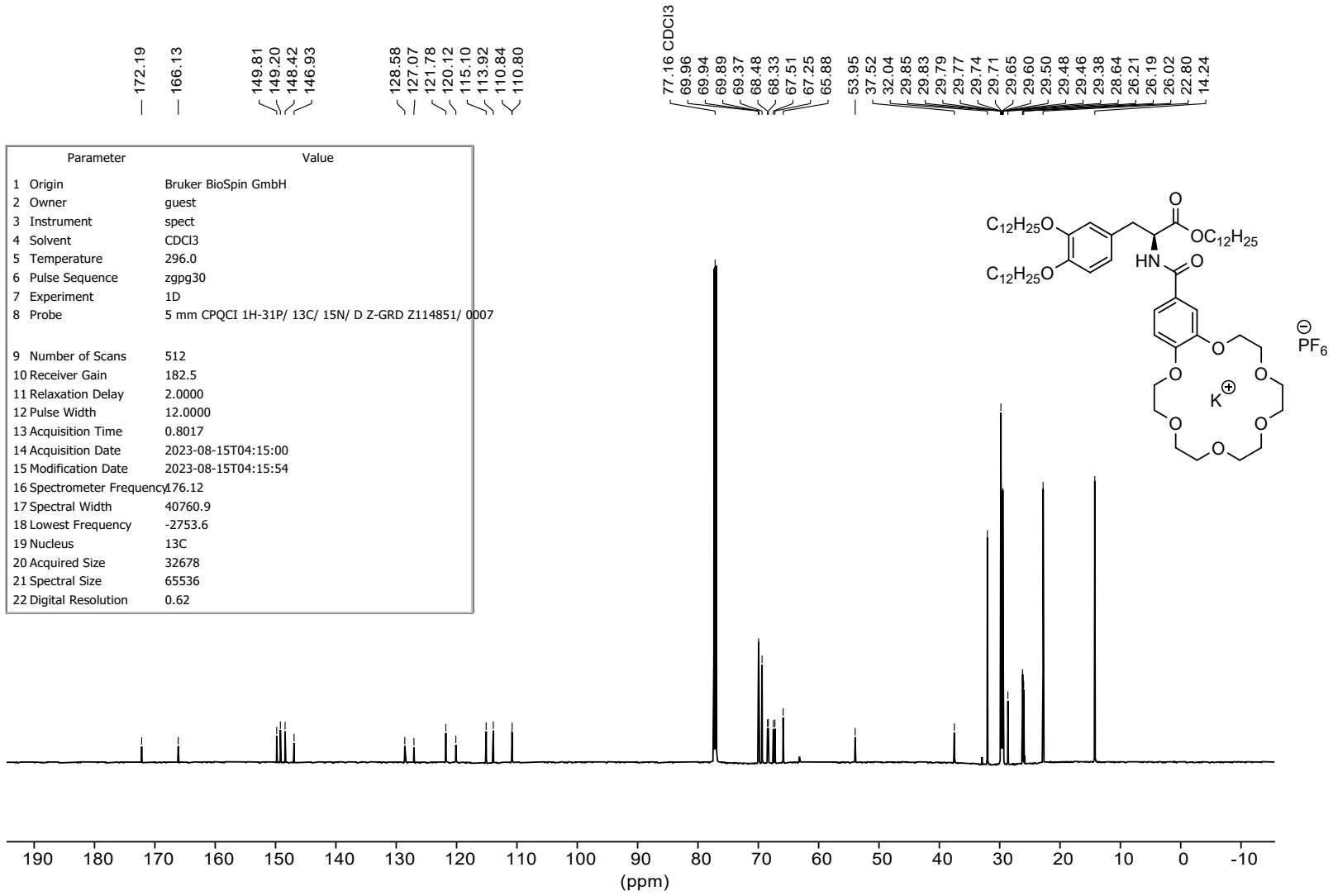

Figure S57: ^{13}C NMR spectrum of **c-DOPA(12) • KPF_6** at 176 MHz.

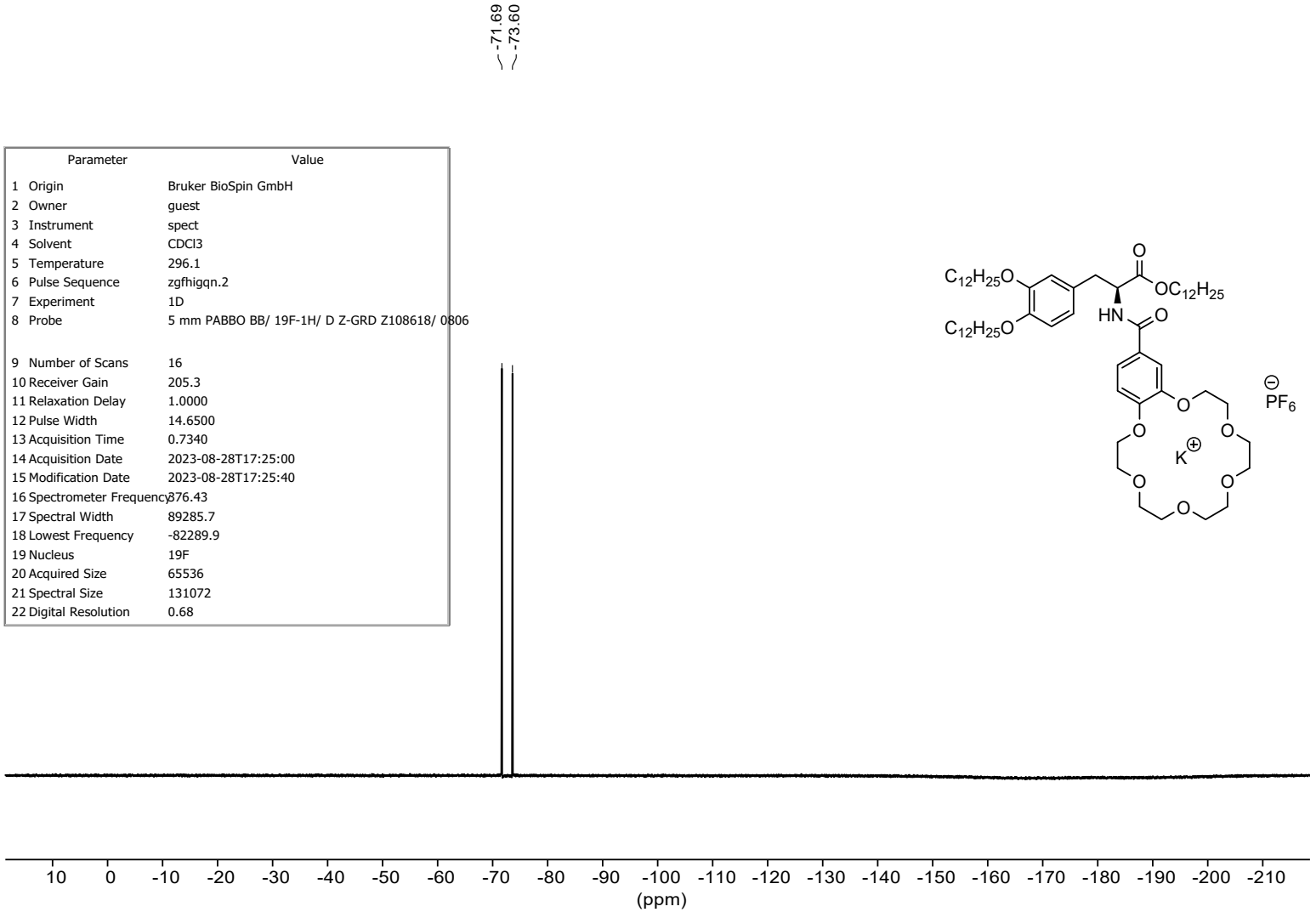

Figure S58: ^{19}F NMR spectrum of **c-DOPA(12) • KPF_6** at 376 MHz.

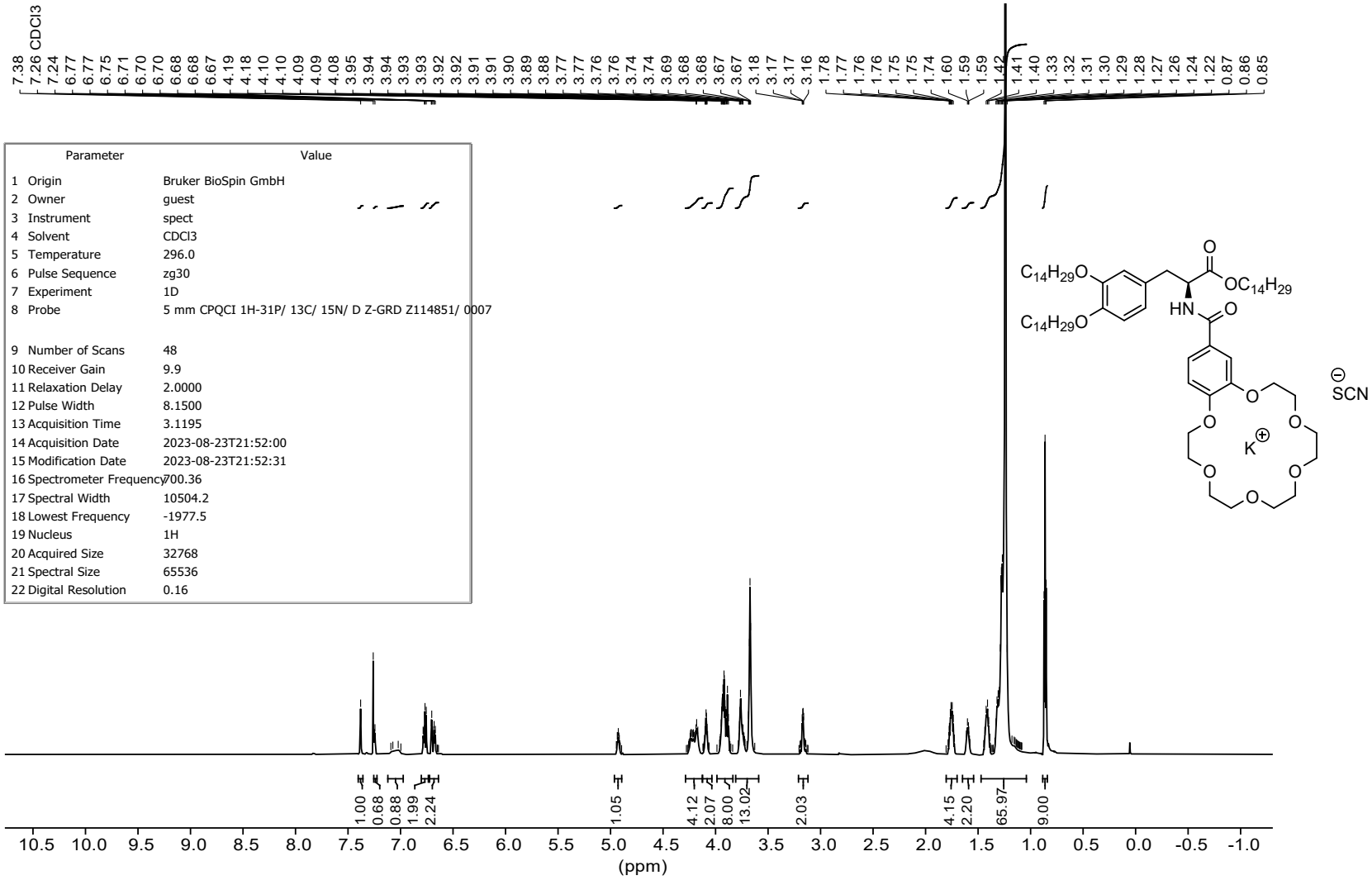

Figure S59: ^{1}H NMR spectrum of **c-DOPA(14) • KSCN** at 700 MHz.

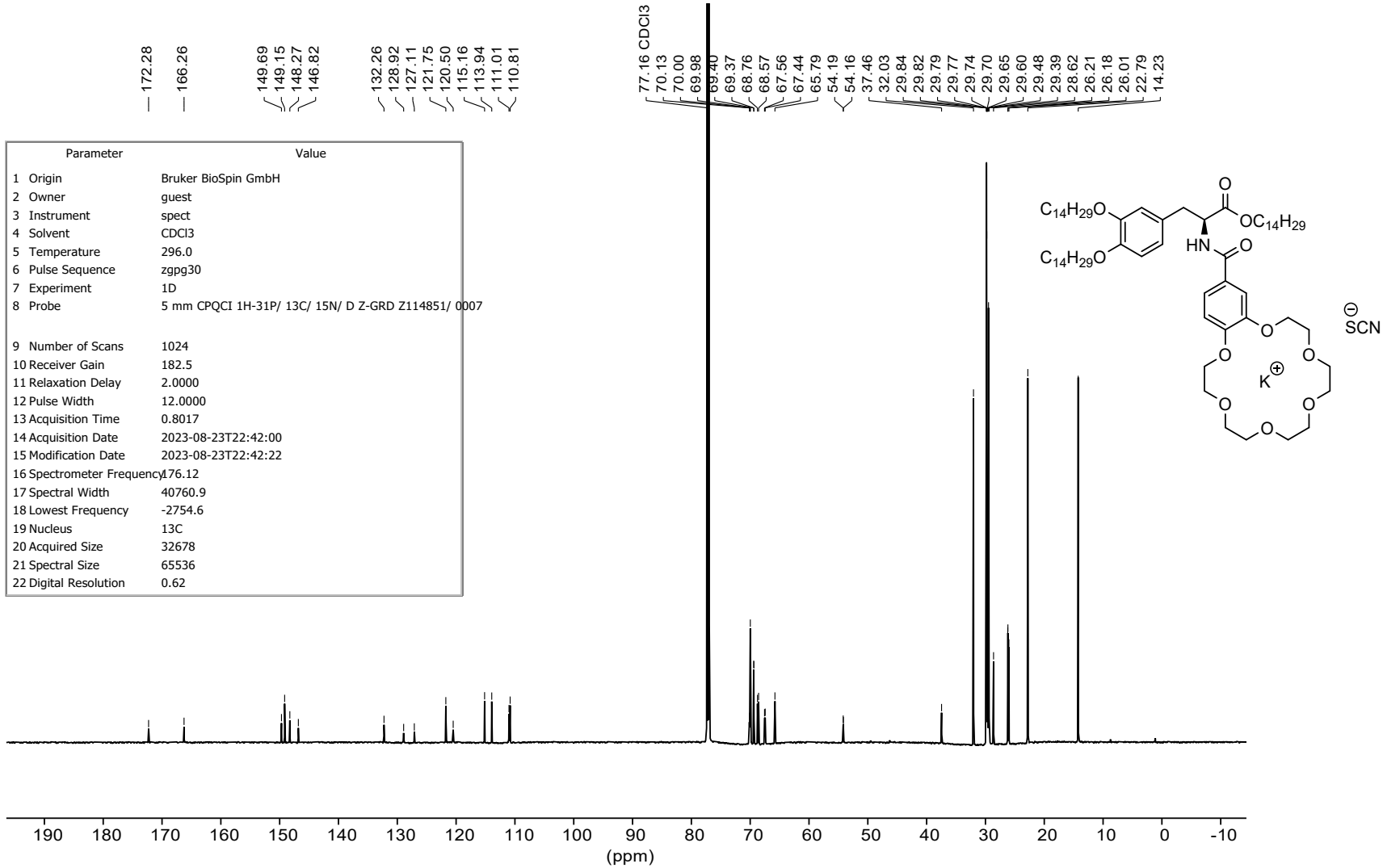

Figure S60: ^{13}C NMR spectrum of **c-DOPA(14) • KSCN** at 176 MHz.

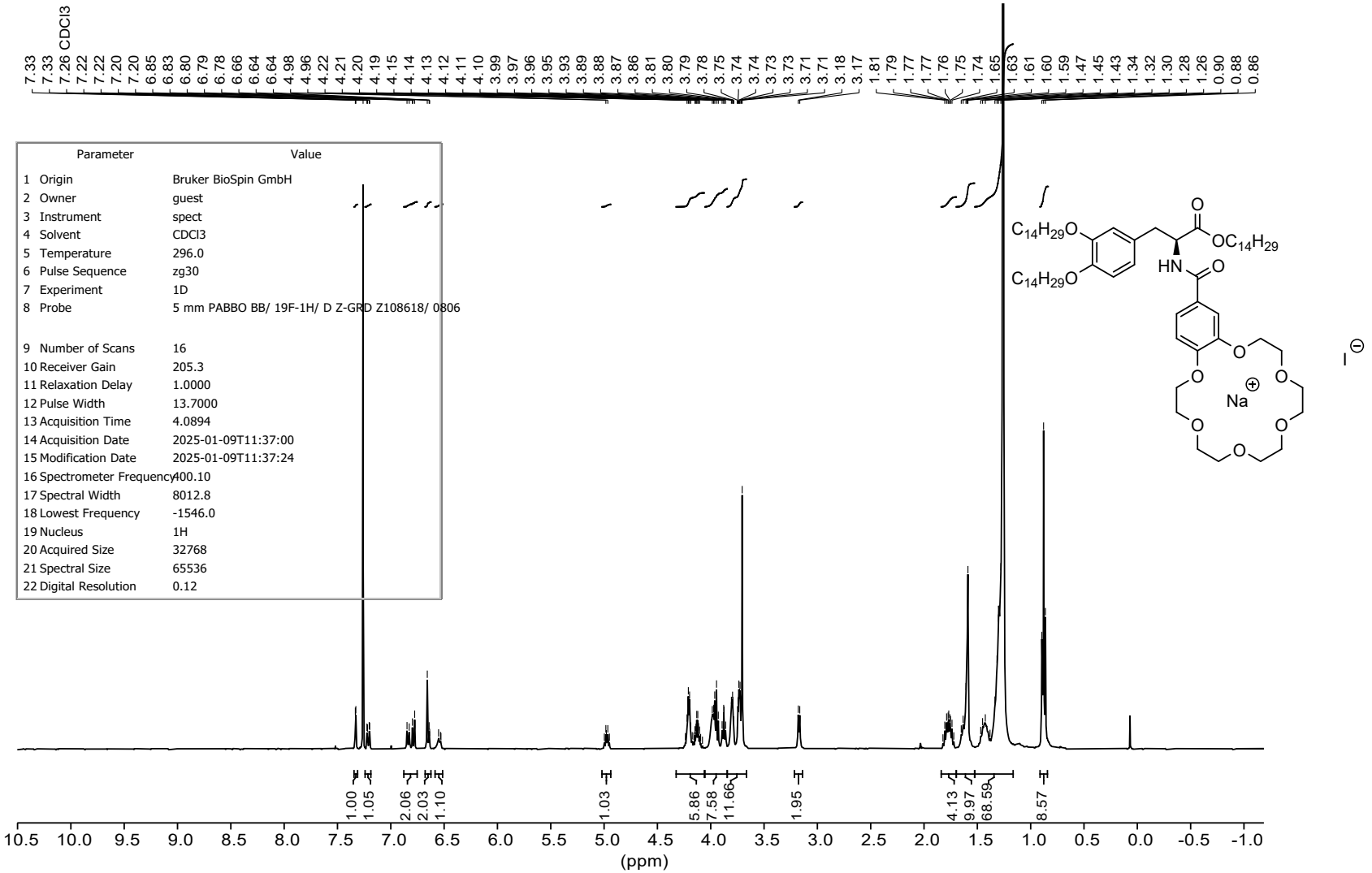

Figure S61: ^{1}H NMR spectrum of **c-DOPA(14) • NaI** at 400 MHz.

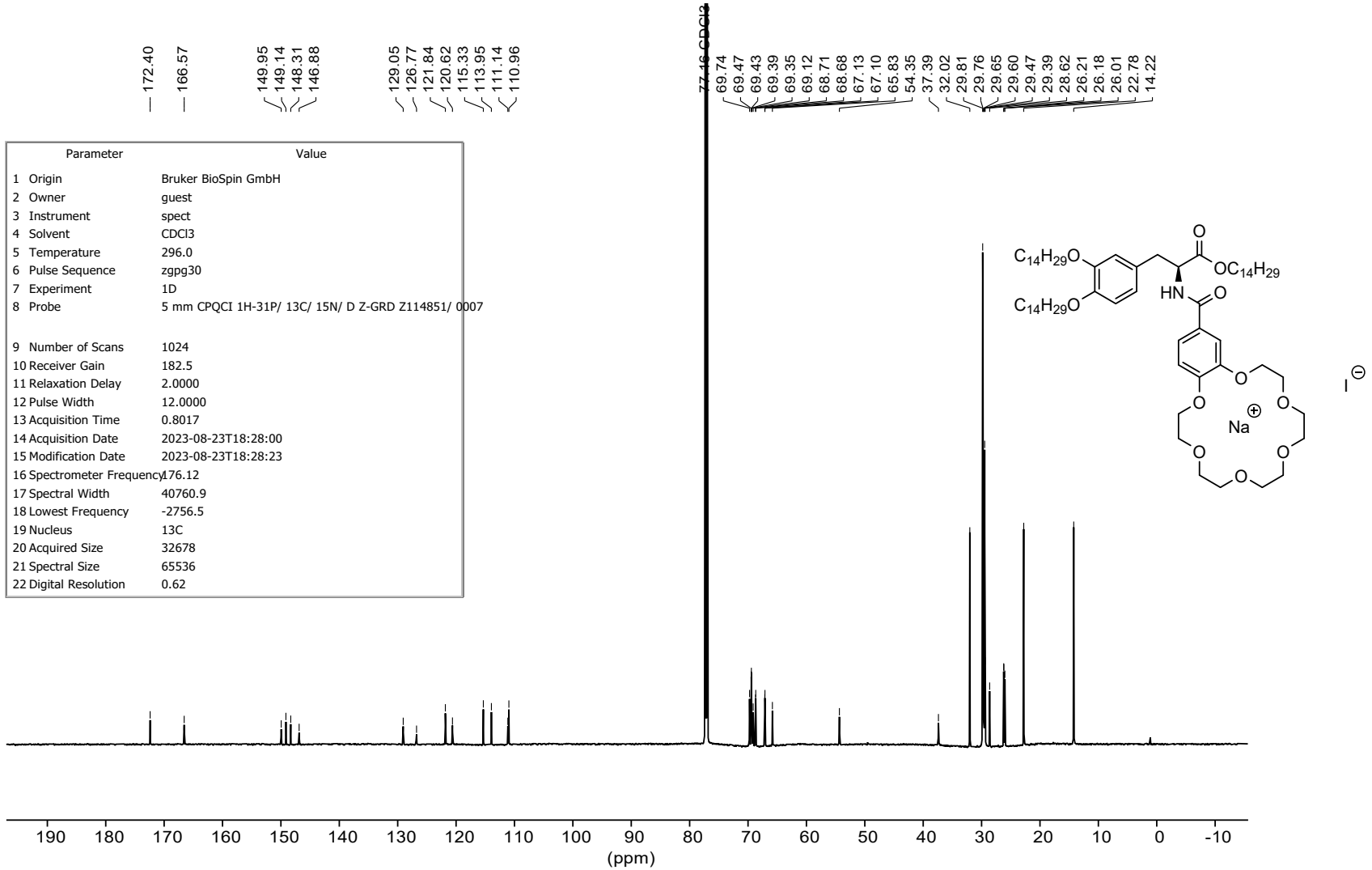

Figure S62: ^{13}C NMR spectrum of **c-DOPA(14) • NaI** at 176 MHz.

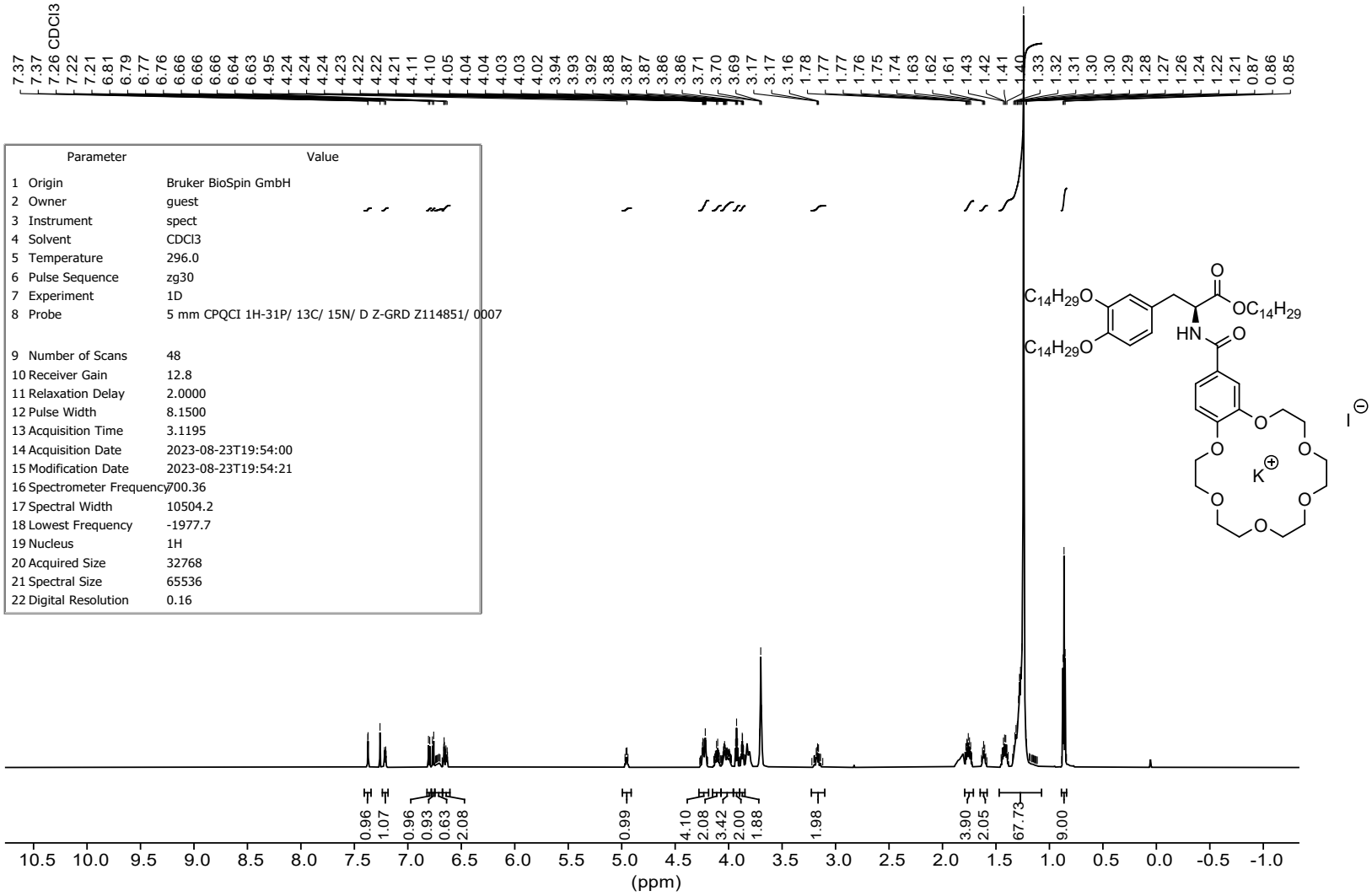

Figure S63: ^{1}H NMR spectrum of **c-DOPA(14) • KI** at 700 MHz.

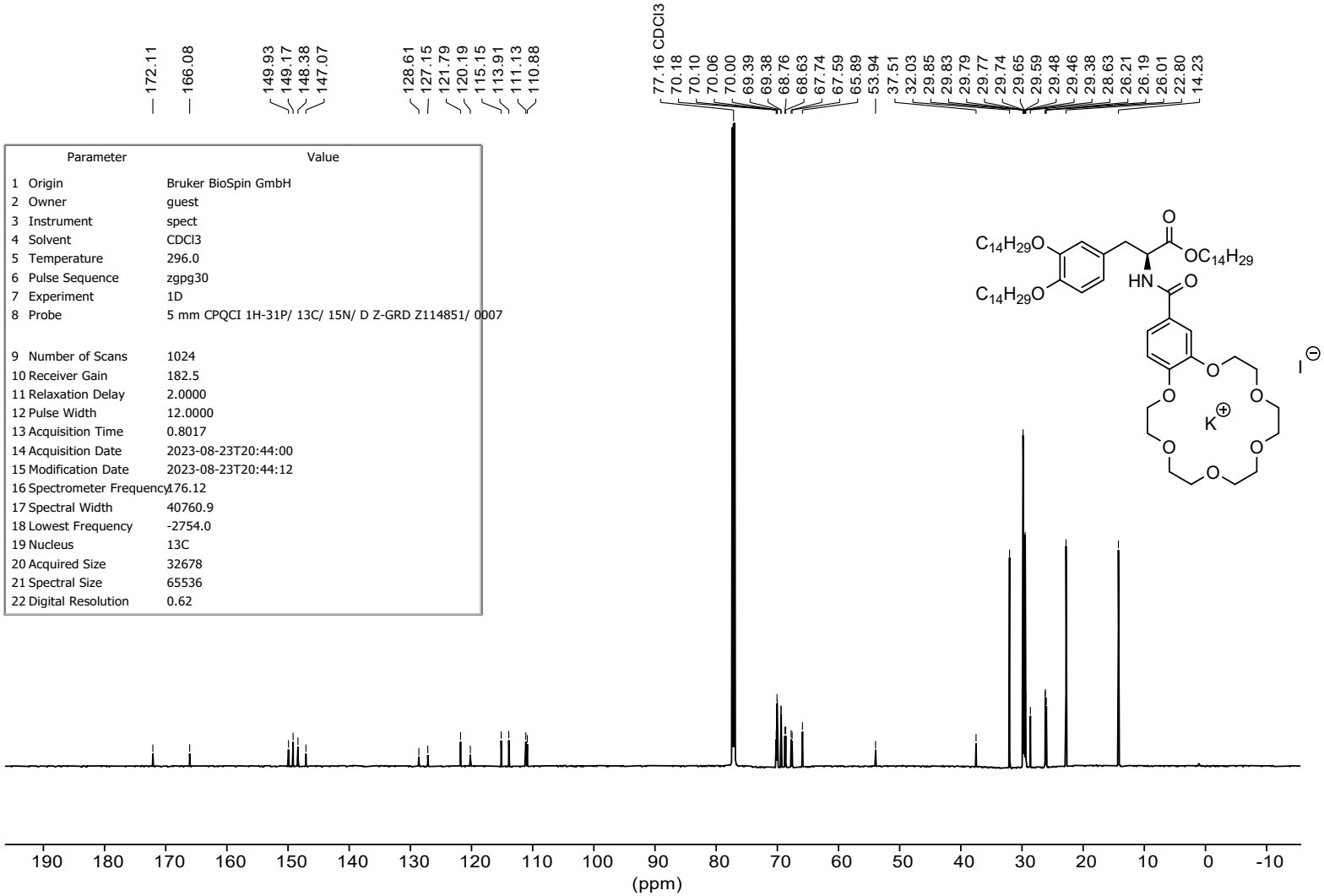

Figure S64: ^{13}C NMR spectrum of **c-DOPA(14) • KI** at 176 MHz.

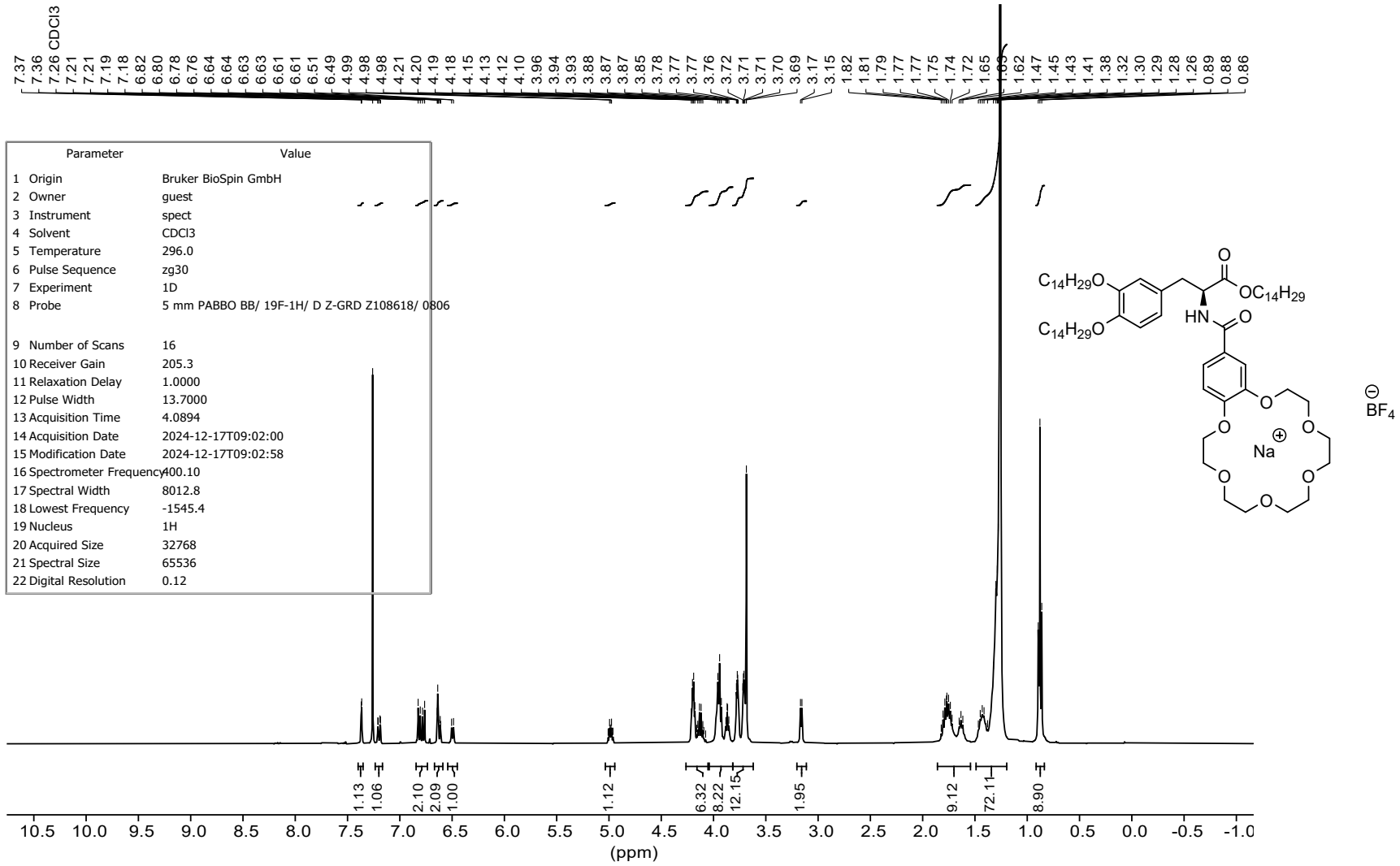

Figure S65: ^{1}H NMR spectrum of **c-DOPA(14) • $NaBF_4$** at 400 MHz.

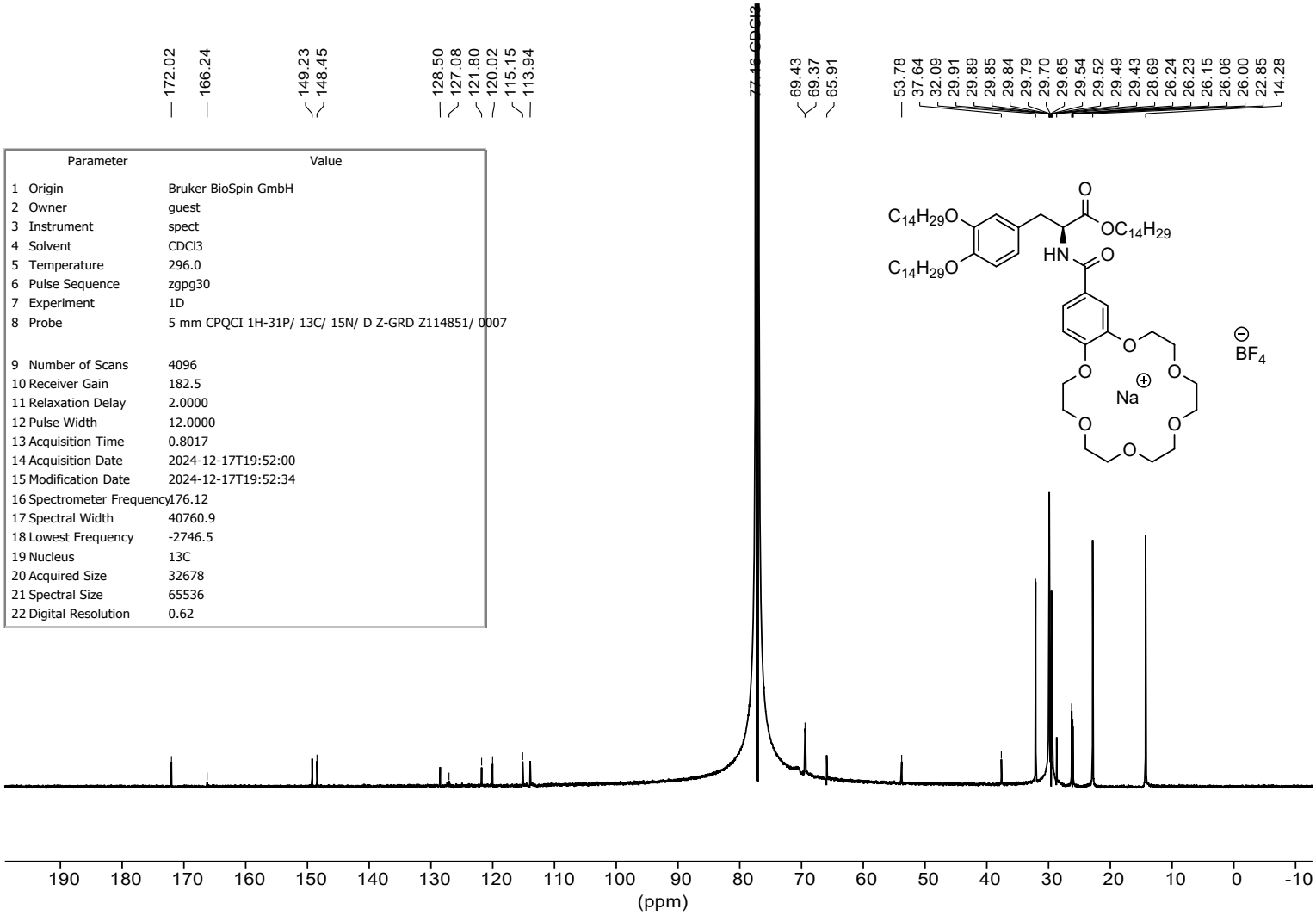

Figure S66: ^{13}C NMR spectrum of **c-DOPA(14) • $NaBF_4$** at 176 MHz.

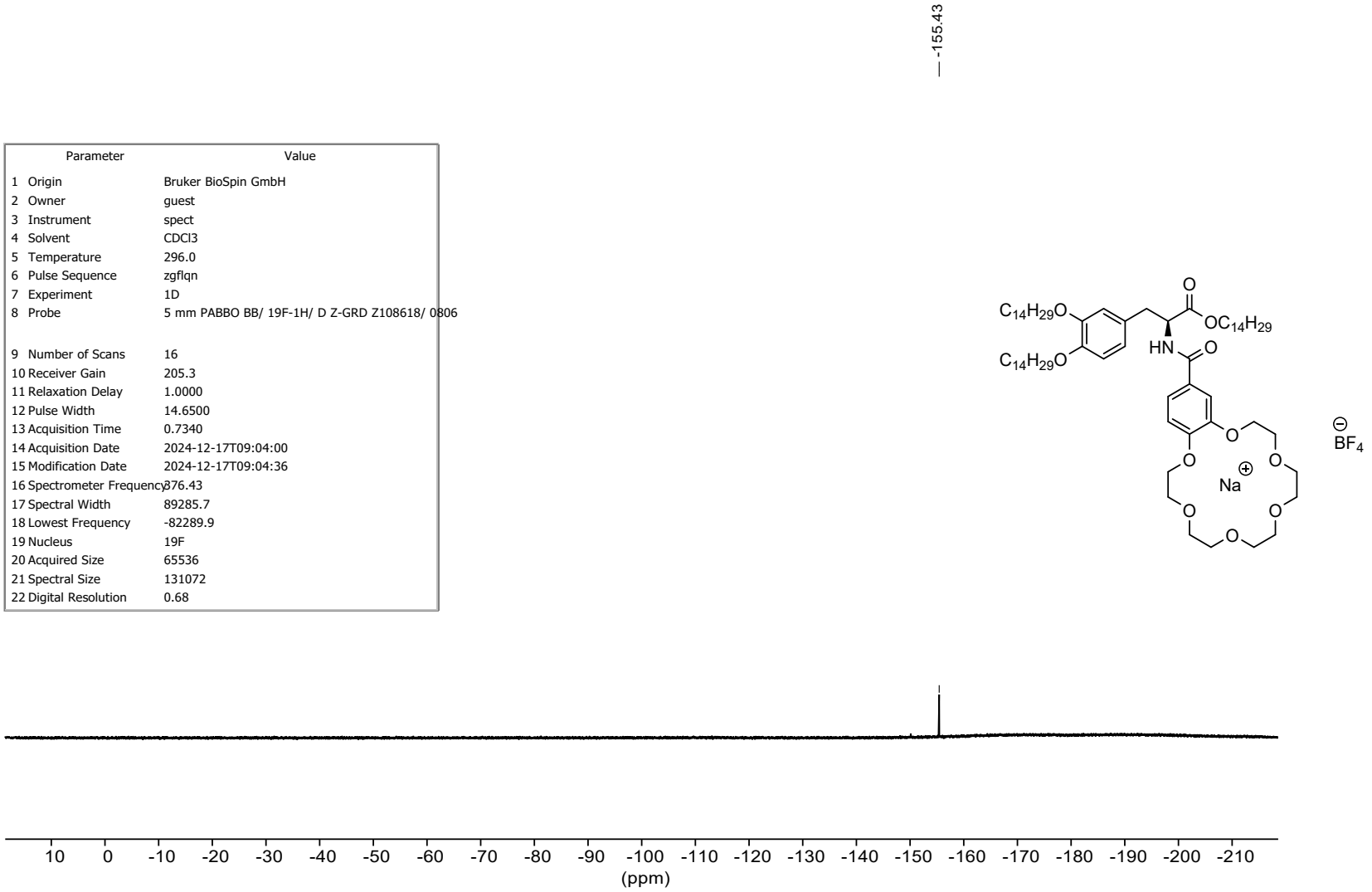

Figure S67: ^{19}F NMR spectrum of **c-DOPA(14) • $NaBF_4$** at 376 MHz.

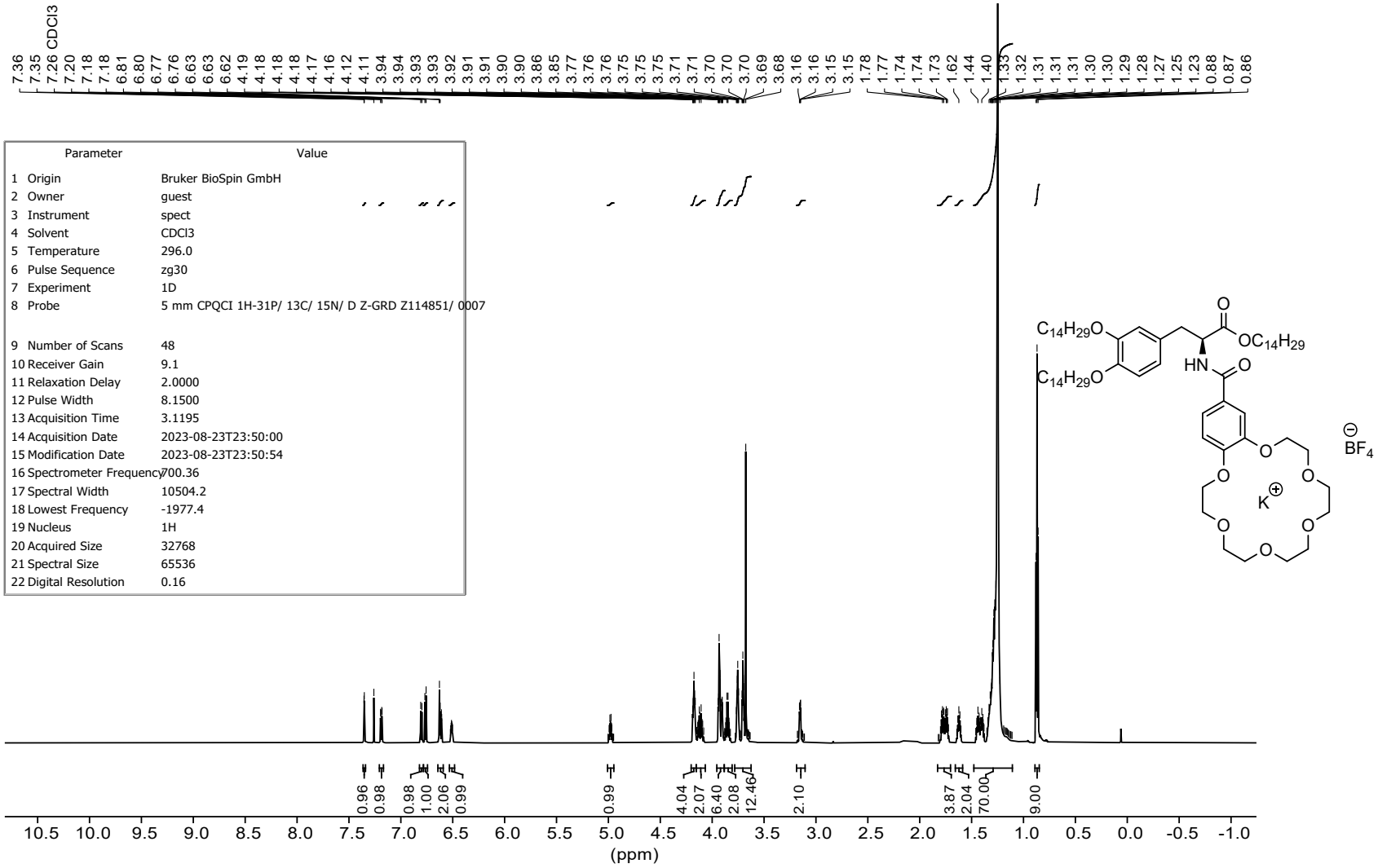

Figure S68: ^{1}H NMR spectrum of **c-DOPA(14) • KBF_4** at 700 MHz.

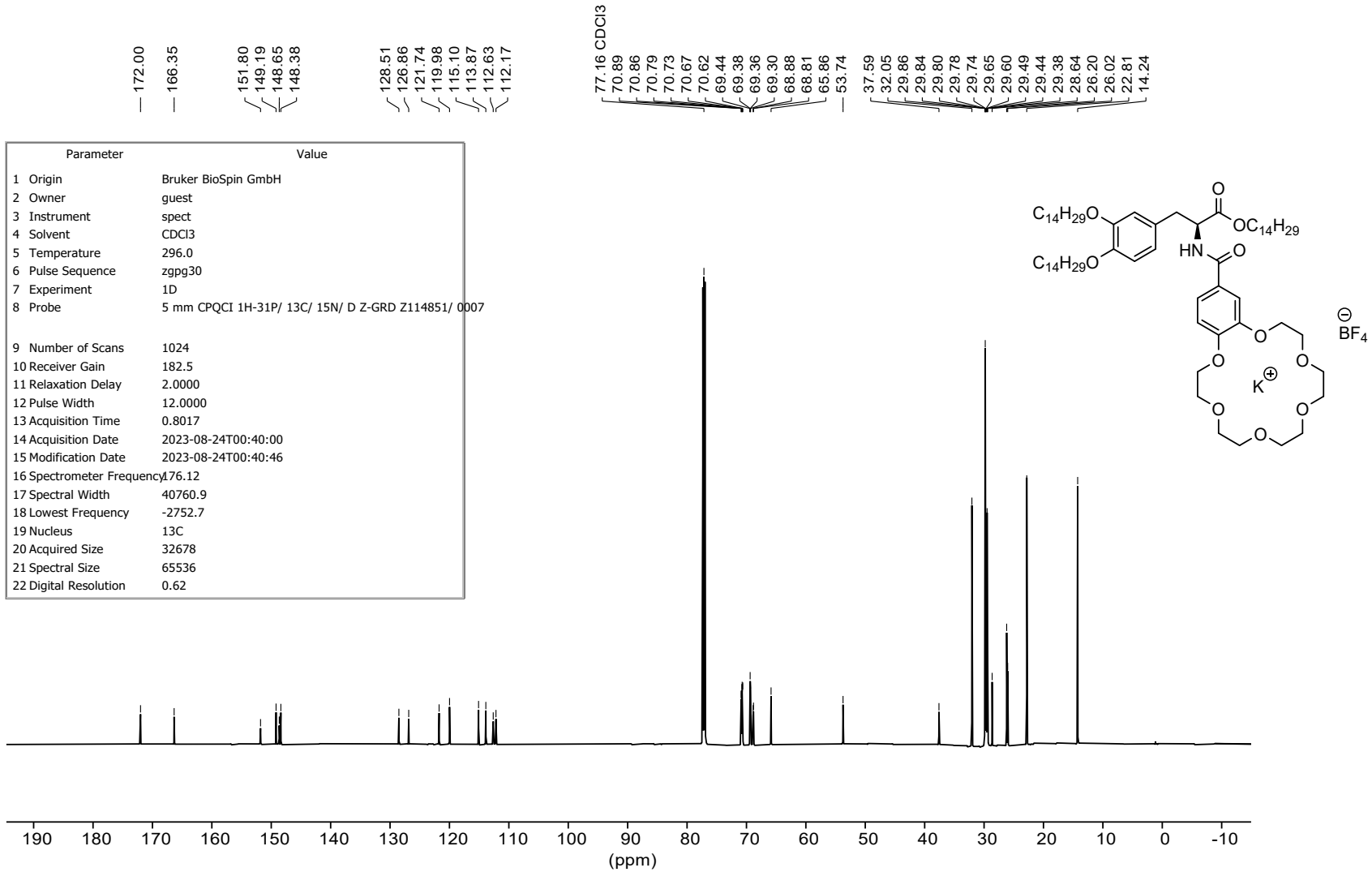

Figure S69: ^{13}C NMR spectrum of **c-DOPA(14) • KBF_4** at 176 MHz.

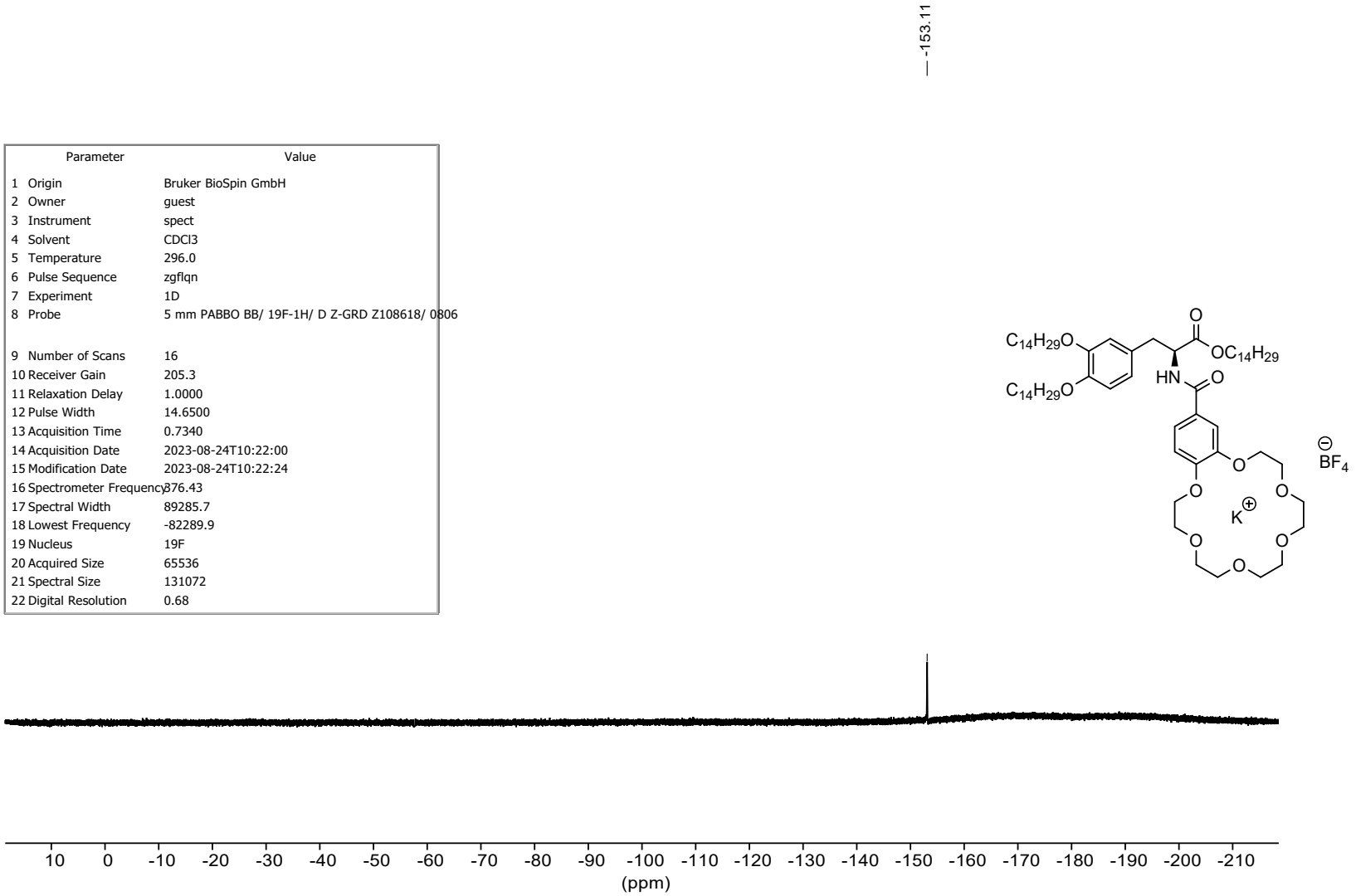

Figure S70: ^{19}F NMR spectrum of **c-DOPA(14) • KBF_4** at 376 MHz.

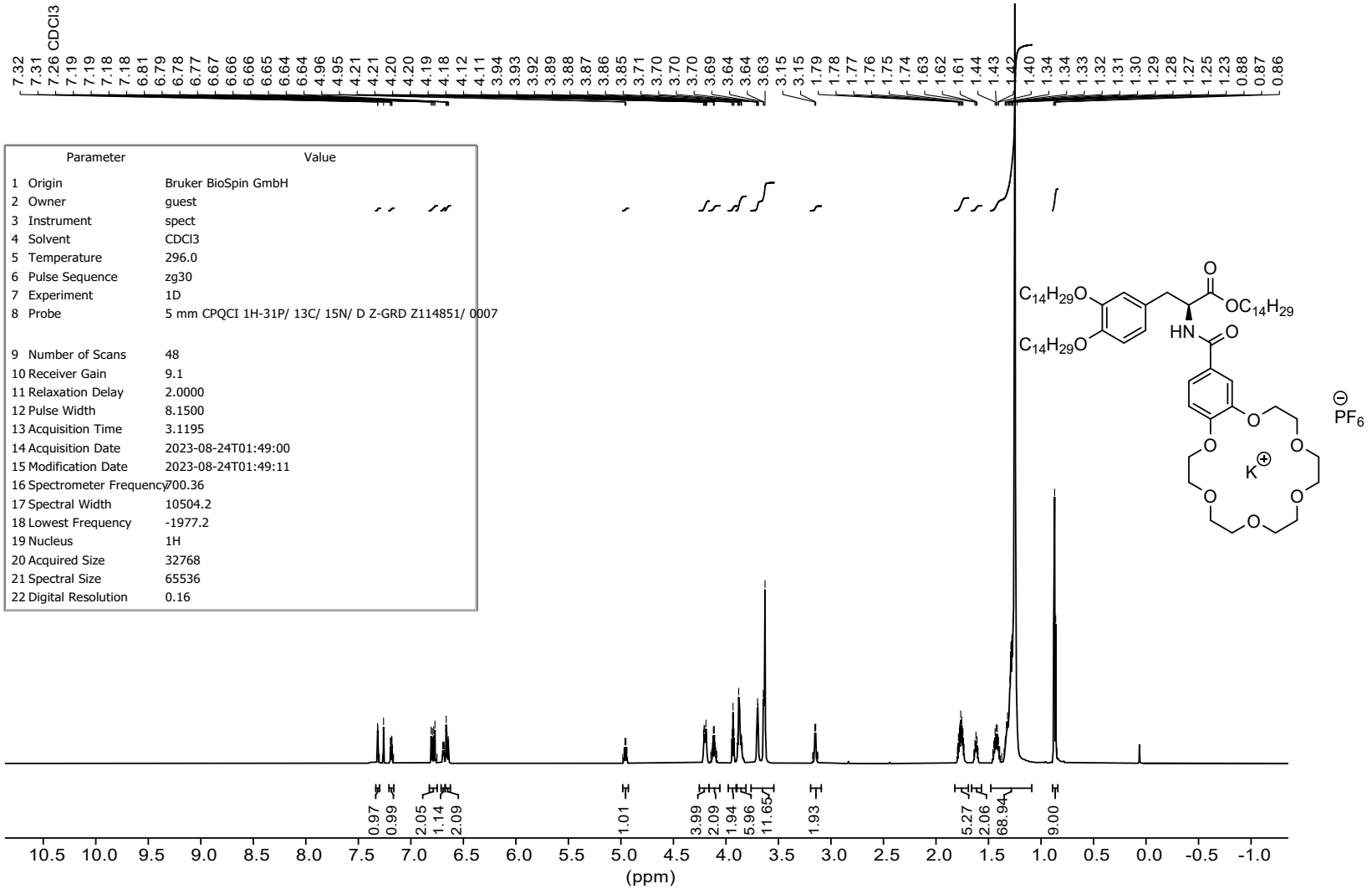

Figure S71: ^{1}H NMR spectrum of **c-DOPA(14) • KPF_6** at 700 MHz.

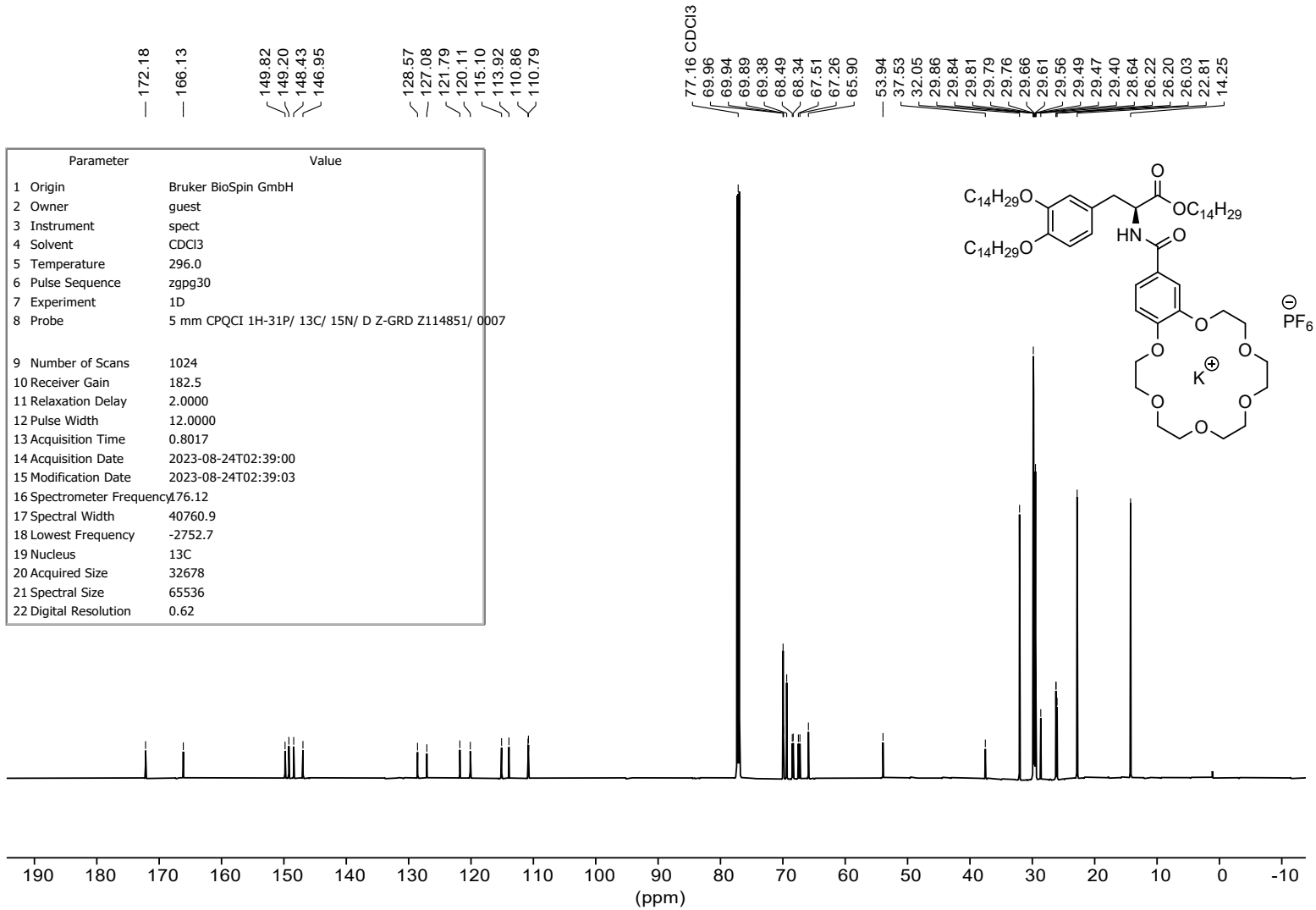

Figure S72: ^{13}C NMR spectrum of **c-DOPA(14) • KPF_6** at 176 MHz.

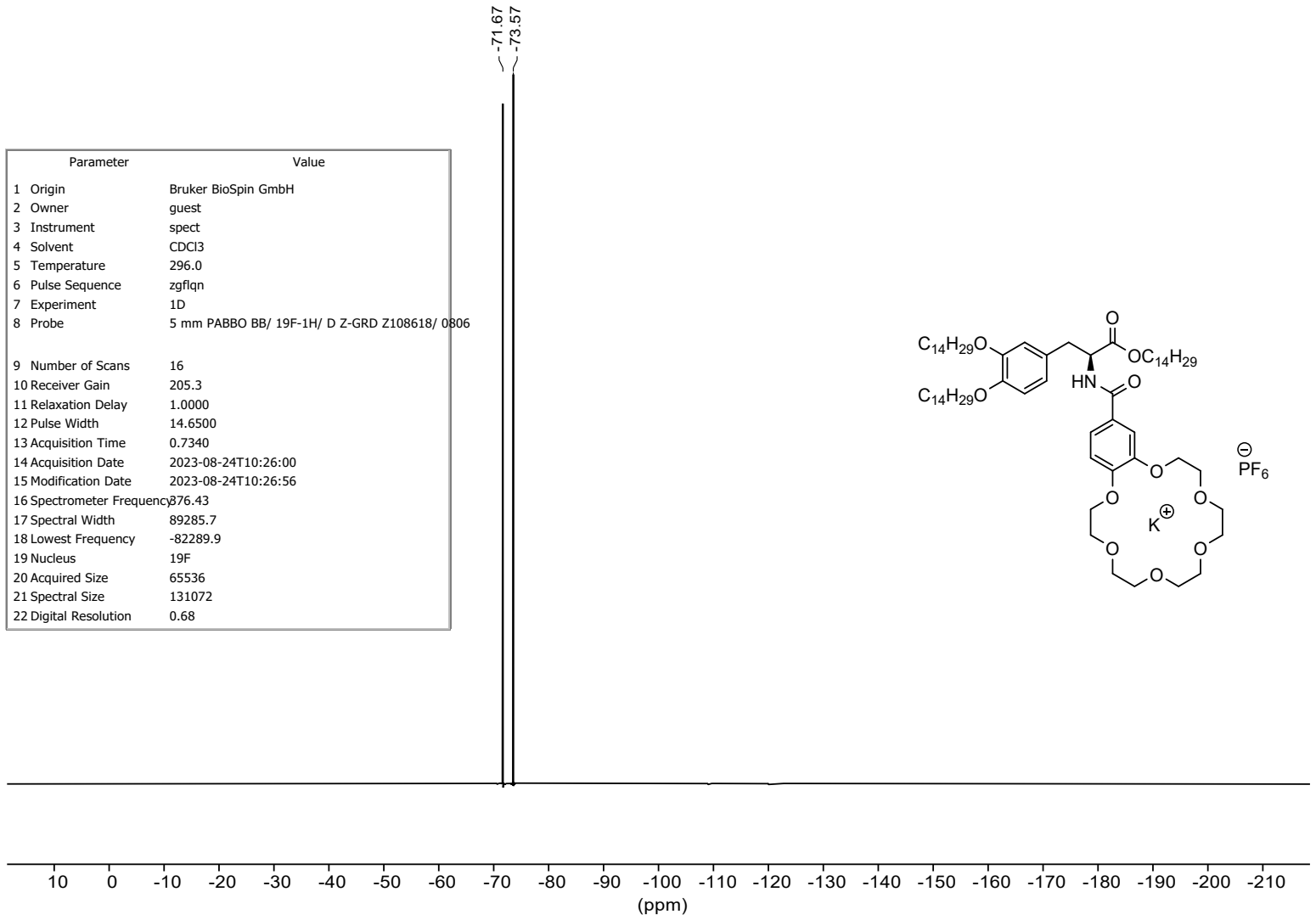

Figure S73: ^{19}F NMR spectrum of **c-DOPA(14) • KPF_6** at 376 MHz.

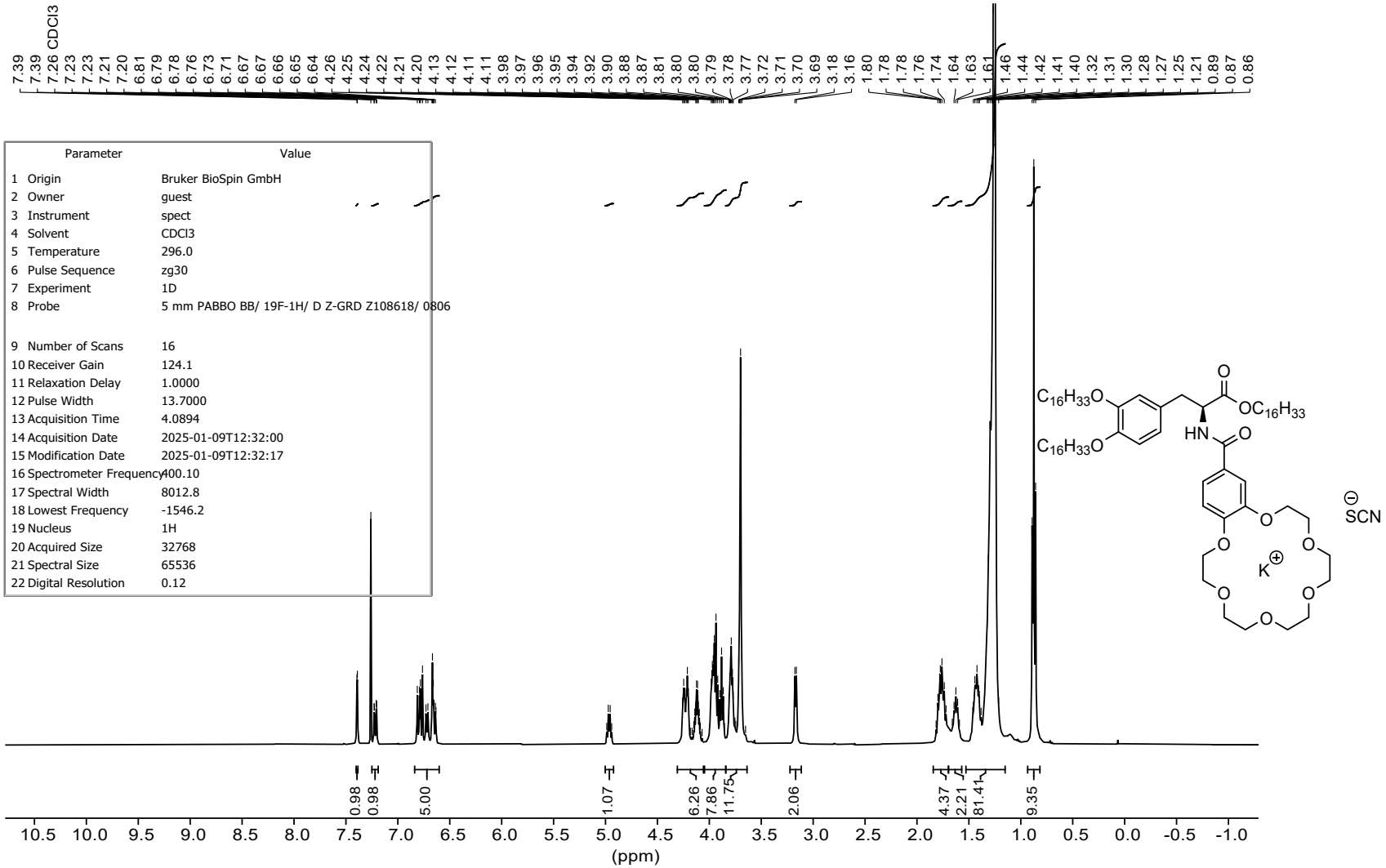

Figure S74: ^{1}H NMR spectrum of **c-DOPA(16) • KSCN** at 400 MHz.

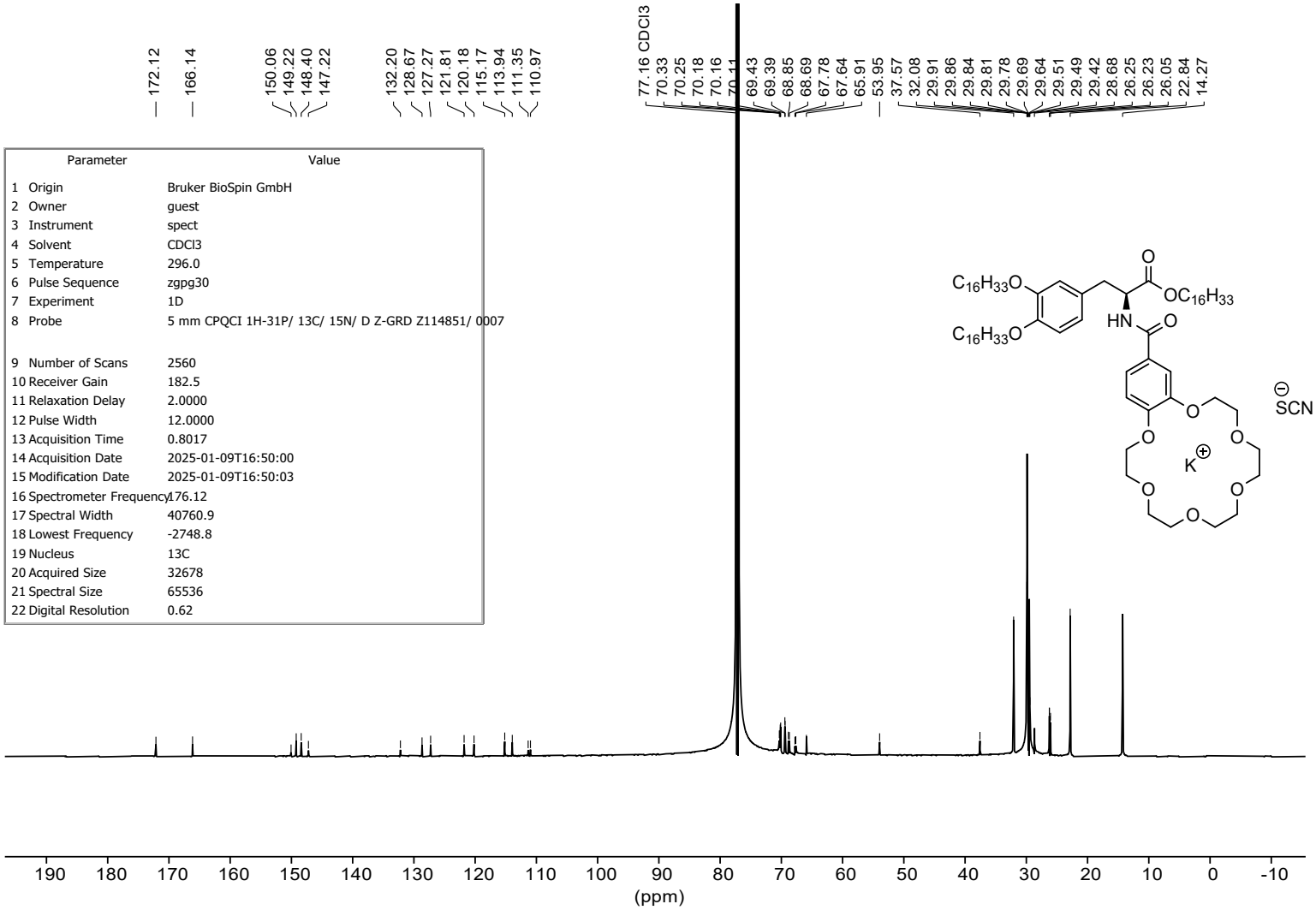

Figure S75: ^{13}C NMR spectrum of **c-DOPA(16) • KSCN** at 176 MHz.

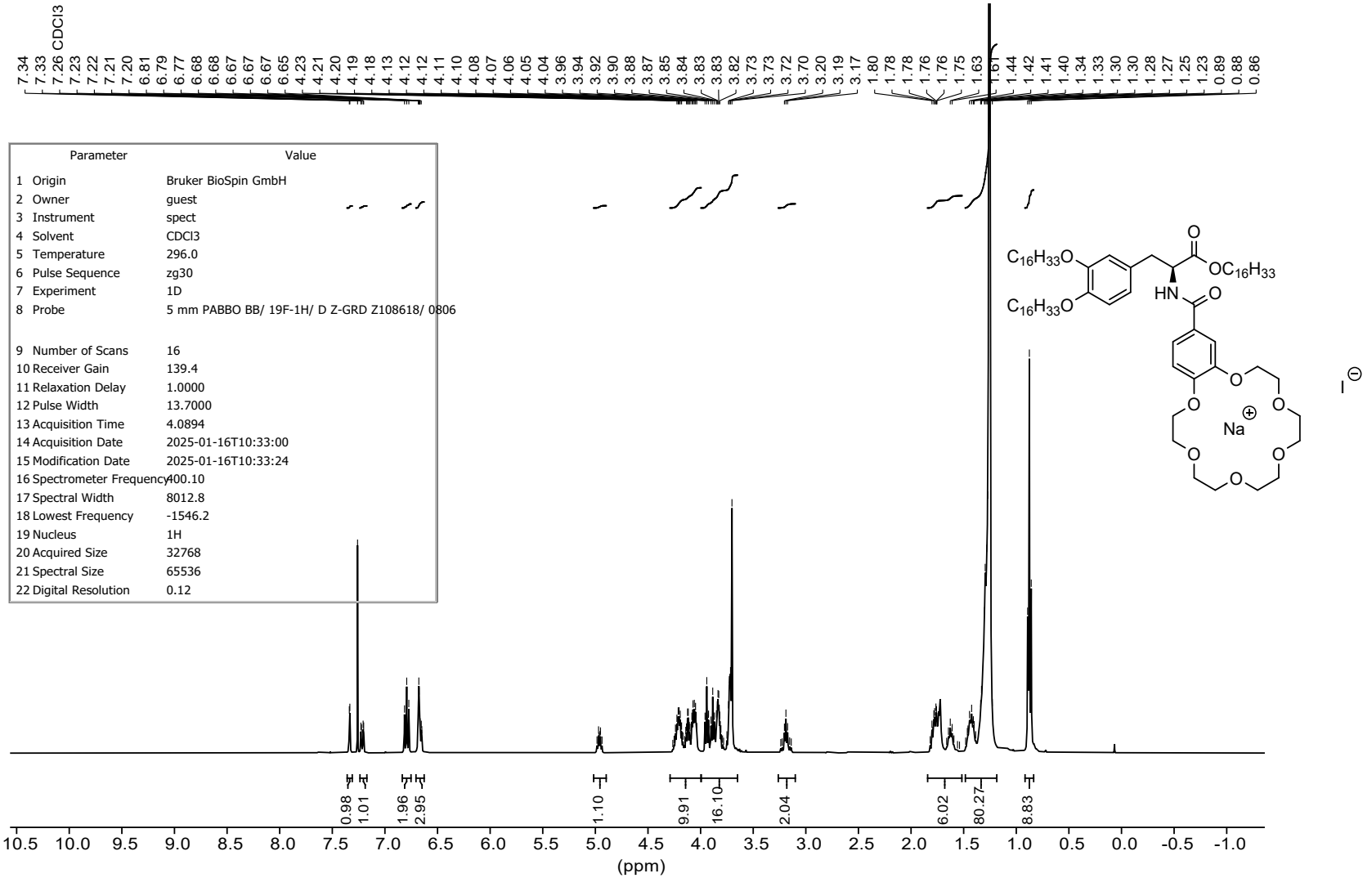

Figure S76: ^{1}H NMR spectrum of **c-DOPA(16) • NaI** at 400 MHz.

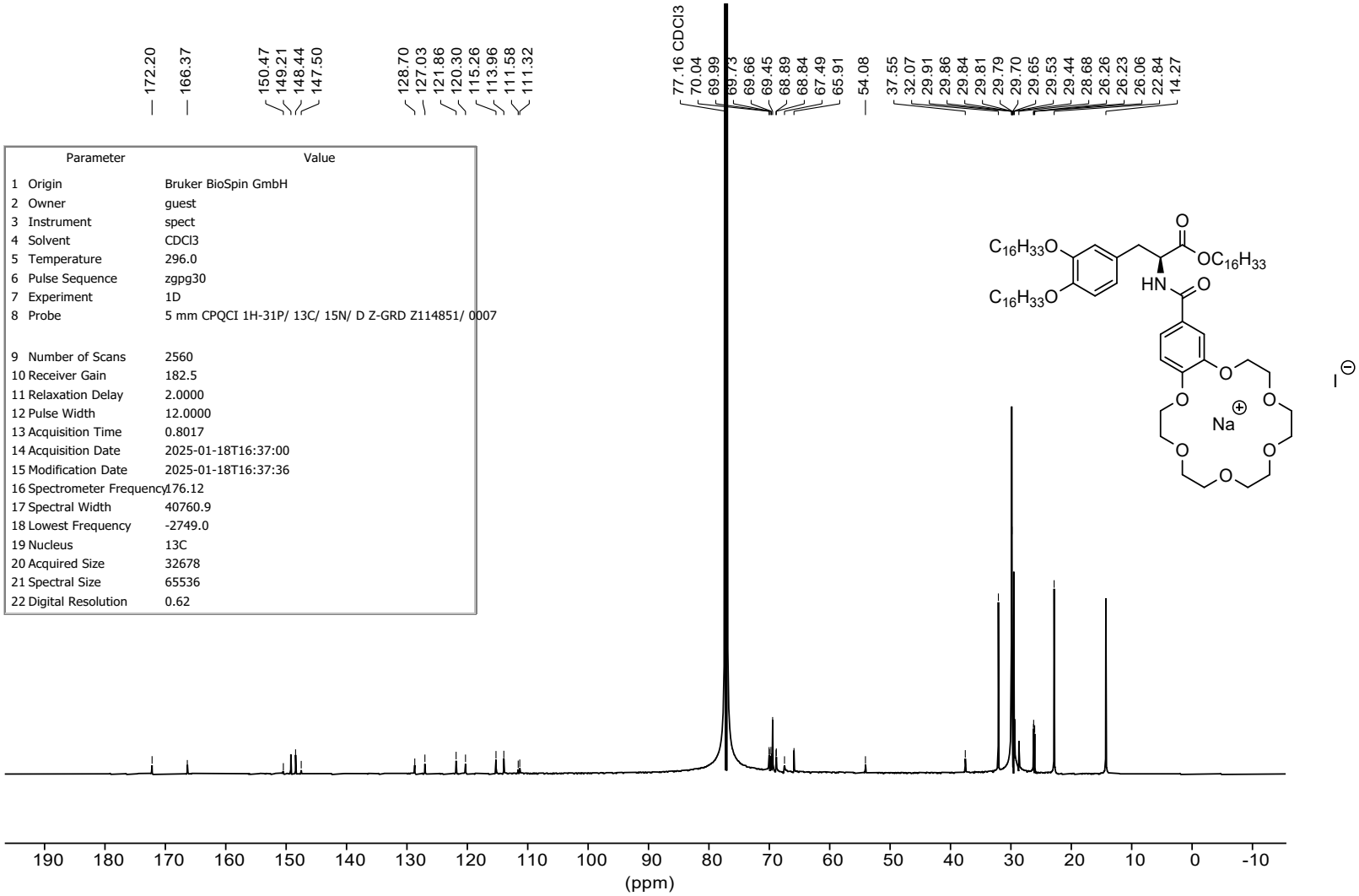

Figure S77: ^{13}C NMR spectrum of **c-DOPA(16) • NaI** at 176 MHz.

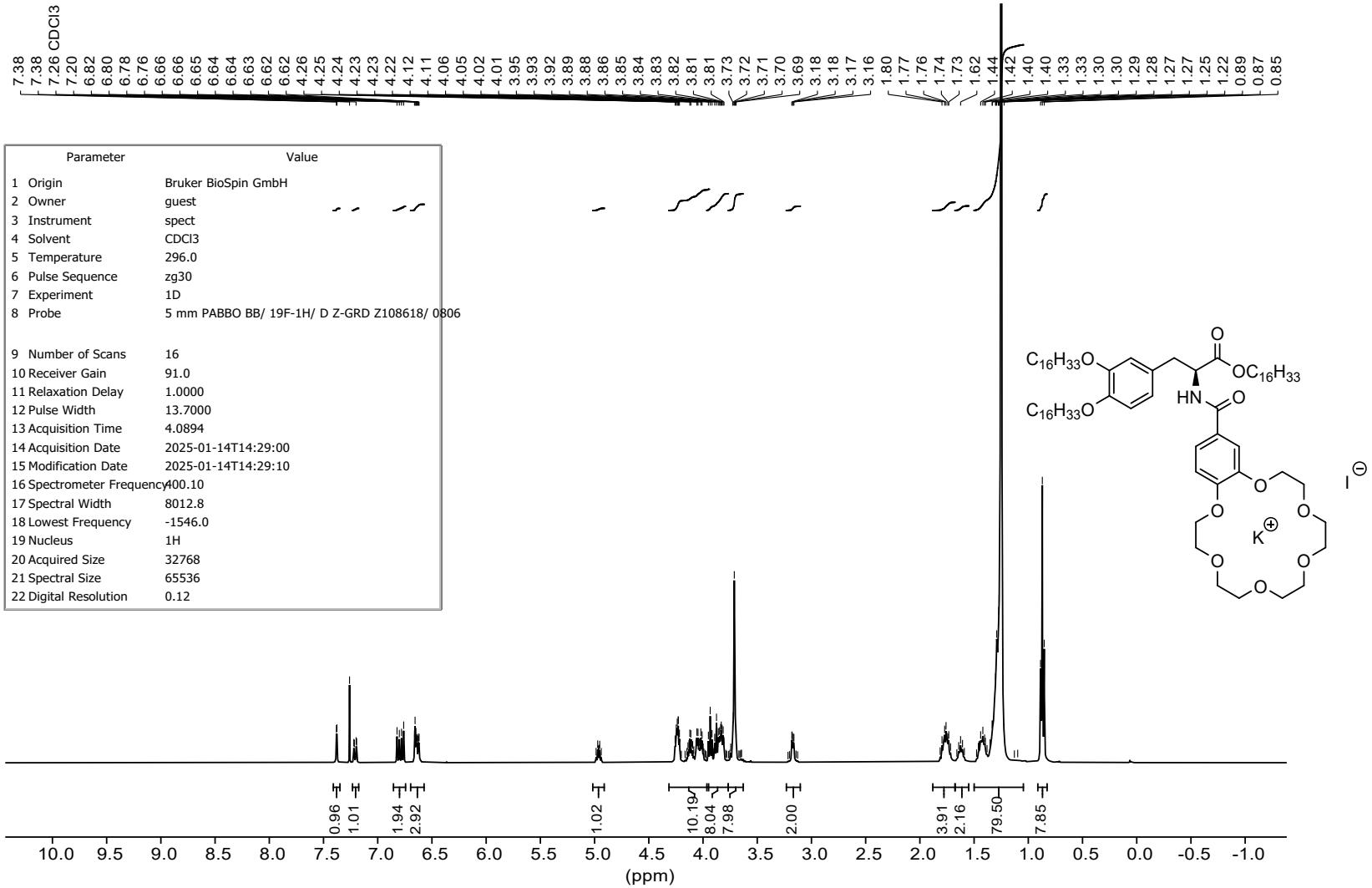

Figure S78: ^{1}H NMR spectrum of **c-DOPA(16) • KI** at 400 MHz.

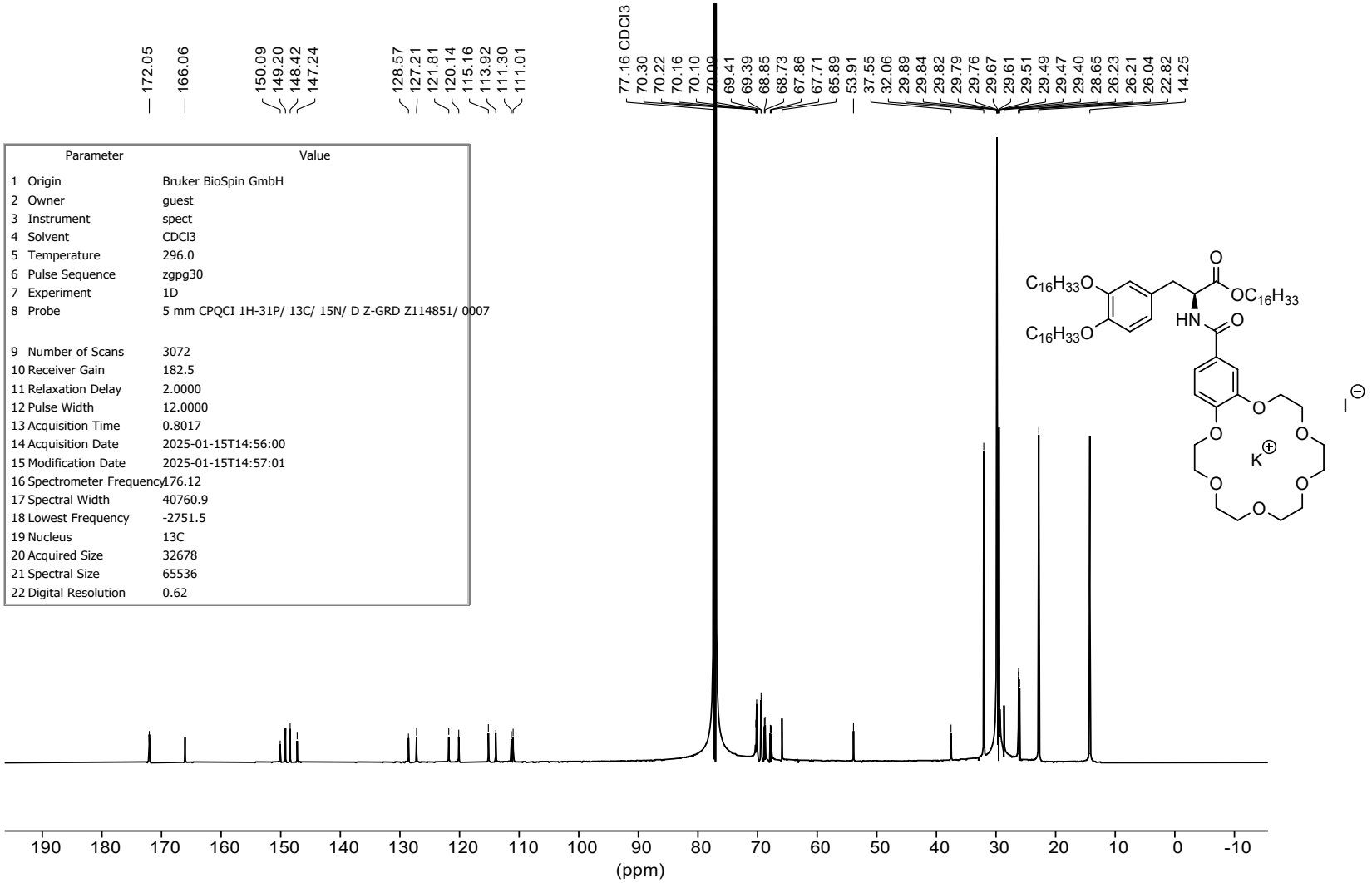

Figure S79: ^{13}C NMR spectrum of **c-DOPA(16) • KI** at 176 MHz.

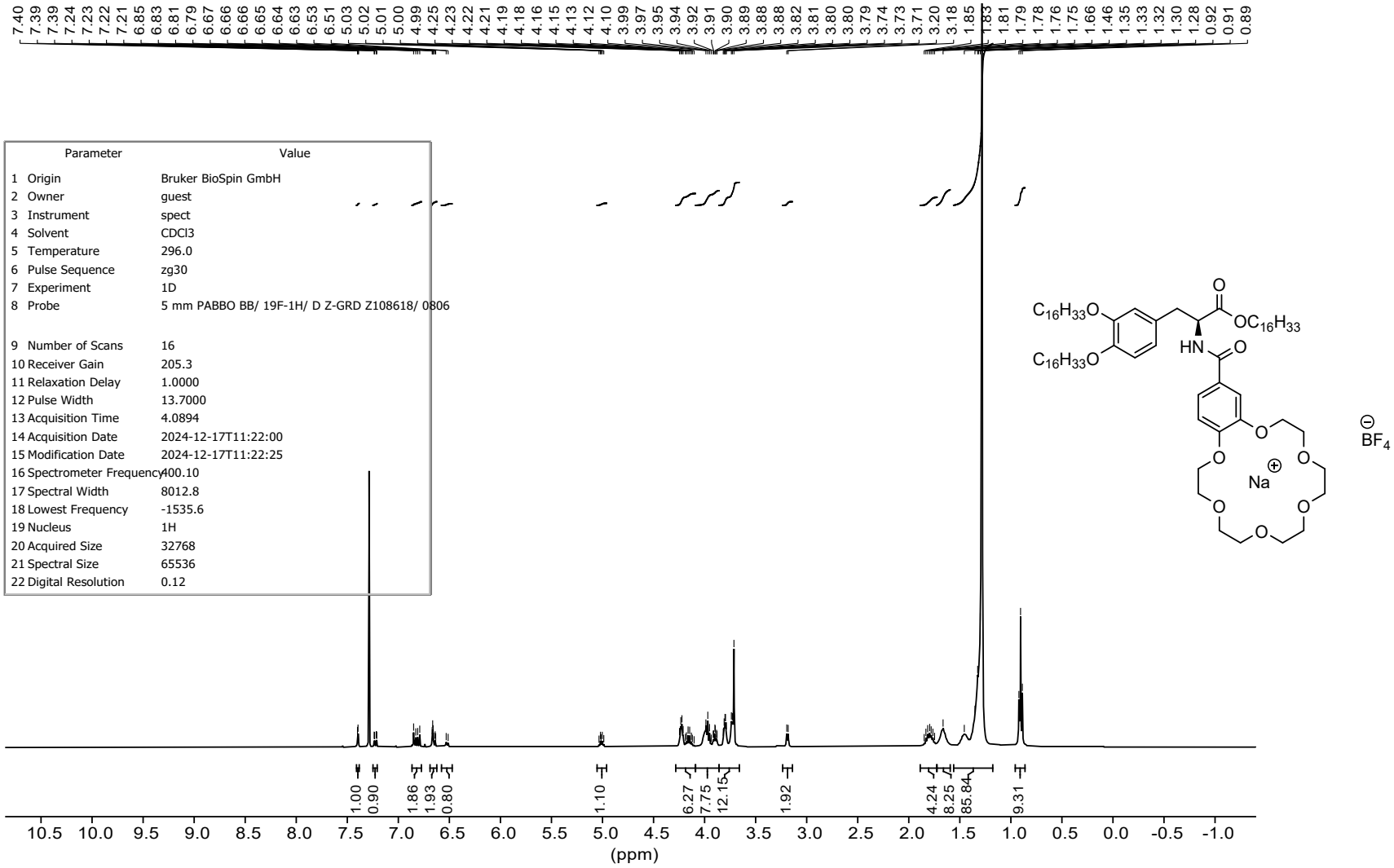

Figure S80: ^{1}H NMR spectrum of **c-DOPA(16) • $NaBF_4$** at 400 MHz.

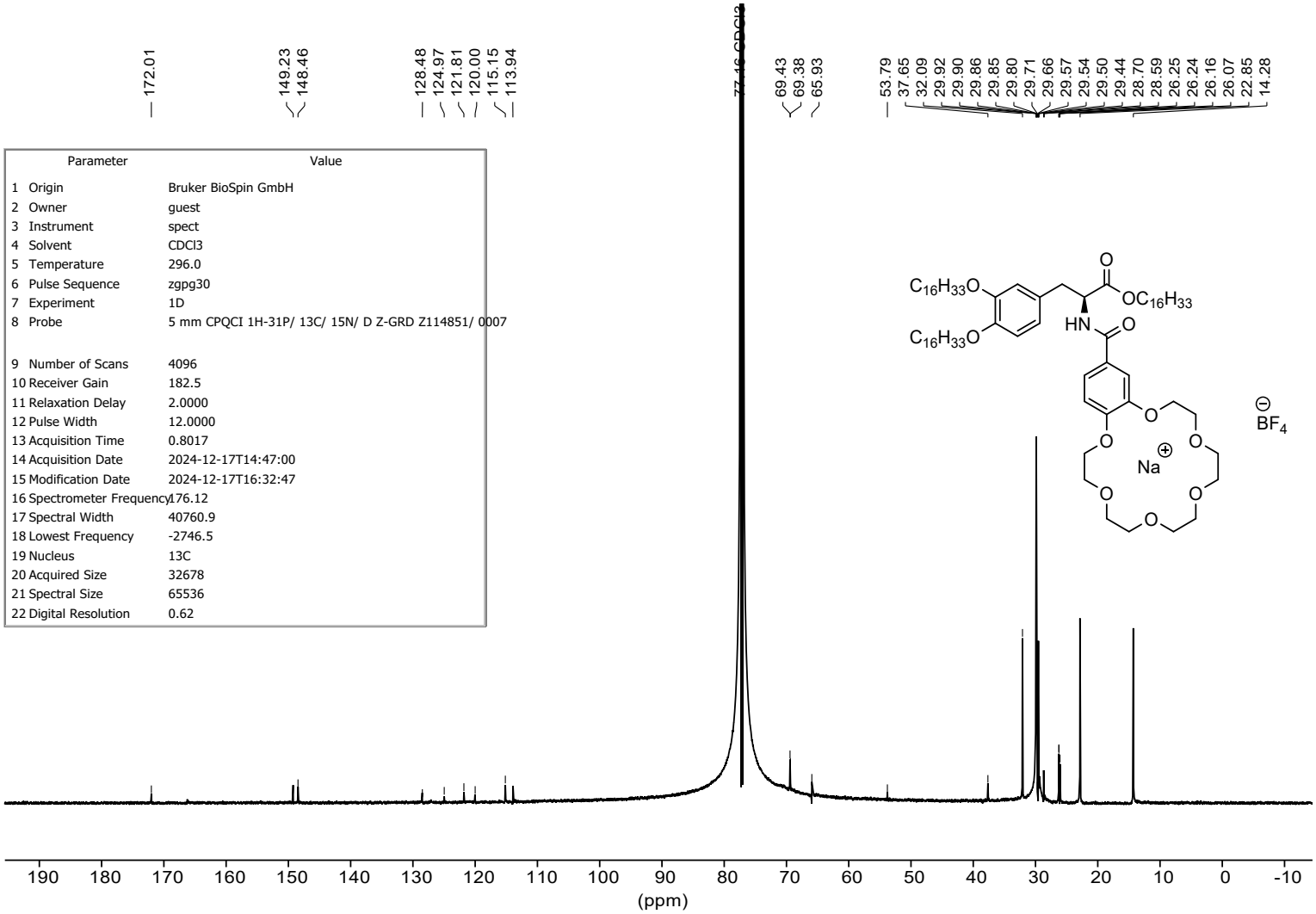

Figure S81: ^{13}C NMR spectrum of **c-DOPA(16) • $NaBF_4$** at 176 MHz.

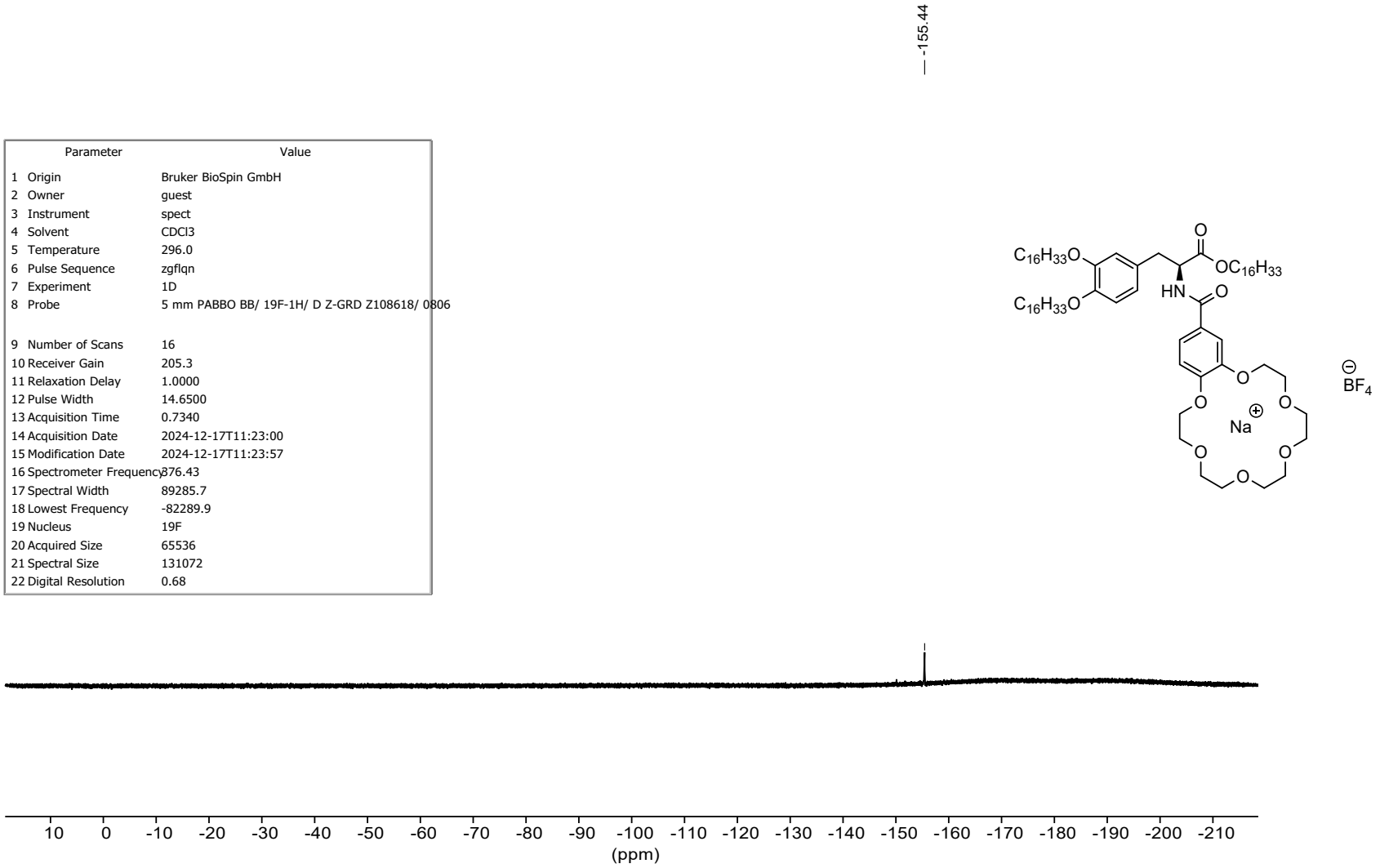

Figure S82: ^{19}F NMR spectrum of **c-DOPA(16) • $NaBF_4$** at 376 MHz.

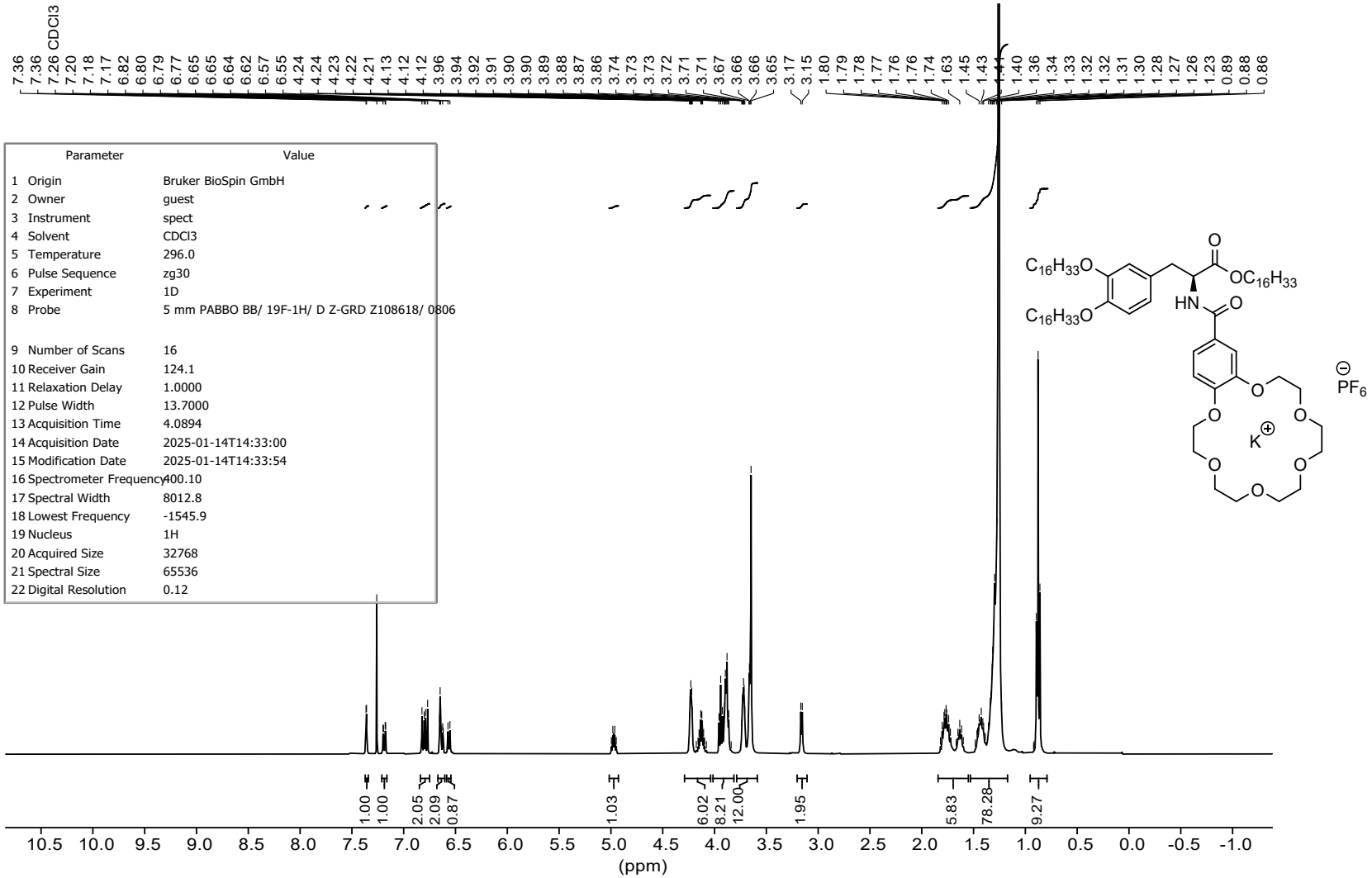

Figure S83: ^{1}H NMR spectrum of **c-DOPA(16) • KPF_6** at 400 MHz.

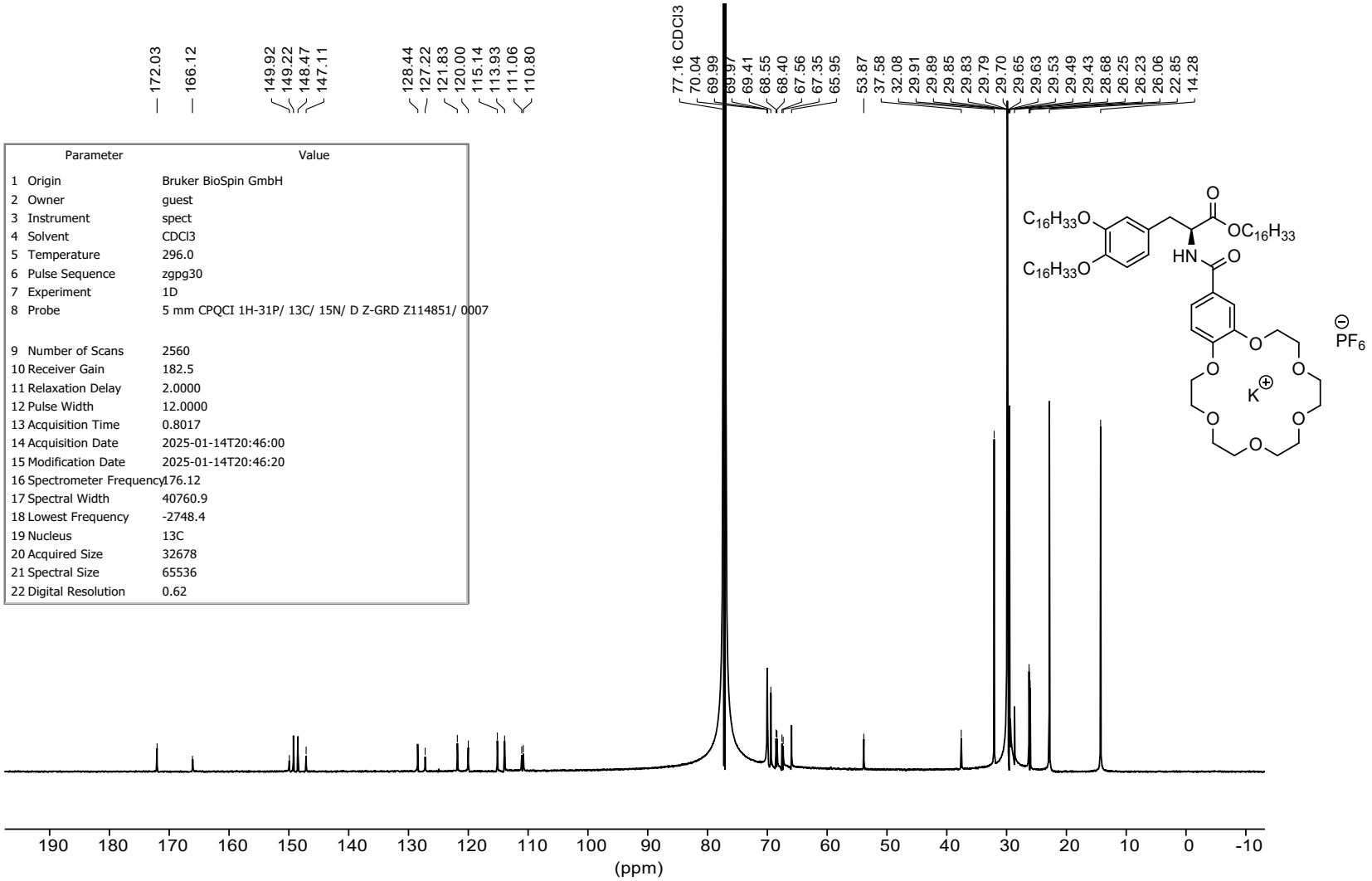

Figure S84: ^{13}C NMR spectrum of **c-DOPA(16) • KPF_6** at 176 MHz.

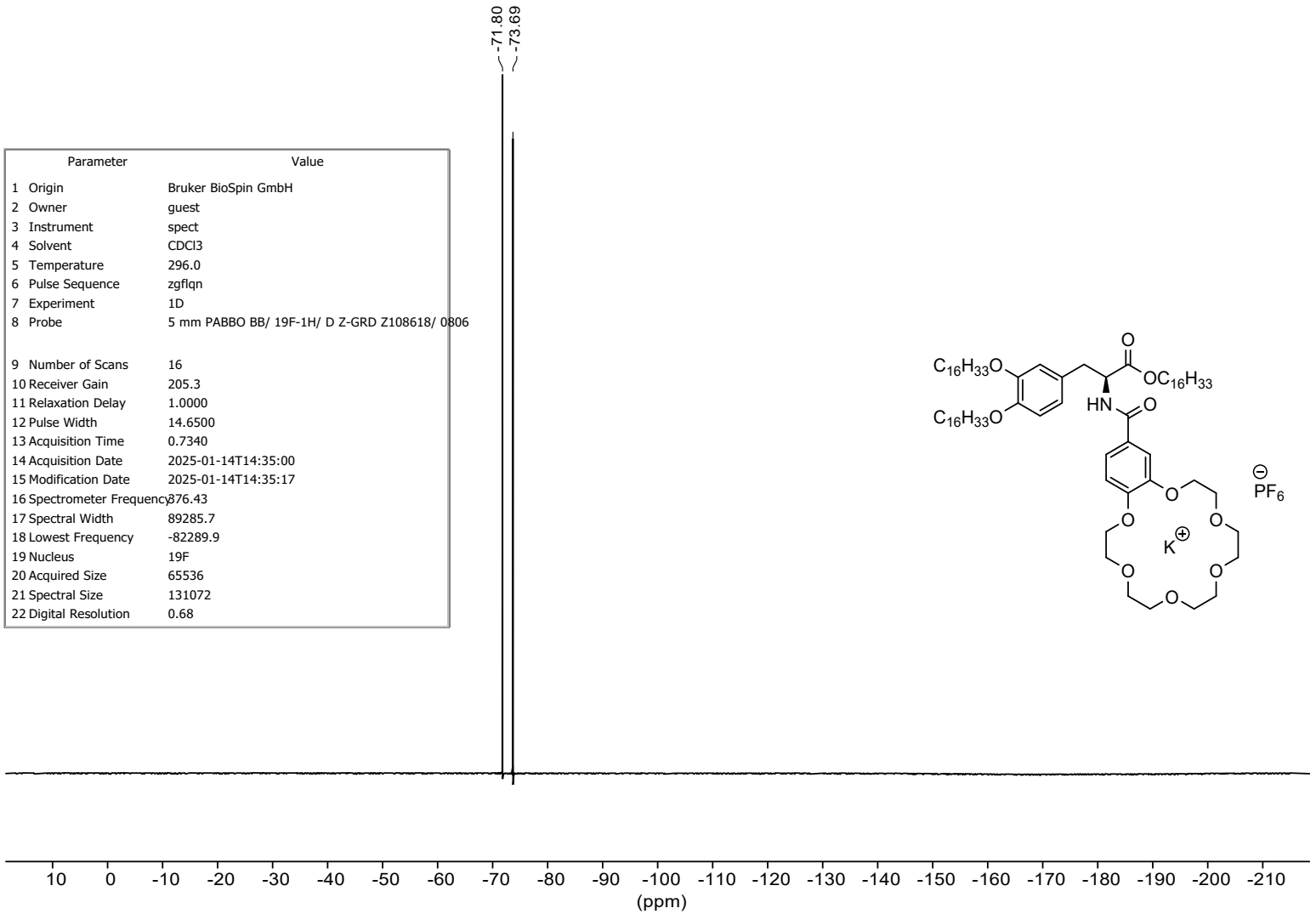

Figure S85: ^{19}F NMR spectrum of **c-DOPA(16) • KPF_6** at 376 MHz.

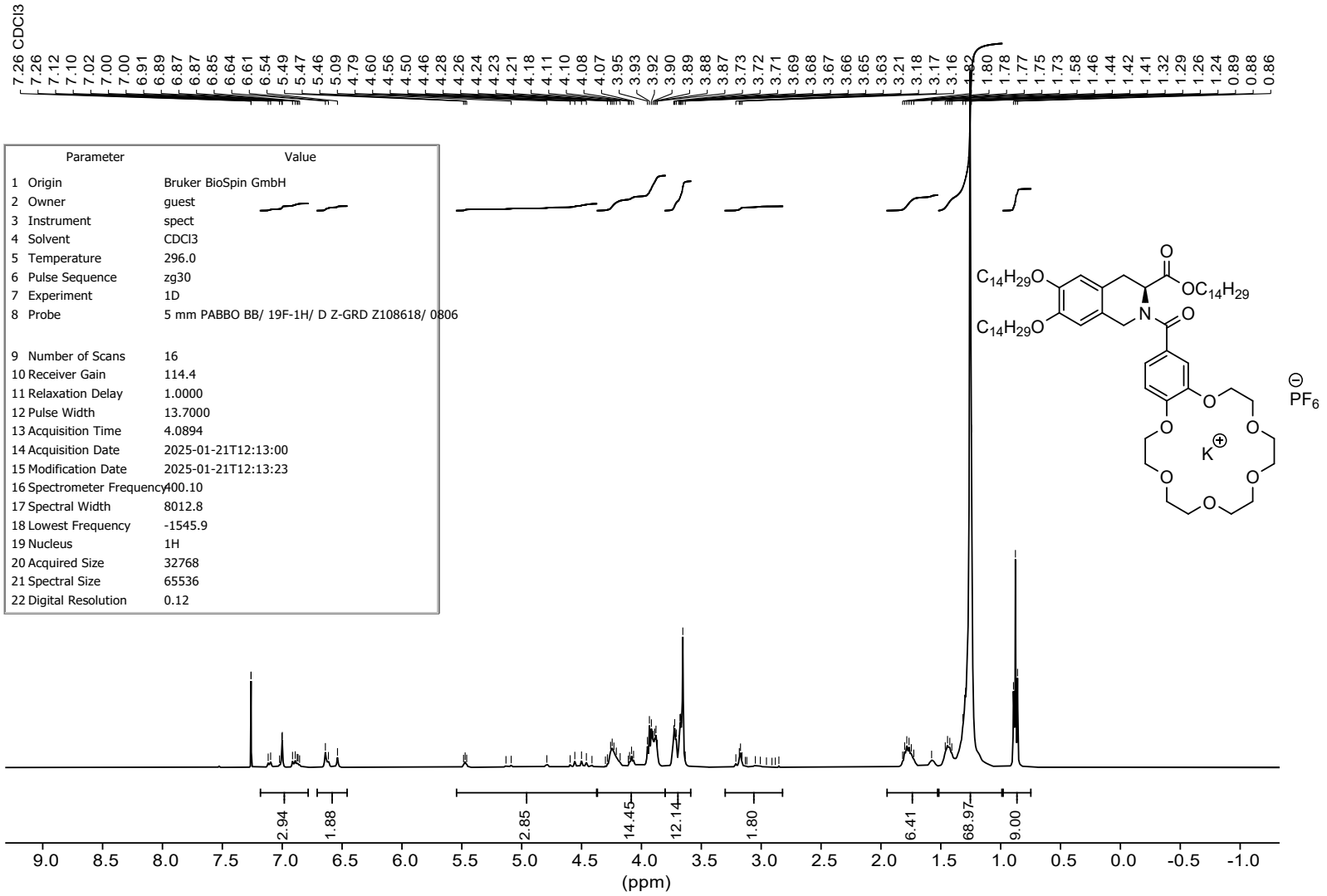

Figure S86: ^{1}H NMR spectrum of **c-THIQ(14) • KPF_6** at 400 MHz.

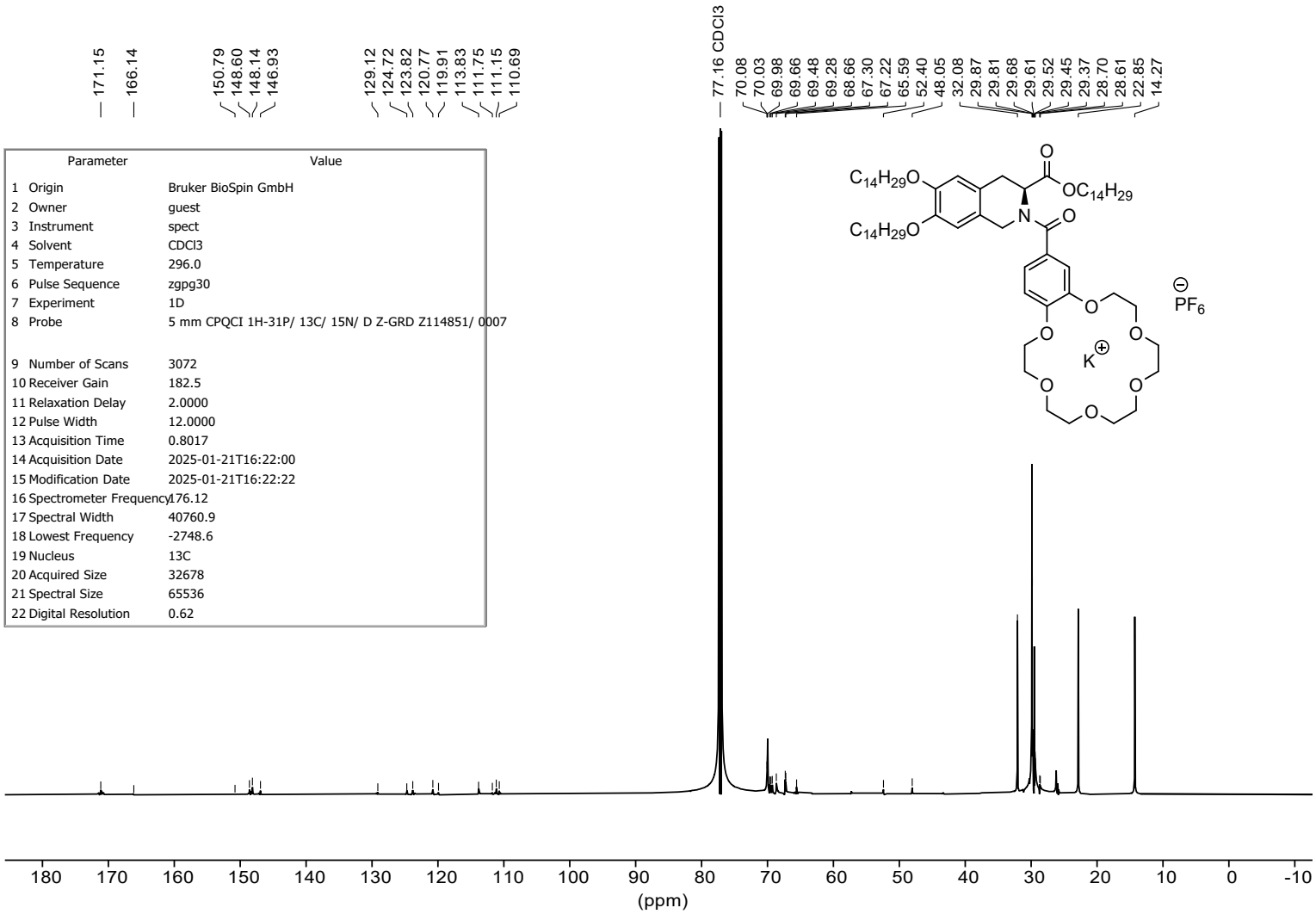

Figure S87: ^{13}C NMR spectrum of **c-THIQ(14) • KPF_6** at 176 MHz.

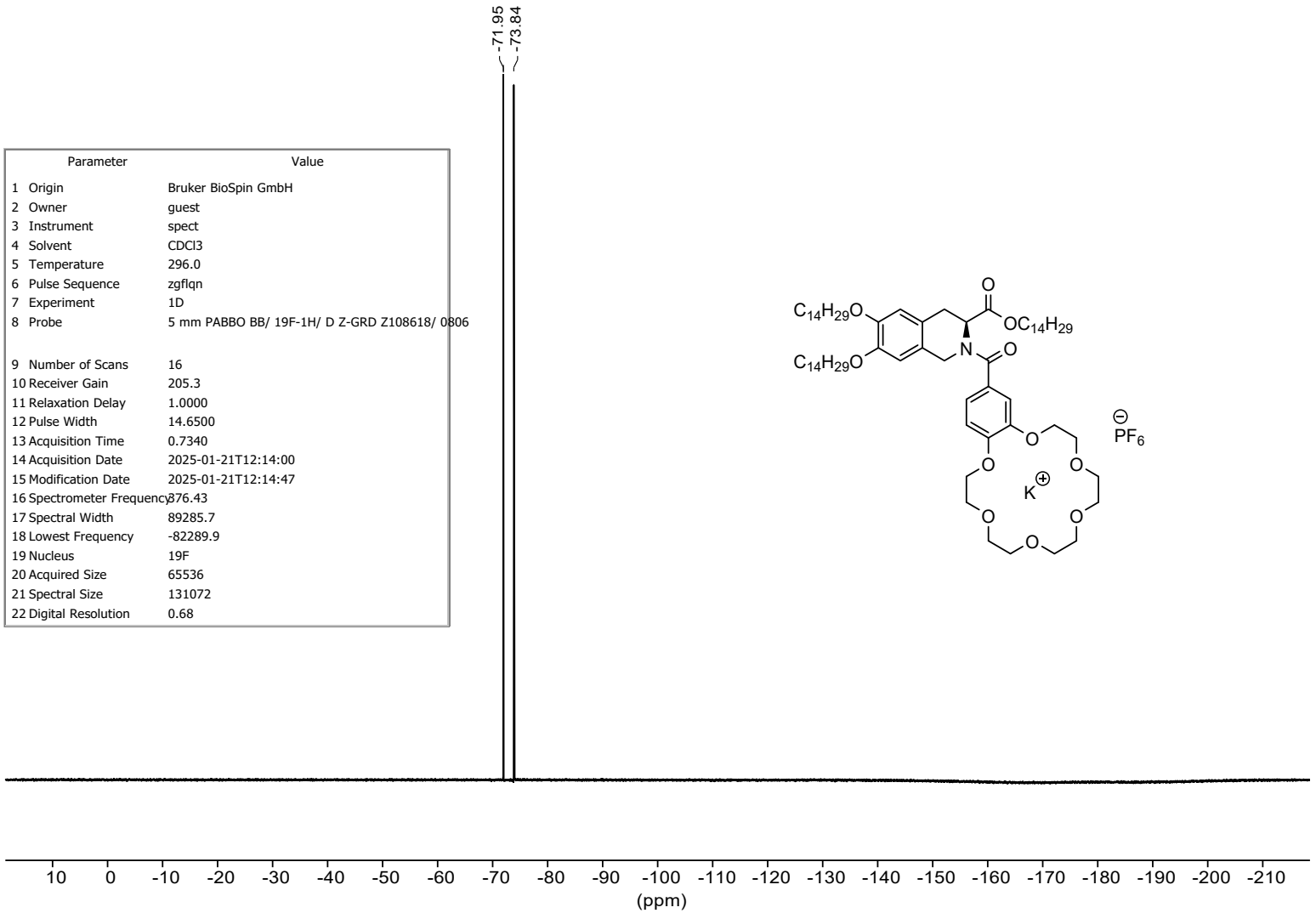

Figure S88: ^{19}F NMR spectrum of **c-THIQ(14) • KPF_6** at 376 MHz.

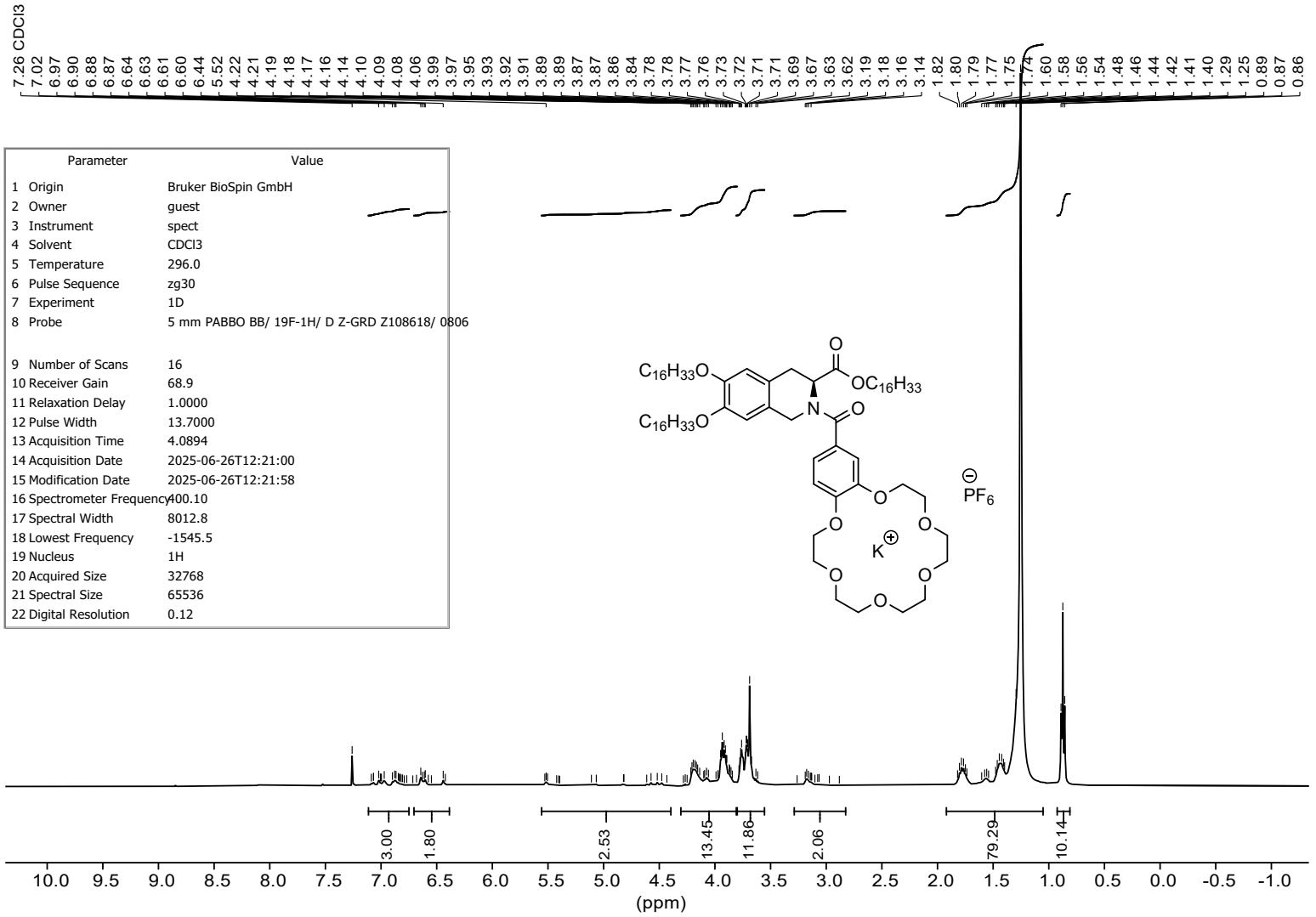

Figure S89: ^{1}H NMR spectrum of **c-THIQ(16) • KPF_6** at 400 MHz.

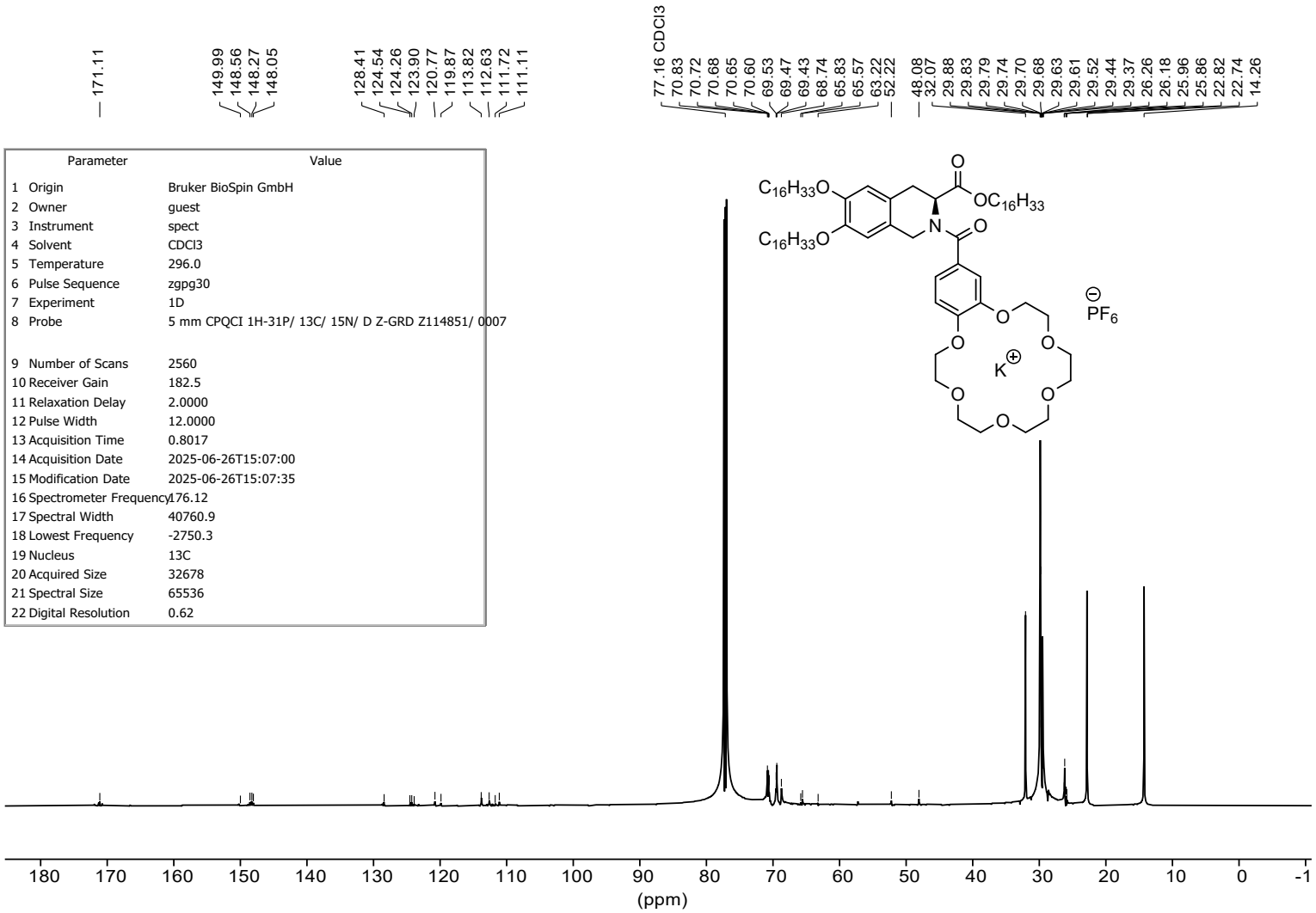

Figure S90: ^{13}C NMR spectrum of **c-THIQ(16) • KPF_6** at 176 MHz.

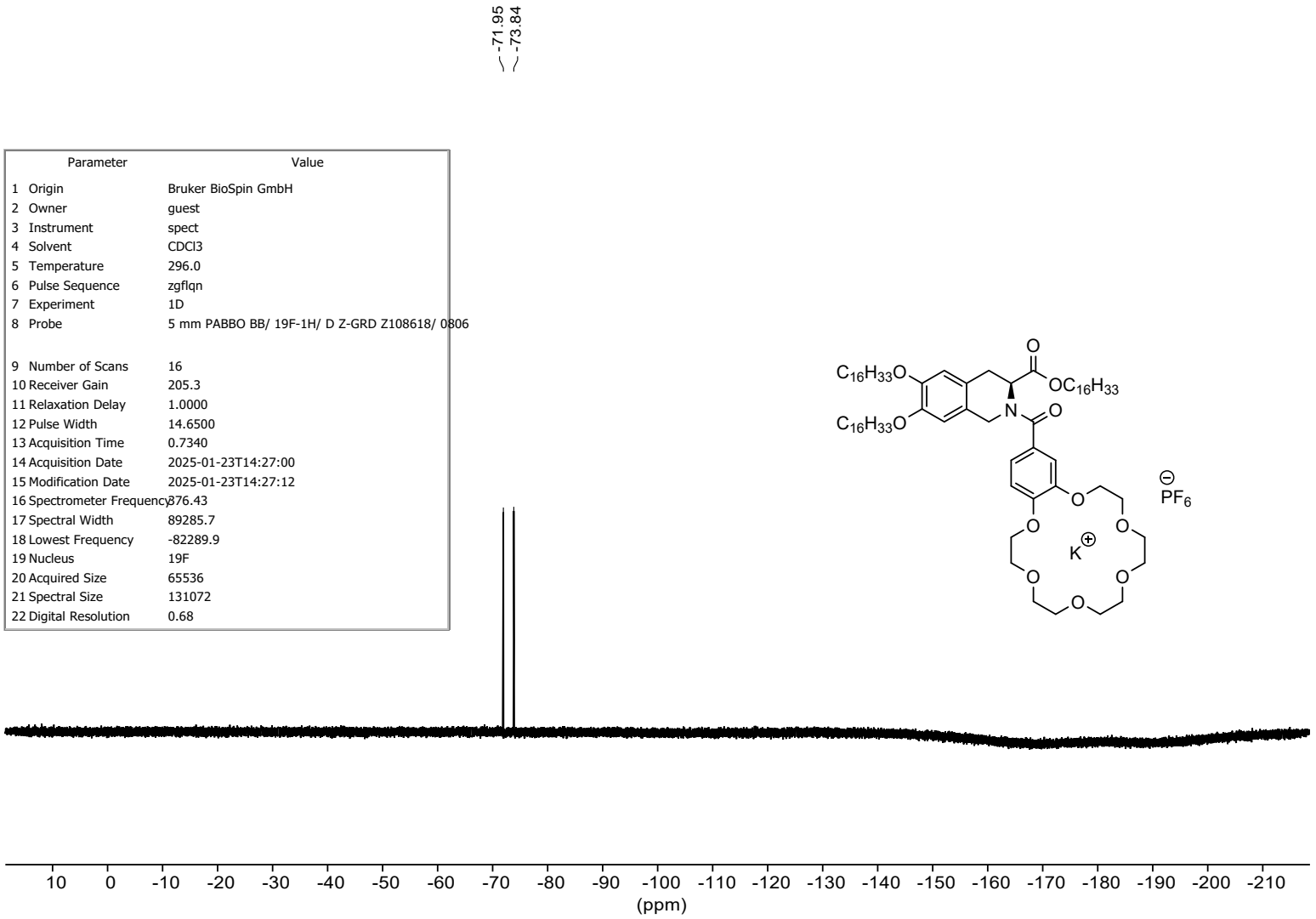

Figure S91: ^{19}F NMR spectrum of **c-THIQ(16) • KPF_6** at 376 MHz.

	Parameter	Value
1	Data File Name	N:/ data/ GRIESSER_400/ nmr/ Jan07-2026/ 201/ fid
2	Title	Jan07-2026.201.fid
3	Comment	02 Griesser ROB-KBF4
4	Origin	Bruker BioSpin GmbH
5	Owner	guest
6	Site	
7	Instrument	spect
8	Author	
9	Solvent	D2O
10	Temperature	293.1
11	Pulse Sequence	zgfhigqn.2
12	Experiment	1D
13	Probe	5 mm PABBO BB/ 19F-1H/ D Z-GRD Z108618/ 0806
14	Number of Scans	16
15	Receiver Gain	205.3
16	Relaxation Delay	1.0000
17	Pulse Width	14.6500
18	Presaturation Frequency	
19	Acquisition Time	0.7340
20	Acquisition Date	2026-01-07T17:30:00
21	Modification Date	2026-01-07T17:30:24
22	Class	
23	Spectrometer Frequency	376.43
24	Spectral Width	89285.7
25	Lowest Frequency	-82289.9
26	Nucleus	19F
27	Acquired Size	65536
28	Spectral Size	131072
29	Digital Resolution	0.68

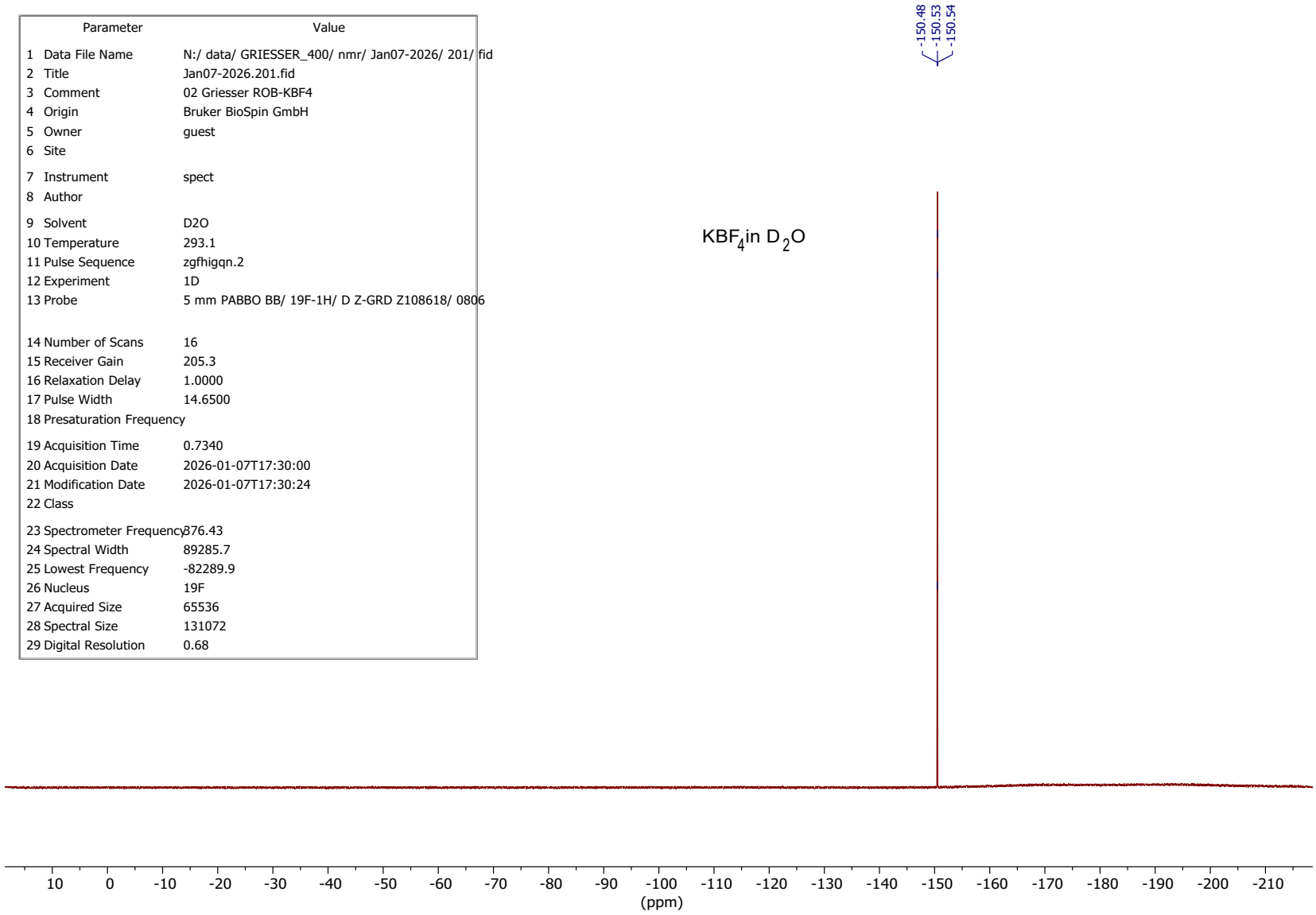

Figure S92: ^{19}F NMR spectrum of KBF_4 in D_2O at 376 MHz.

Parameter	Value
1 Data File Name	N:/ data/ GRIESSER_400/ nmr/ Jan07-2026/ 191/ fid
2 Title	Jan07-2026.191.fid
3 Comment	02 Griesser ROB-NaBF4
4 Origin	Bruker BioSpin GmbH
5 Owner	guest
6 Site	
7 Instrument	spect
8 Author	
9 Solvent	D2O
10 Temperature	293.0
11 Pulse Sequence	zgfhigqn.2
12 Experiment	1D
13 Probe	5 mm PABBO BB/ 19F-1H/ D Z-GRD Z108618/ 0806
14 Number of Scans	16
15 Receiver Gain	205.3
16 Relaxation Delay	1.0000
17 Pulse Width	14.6500
18 Presaturation Frequency	
19 Acquisition Time	0.7340
20 Acquisition Date	2026-01-07T17:25:00
21 Modification Date	2026-01-07T17:25:26
22 Class	
23 Spectrometer Frequency	376.43
24 Spectral Width	89285.7
25 Lowest Frequency	-82289.9
26 Nucleus	19F
27 Acquired Size	65536
28 Spectral Size	131072
29 Digital Resolution	0.68

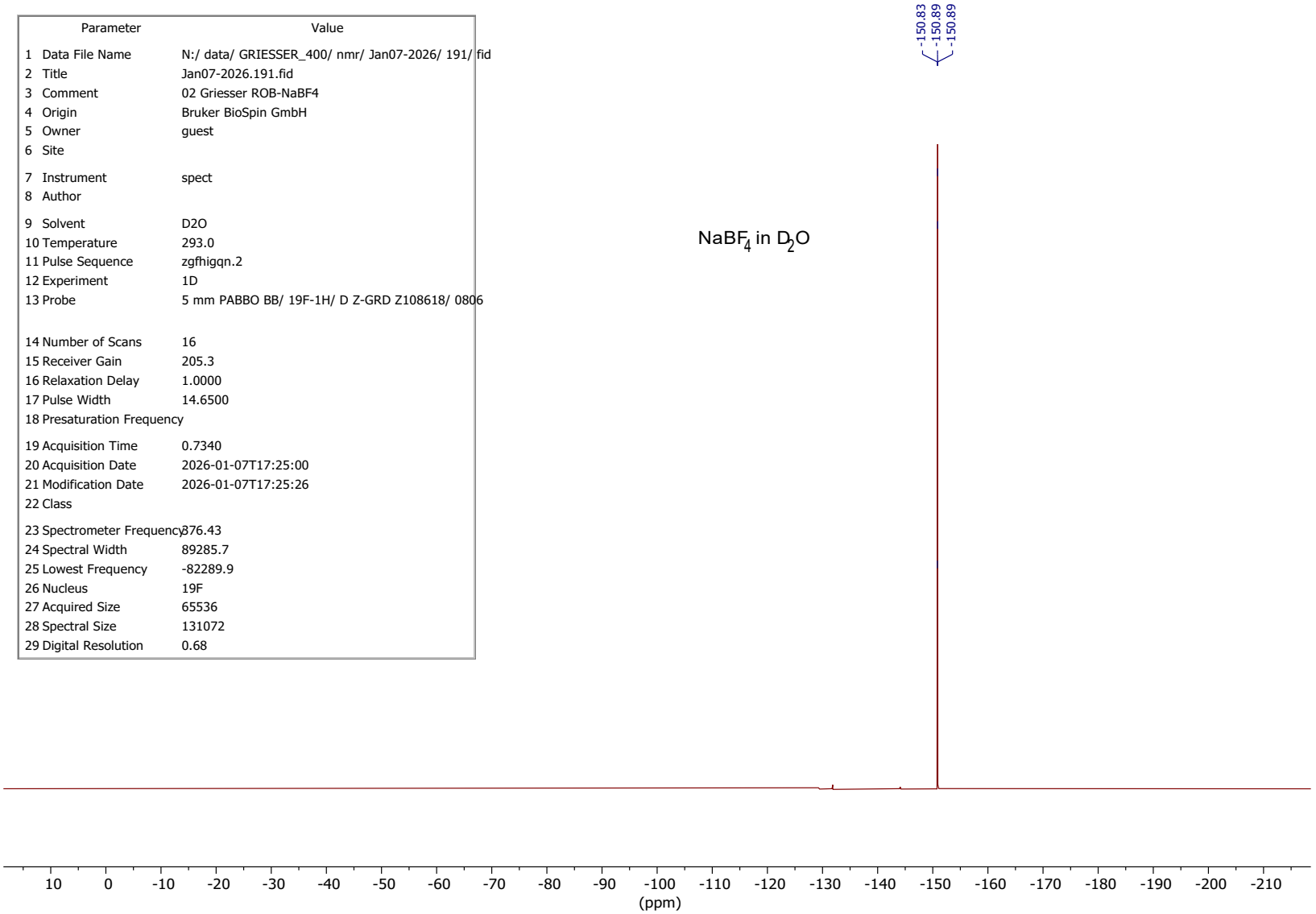

Figure S93: ^{19}F NMR spectrum of $NaBF_4$ in D_2O at 376 MHz.

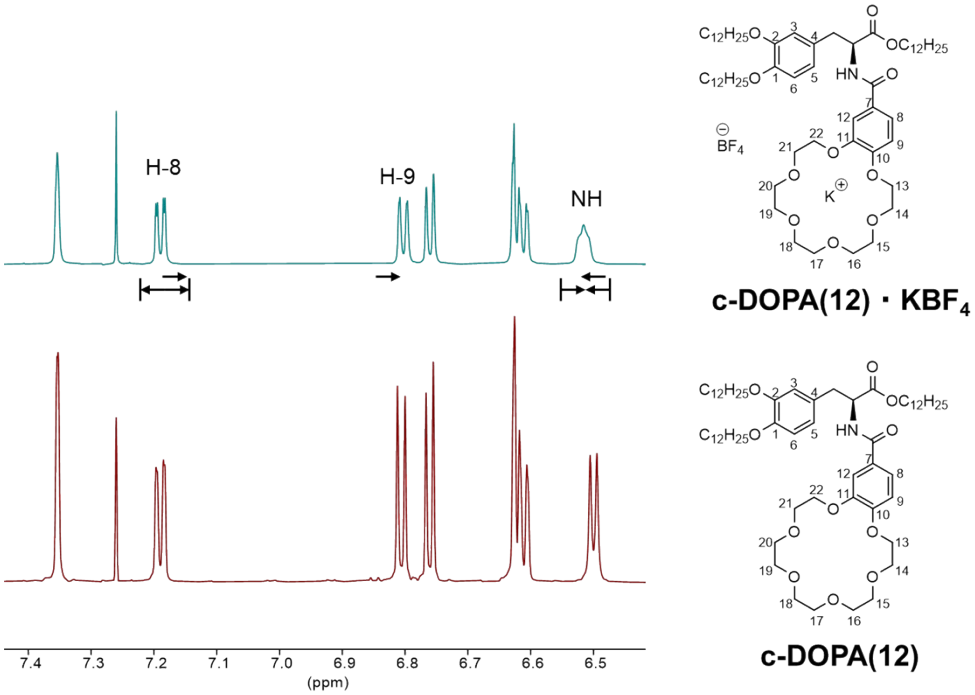

Figure S94: Selected region of the ^{1}H NMR spectrum (6.0 - 7.5 ppm) of **c-DOPA(12) • KBF$_4$** (top) compared to **c-DOPA(12)** (bottom).

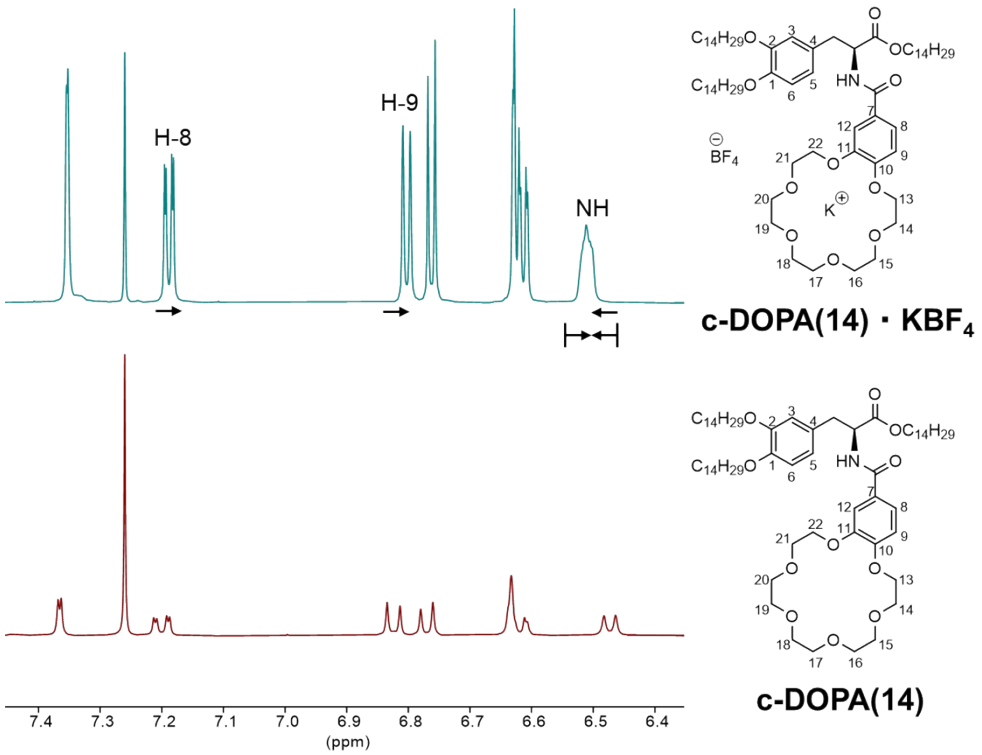

Figure S95: Selected region of the ^{1}H NMR spectrum (6.0 - 7.5 ppm) of **c-DOPA(14) • KBF$_4$** (top) compared to **c-DOPA(14)** (bottom).

4 Polarizing Optical Microscopy (POM)

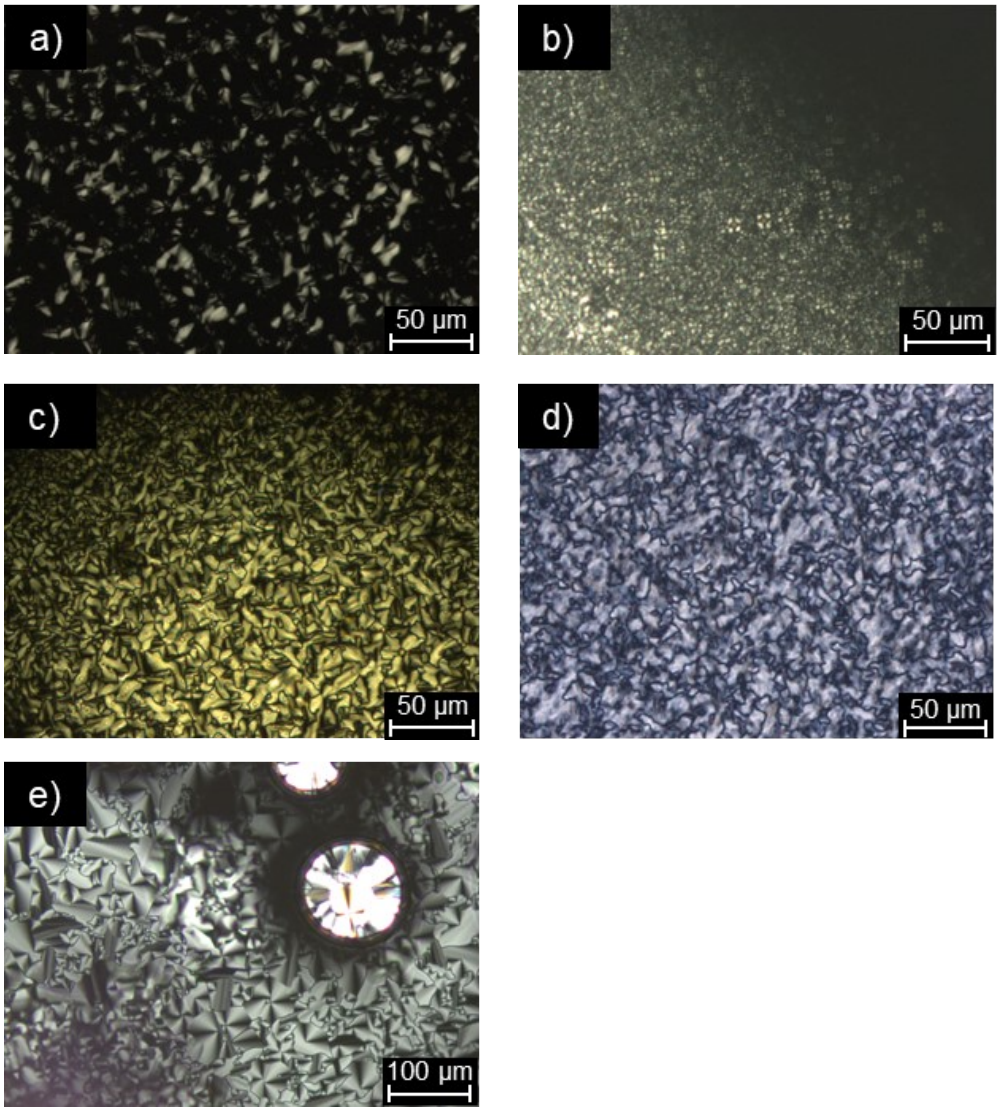

Figure S96: Optical micrographs of the SmA_d phase of the **c-DOPA(12) • MX** salt complexes between crossed polarizers upon cooling from the isotropic phase or heating from the crystalline phase: MX = c) **KSCN** at 92 °C (C) in 2 K/min. b) **NaI** at 75 °C (C) in 1 K/min on silylated slide. c) **KI** at 89 °C (C) in 1 K/min on silylated slide. d) **$NaBF_4$** at 85 °C (C) in 1 K/min. e) **KPF_6** at 100 °C (C) in 1 K/min; C = cooling.

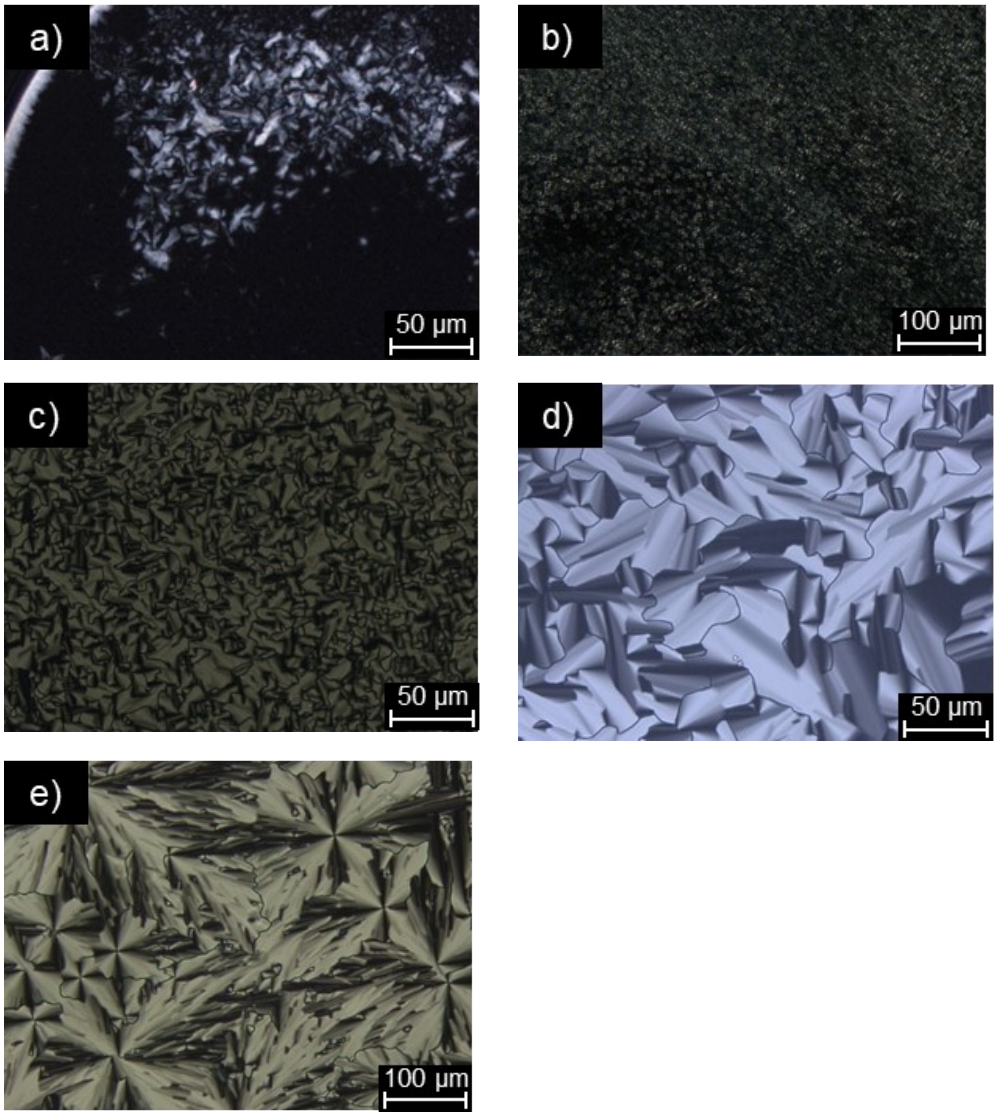

Figure S97: Optical micrographs of the mesophase of the **c-DOPA(14) • MX** salt complexes between crossed polarizers upon cooling from the isotropic phase or heating from the crystalline phase: MX = c) **KSCN** at 84 °C (C, SmA_d) in 1 K/min. a) **NaI** at 85 °C (C, SmA_d) in 1 K/min. b) **KI** at 110 °C (C, SmA_d) in 1 K/min. d) **$NaBF_4$** at 105 °C (C, SmA_d) in 1 K/min. e) **KPF_6** at 139 °C (C, Col_h) in 1 K/min; C = cooling.

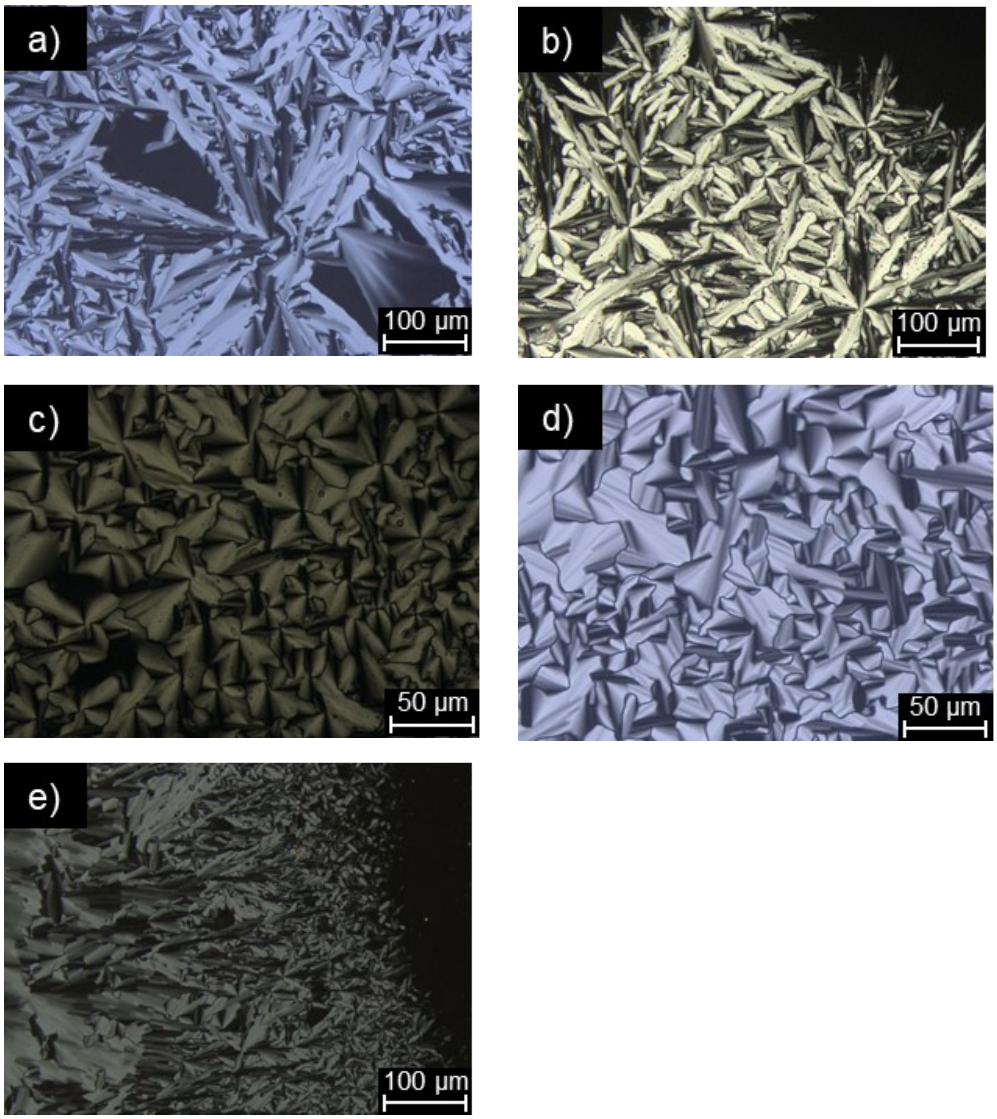

Figure S98: Optical micrographs of the Col_h phase of the **c-DOPA(16) • MX** salt complexes between crossed polarizers upon cooling from the isotropic phase: MX = a) **NaI** at 141 °C (C) in 1 K/min. b) **KI** at 132 °C (C) in 1 K/min. c) **KSCN** at 110 °C (C) in 1 K/min. d) **$NaBF_4$** at 119 °C (C) in 1 K/min. e) **KPF_6** at 130 °C (C) in 1 K/min; C = cooling.

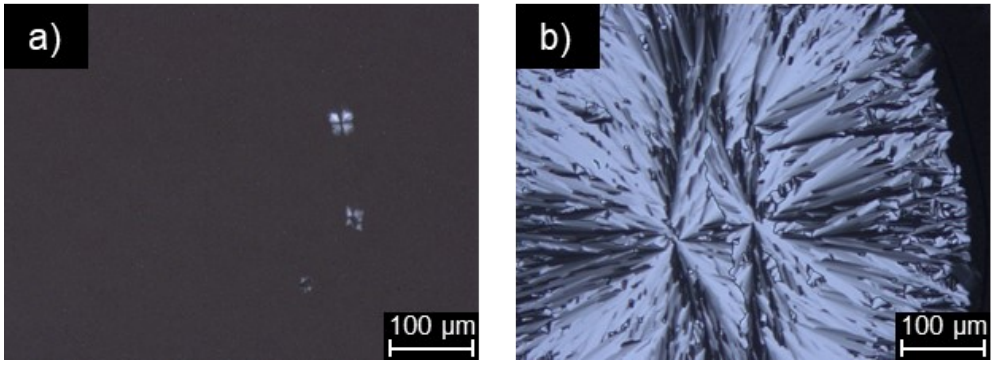

Figure S99: Optical micrographs of the mesophase of the **c-THIQ(n) • KPF_6** complexes between crossed polarizers upon cooling from the isotropic phase: n = a) **14** at 112 °C (C, SmA_d) in 1 K/min. b) **16** at 51 °C (C, Col_h) in 1 K/min; C = cooling.

5 Differential Scanning Calorimetry (DSC)

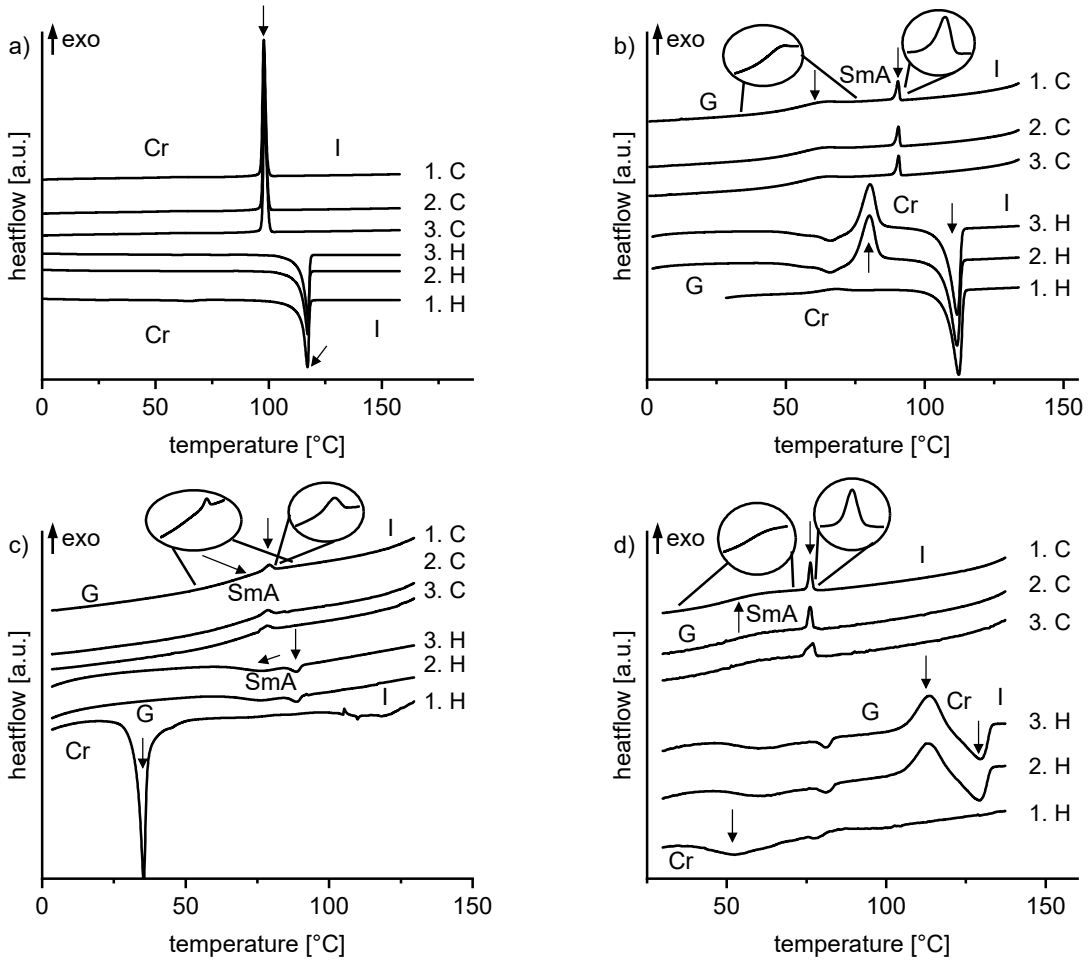

Figure S100: DSC measurement of a) **c-DOPA(12)**, b) **c-DOPA(12) • KSCN**, c) **c-DOPA(12) • NaI** and d) **c-DOPA(12) • KI** over three heating (H) and cooling (C) cycles, heating and cooling rate = 5 K/min.

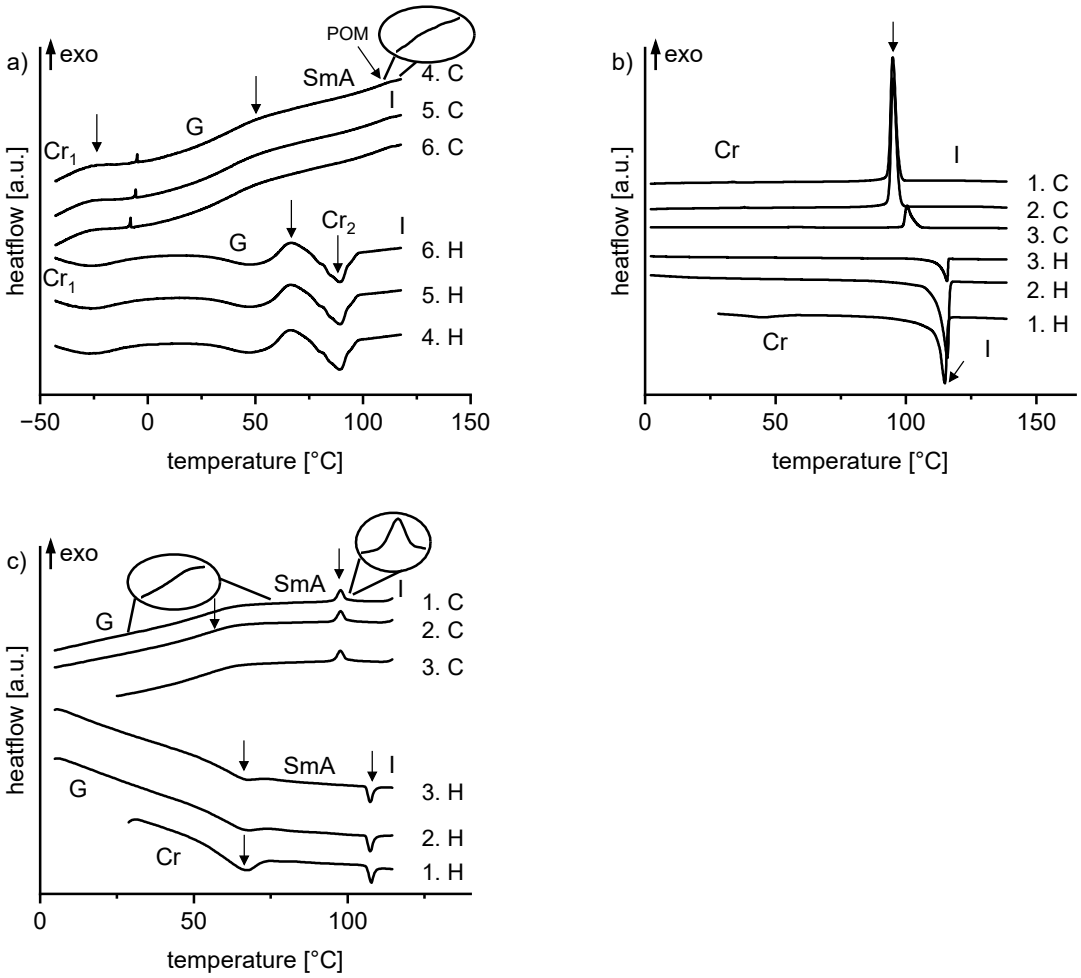

Figure S101: DSC measurement of a) **c-DOPA(12) • $NaBF_4$**, b) **c-DOPA(12) • KBF_4** and c) **c-DOPA(12) • KPF_6** over three heating (H) and cooling (C) cycles, heating and cooling rate = 5 K/min.

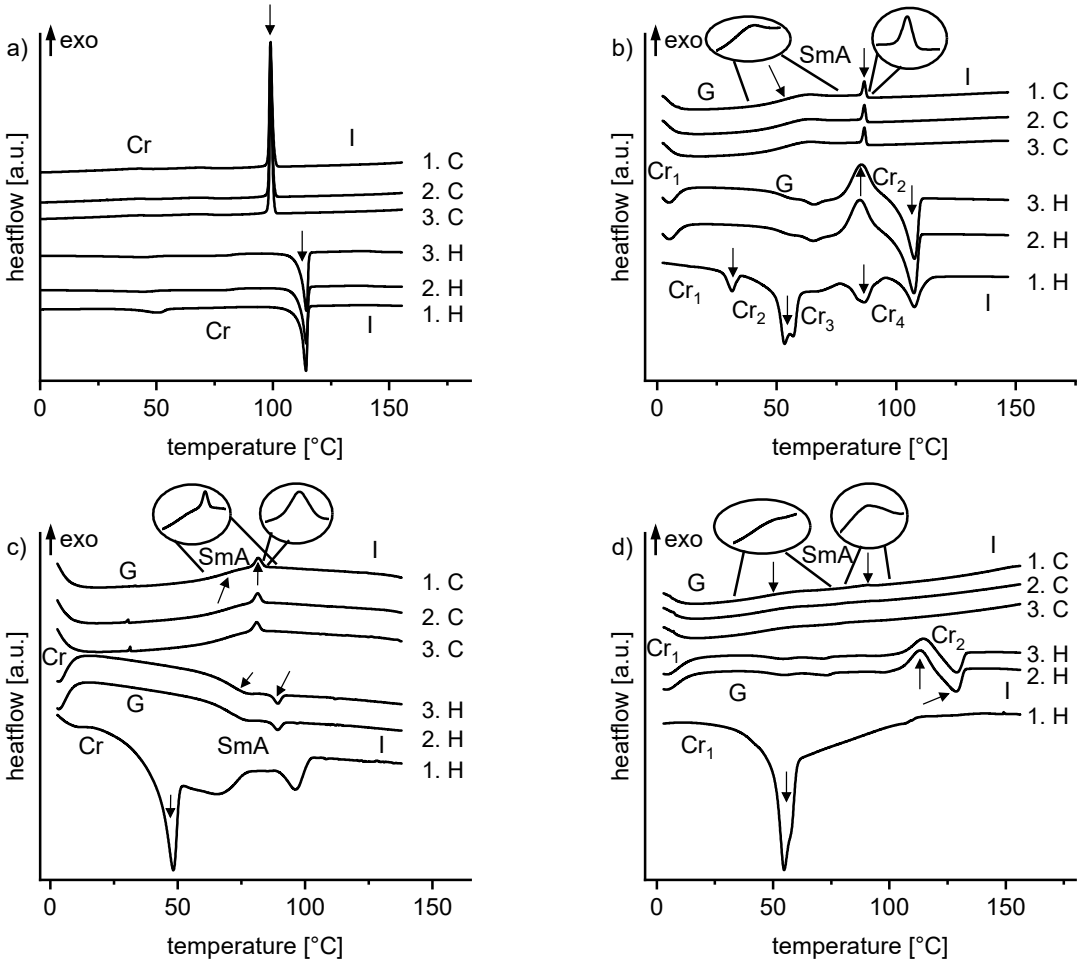

Figure S102: DSC measurement of a) **c-DOPA(14)**, b) **c-DOPA(14) • KSCN**, c) **c-DOPA(14) • NaI** and d) **c-DOPA(14) • KI** over three heating (H) and cooling (C) cycles, heating and cooling rate = 5 K/min.

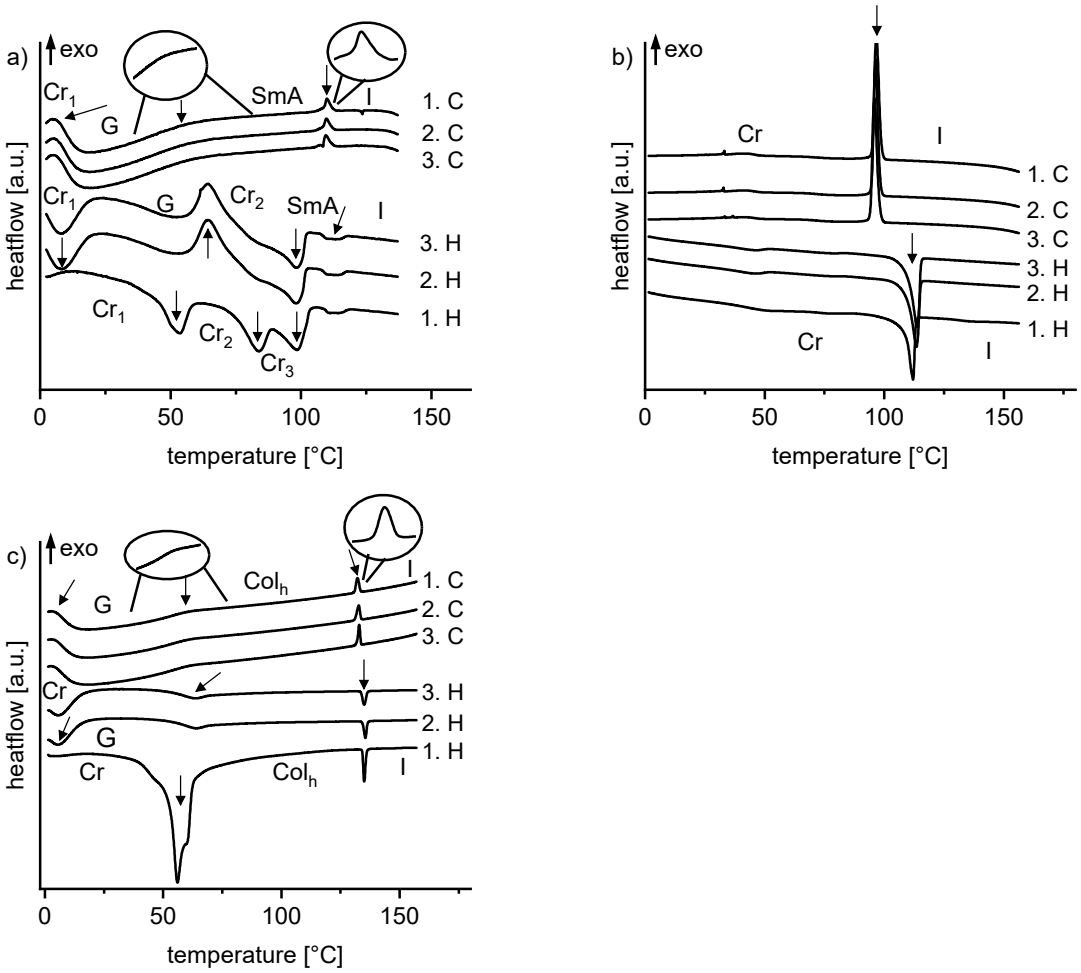

Figure S103: DSC measurement of a) **c-DOPA(14) • $NaBF_4$**, b) **c-DOPA(14) • KBF_4** and c) **c-DOPA(14) • KPF_6** over three heating (H) and cooling (C) cycles, heating and cooling rate = 5 K/min.

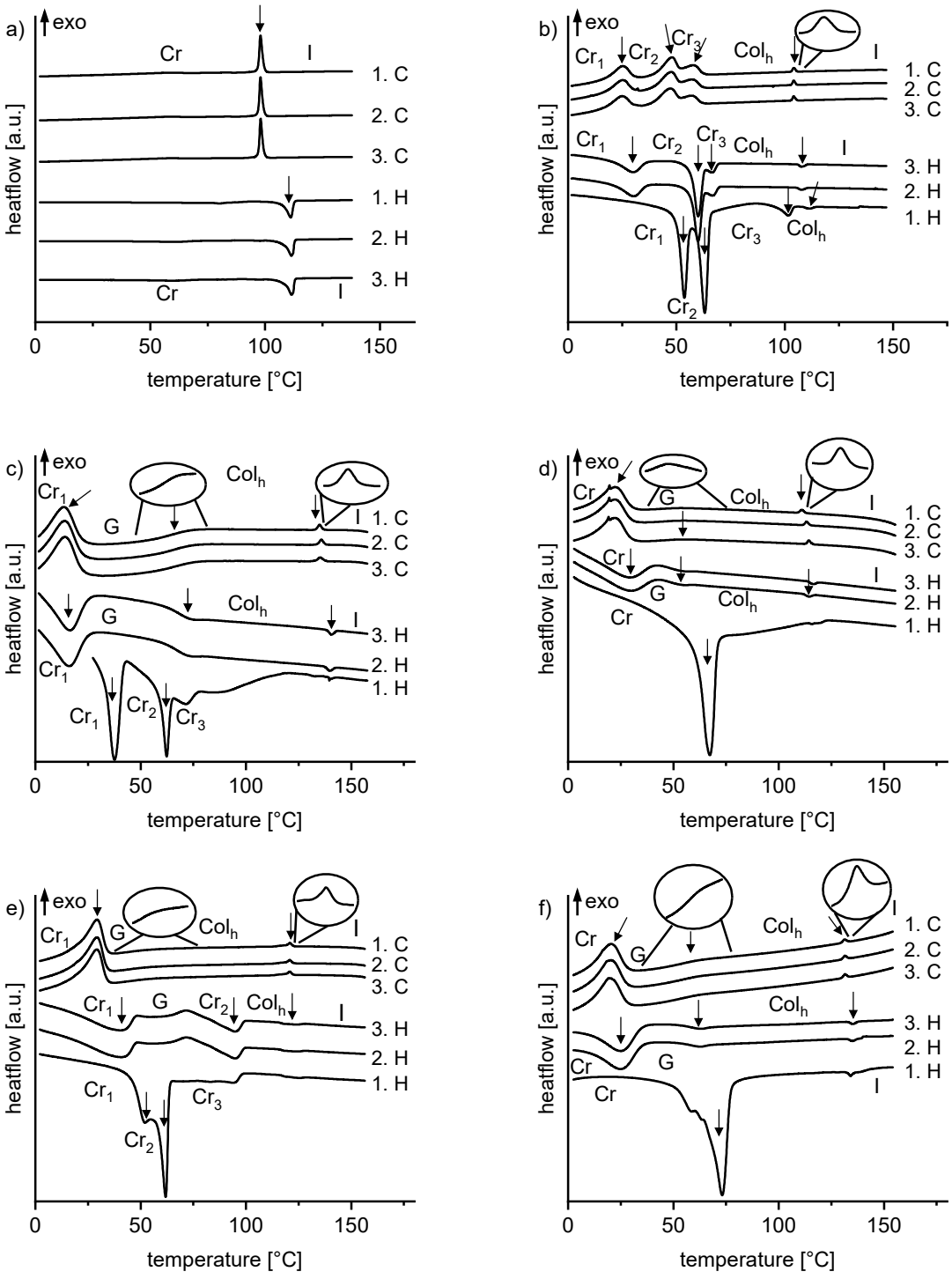

Figure S104: DSC measurement of a) **c-DOPA(16)**, b) **c-DOPA(16) • KSCN**, c) **c-DOPA(16) • NaI**, d) **c-DOPA(16) • KI**, e) **c-DOPA(16) • $NaBF_4$** and f) **c-DOPA(16) • KPF_6** over three heating (H) and cooling (C) cycles, heating and cooling rate = 5 K/min.

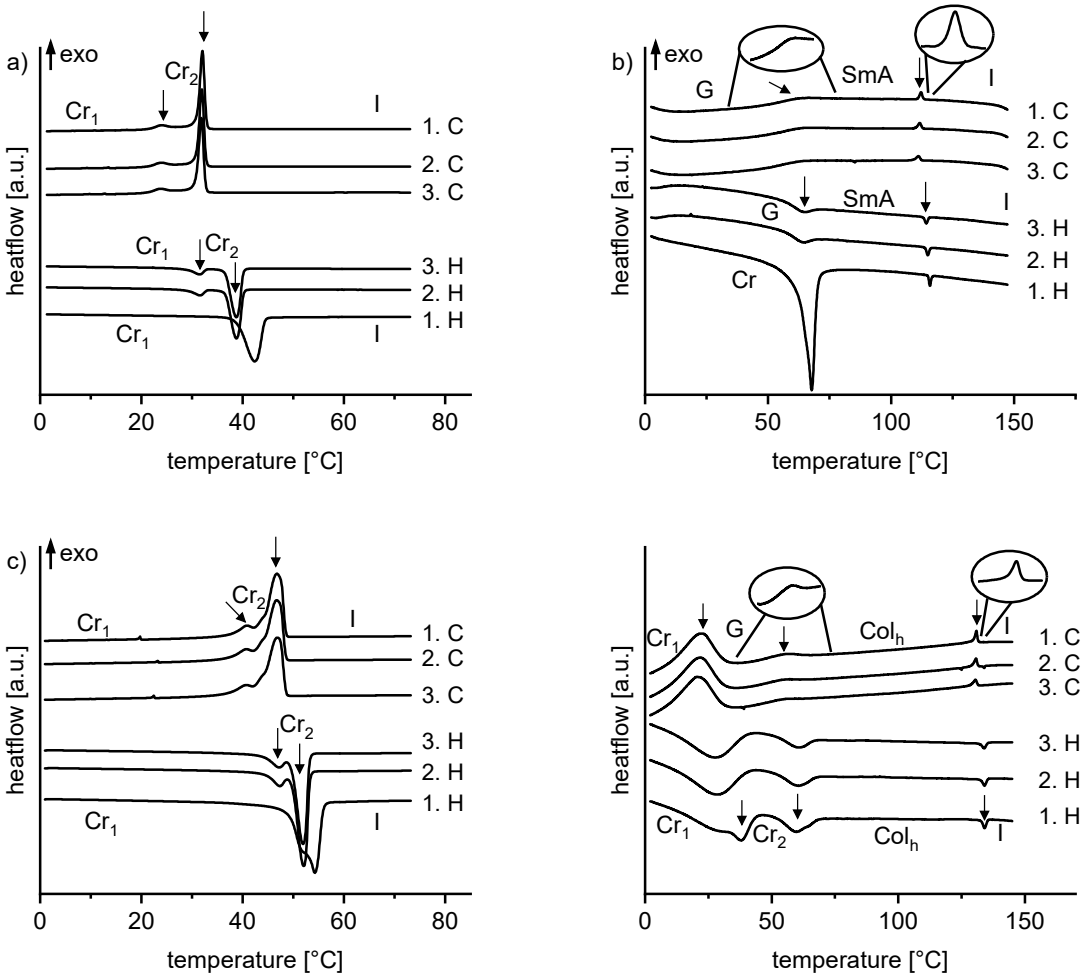

Figure S105: DSC measurement of a) **c-THIQ(14)**, b) **c-THIQ(14) • KPF_6**, c) **c-THIQ(16)** and d) **c-THIQ(16) • KPF_6** over three heating (H) and cooling (C) cycles, heating and cooling rate = 5 K/min.

Table S1: Phase transition temperatures [°C] (enthalpies [kJ/mol]) of **c-DOPA/THIQ(n)** parent compounds determined by DSC during heating (H) and cooling (C); G: glass, Cr: crystalline, SmA_d: smectic A_d phase, I: isotropic phase , • observed, - not observed.[a]

Compound		G	Cr		SmA_d	I
c-DOPA(12)	1st H	-	•	114 (-71.9)	-	•
	1st C	-	•	100 (70.6)	-	•
c-DOPA(14)	1st H	-	•	112 (-61.7)	-	•
	1st C	-	•	101 (70.0)	-	•
c-DOPA(16)	1st H	-	•	108 (-47.3)	-	•
	1st C	-	•	100 (49.1)	-	•
c-THIQ(14)	1st H	-	•	39 (-56.7)	-	•
	1st C	-	•	33 (35.0)	-	•
c-THIQ(16)	1st H	-	•	49 (-75.6)	-	•
	1st C	-	•	49 (62.6)	-	•

[a] Heating/Cooling rate: 5 K/min, Cr-Cr transitions are not listed.

Table S2: Phase transition temperatures [°C] (enthalpies [kJ/mol]) of non-liquid crystalline **c-DOPA(n) • KBF_4** complexes determined by DSC during heating (H) and cooling (C); G: glass, Cr: crystalline, SmA_d: smectic A_d phase, I: isotropic phase , • observed, - not observed.[a]

n		G	Cr		SmA_d	I
12	1st H	-	•	112 (-42.5)	-	•
	1st C	-	•	97 (61.1)	-	•
14	1st H	-	•	109 (-47.4)	-	•
	1st C	-	•	99 (69.1)	-	•

[a] Heating/Cooling rate: 5 K/min, Cr-Cr transitions are not listed.

Table S3: Phase transition temperatures [°C] (enthalpies [kJ/mol]) of **c-DOPA(12) • MX** complexes determined by DSC during heating (H) and cooling (C); G: glass, Cr: crystalline, SmA_d: smectic A_d phase, I: isotropic phase , • observed, - not observed.[a]

MX		G		Cr		SmA_d		I
KSCN	3rd H	•	75 (13.1) [c]	•	107 (-24.0)	-		•
	3rd C	•	61	-		•	91 (1.6)	•
NaI	3rd H	•	64	-		•	85 (-0.9)	•
	3rd C	•	81	-		•	83 (1.0)	•
KI	3rd H	•	105 (9.8) [c]	•	120 (-8.5)	-		•
	3rd C	•	63	-		•	77 (1.2)	•
$NaBF_4$	6th H	•	57 (5.2) [c]	•	-41 (-4.0) [b] 80 (-6.3)	-		•
	6th C	•	32	-	-19 (2.6) [b]	•	115 (0.1)	•
KPF_6	3rd H	-		•	56 (-1.9)	•	105 (-0.6)	•
	3rd C	•	69	-		•	101 (0.4)	•

[a] Heating/Cooling rate: 5 K/min, Cr-Cr transitions are not listed. [b] Cr-G transition observed below the G-Col_h transition. [c] Cold crystallization during heating.

Table S4: Phase transition temperatures [°C] (enthalpies [kJ/mol]) of **c-DOPA(14) • MX** complexes determined by DSC during heating (H) and cooling (C); G: glass, Cr: crystalline, SmA_d: smectic A_d phase, Col_h: columnar hexagonal phase, I: isotropic phase , • observed, - not observed. [a]

MX		G		Cr		SmA_d / Col_h[a)]		I
KSCN	3rd H	•	78 (17.6) [c]	•	101 (-18.7)	-		•
	3rd C	•	61	-		•	88 (1.2)	•
NaI	3rd H	•	59	-		•	87 (-0.8)	•
	3rd C	•	81	-		•	83 (1.0)	•
KI	3rd H	•	105 (8.3) [c]	•	121 (-7.0)	-		•
	3rd C	•	57	-		•	98 (0.4)	•
$NaBF_4$	3rd H	•	60 (6.8) [c]	•	2 (-2.3) [b] 86 (-11.1)	•	107 (-0.7)	•
	3rd C	•	58	•	12 (2.2) [b]	•	112 (0.5)	•
KPF_6[a)]	3rd H	•	52	-		•	134 (-0.8)	•
	3rd C	•	57	-		•	134 (0.8)	•

[a] Heating/Cooling rate: 5 K/min, Cr-Cr transitions are not listed. [b] Cr-G transition observed below the G-Col_h transition. [c] Cold crystallization during heating.

Table S5: Phase transition temperatures [°C] (enthalpies [kJ/mol]) of **c-DOPA(16) • MX** complexes determined by DSC during heating (H) and cooling (C); G: glass, Cr: crystalline, Col_h: columnar hexagonal phase, I: isotropic phase , • observed, - not observed. [a]

MX		G		Cr		Col_h		I
KSCN	3rd H	-		•	57 (-24.0)	•	106 (-0.6)	•
	3rd C	-		•	53 (17.3)	•	106 (0.6)	•
NaI	3rd H	•	60	-	6 (-13.0) [b]	•	139 (-0.4)	•
	3rd C	•	75	-	22 (13.8) [b]	•	137 (0.2)	•
KI	3rd H	•	47	•	10 (-16.7) [b]	•	114 (-0.4)	•
	3rd C	•	54	•	30 (17.5) [b]	•	116 (0.4)	•
$NaBF_4$	3rd H	•	64 (4.6) [c]	•	82 (-8.0)	•	113 (-0.8)	•
	3rd C	•	50	•	34 (28.1) [b]	•	122 (0.4)	•
KPF_6	3rd H	•	51	•	10 (-17.5) [b]	•	133 (-0.4)	•
	3rd C	•	69	•	28 (18.0) [b]	•	133 (0.4)	•

[a] Heating/Cooling rate: 5 K/min, Cr-Cr transitions are not listed. [b] Cr-G transition observed below the G-Col_h transition. [c] Cold crystallization during heating.

Table S6: Phase transition temperatures [°C] (enthalpies [kJ/mol]) of **c-THIQ(n) • KPF_6** complexes determined by DSC during heating (H) and cooling (C); G: glass, Cr: crystalline, SmA_d: smectic A_d phase, Col_h: columnar hexagonal phase, I: isotropic phase , • observed, - not observed. [a]

n		G		Cr		SmA_d / Col_h [a)]		I
14	3rd H	•	47	-		•	113 (-0.4)	•
	3rd C	•	65	-		•	112 (0.4)	•
16 [a)]	3rd H	-		•	52 (-3.4)	•	132 (-0.4)	•
	3rd C	•	54	•	31 (18.1) [b]	•	132 (0.4)	•

[a] Heating/Cooling rate: 5 K/min. [b] Cr-G transition observed below the G-Col_h transition

6 Ion properties

Table S7: Relevant ionic radii and polarizabilities.

Ion	Ionic radius / Å		Polarizability / Å^3	
Na^+	1.02 (CN = 6)	Ref. [14]	0.408 (0.279)	Ref. [15,16]
K^+	1.38 (CN = 6)	Ref. [14]	1.334 (0.873)	Ref. [15,16]
SCN^-	2.09	Ref. [17]	10.406	Ref. [18]
I^-	2.11 (2.20)	Ref. [17,19]	6.431 (7.197)	Ref. [15,16]
BF_4^-	2.05 (2.11)	Ref. [17,19]	3.118	Ref. [18]
PF_6^-	2.42	Ref. [17,19]	4.397	Ref. [18]

7 X-ray characterization (WAXS, SAXS)

Table S8: Reflexes in XRD measurements of **c-DOPA(12) • MX**.

MX	Phase	Spacing / Å		Miller indices (*hkl*)
		Obs.	Calc.	
KSCN	(SmA_d at 85 °C)	38.8 4.5		(001) halo
NaI	(SmA_d at 64 °C)	38.0 4.2		(001) halo
	(SmA_d at 69 °C)	38.0 4.2		(001) halo
	(SmA_d at 72 °C)	37.9 4.2		(001) halo
	(SmA_d at 77 °C)	37.9 4.1		(001) halo
KI	(SmA_d at 68 °C)	36.9 4.4		(001) halo
	(SmA_d at 70 °C)	36.9 18.5 4.4	18.4	(001) (002) halo
	(SmA_d at 72 °C)	36.9 18.6 4.4	18.4	(001) (002) halo
	(SmA_d at 76 °C)	36.9 18.4 4.4	18.4	(001) (002) halo
	(SmA_d at 80 °C)	36.9 4.4		(001) halo
$NaBF_4$	(SmA_d at 80 °C)	42.7 4.5		(001) halo
	(SmA_d at 85 °C)	41.9 4.5		(001) halo
	(SmA_d at 90 °C)	41.9 4.5		(001) halo
	(SmA_d at 95 °C)	41.7 4.5		(001) (halo)
KPF_6	(SmA_d at 70 °C)	45.9 4.1		(001) halo
	(SmA_d at 75 °C)	45.6 4.5		(001) halo
	(SmA_d at 83 °C)	45.1 4.1		(001) halo
	(SmA_d at 93 °C)	44.5 4.1		(001) halo
	(SmA_d at 102 °C)	44.1 4.1		(001) halo

Table S9: Reflexes in XRD measurements of **c-DOPA(14) • MX**.

MX	Phase	Spacing / Å		Miller indices (*hkl*)
		Obs.	Calc.	
KSCN	(SmA_d at 85 °C)	41.1 4.6		(001) halo
NaI	(SmA_d at 65 °C)	39.4 4.4		(001) halo
	(SmA_d at 68 °C)	39.3 4.4		(001) halo
	(SmA_d at 72 °C)	39.3 4.5		(001) halo
	(SmA_d at 75 °C)	39.4 4.5		(001) halo
	(SmA_d at 78 °C)	39.5 4.5		(001) halo
KI	(SmA_d at 74 °C)	40.0 20.0 4.2	20.0	(001) (002) halo
	(SmA_d at 80 °C)	40.1 20.0 4.2	20.1	(001) (002) halo
	(SmA_d at 88 °C)	40.1 20.1 4.2	20.1	(001) (002) halo
	(SmA_d at 95 °C)	40.2 20.1 4.2	20.1	(001) (002) halo
	(SmA_d at 105 °C)	40.4 20.1 4.2	20.2	(001) (002) halo
$NaBF_4$	(SmA_d at 60 °C)	48.6 4.4		(001) halo
	(SmA_d at 65 °C)	47.9 4.4		(001) halo
	(SmA_d at 70 °C)	47.3 4.4		(001) halo
	(SmA_d at 75 °C)	46.8 4.4		(001) halo
	(SmA_d at 80 °C)	46.3 4.4		(001) halo
	(SmA_d at 85 °C)	45.9 4.4		(001) halo
	(SmA_d at 90 °C)	45.5 4.4		(001) halo
	(SmA_d at 95 °C)	45.2 4.4		(001) halo
	(SmA_d at 100 °C)	44.9 4.4		(001) halo
	(SmA_d at 105 °C)	44.6 4.4		(001) halo
	(SmA_d at 110 °C)	44.3 4.4		(001) (halo)

Table S10: Lattice constants and reflexes in XRD measurements of **c-DOPA(14) • KPF_6**.

	Phase	Spacing / Å		Miller indices (*hkl*)	*a* / Å
		Obs.	Calc.		
c-DOPA(14) • KPF_6	(Col_h at 60 °C)	49.6		(100)	57.2
		28.7	28.6	(110)	
		24.8	24.8	(200)	
		4.5		halo	
	(Col_h at 65 °C)	49.1		(100)	56.7
		28.4	28.4	(110)	
		24.6	24.6	(200)	
		4.5		halo	
	(Col_h at 70 °C)	48.7		(100)	56.2
		28.2	28.1	(110)	
		24.4	24.3	(200)	
		4.6		halo	
	(Col_h at 75 °C)	48.3		(100)	55.8
		27.9	27.9	(110)	
		24.2	24.1	(200)	
		4.6		halo	
	(Col_h at 80 °C)	47.9		(100)	55.3
		27.7	27.6	(110)	
		23.9	23.9	(200)	
		4.6		halo	
	(Col_h at 85 °C)	47.5		(100)	54.9
		27.6	27.5	(110)	
		24.1	23.8	(200)	
		4.6		halo	
	(Col_h at 90 °C)	47.2		(100)	54.5
		27.5	27.3	(110)	
		23.8	23.6	(200)	
		4.6		halo	
	(Col_h at 95 °C)	47.0		(100)	54.2
		23.6	23.5	(200)	
		4.7		halo	
	(Col_h at 100 °C)	46.6		(100)	53.8
		27.0	26.9	(110)	
		23.4	23.3	(200)	
		4.7		halo	
	(Col_h at 105 °C)	46.3		(100)	53.5
		26.8	26.8	(110)	
		23.3	23.2	(200)	
		4.7		halo	
	(Col_h at 110 °C)	46.1		(100)	53.2
		26.8	26.6	(110)	
		23.2	23.1	(200)	
		4.7		halo	
	(Col_h at 115 °C)	45.9		(100)	53.0
		26.7	26.5	(110)	
		23.0	23.0	(200)	
		4.7		halo	
	(Col_h at 120 °C)	45.6		(100)	52.7
		26.3	26.3	(110)	
		22.9	22.8	(200)	
		4.7		halo	

	(Col_h at 125 °C)	45.4 26.4 22.8 4.7	 26.2 22.7 	(100) (110) (200) halo	52.4
	(Col_h at 130 °C)	45.1 26.4 22.8 4.7	 26.0 22.6 	(100) (110) (200) halo	51.6

Table S11: Lattice constants and reflexes in XRD measurements of **c-DOPA(16) • KSCN**.

	Phase	Spacing / Å		Miller indices (*hkl*)	*a* / Å
		Obs.	Calc.		
c-DOPA(16) • KSCN	(Col_h at 60 °C)	52.4 30.2 26.3 4.5	 30.3 26.2 	(100) (110) (200) halo	60.5
	(Col_h at 65 °C)	51.6 29.8 25.7 4.5	 29.8 25.8 	(100) (110) (200) halo	59.6
	(Col_h at 70 °C)	50.8 29.5 25.4 4.6	 29.3 25.4 	(100) (110) (200) halo	58.7
	(Col_h at 75 °C)	50.1 28.8 25.0 4.6	 28.9 25.1 	(100) (110) (200) halo	57.9
	(Col_h at 80 °C)	49.3 28.4 24.8 4.6	 28.5 24.7 	(100) (110) (200) halo	56.9
	(Col_h at 85 °C)	48.7 28.3 24.3 4.6	 28.1 24.4 	(100) (110) (200) halo	56.2
	(Col_h at 90 °C)	48.2 4.6	 	(100) halo	55.6
	(Col_h at 95 °C)	47.6 4.6	 	(100) halo	54.9
	(Col_h at 100 °C)	47.0 4.6	 	(100) halo	54.3
	(Col_h at 105 °C)	46.6 4.7	 	(100) halo	53.8

Table S12: Lattice constants and reflexes in XRD measurements of **c-DOPA(16) • NaI**.

	Phase	Spacing / Å		Miller indices (*hkl*)	*a* / Å
		Obs.	Calc.		
c-DOPA(16) • NaI	(Col_h at 93 °C)	53.7		(100)	62.0
		30.8	31.0	(110)	
		26.9	26.8	(200)	
		4.4		halo	
	(Col_h at 102 °C)	53.0		(100)	61.2
		30.7	30.6	(110)	
		26.5	26.5	(200)	
		4.3		halo	
	(Col_h at 107 °C)	52.6		(100)	60.8
		4.4		halo	
	(Col_h at 112 °C)	52.3		(100)	60.4
		4.4		halo	
	(Col_h at 116 °C)	52.1		(100)	60.1
		4.3		halo	
	(Col_h at 121 °C)	51.7		(100)	59.7
		4.4		halo	
	(Col_h at 126 °C)	51.5		(100)	59.4
		4.4		halo	
	(Col_h at 131 °C)	51.2		(100)	59.1
		4.4		halo	
	(Col_h at 135 °C)	51.0		(100)	58.8
		4.4		halo	
	(Col_h at 140 °C)	50.8		(100)	58.6
		4.5		halo	
	(Col_h at 145 °C)	50.6		(100)	58.5
		4.5		halo	
	(Col_h at 150 °C)	50.2		(100)	58.0
		4.5		halo	
	(Col_h at 154 °C)	50.0		(100)	57.8
		29.2	28.9	(110)	
		25.3	25.0	(200)	
		4.6		halo	

Table S13: Lattice constants and reflexes in XRD measurements of **c-DOPA(16) • KI**.

	Phase	Spacing / Å		Miller indices (*hkl*)	*a* / Å
		Obs.	Calc.		
c-DOPA(16) • KI	(Col_h at 70 °C)	53.0		(100)	61.2
		30.6	30.6	(110)	
		26.7	26.5	(200)	
		4.5		halo	
	(Col_h at 75 °C)	53.0		(100)	60.4
		4.5		halo	
	(Col_h at 80 °C)	52.3		(100)	59.6
		4.5		halo	
	(Col_h at 84 °C)	51.6		(100)	59.1
		4.5		halo	
	(Col_h at 90 °C)	51.1		(100)	58.4
		4.5		halo	
	(Col_h at 95 °C)	52.2		(100)	57.9
		30.3	30.2	(110)	
		26.3	26.1	(200)	
		4.5		halo	
	(Col_h at 100 °C)	50.6		(100)	57.3
		4.5		halo	
	(Col_h at 105 °C)	50.2		(100)	56.8
		4.5		halo	

Table S14: Lattice constants and reflexes in XRD measurements of **c-DOPA(16) • $NaBF_4$**.

	Phase	Spacing / Å		Miller indices (*hkl*)	*a* / Å
		Obs.	Calc.		
c-DOPA(16) • $NaBF_4$	(Col_h at 75 °C)	47.6		(100)	54.9
		28.3	27.5	(110)	
		24.0	23.8	(200)	
		4.6		halo	
	(Col_h at 80 °C)	47.0		(100)	54.2
		27.1	27.1	(110)	
		23.7	23.5	(200)	
		4.6		halo	
	(Col_h at 85 °C)	46.6		(100)	53.8
		4.6		halo	
	(Col_h at 90 °C)	46.2		(100)	53.4
		4.6		halo	
	(Col_h at 95 °C)	45.9		(100)	53.0
		4.6		halo	
	(Col_h at 100 °C)	45.5		(100)	52.5
		4.6		halo	
	(Col_h at 105 °C)	45.3		(100)	52.3
		4.6		halo	
	(Col_h at 110 °C)	45.0		(100)	52.0
		4.7		halo	
	(Col_h at 115 °C)	44.6		(100)	51.5
		4.7		halo	
	(Col_h at 120 °C)	44.5		(100)	51.4
		4.7		halo	

Table S15: Lattice constants and reflexes in XRD measurements of **c-DOPA(16) • KPF_6**.

	Phase	Spacing / Å		Miller indices (*hkl*)	*a* / Å
		Obs.	Calc.		
c-DOPA(16) • KPF_6	(Col_h at 70 °C)	56.8		(100)	65.6
		29.1	28.4	(200)	
		4.6		halo	
	(Col_h at 74 °C)	56.8		(100)	65.6
		33.1	32.8	(110)	
		28.6	28.4	(200)	
		4.4		halo	
	(Col_h at 80 °C)	55.5		(100)	64.0
		32.6	32.0	(110)	
		28.4	27.7	(200)	
		4.6		halo	
	(Col_h at 84 °C)	55.0		(100)	63.5
		28.1	27.5	(200)	
		4.7		halo	
	(Col_h at 90 °C)	54.4		(100)	62.8
		27.8	27.2	(200)	
		4.7		halo	
	(Col_h at 95 °C)	53.9		(100)	62.3
		27.5	27.0	(200)	
		4.7		halo	
	(Col_h at 100 °C)	53.4		(100)	61.7
		27.2	26.7	(200)	
		4.7		halo	
	(Col_h at 105 °C)	53.2		(100)	61.5
		27.1	26.6	(200)	
		4.7		halo	
	(Col_h at 110 °C)	52.9		(100)	61.0
		31.0	30.5	(110)	
		27.0	26.4	(200)	
		4.7		halo	
	(Col_h at 115 °C)	52.6		(100)	60.8
		30.8	30.4	(110)	
		26.5	26.3	(200)	
		4.7		halo	
	(Col_h at 120 °C)	52.2		(100)	60.3
		26.4	26.1	(200)	
		4.7		halo	
	(Col_h at 125 °C)	51.9		(100)	59.9
		26.4	25.9	(200)	
		4.7		halo	
	(Col_h at 130 °C)	51.6		(100)	59.5
		30.4	29.8	(110)	
		26.3	25.8	(200)	
		4.7		halo	

Table S16: Reflexes in XRD measurements of **c-THIQ(14) • KPF_6**.

	Phase	Spacing / Å		Miller indices (*hkl*)
		Obs.	Calc.	
c-THIQ(14) • KPF_6	(SmA_d at 60 °C)	48.3		(001)
		4.5		halo
	(SmA_d at 65 °C)	47.7		(001)
		4.5		halo
	(SmA_d at 70 °C)	47.2		(001)
		4.5		halo
	(SmA_d at 75 °C)	46.8		(001)
		4.5		halo
	(SmA_d at 80 °C)	46.3		(001)
		4.5		halo
	(SmA_d at 85 °C)	45.9		(001)
		4.5		halo
	(SmA_d at 90 °C)	45.6		(001)
		4.5		halo
	(SmA_d at 95 °C)	45.3		(001)
		4.5		halo

Table S17: Lattice constants and reflexes in XRD measurements of **c-THIQ(16) • KPF_6**.

	Phase	Spacing / Å		Miller indices (*hkl*)	*a* / Å
		Obs.	Calc.		
c-THIQ(16) • KPF_6	(Col_h at 60 °C)	53.3		(100)	61.5
		30.9	30.8	(110)	
		26.7	26.7	(200)	
		4.5		halo	
	(Col_h at 65 °C)	52.5		(100)	60.6
		30.6	30.3	(110)	
		26.3	26.3	(200)	
		4.5		halo	
	(Col_h at 70 °C)	51.8		(100)	59.8
		29.6	29.9	(110)	
		26.0	25.9	(200)	
		4.5		halo	
	(Col_h at 75 °C)	51.2		(100)	59.1
		29.7	29.6	(110)	
		25.6	25.6	(200)	
		4.5		halo	
	(Col_h at 80 °C)	50.6		(100)	58.5
		29.4	29.2	(110)	
		25.4	25.3	(200)	
		4.5		halo	
	(Col_h at 85 °C)	50.2		(100)	58.0
		29.6	29.0	(110)	
		25.2	25.1	(200)	
		4.5		halo	
	(Col_h at 90 °C)	49.7		(100)	57.4
		25.2	24.9	(200)	
		4.5		halo	
	(Col_h at 95 °C)	49.3		(100)	56.9
		28.7	28.4	(110)	
		24.9	24.6	(200)	
		4.5		halo	
	(Col_h at 100 °C)	49.0		(100)	56.6
		24.6	24.5	(200)	
		4.5		halo	
	(Col_h at 105 °C)	48.8		(100)	56.4
		4.6		halo	
	(Col_h at 110 °C)	48.5		(100)	56.0
		4.5		halo	
	(Col_h at 115 °C)	48.5		(100)	56.0
		4.6		halo	
	(Col_h at 120 °C)	48.2		(100)	55.7
		4.6		halo	
	(Col_h at 125 °C)	47.8		(100)	55.2
		4.6		halo	
	(Col_h at 130 °C)	47.4		(100)	54.8
		4.6		halo	

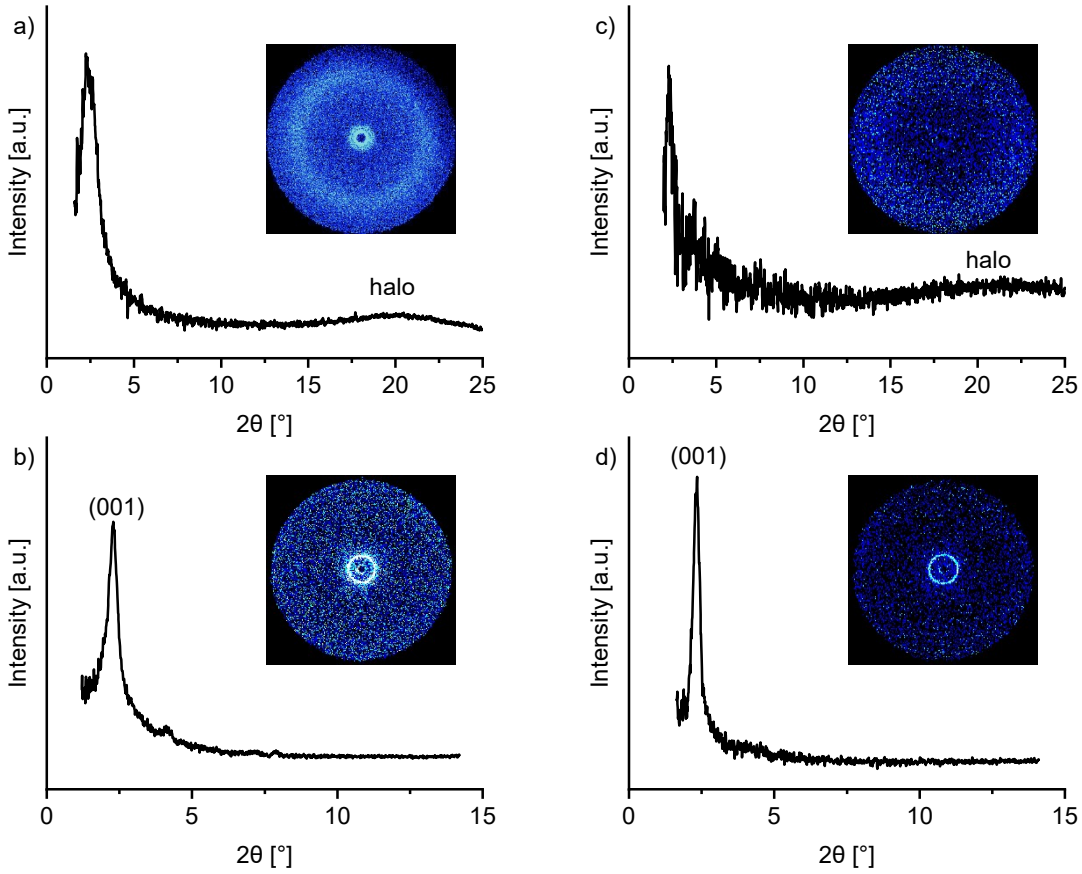

Figure S106: a) WAXS and b) SAXS diffractogram of **c-DOPA(12) • KSCN** at 85 °C as well as c) WAXS and d) SAXS diffractogram of **c-DOPA(12) • NaI** at 64 °C with diffraction patterns as inset.

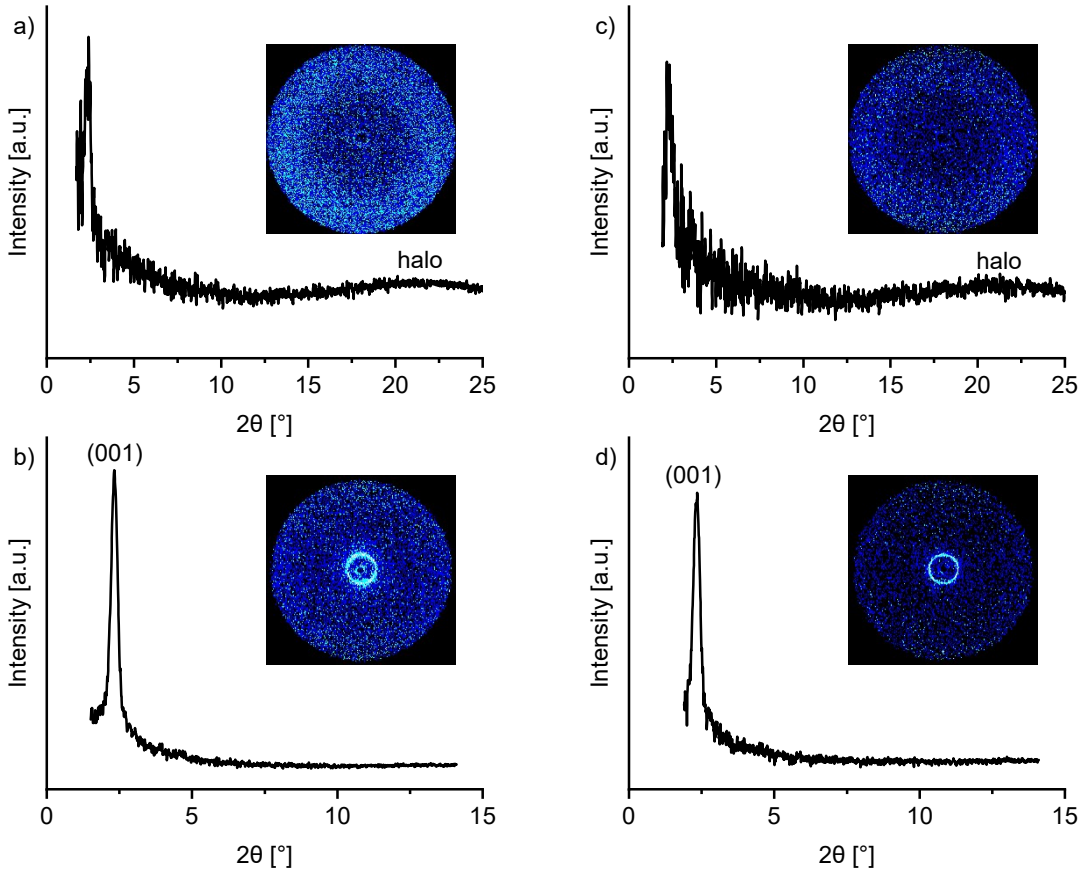

Figure S107: WAXS and SAXS diffractogram of **c-DOPA(12) • NaI** at 69 °C (a, b) as well as 72 °C (c, d) with diffraction patterns as inset.

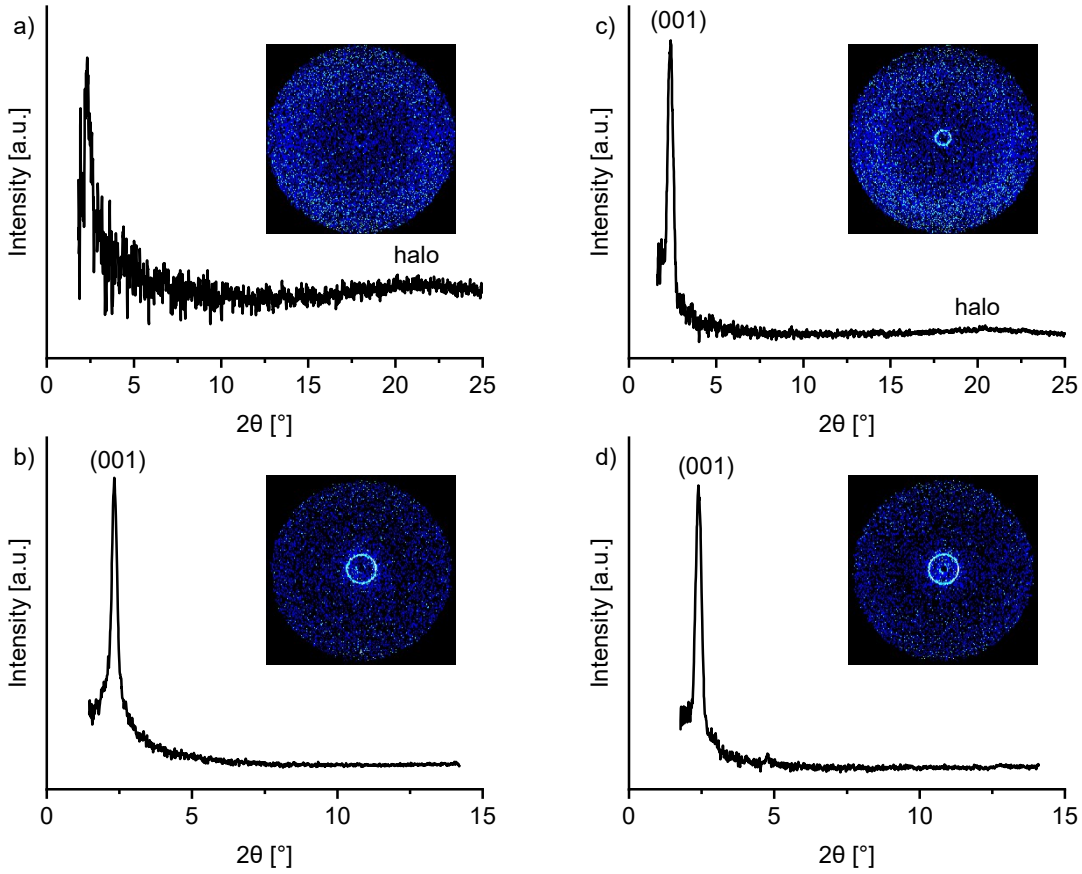

Figure S108: a) WAXS and b) SAXS diffractogram of **c-DOPA(12) • NaI** at 77 °C as well as c) WAXS and d) SAXS diffractogram of **c-DOPA(12) • KI** at 68 °C with diffraction patterns as inset.

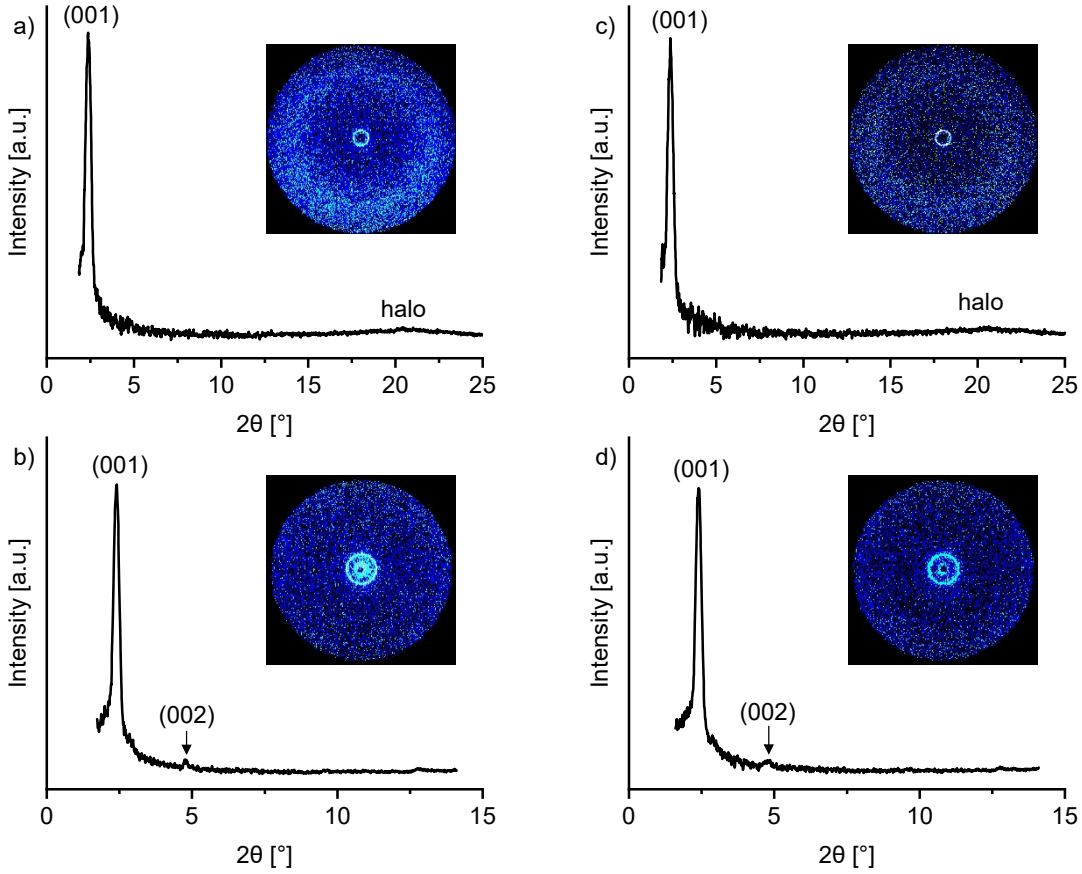

Figure S109: WAXS and SAXS diffractogram of **c-DOPA(12) • KI** at 70 °C (a, b) as well as 72 °C (c, d) with diffraction patterns as inset.

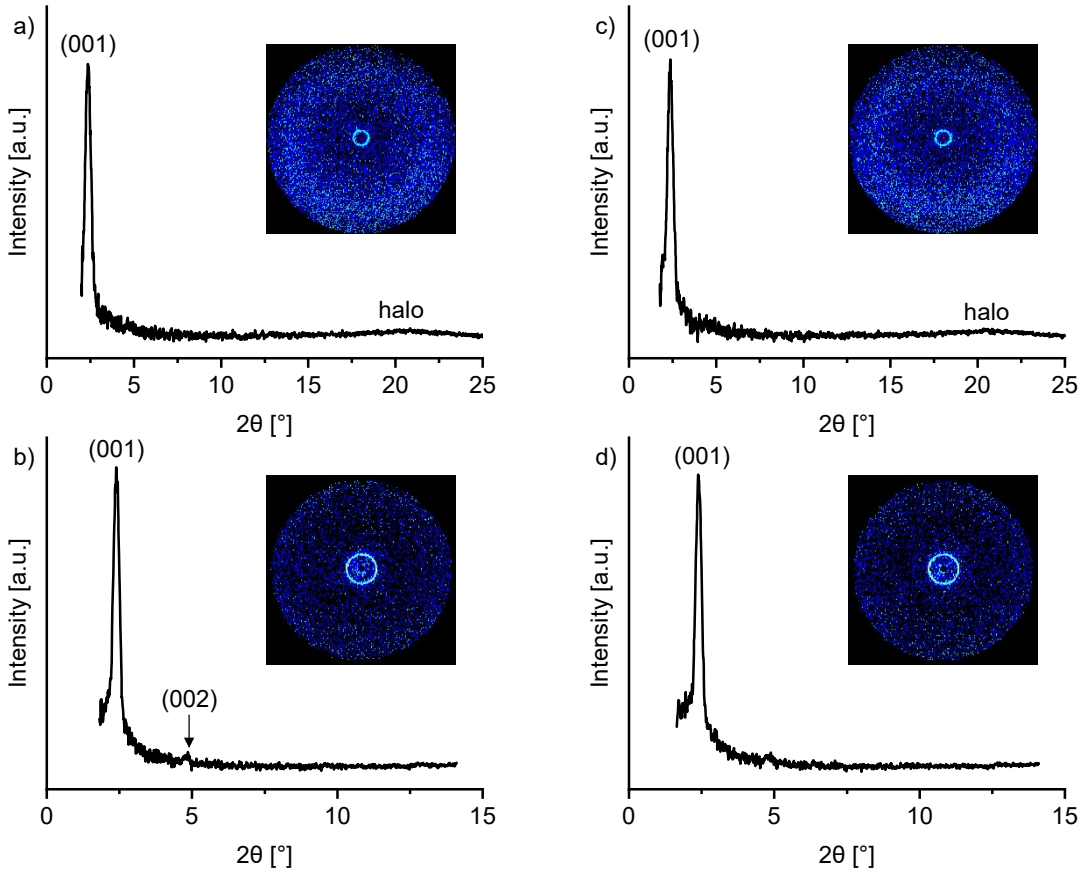

Figure S110: WAXS and SAXS diffractogram of **c-DOPA(12) • KI** at 76 °C (a, b) as well as 80 °C (c, d) with diffraction patterns as inset.

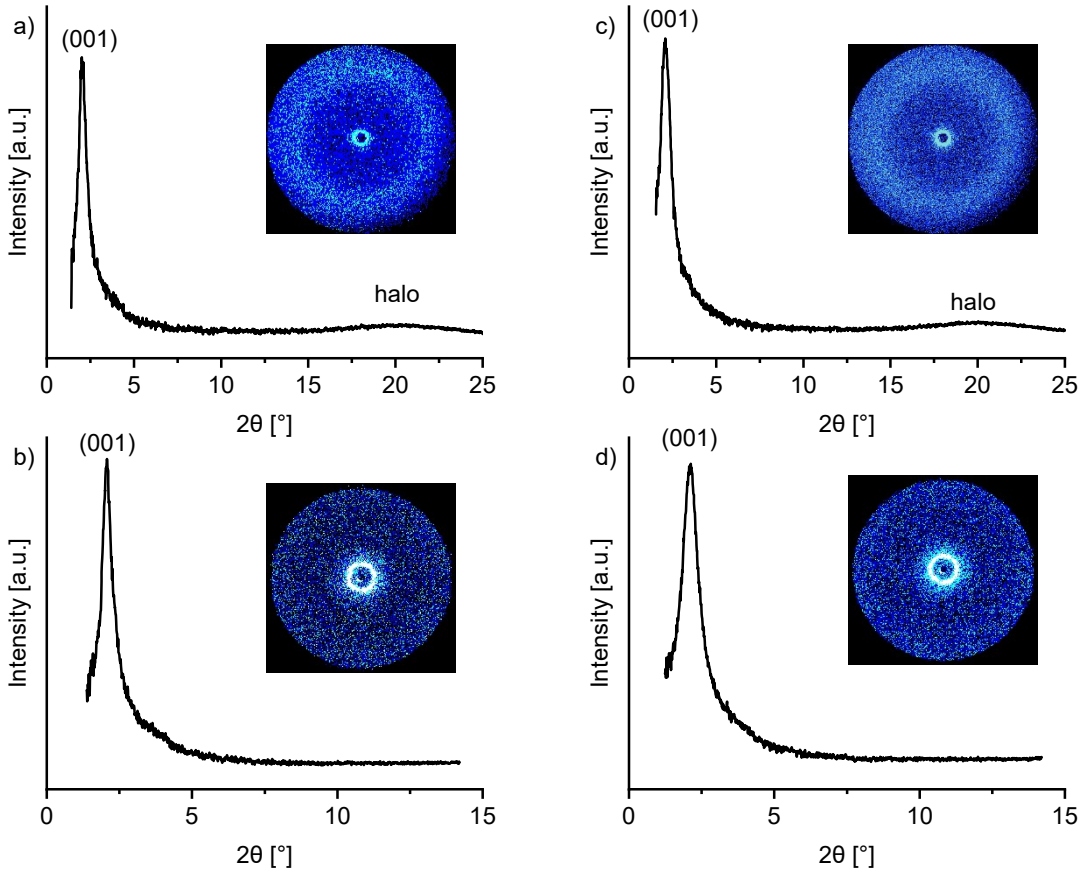

Figure S111: WAXS and SAXS diffractogram of **c-DOPA(12) • $NaBF_4$** at 80 °C (a, b) as well as 85 °C (c, d) with diffraction patterns as inset.

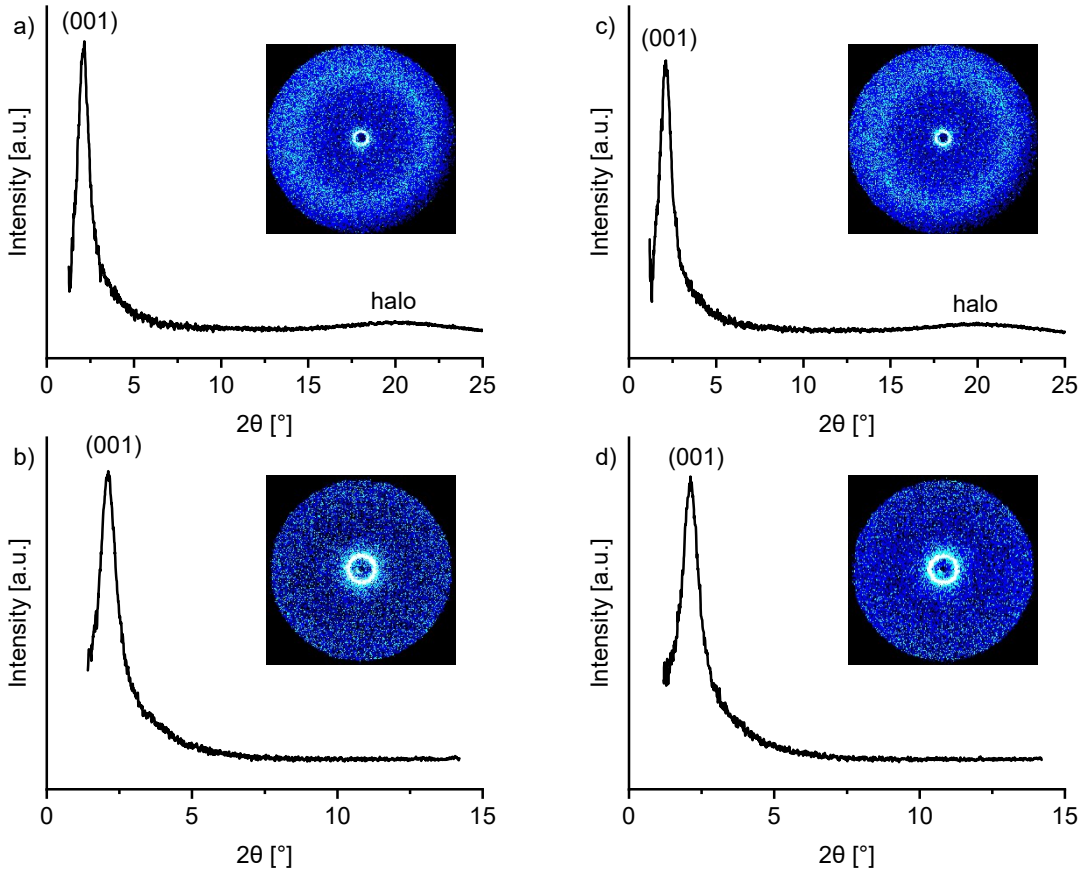

Figure S112: WAXS and SAXS diffractogram of **c-DOPA(12) • $NaBF_4$** at 90 °C (a, b) as well as 95 °C (c, d) with diffraction patterns as inset.

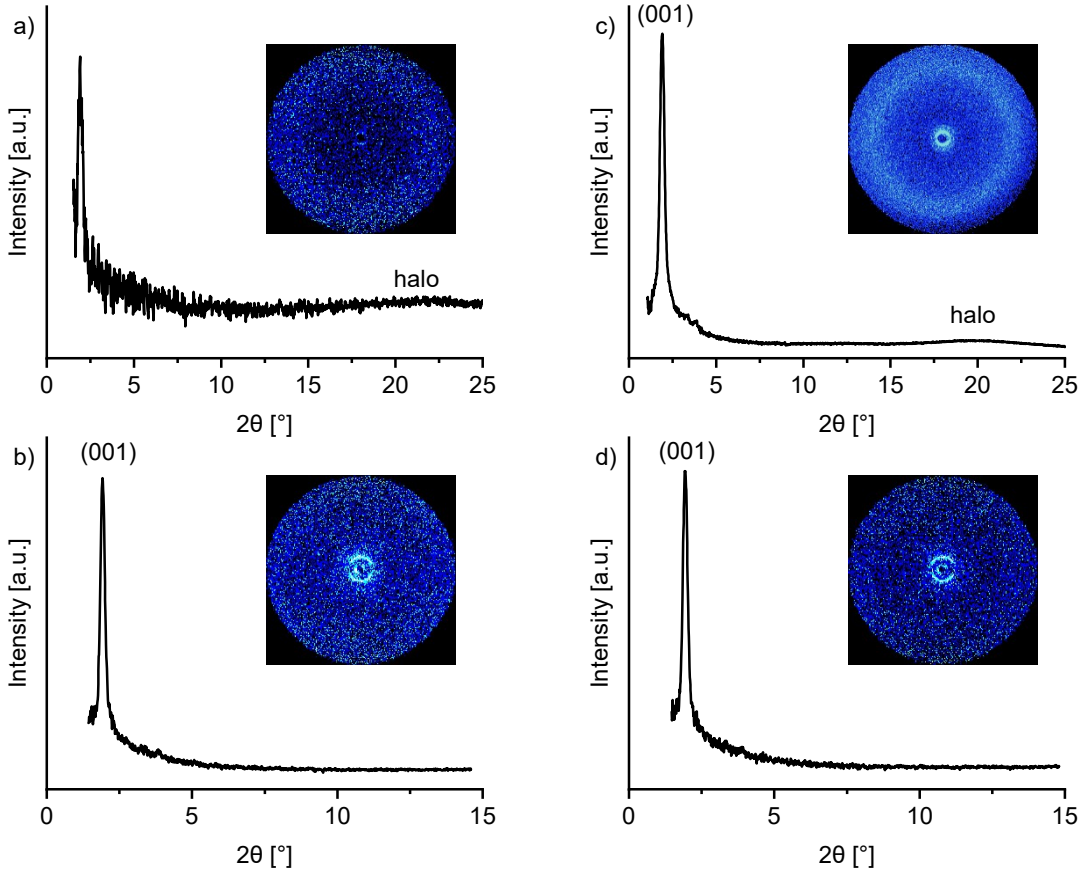

Figure S113: WAXS and SAXS diffractogram of **c-DOPA(12) • KPF_6** at 70 °C (a, b) as well as 75 °C (c, d) with diffraction patterns as inset.

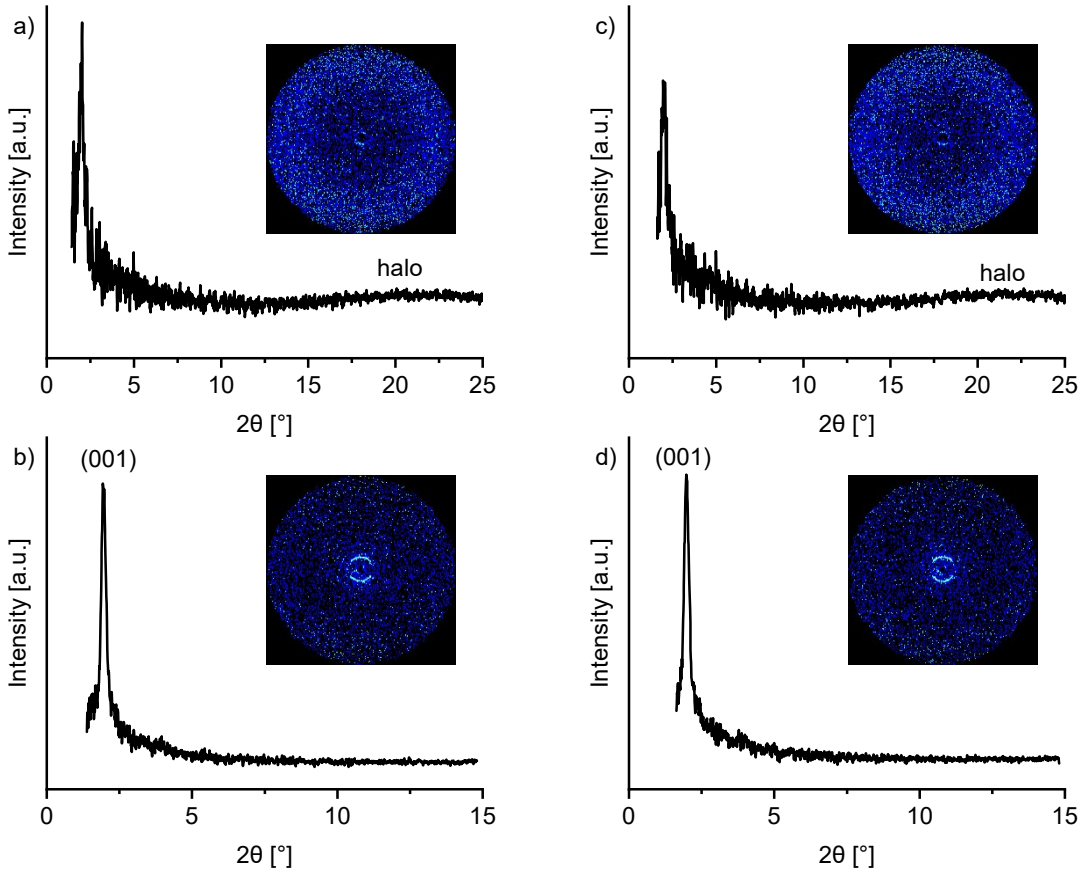

Figure S114: WAXS and SAXS diffractogram of **c-DOPA(12) • KPF_6** at 83 °C (a, b) as well as 93 °C (c, d) with diffraction patterns as inset.

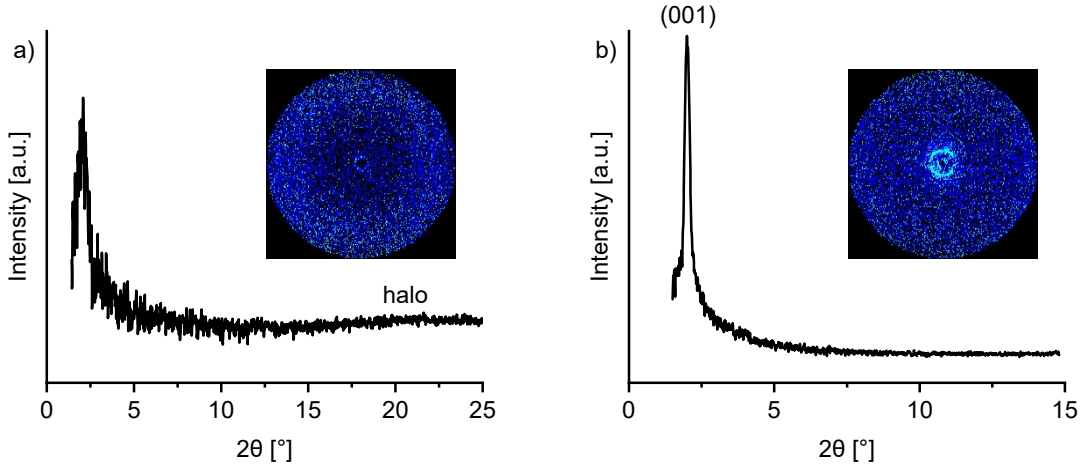

Figure S115: a) WAXS and b) SAXS diffractogram of **c-DOPA(12) • KPF_6** at 102 °C with diffraction patterns as inset.

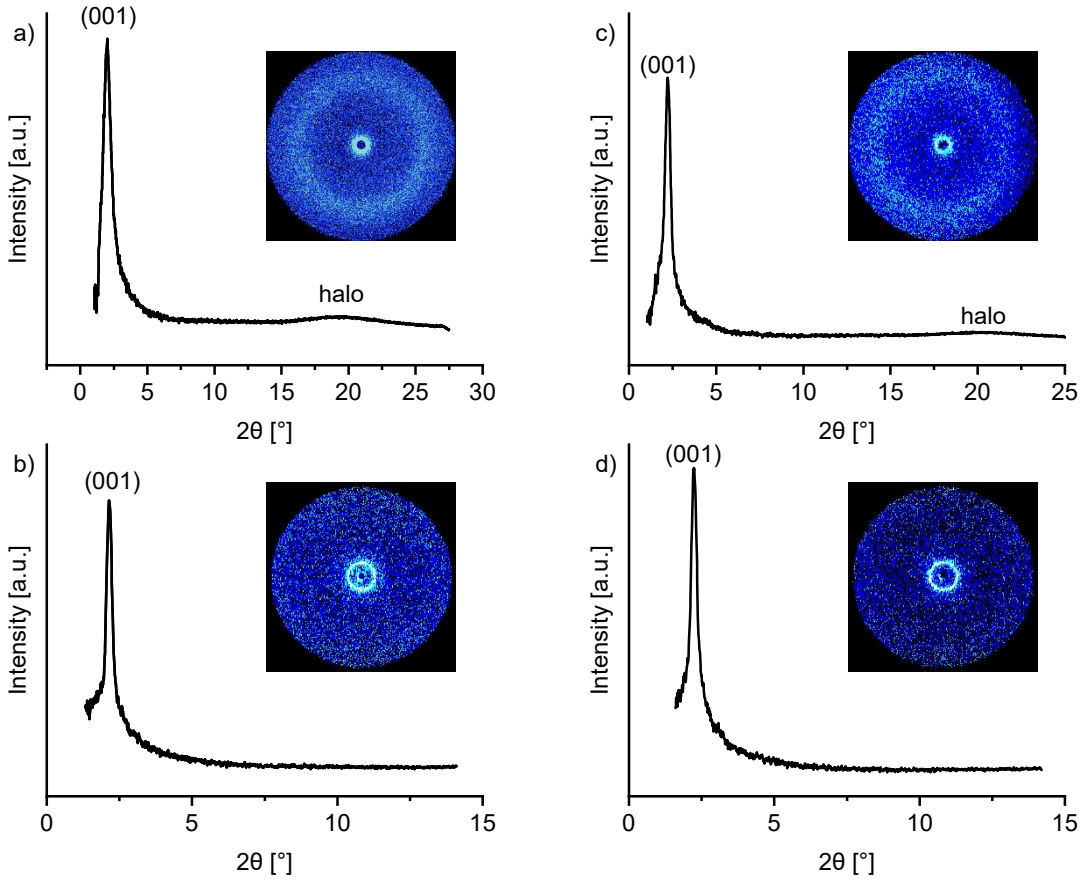

Figure S116: a) WAXS and b) SAXS diffractogram of **c-DOPA(14) • KSCN** at 85 °C as well as c) WAXS and d) SAXS diffractogram of **c-DOPA(14) • NaI** at 65 °C with diffraction patterns as inset.

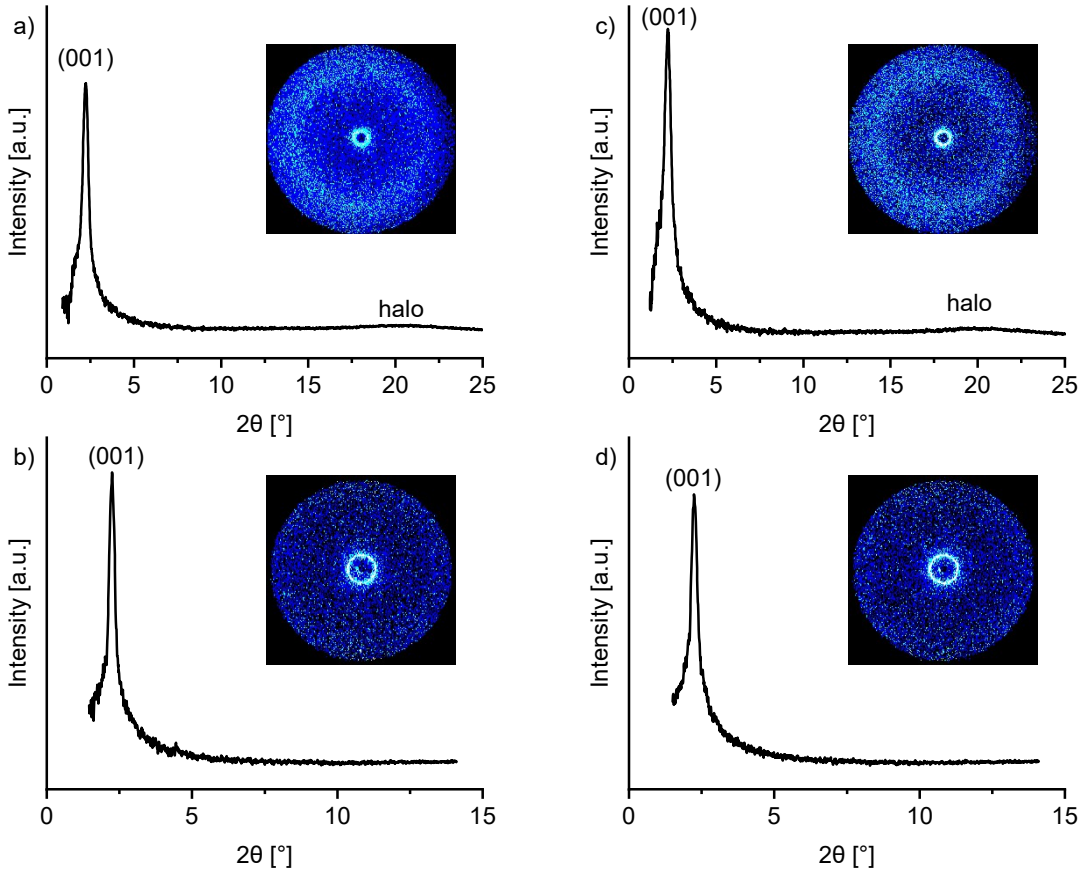

Figure S117: WAXS and SAXS diffractogram of **c-DOPA(14) • NaI** at 68 °C (a, b) as well as 72 °C (c, d) with diffraction patterns as inset.

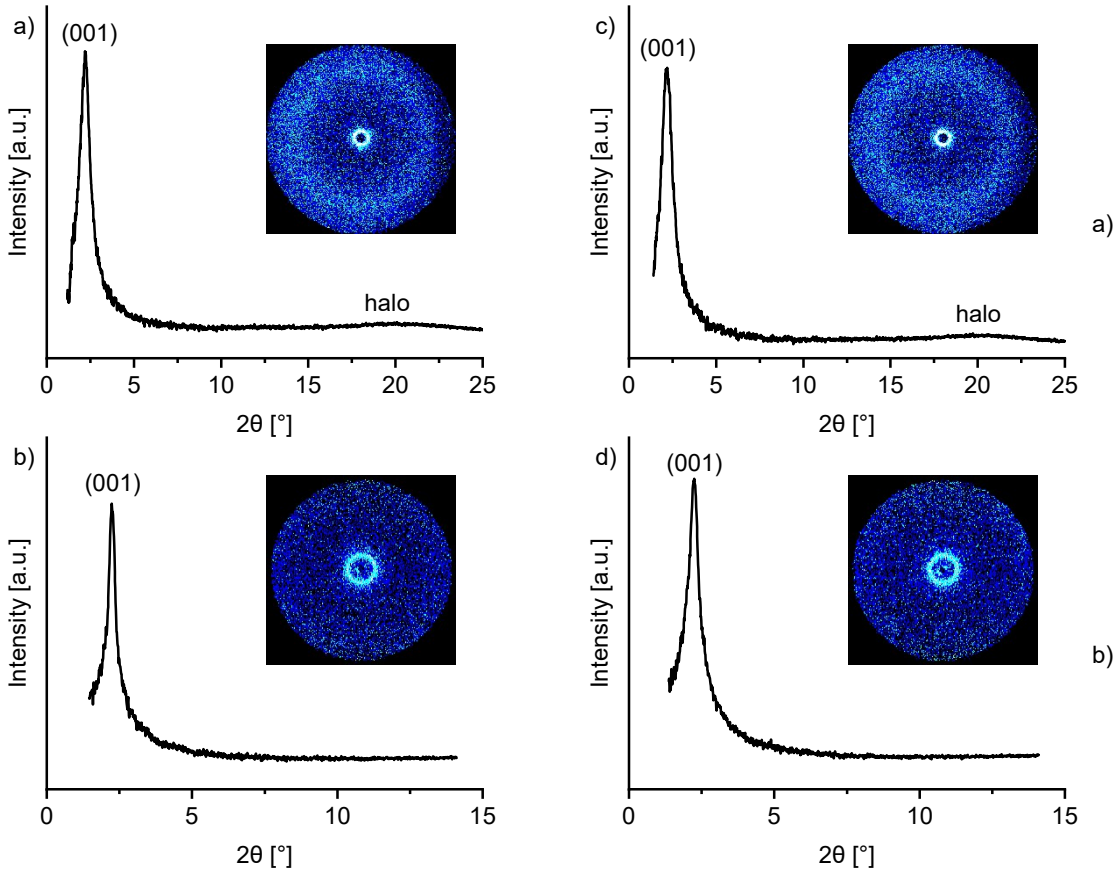

Figure S118: WAXS and SAXS diffractogram of **c-DOPA(14) • NaI** at 75 °C (a, b) as well as 78 °C (c, d) with diffraction patterns as inset.

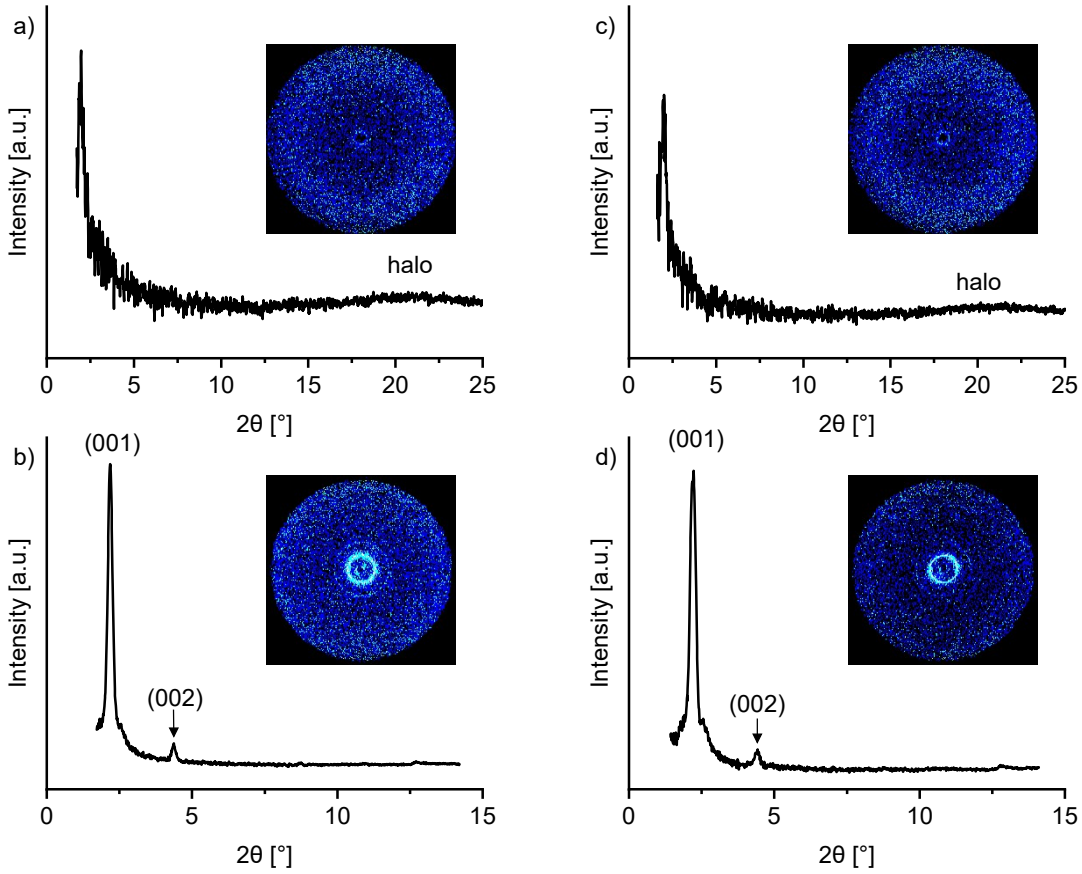

Figure S119: WAXS and SAXS diffractogram of **c-DOPA(14) • KI** at 74 °C (a, b) as well as 80 °C (c, d) with diffraction patterns as inset.

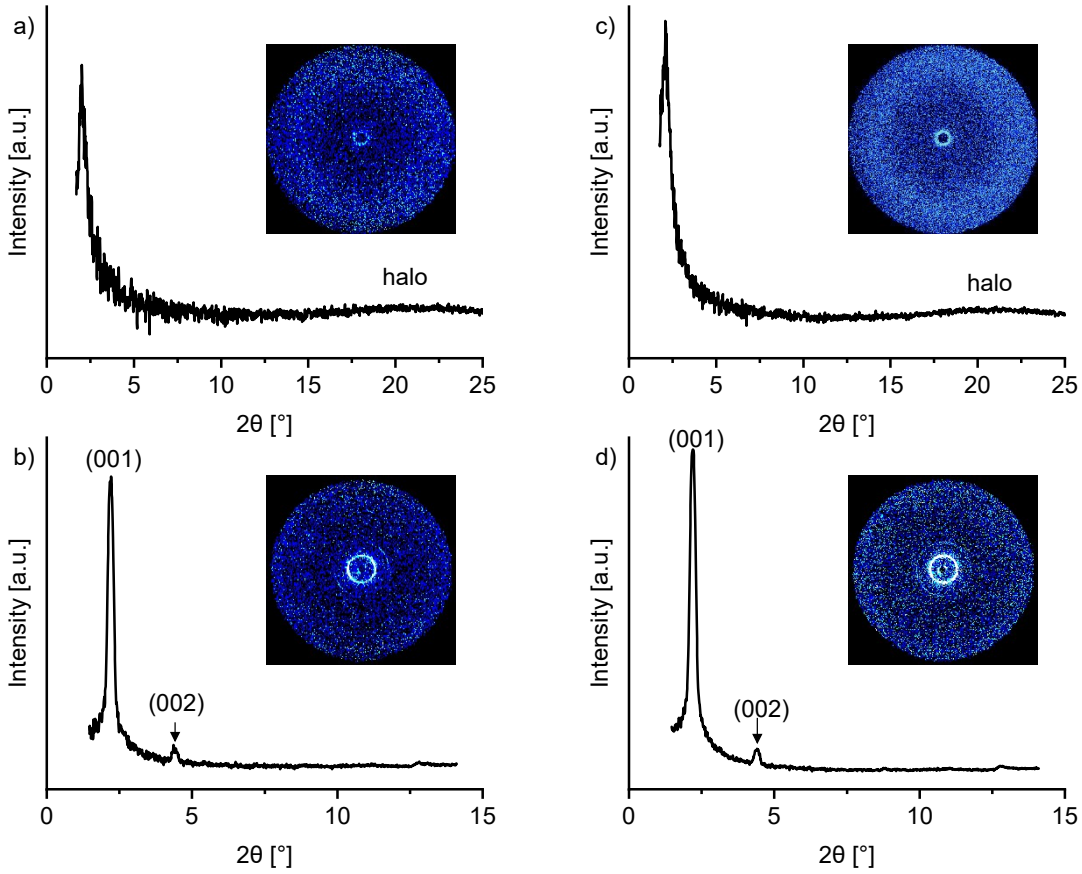

Figure S120: WAXS and SAXS diffractogram of **c-DOPA(14) • KI** at 88 °C (a, b) as well as 95 °C (c, d) with diffraction patterns as inset.

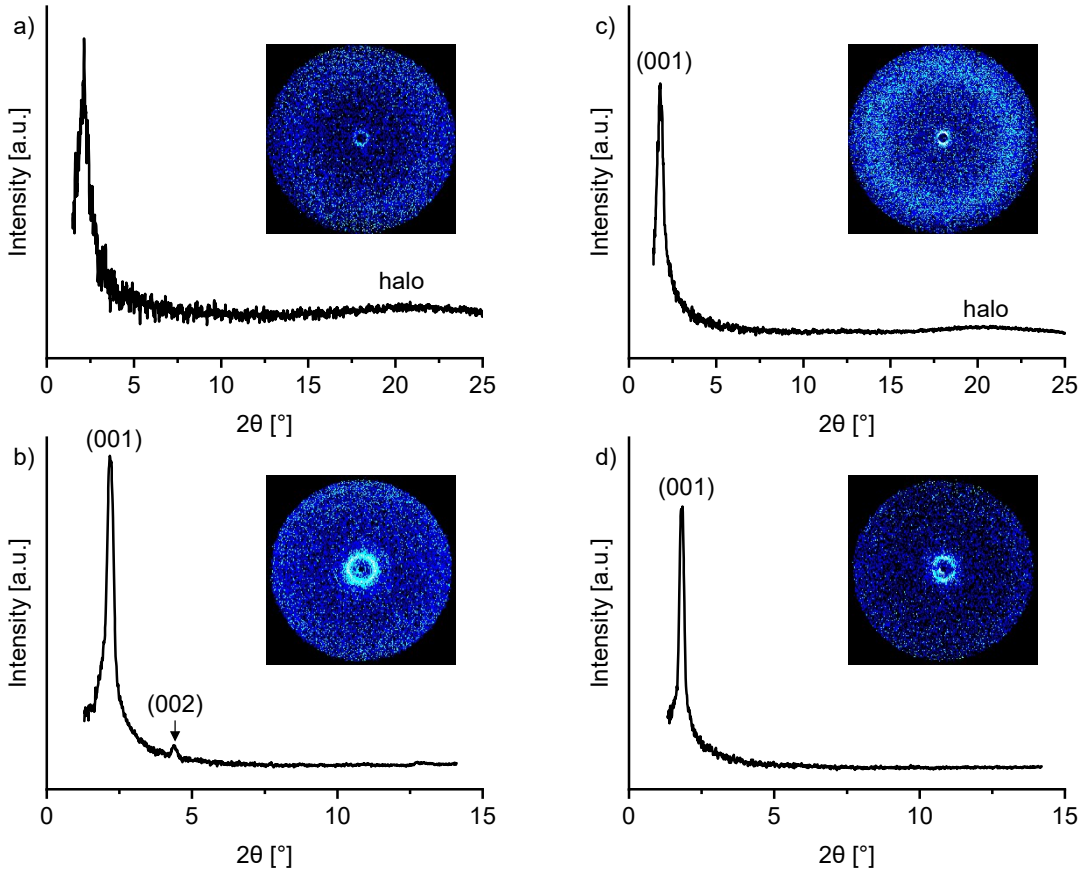

Figure S121: a) WAXS and b) SAXS diffractogram of **c-DOPA(14) • KI** at 105 °C as well as c) WAXS and d) SAXS diffractogram of **c-DOPA(14) • $NaBF_4$** at 60 °C with diffraction patterns as inset.

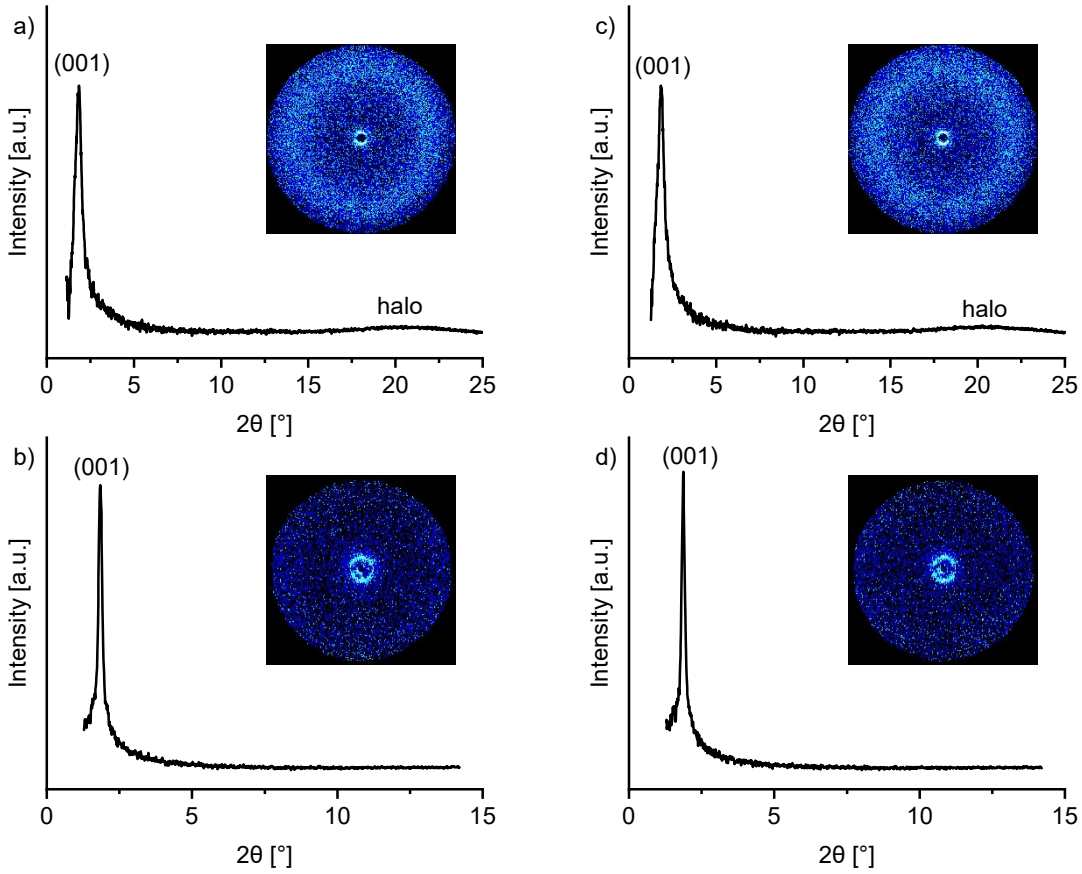

Figure S122: WAXS and SAXS diffractogram of **c-DOPA(14) • $NaBF_4$** at 65 °C (a, b) as well as 70 °C (c, d) with diffraction patterns as inset.

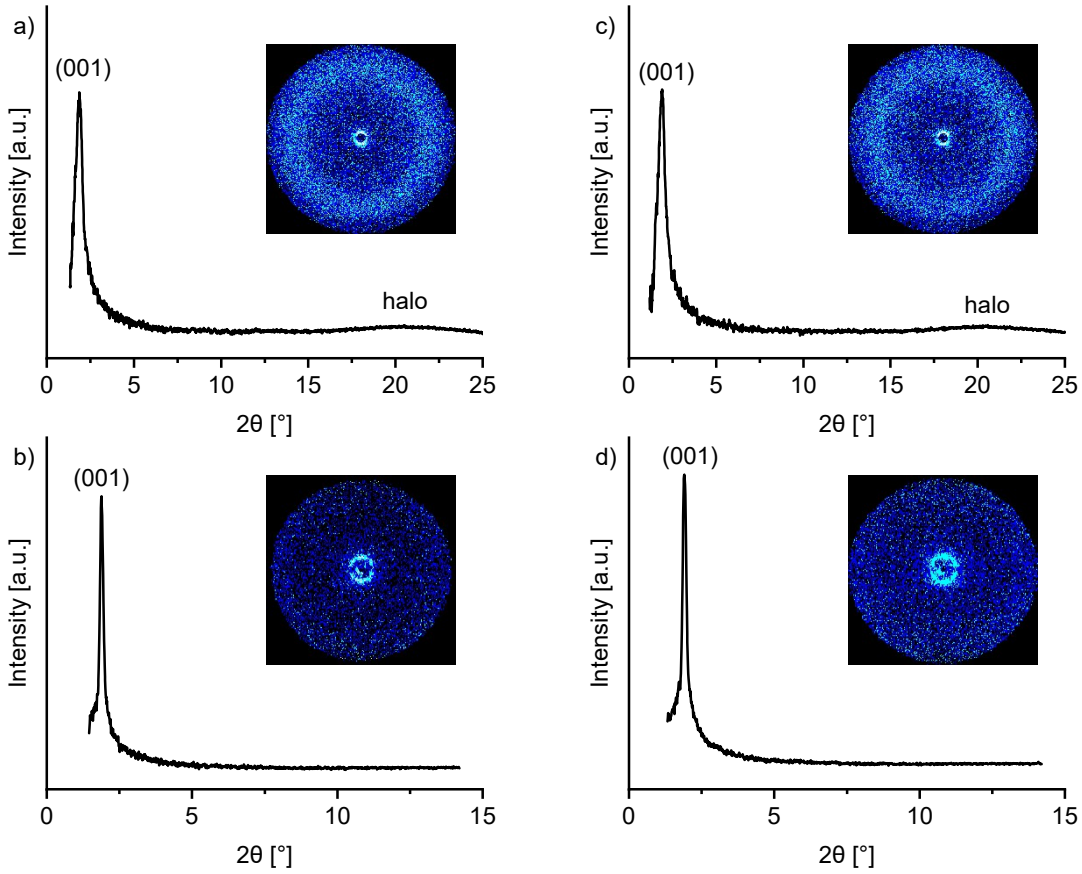

Figure S123: WAXS and SAXS diffractogram of **c-DOPA(14) • $NaBF_4$** at 75 °C (a, b) as well as 80 °C (c, d) with diffraction patterns as inset.

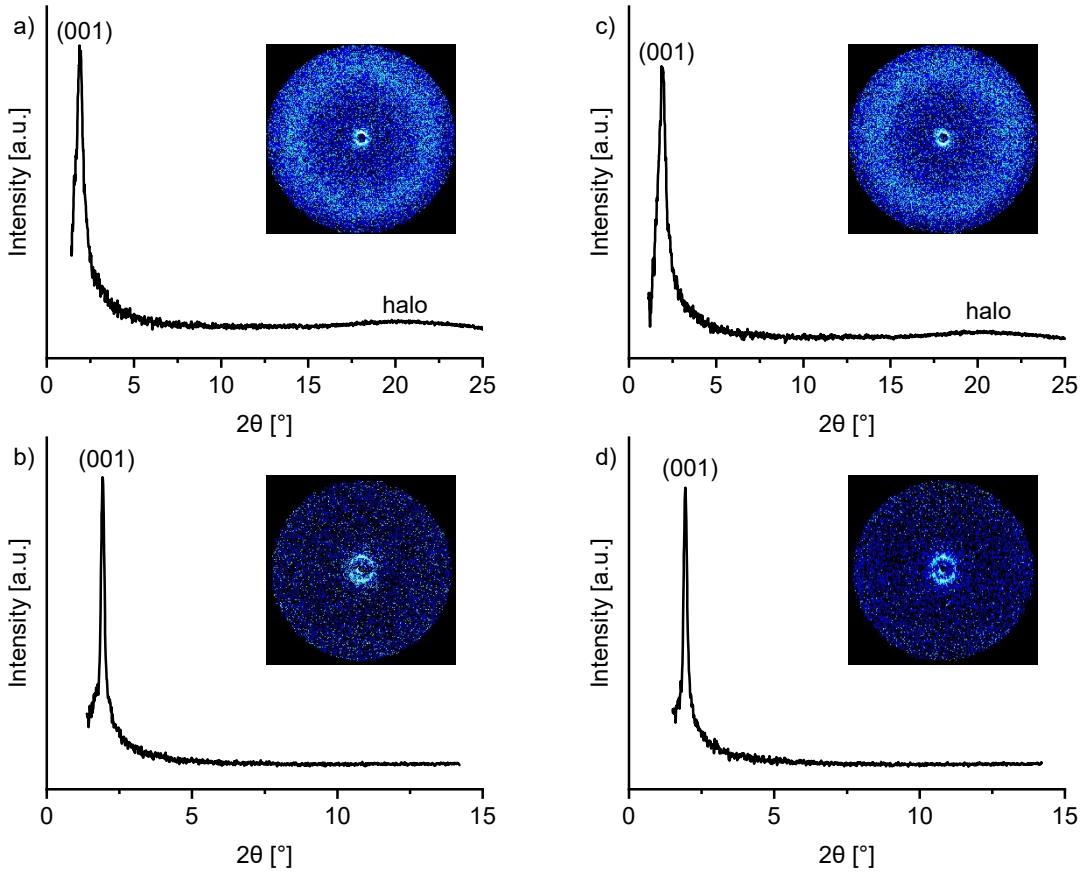

Figure S124: WAXS and SAXS diffractogram of **c-DOPA(14) • $NaBF_4$** at 85 °C (a, b) as well as 90 °C (c, d) with diffraction patterns as inset.

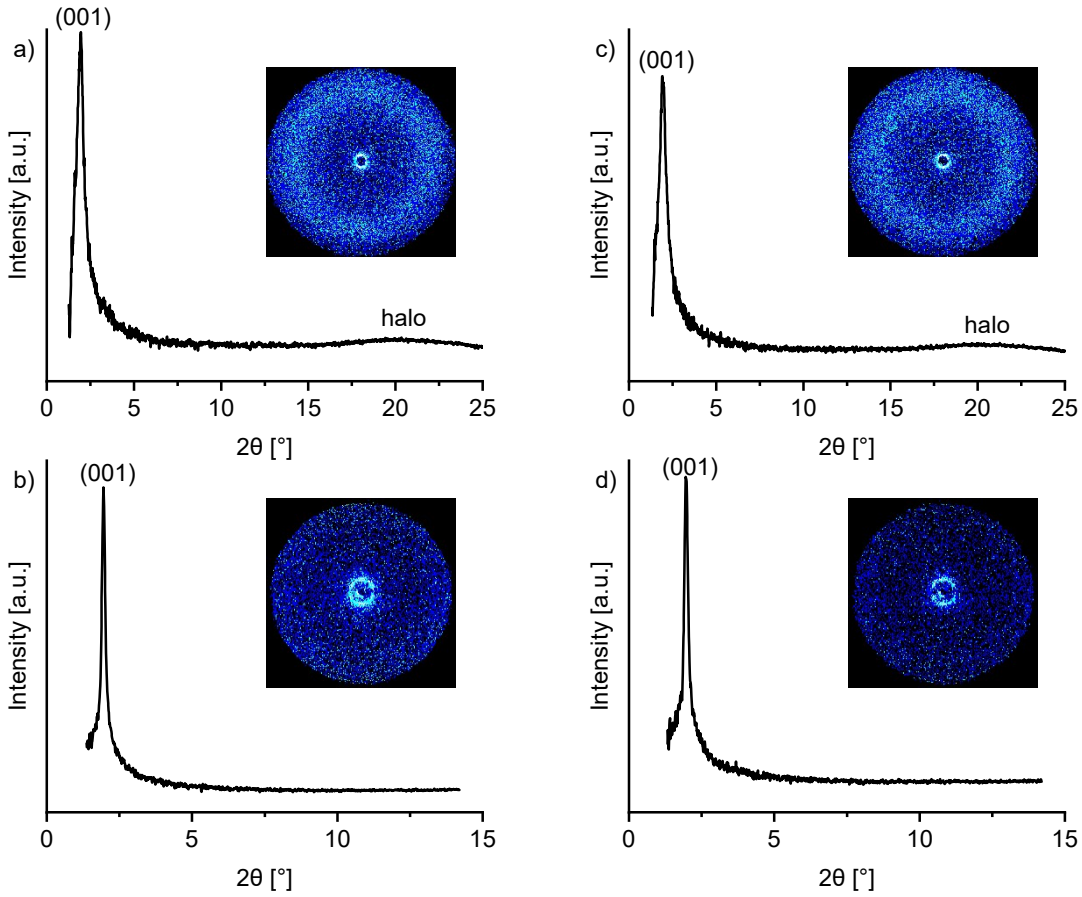

Figure S125: WAXS and SAXS diffractogram of **c-DOPA(14) • $NaBF_4$** at 95 °C (a, b) as well as 100 °C (c, d) with diffraction patterns as inset.

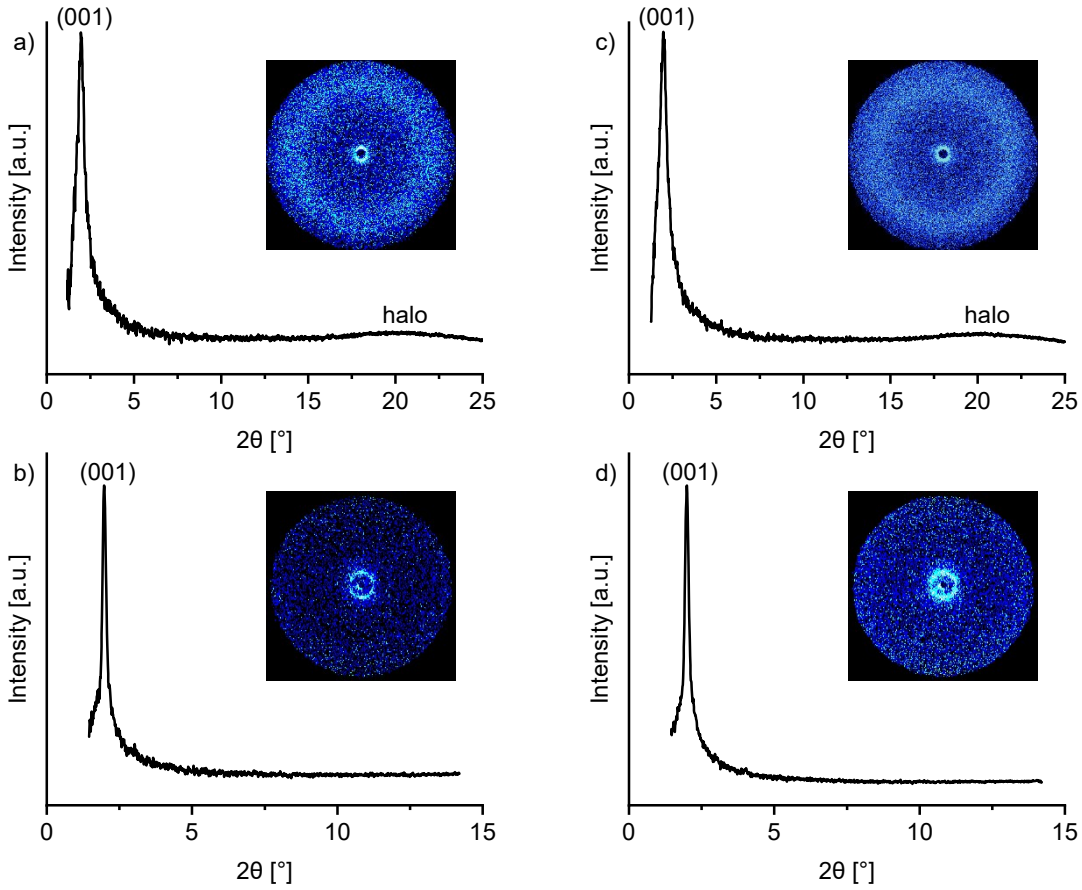

Figure S126: WAXS and SAXS diffractogram of **c-DOPA(14) • $NaBF_4$** at 105 °C (a, b) as well as 110 °C (c, d) with diffraction patterns as inset.

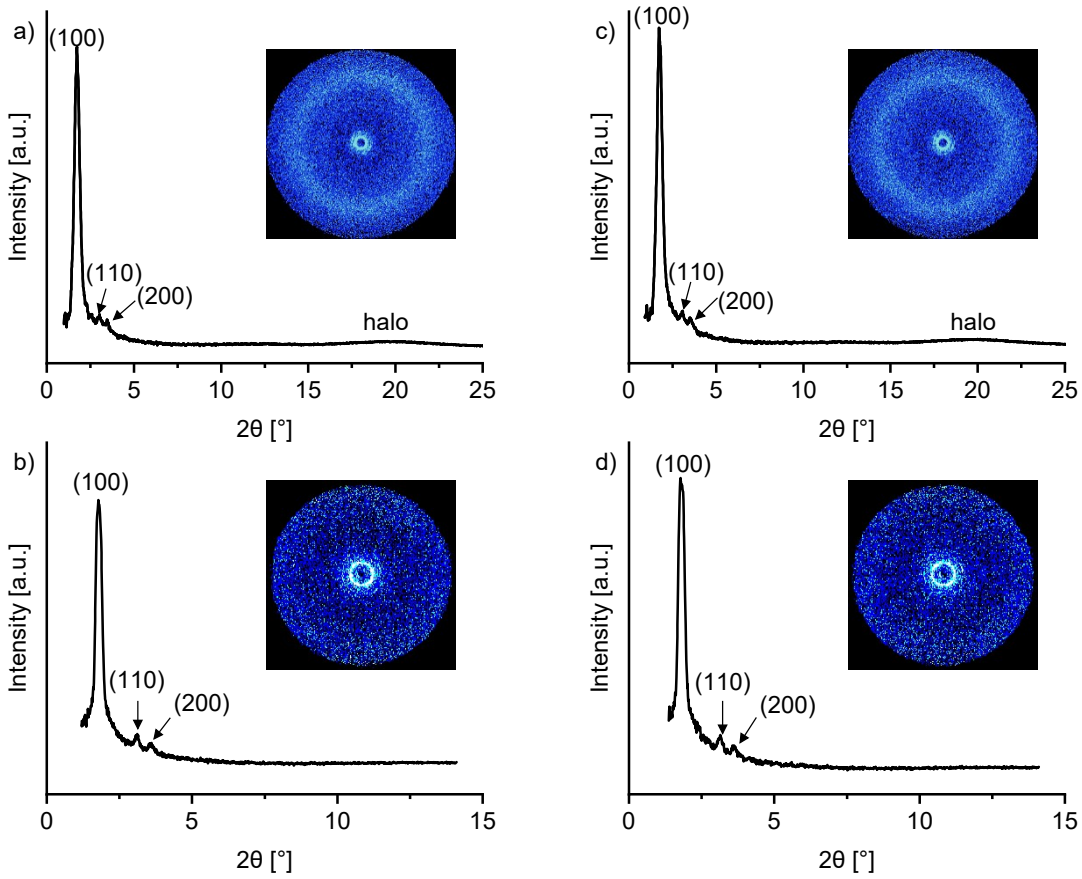

Figure S127: WAXS and SAXS diffractogram of **c-DOPA(14) • KPF_6** at 60 °C (a, b) as well as 65 °C (c, d) with diffraction patterns as inset.

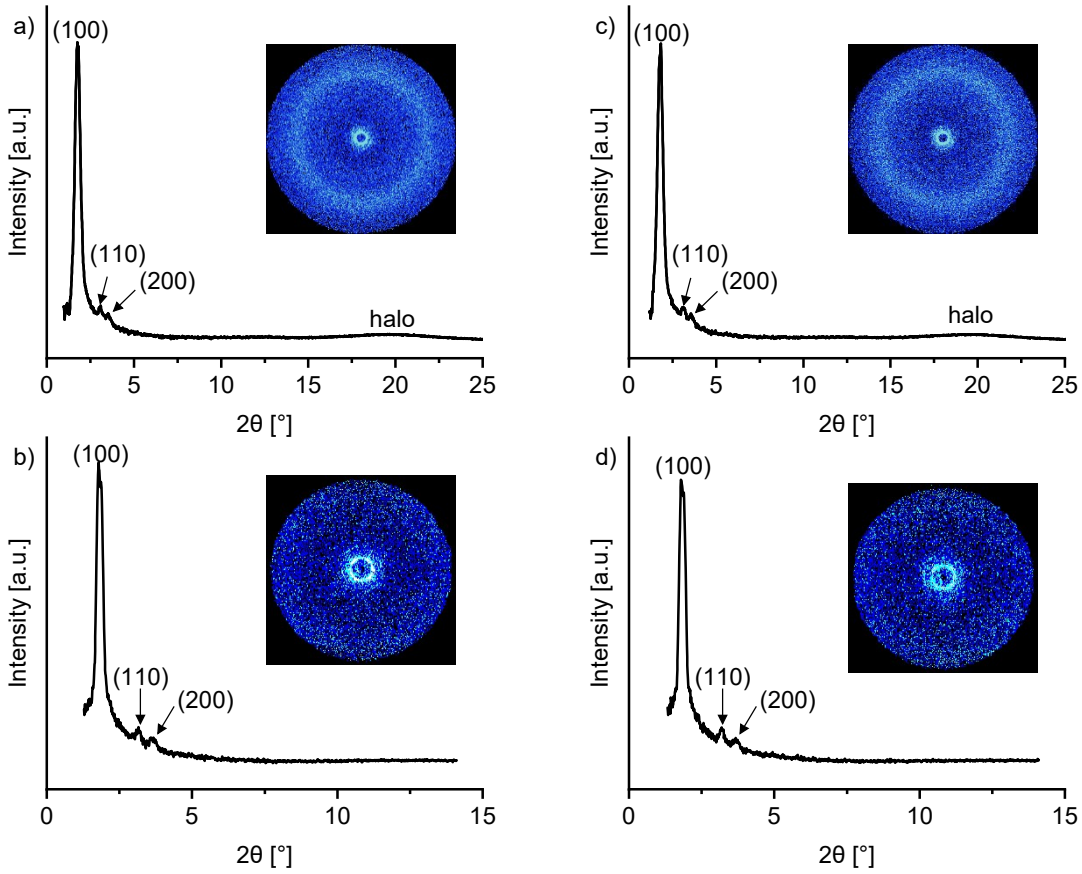

Figure S128: WAXS and SAXS diffractogram of **c-DOPA(14) • KPF_6** at 70 °C (a, b) as well as 75 °C (c, d) with diffraction patterns as inset.

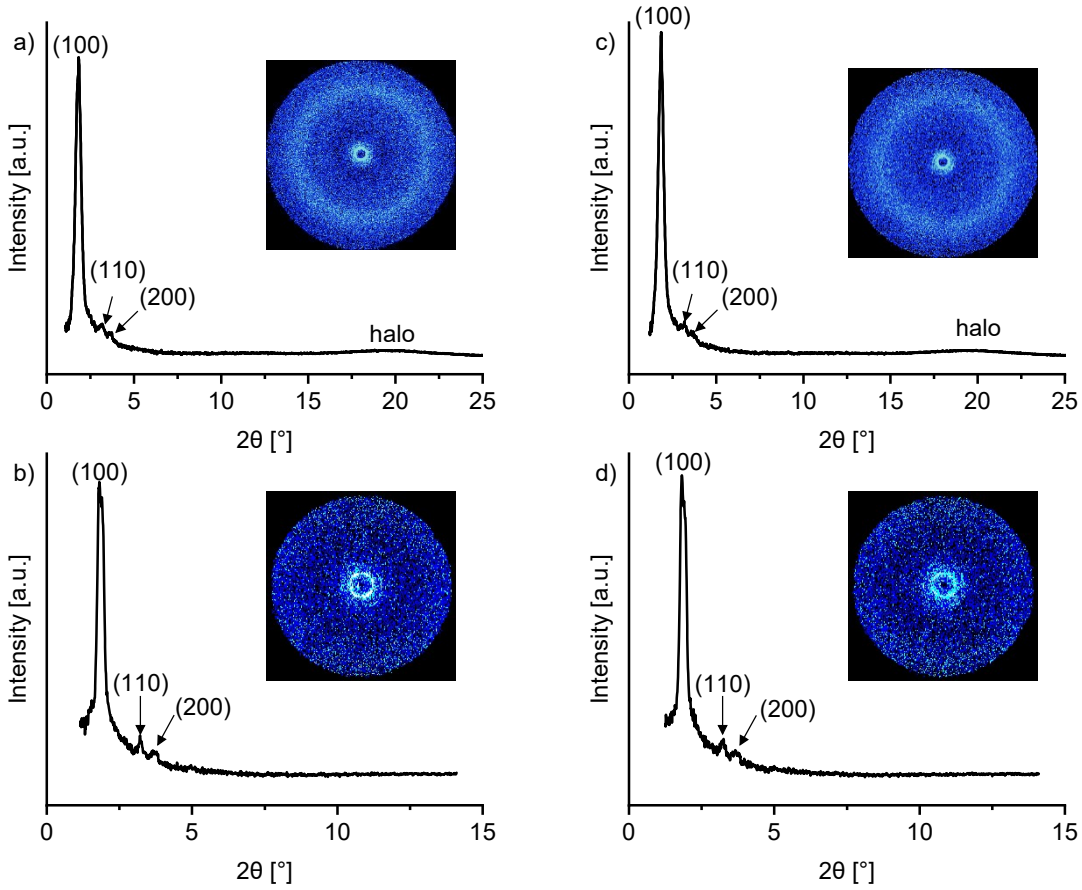

Figure S129: WAXS and SAXS diffractogram of **c-DOPA(14) • KPF_6** at 80 °C (a, b) as well as 85 °C (c, d) with diffraction patterns as inset.

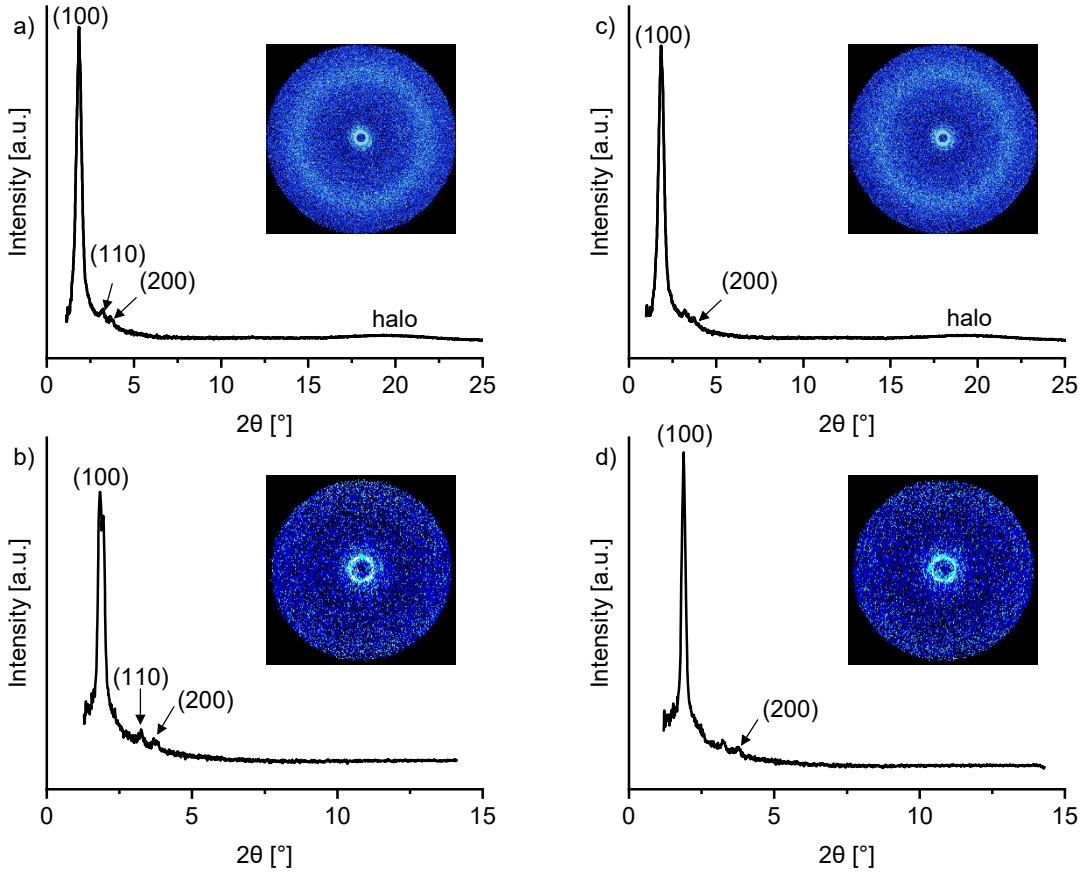

Figure S130: WAXS and SAXS diffractogram of **c-DOPA(14) • KPF_6** at 90 °C (a, b) as well as 95 °C (c, d) with diffraction patterns as inset.

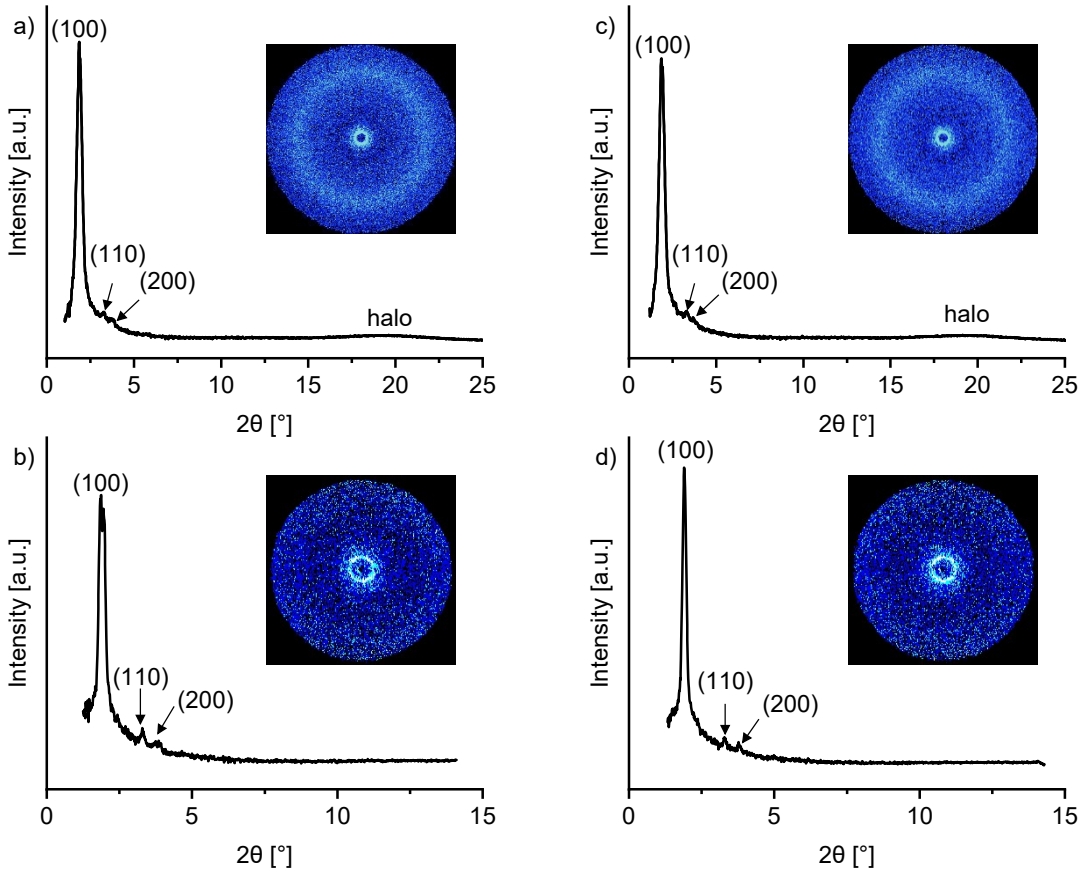

Figure S131: WAXS and SAXS diffractogram of **c-DOPA(14) • KPF_6** at 100 °C (a, b) as well as 105 °C (c, d) with diffraction patterns as inset.

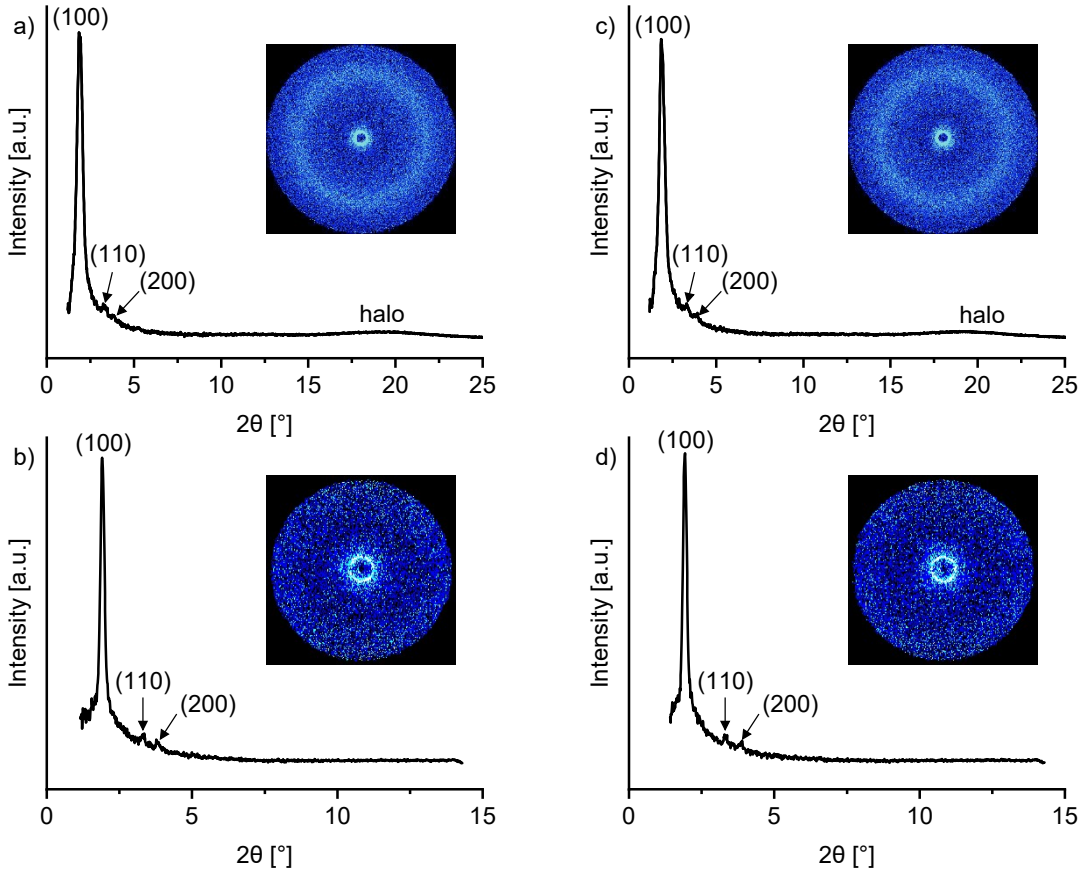

Figure S132: WAXS and SAXS diffractogram of **c-DOPA(14) • KPF_6** at 110 °C (a, b) as well as 115 °C (c, d) with diffraction patterns as inset.

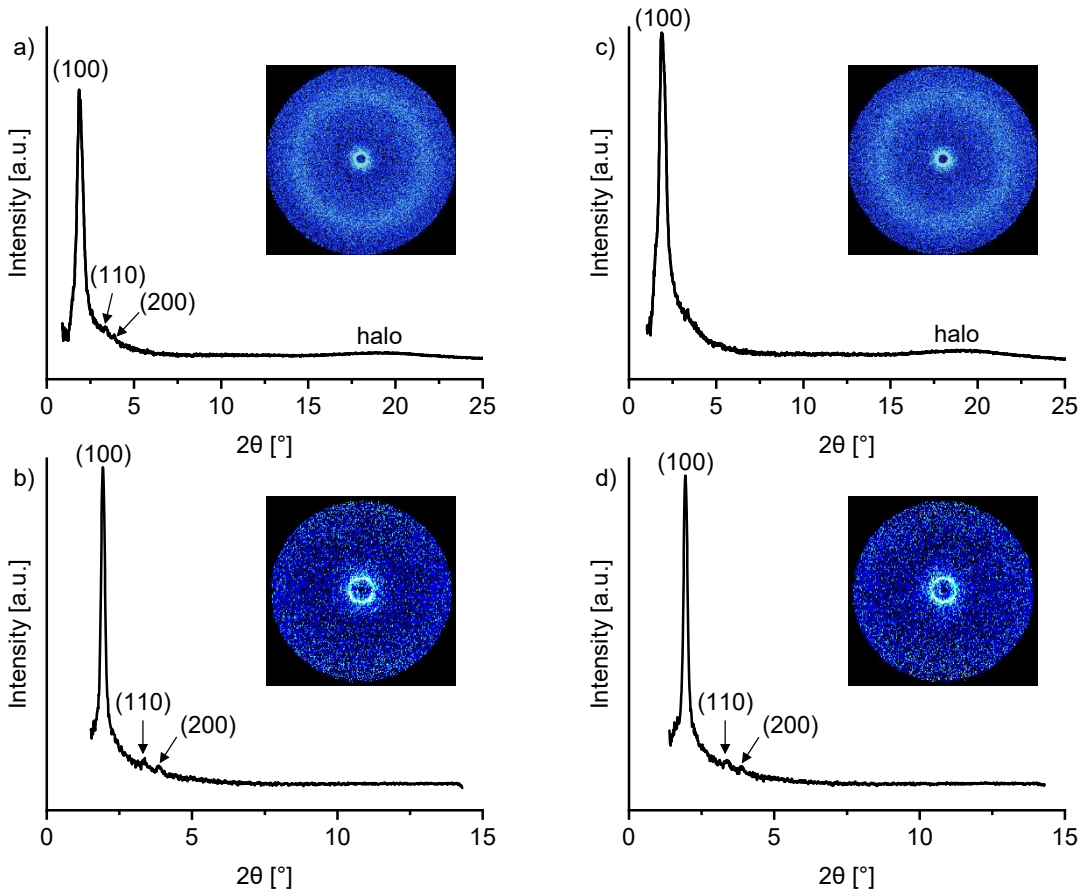

Figure S133: WAXS and SAXS diffractogram of **c-DOPA(14) • KPF_6** at 120 °C (a, b) as well as 125 °C (c, d) with diffraction patterns as inset.

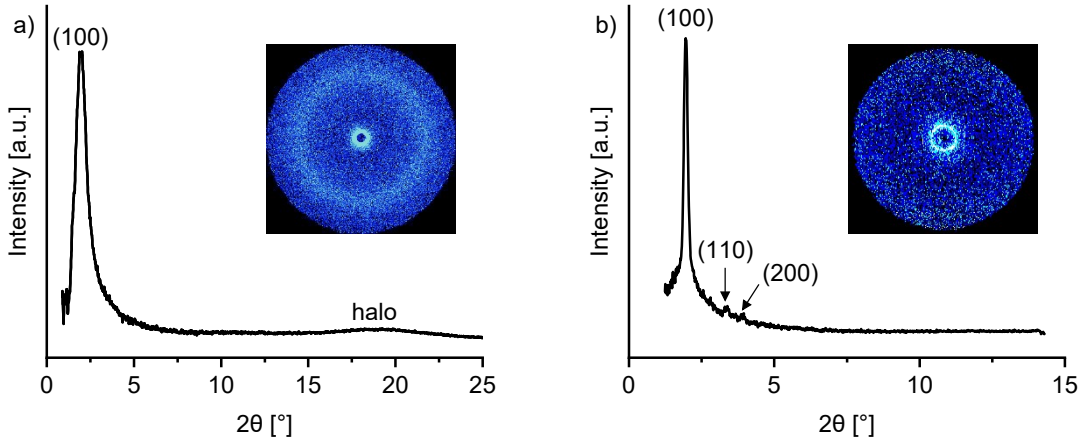

Figure S134: a) WAXS and b) SAXS diffractogram of **c-DOPA(14) • KPF_6** at 130 °C with diffraction patterns as inset.

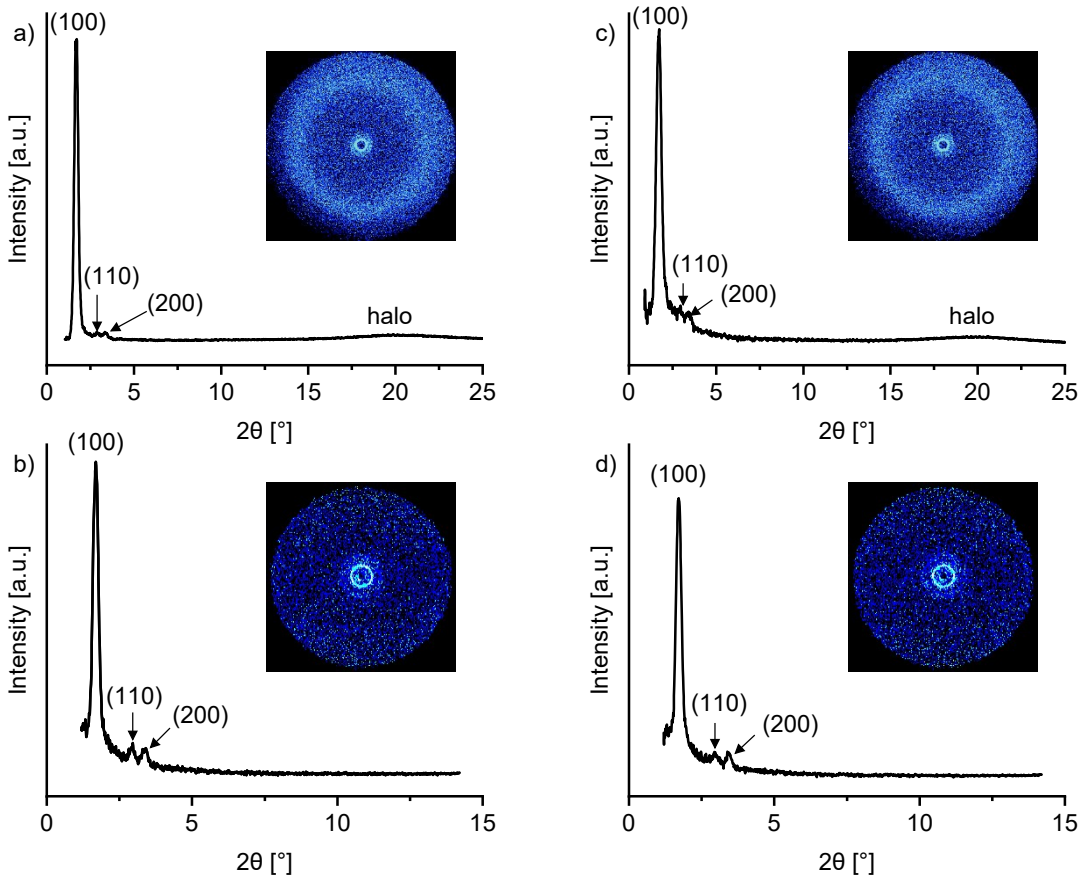

Figure S135: WAXS and SAXS diffractogram of **c-DOPA(16) • KSCN** at 60 °C (a, b) as well as 65 °C (c, d) with diffraction patterns as inset.

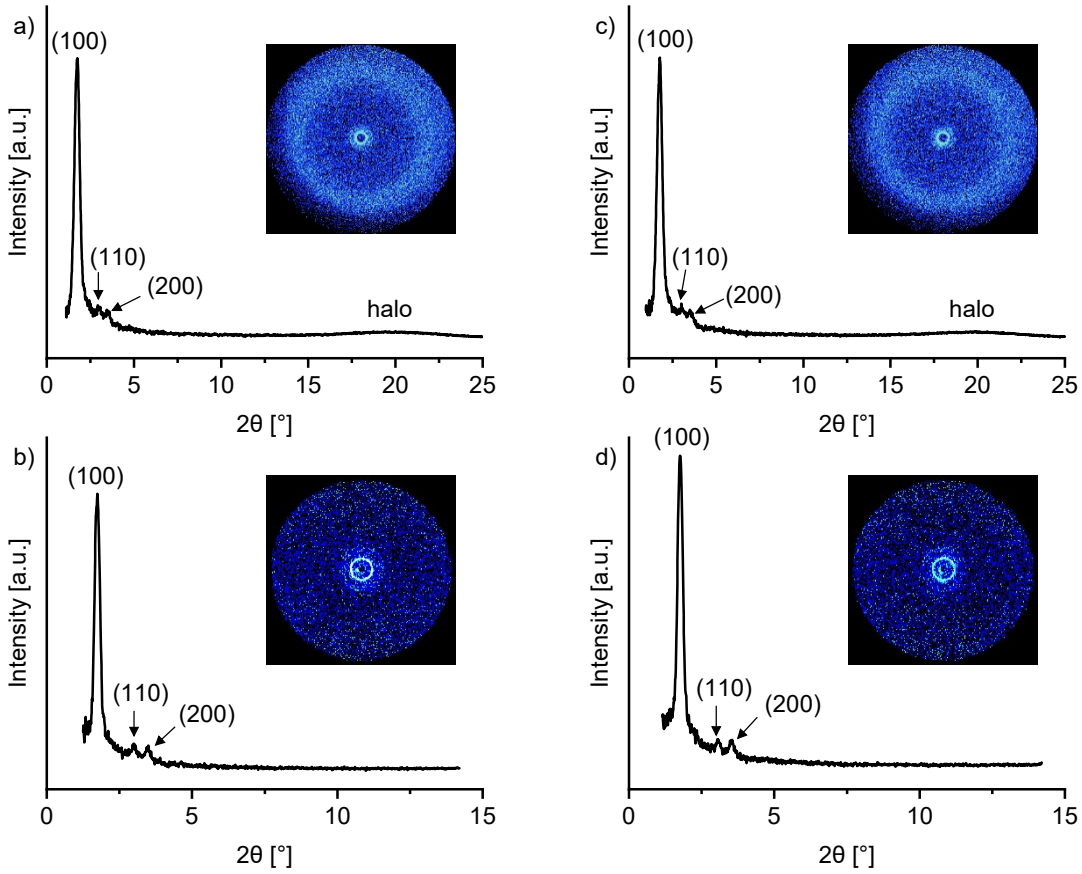

Figure S136: WAXS and SAXS diffractogram of **c-DOPA(16) • KSCN** at 70 °C (a, b) as well as 75 °C (c, d) with diffraction patterns as inset.

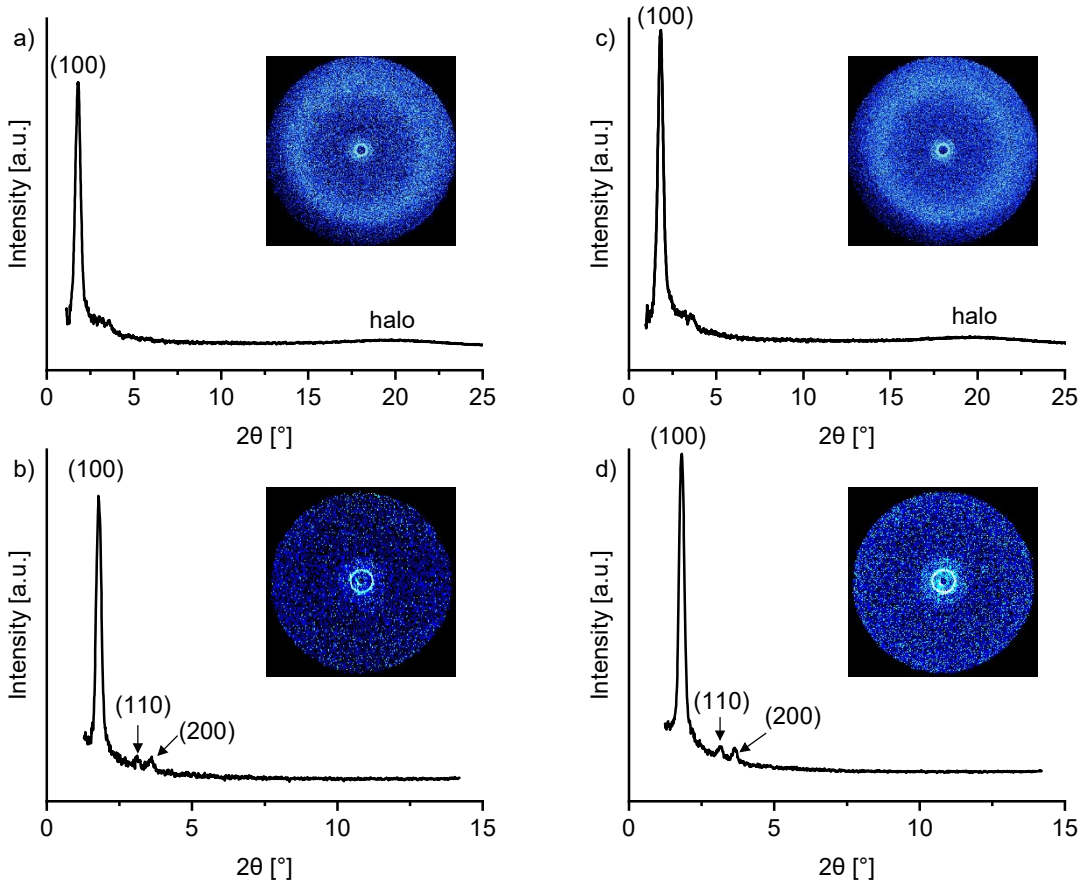

Figure S137: WAXS and SAXS diffractogram of **c-DOPA(16) • KSCN** at 80 °C (a, b) as well as 85 °C (c, d) with diffraction patterns as inset.

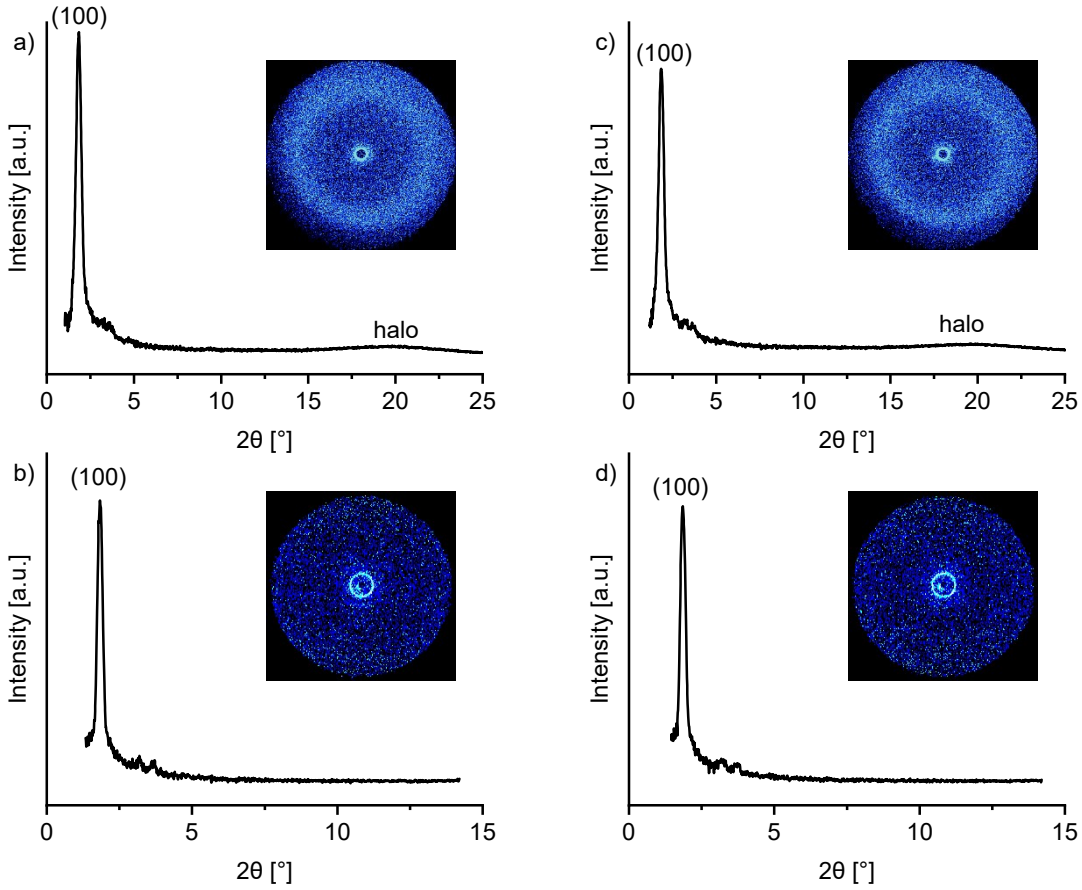

Figure S138: WAXS and SAXS diffractogram of **c-DOPA(16) • KSCN** at 90 °C (a, b) as well as 95 °C (c, d) with diffraction patterns as inset.

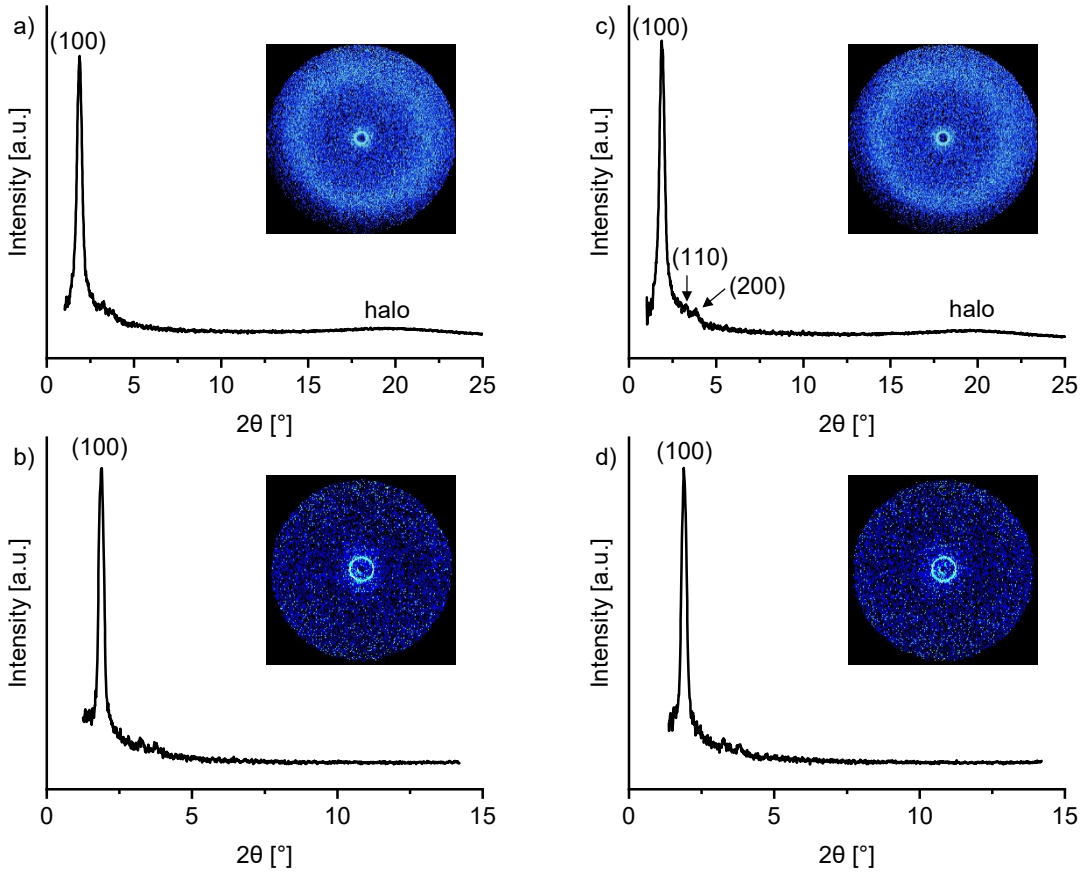

Figure S139: WAXS and SAXS diffractogram of **c-DOPA(16) • KSCN** at 100 °C (a, b) as well as 105 °C (c, d) with diffraction patterns as inset.

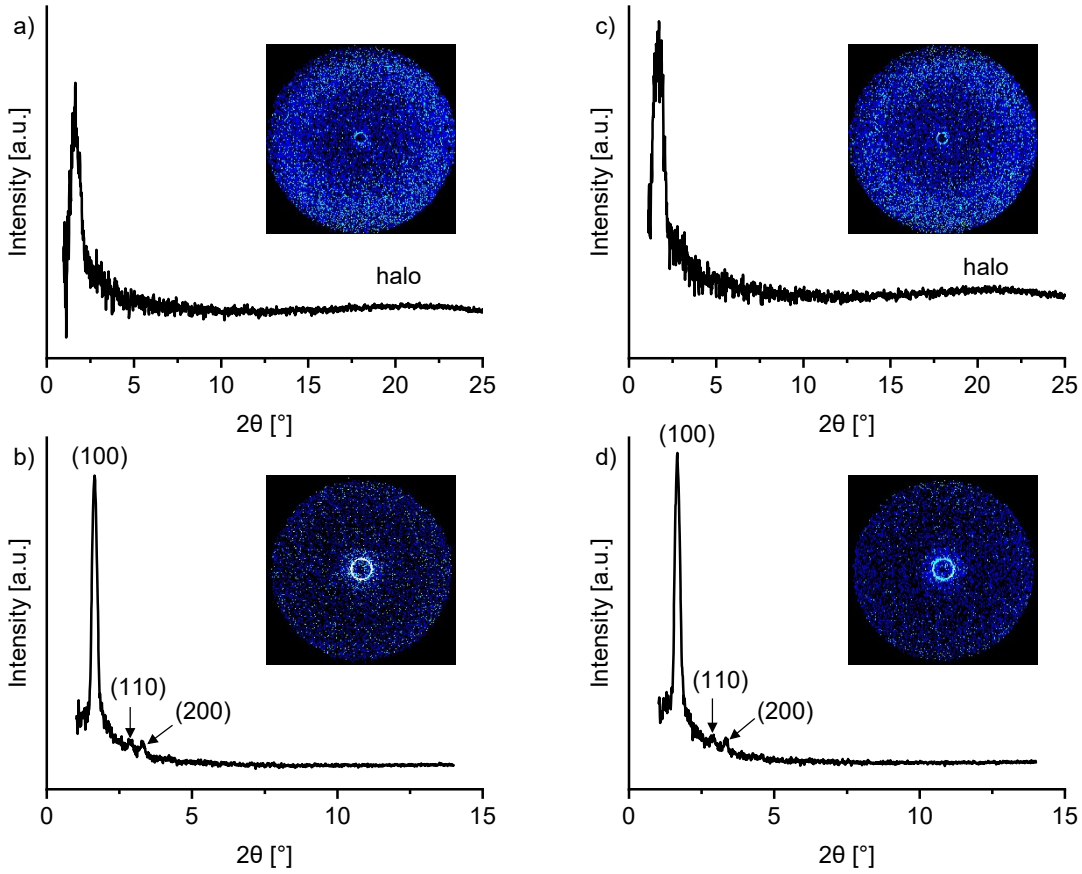

Figure S140: WAXS and SAXS diffractogram of **c-DOPA(16) • NaI** at 93 °C (a, b) as well as 102 °C (c, d) with diffraction patterns as inset.

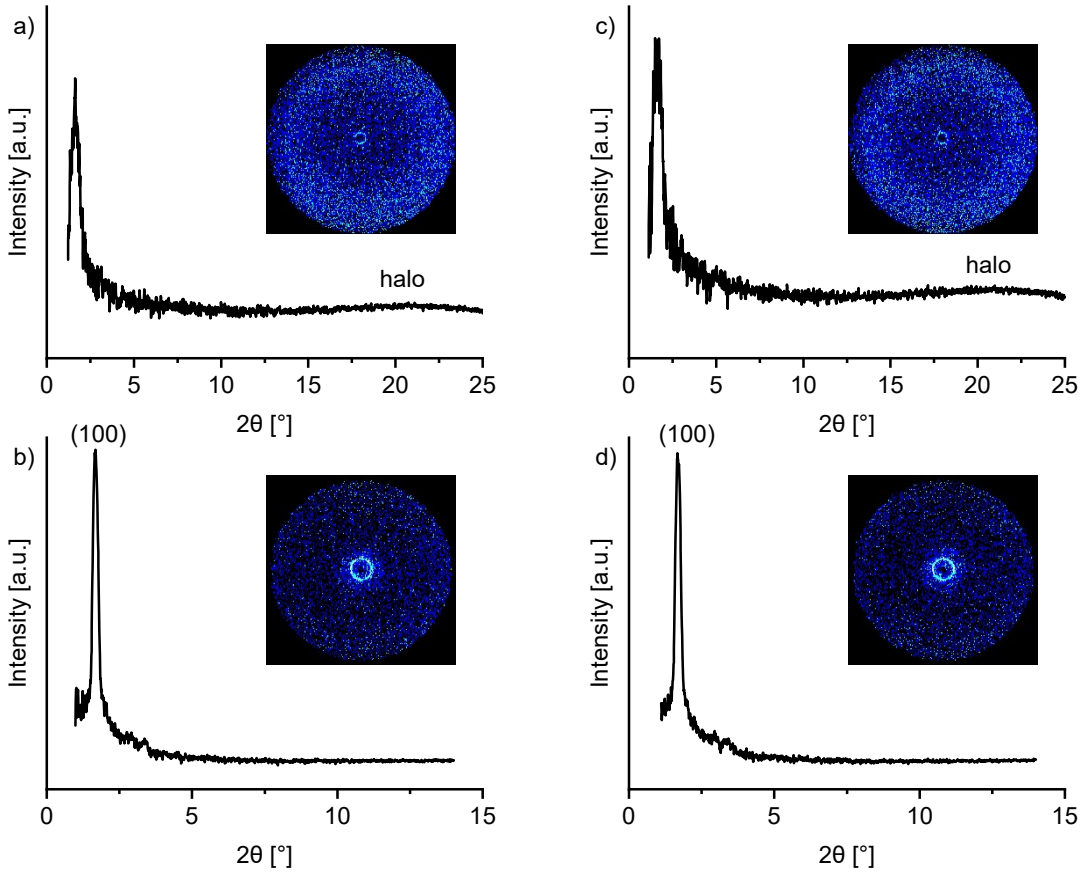

Figure S141: WAXS and SAXS diffractogram of **c-DOPA(16) • NaI** at 107 °C (a, b) as well as 112 °C (c, d) with diffraction patterns as inset.

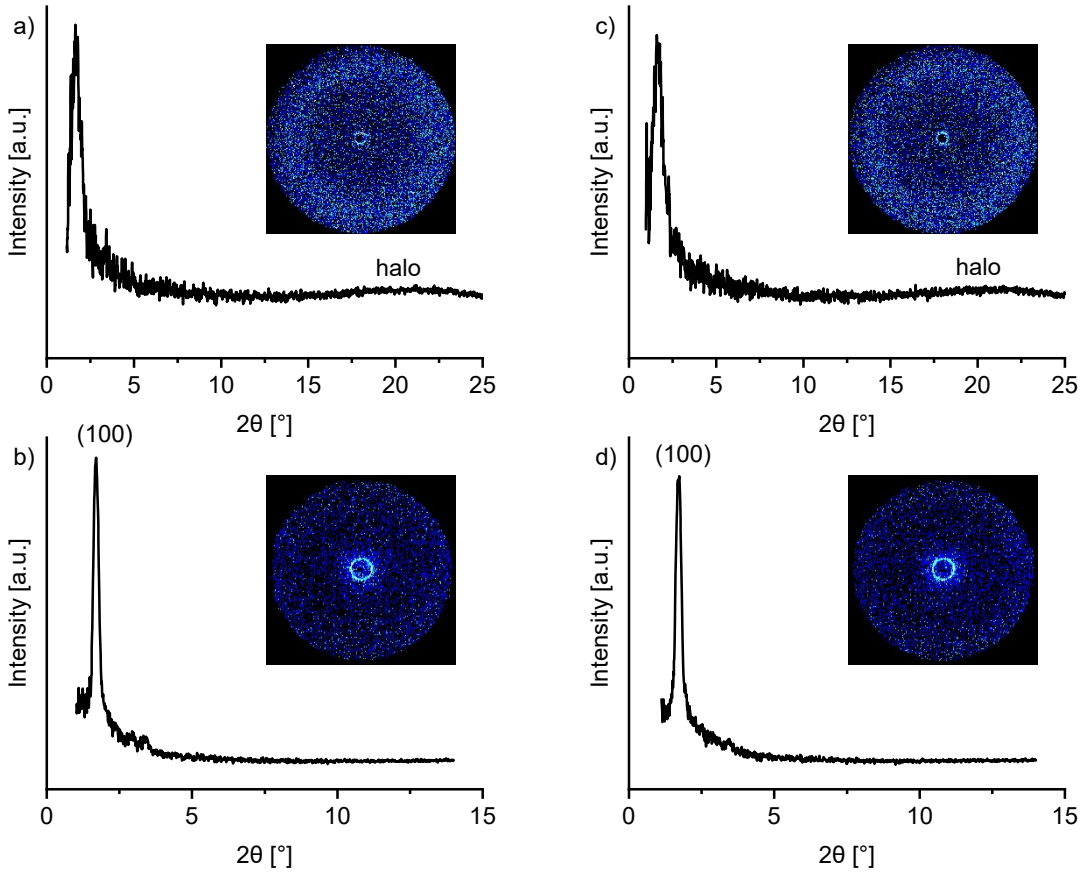

Figure S142: WAXS and SAXS diffractogram of **c-DOPA(16) • NaI** at 116 °C (a, b) as well as 121 °C (c, d) with diffraction patterns as inset.

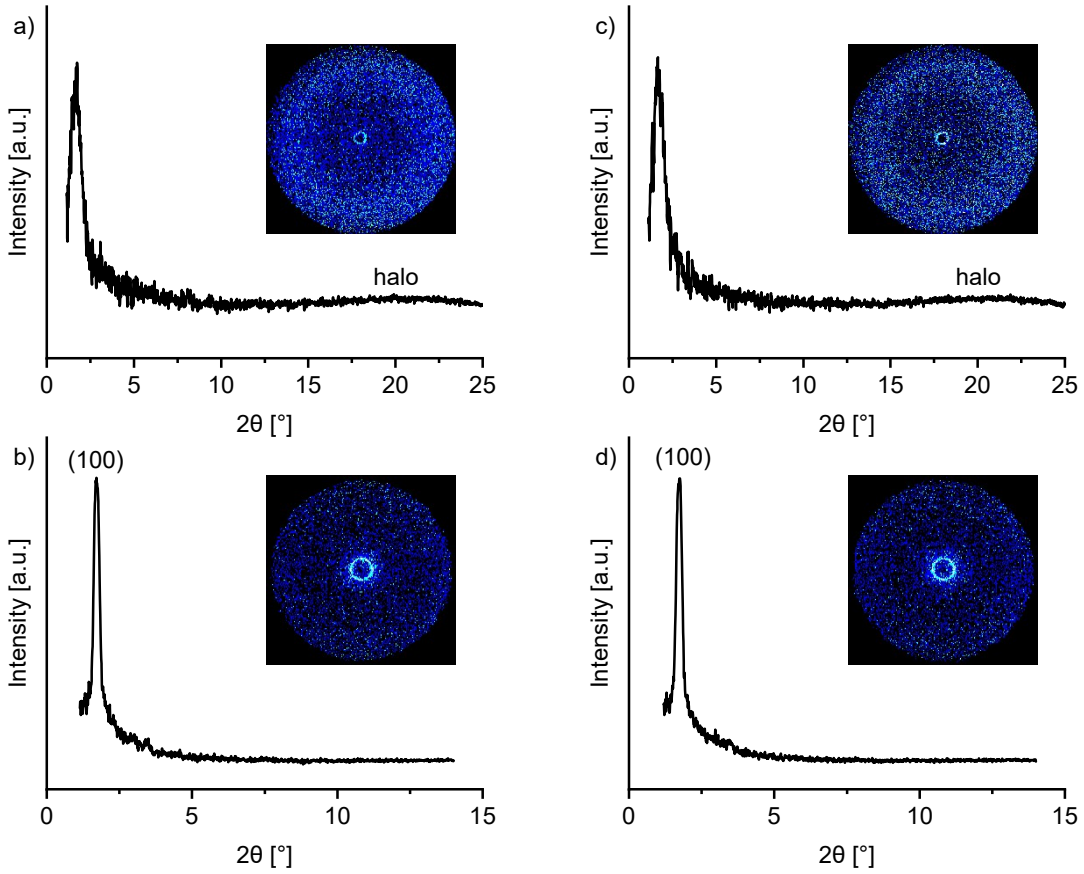

Figure S143: WAXS and SAXS diffractogram of **c-DOPA(16) • NaI** at 126 °C (a, b) as well as 131 °C (c, d) with diffraction patterns as inset.

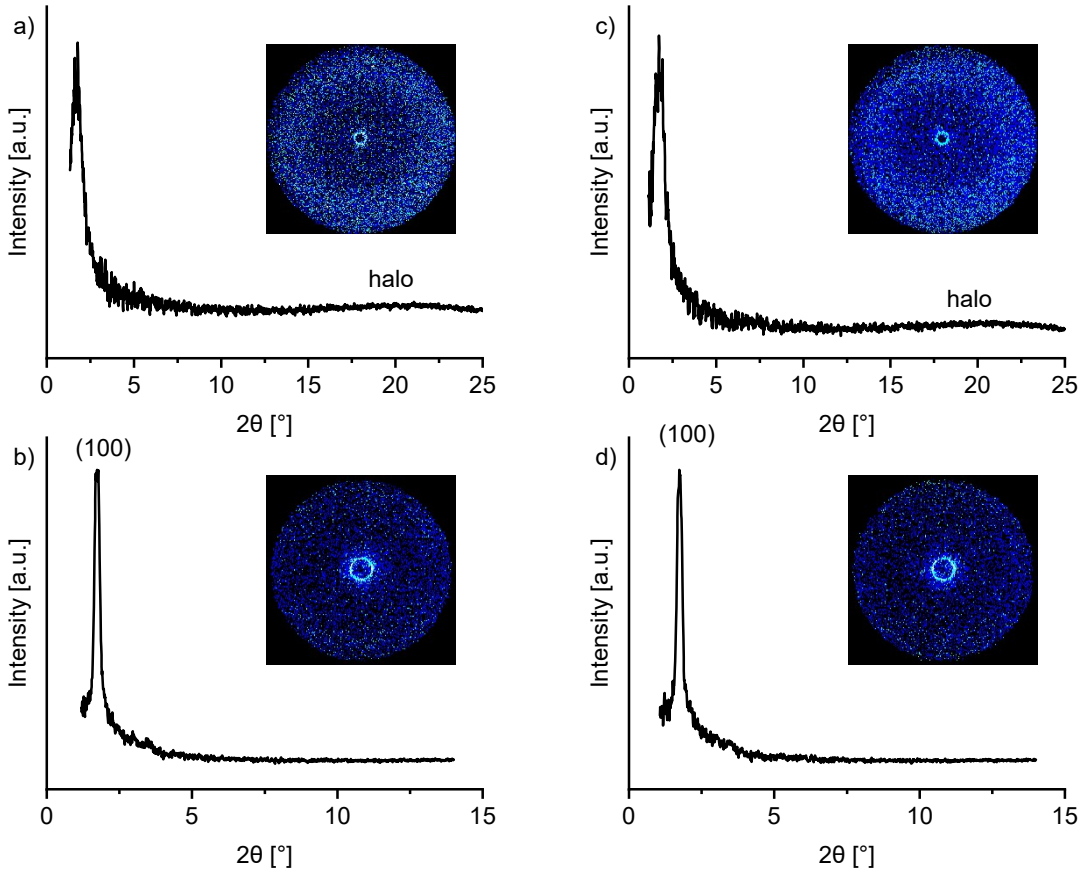

Figure S144: WAXS and SAXS diffractogram of **c-DOPA(16) • NaI** at 135 °C (a, b) as well as 140 °C (c, d) with diffraction patterns as inset.

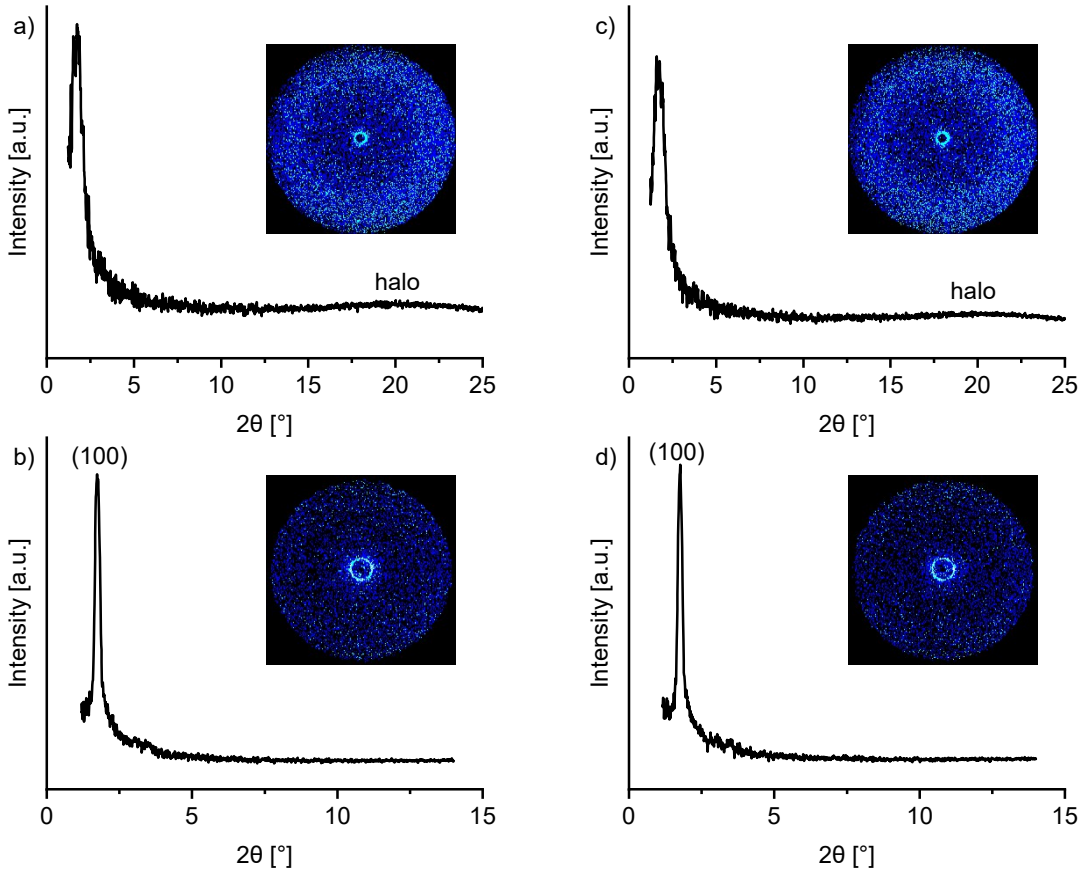

Figure S145: WAXS and SAXS diffractogram of **c-DOPA(16) • NaI** at 145 °C (a, b) as well as 150 °C (c, d) with diffraction patterns as inset.

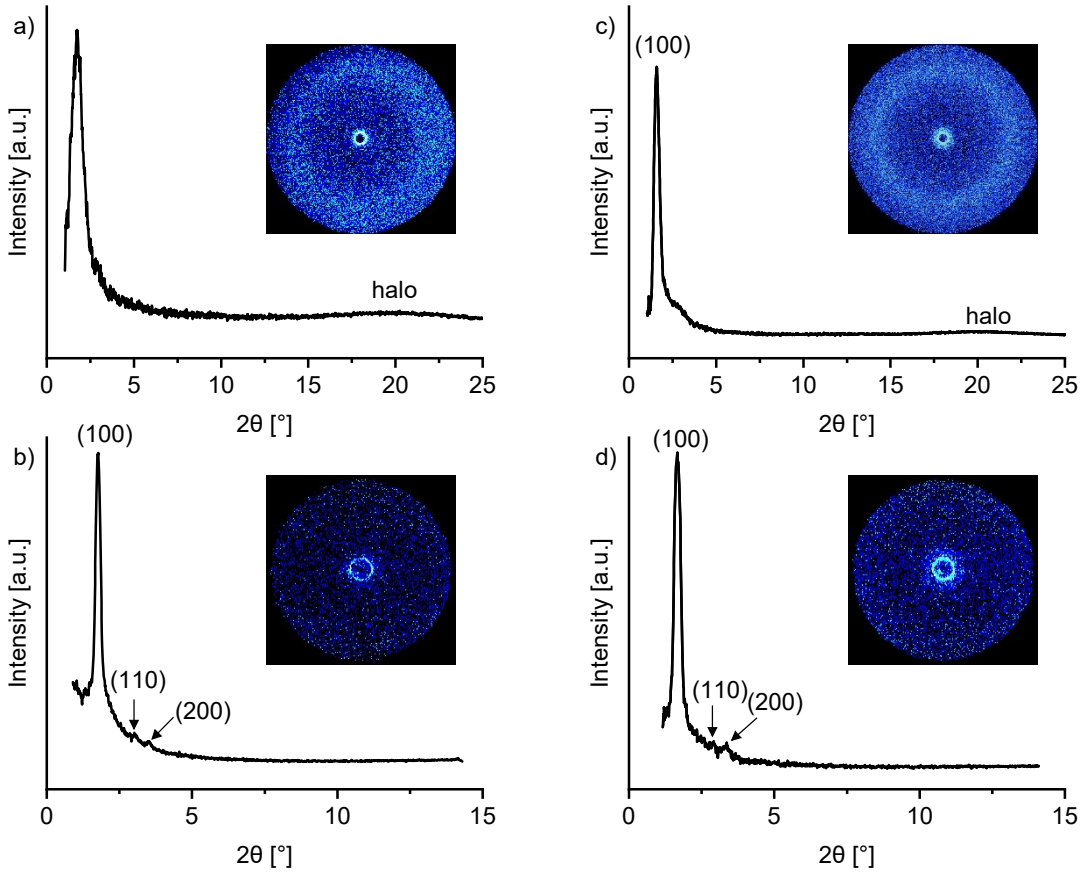

Figure S146: a) WAXS and b) SAXS diffractogram of **c-DOPA(16) • NaI** at 154 °C as well as c) WAXS and d) SAXS diffractogram of **c-DOPA(16) • KI** at 70 °C with diffraction patterns as inset.

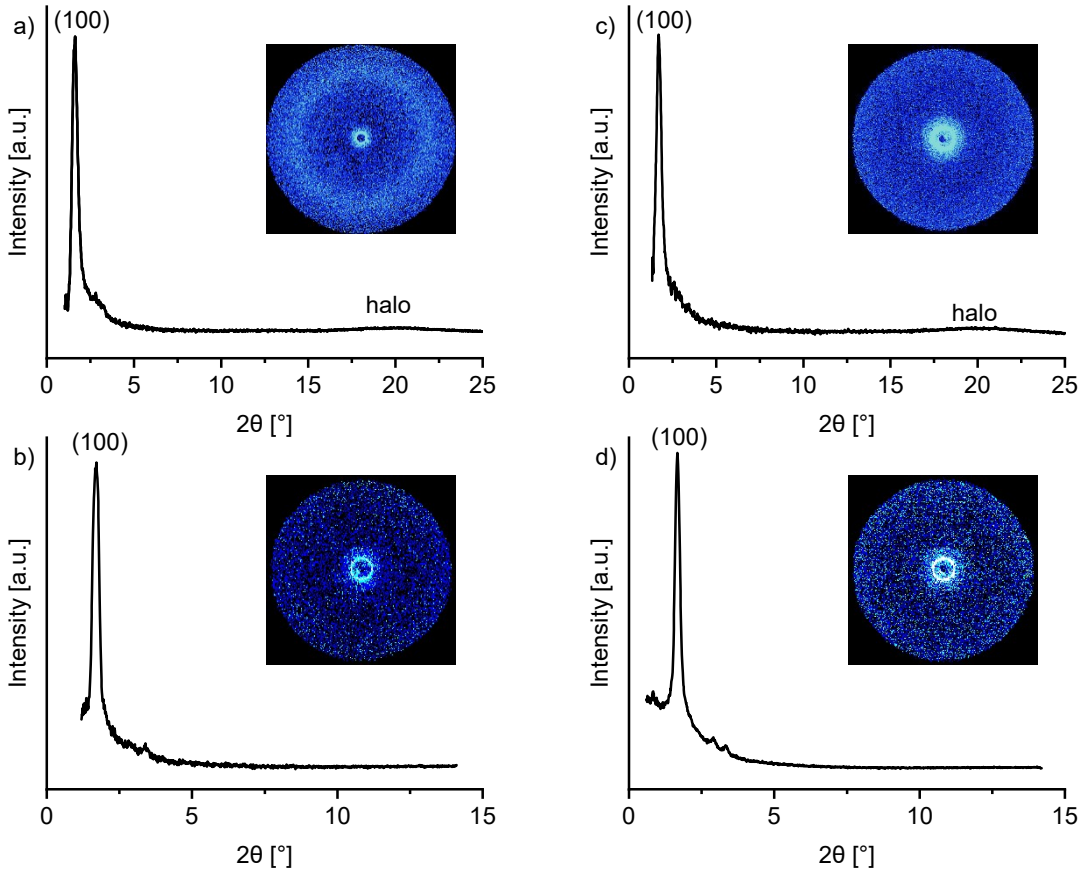

Figure S147: WAXS and SAXS diffractogram of **c-DOPA(16) • KI** at 75 °C (a, b) as well as 80 °C (c, d) with diffraction patterns as inset.

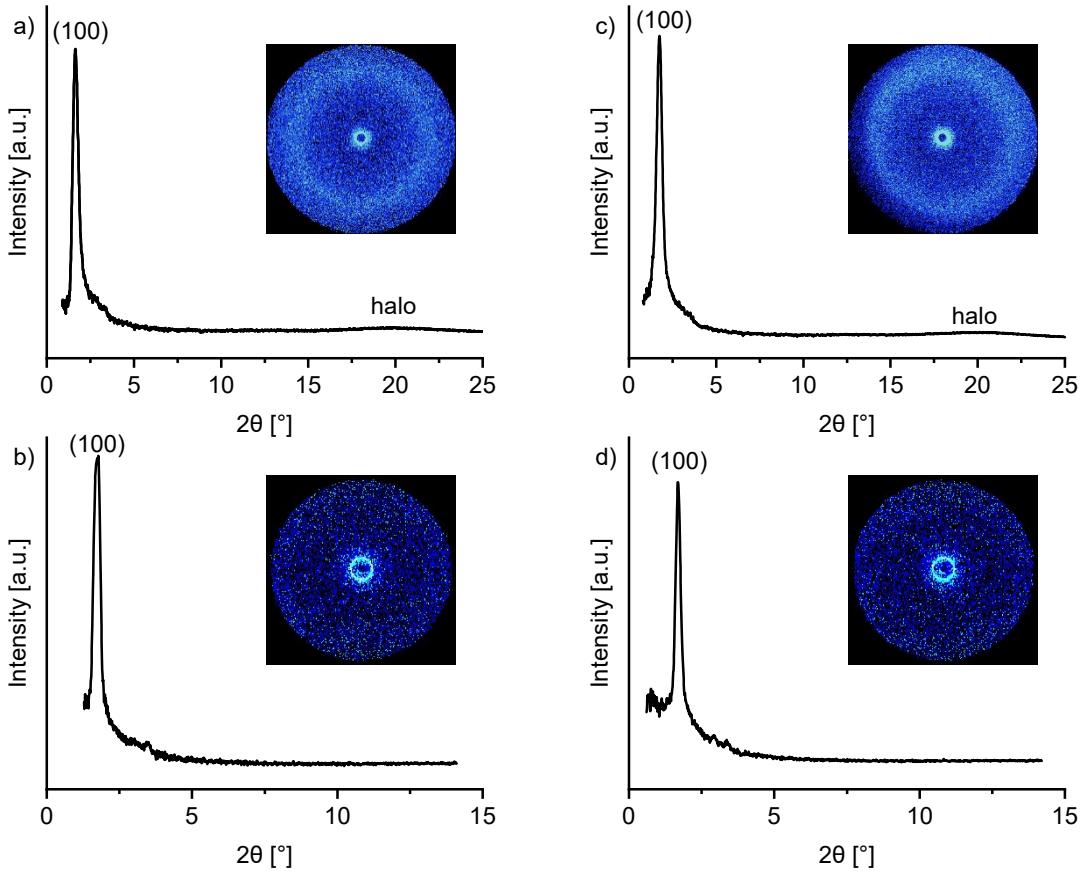

Figure S148: WAXS and SAXS diffractogram of **c-DOPA(16) • KI** at 84 °C (a, b) as well as 90 °C (c, d) with diffraction patterns as inset.

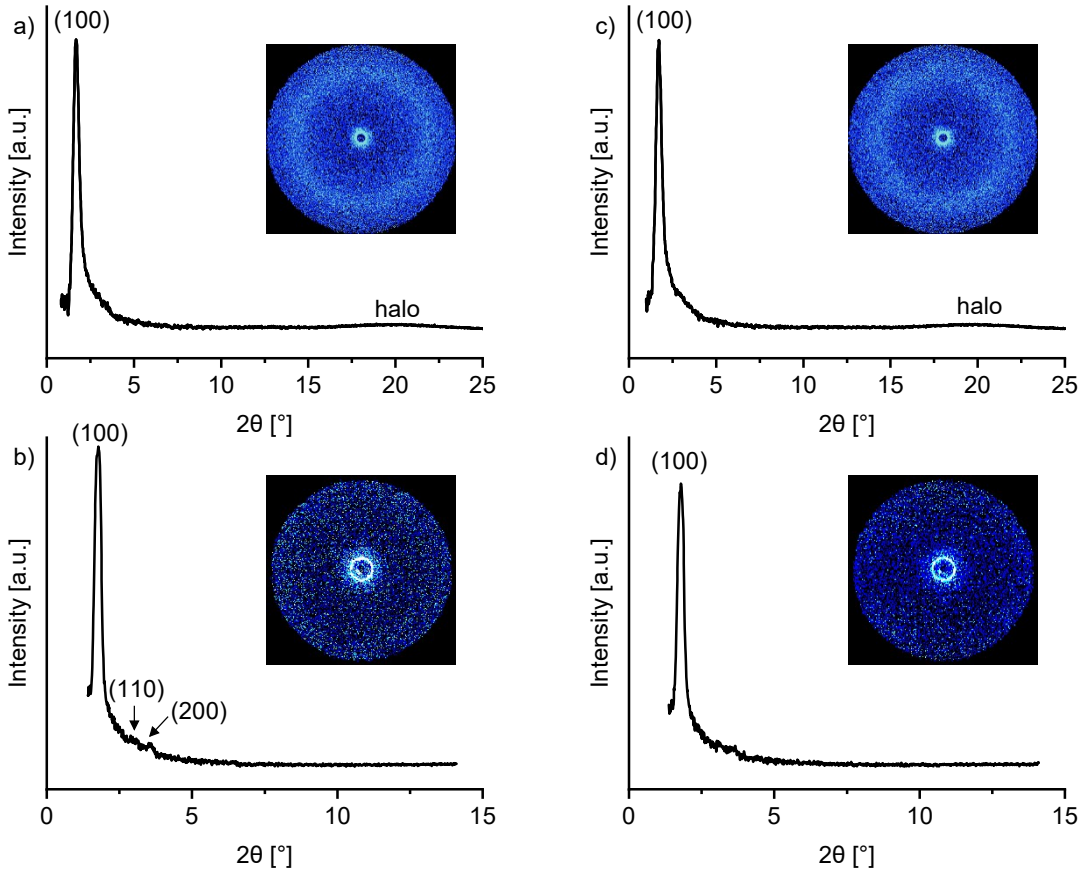

Figure S149: WAXS and SAXS diffractogram of **c-DOPA(16) • KI** at 95 °C (a, b) as well as 100 °C (c, d) with diffraction patterns as inset.

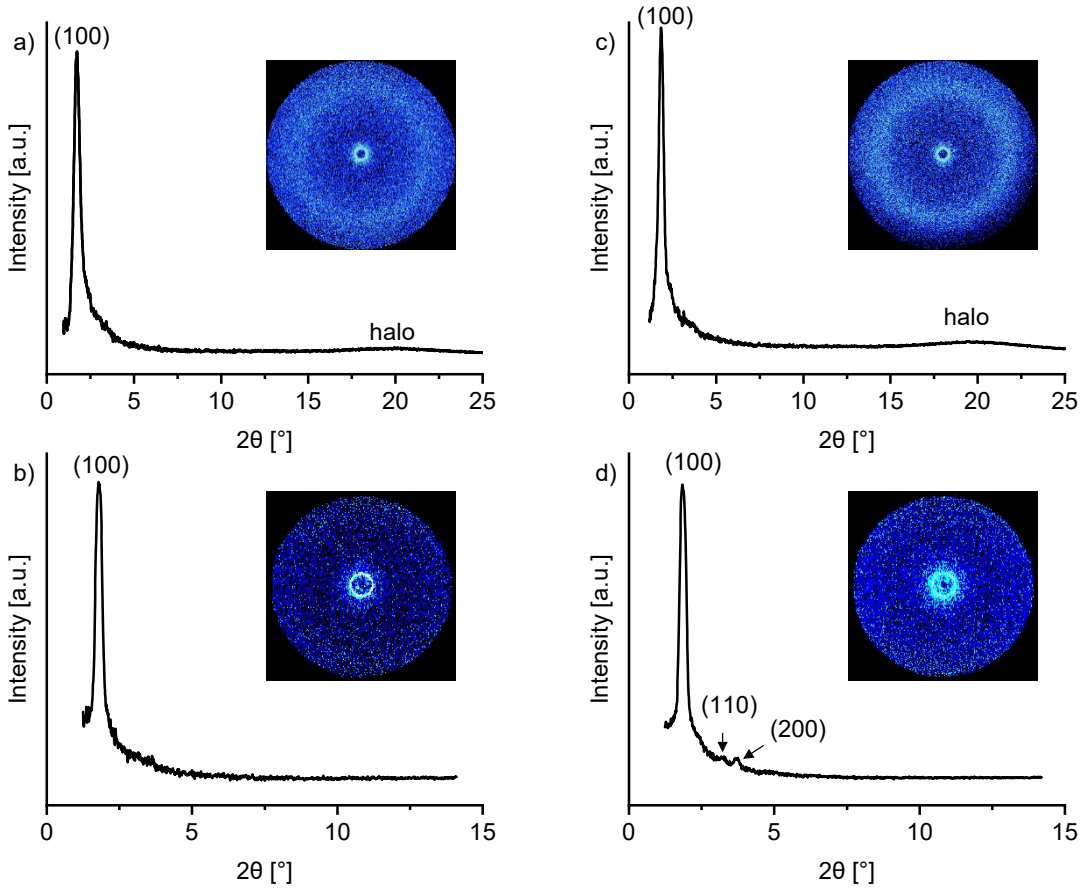

Figure S150: a) WAXS and b) SAXS diffractogram of **c-DOPA(16) • KI** at 105 °C as well as c) WAXS and d) SAXS diffractogram of **c-DOPA(16) • $NaBF_4$** at 75 °C with diffraction patterns as inset.

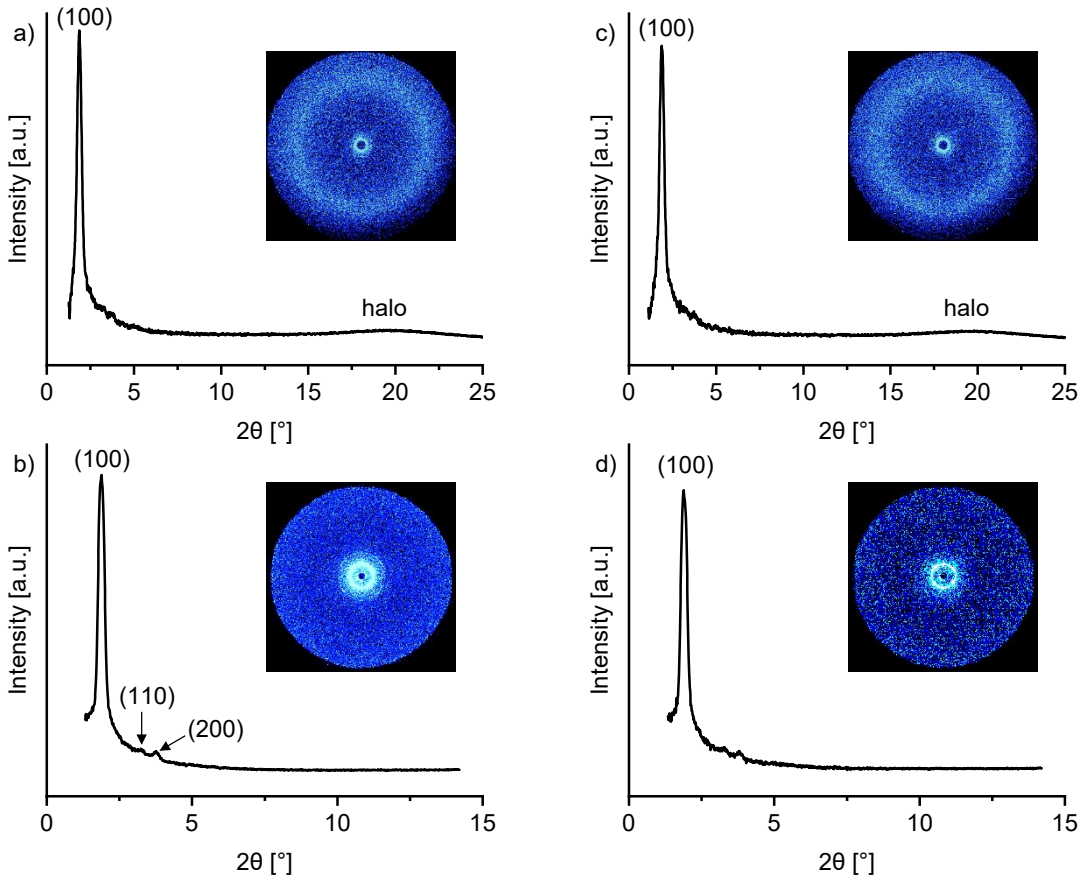

Figure S151: WAXS and SAXS diffractogram of **c-DOPA(16) • $NaBF_4$** at 80 °C (a, b) as well as 85 °C (c, d) with diffraction patterns as inset.

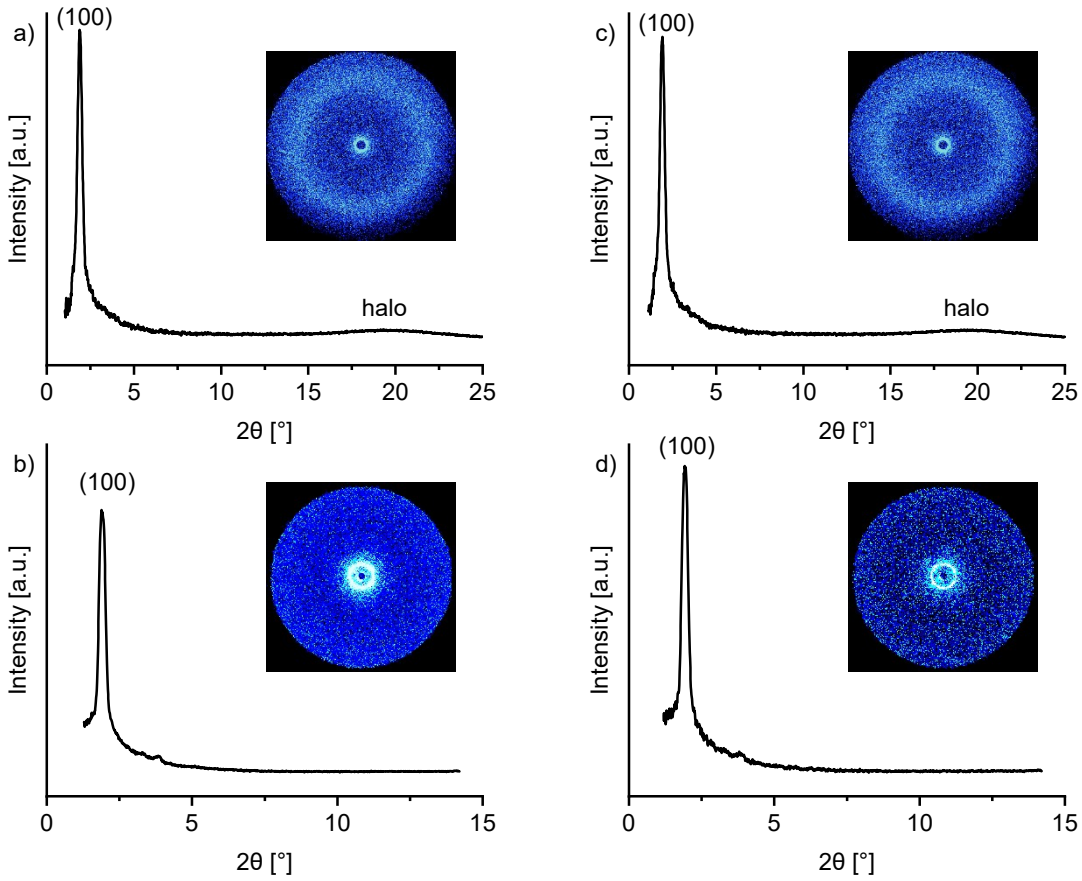

Figure S152: WAXS and SAXS diffractogram of **c-DOPA(16) • $NaBF_4$** at 90 °C (a, b) as well as 95 °C (c, d) with diffraction patterns as inset.

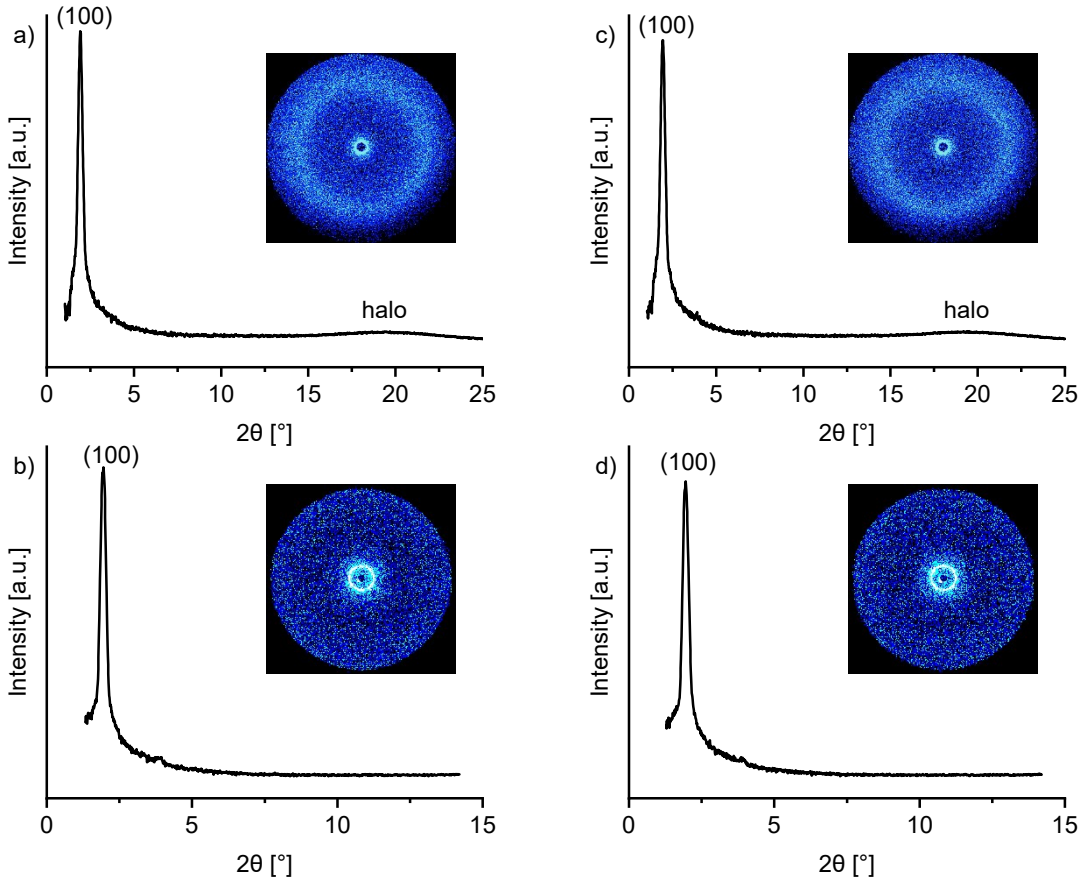

Figure S153: WAXS and SAXS diffractogram of **c-DOPA(16) • $NaBF_4$** at 100 °C (a, b) as well as 105 °C (c, d) with diffraction patterns as inset.

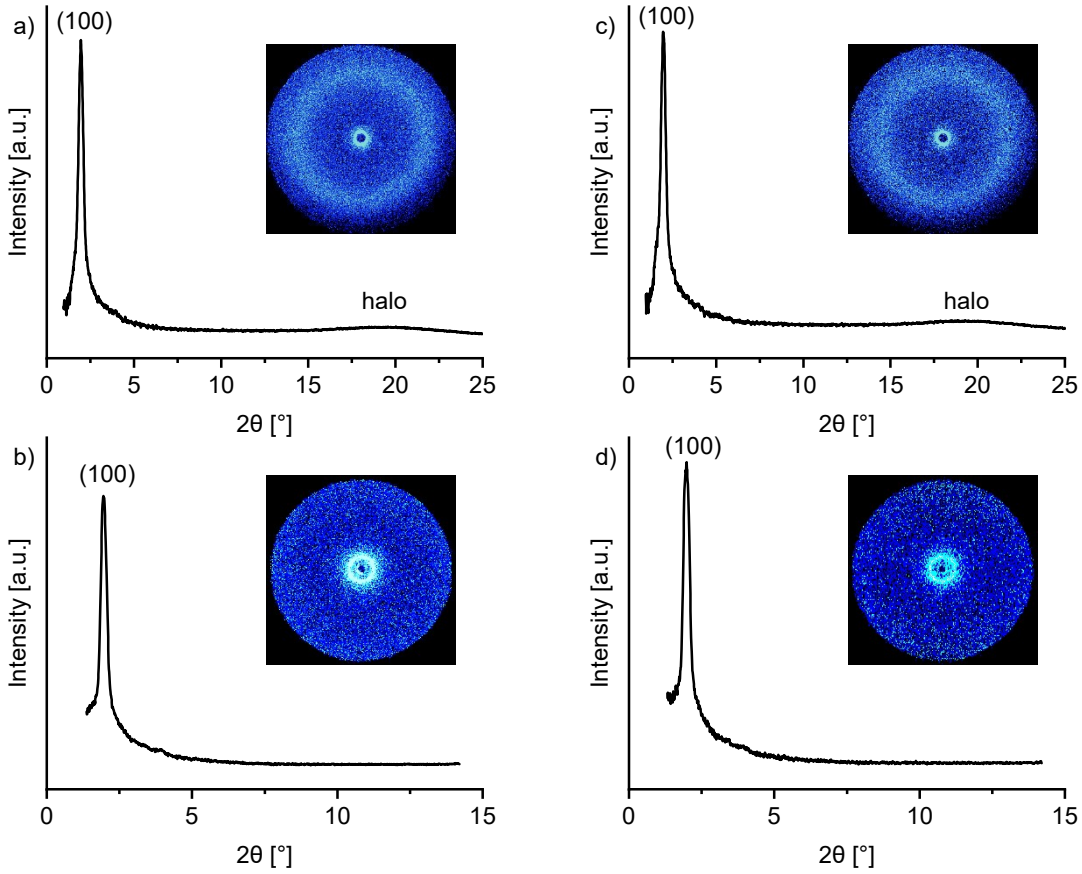

Figure S154: WAXS and SAXS diffractogram of **c-DOPA(16) • $NaBF_4$** at 110 °C (a, b) as well as 115 °C (c, d) with diffraction patterns as inset.

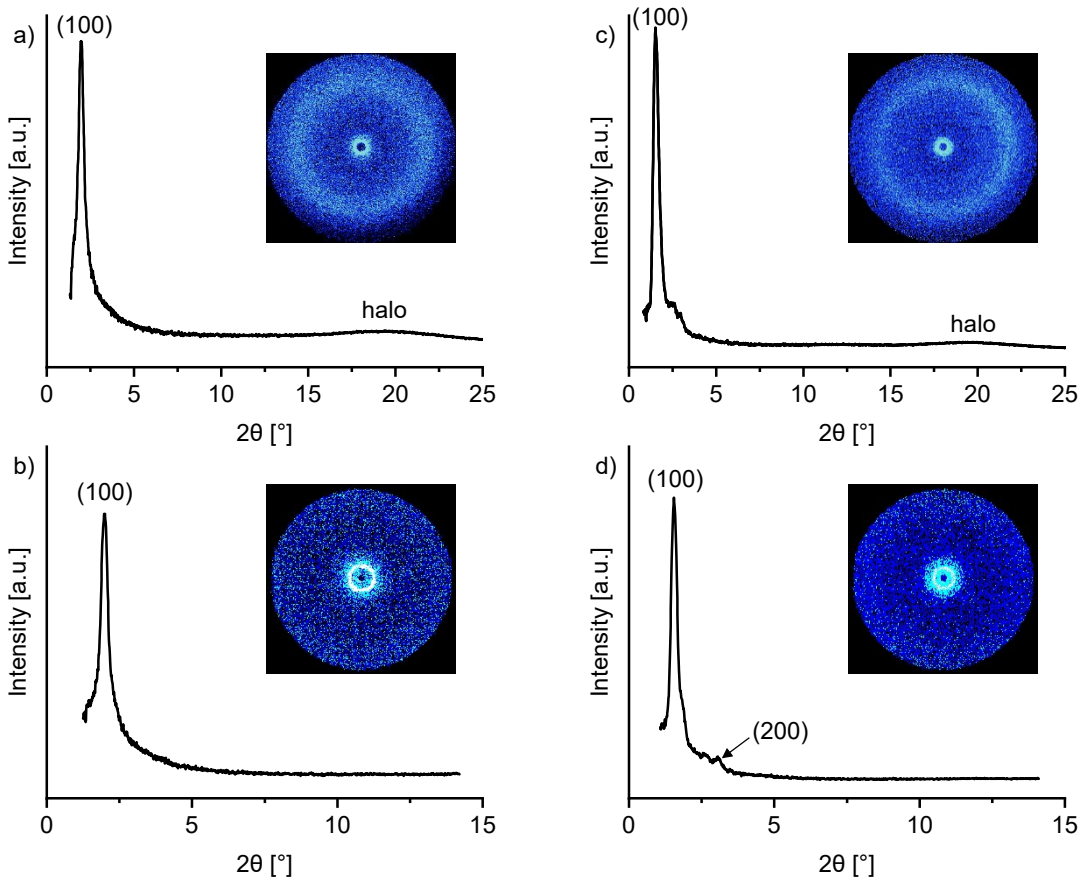

Figure S155: a) WAXS and b) SAXS diffractogram of **c-DOPA(16) • $NaBF_4$** at 120 °C as well as c) WAXS and d) SAXS diffractogram of **c-DOPA(16) • KPF_6** at 70 °C with diffraction patterns as inset.

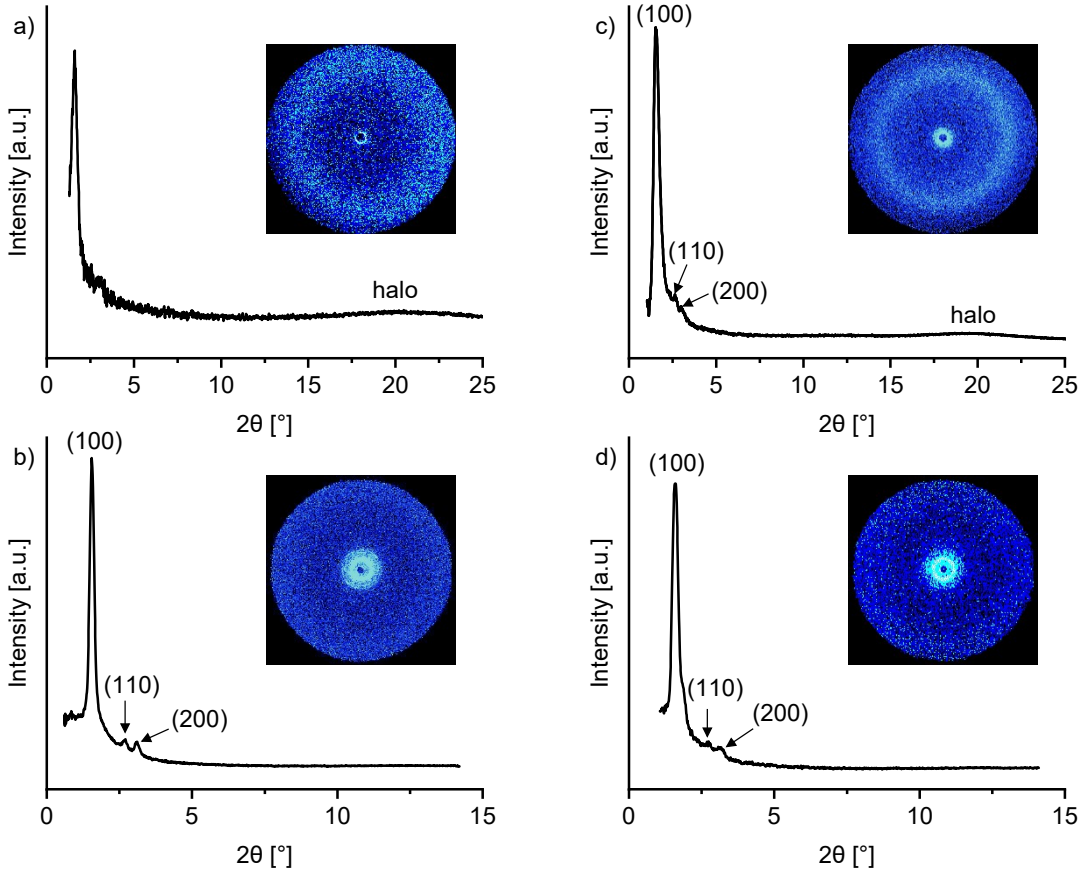

Figure S156: WAXS and SAXS diffractogram of **c-DOPA(16) • KPF_6** at 74 °C (a, b) as well as 80 °C (c, d) with diffraction patterns as inset.

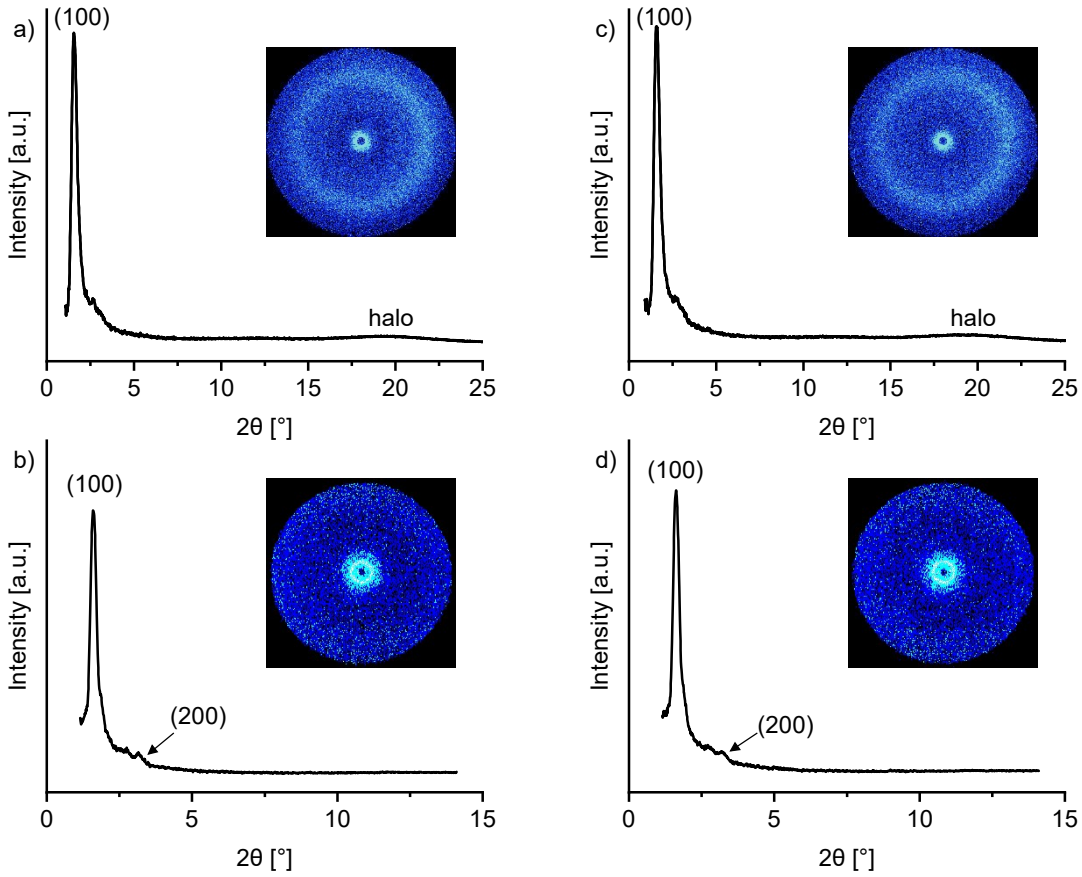

Figure S157: WAXS and SAXS diffractogram of **c-DOPA(16) • KPF_6** at 84 °C (a, b) as well as 90 °C (c, d) with diffraction patterns as inset.

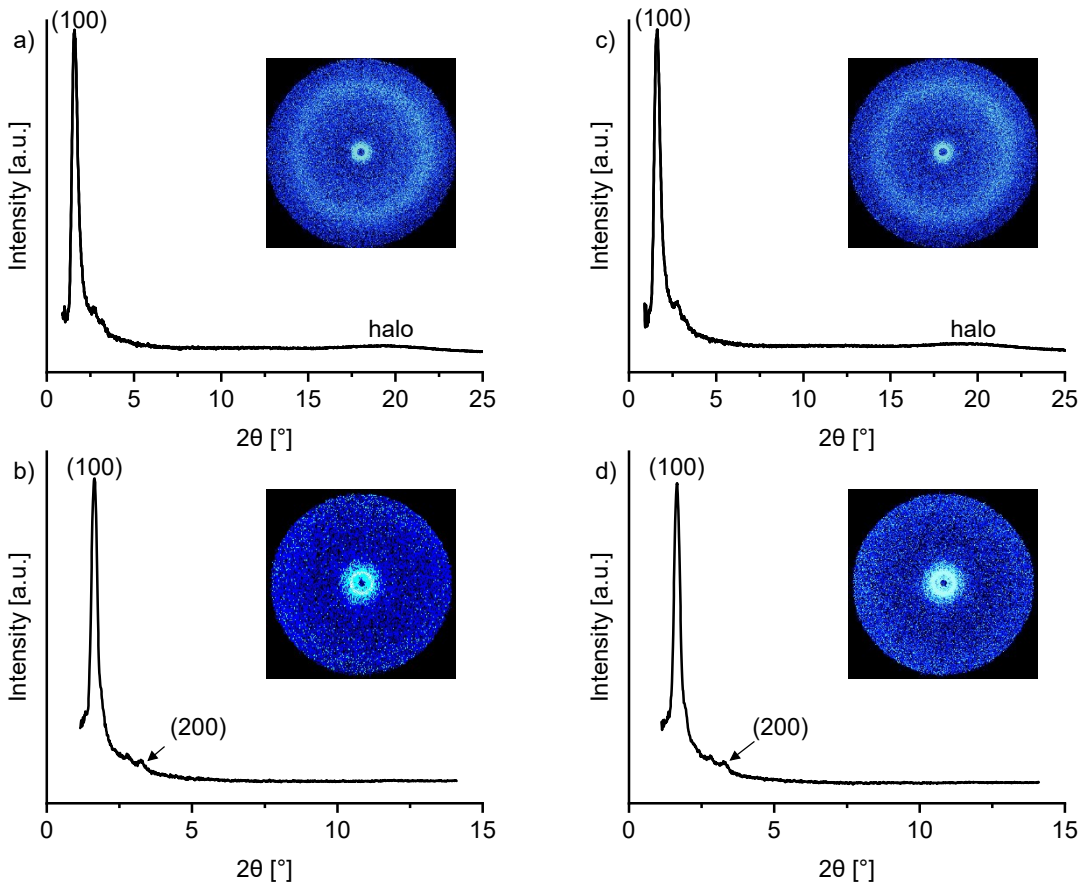

Figure S158: WAXS and SAXS diffractogram of **c-DOPA(16) • KPF_6** at 95 °C (a, b) as well as 100 °C (c, d) with diffraction patterns as inset.

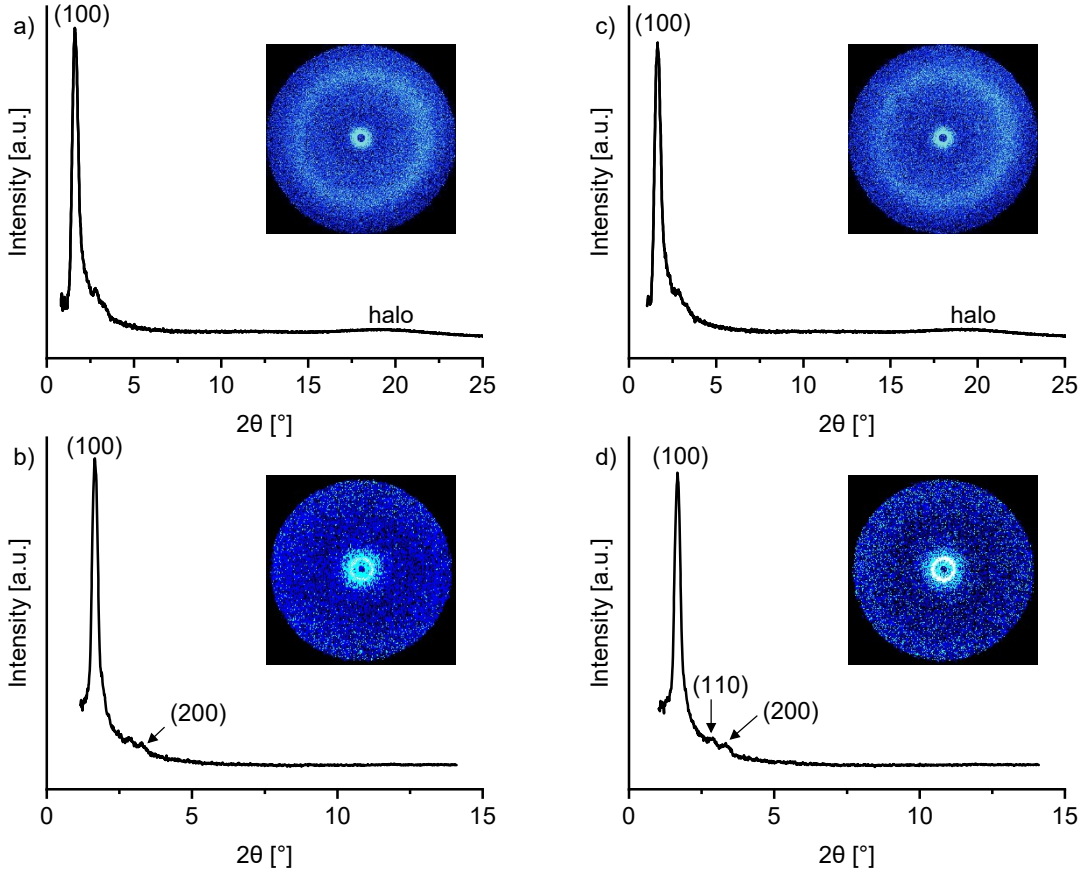

Figure S159: WAXS and SAXS diffractogram of **c-DOPA(16) • KPF_6** at 105 °C (a, b) as well as 110 °C (c, d) with diffraction patterns as inset.

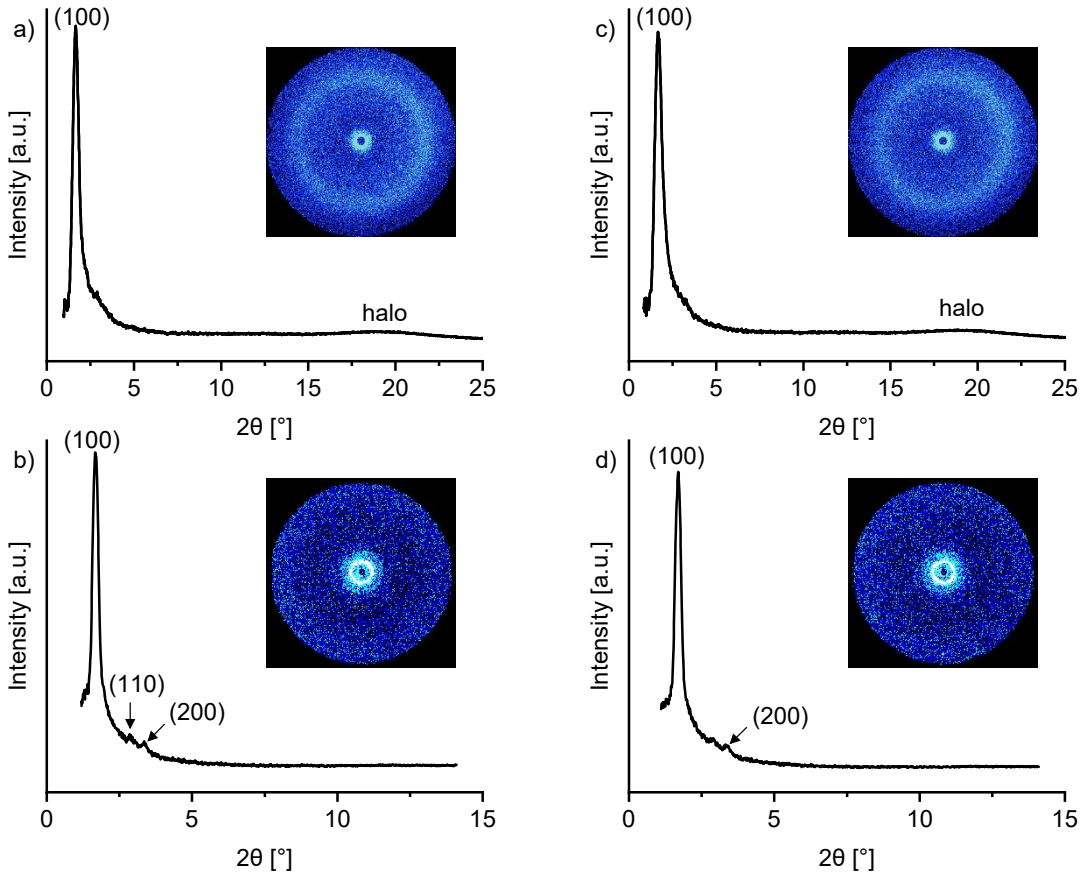

Figure S160: WAXS and SAXS diffractogram of **c-DOPA(16) • KPF_6** at 115 °C (a, b) as well as 120 °C (c, d) with diffraction patterns as inset.

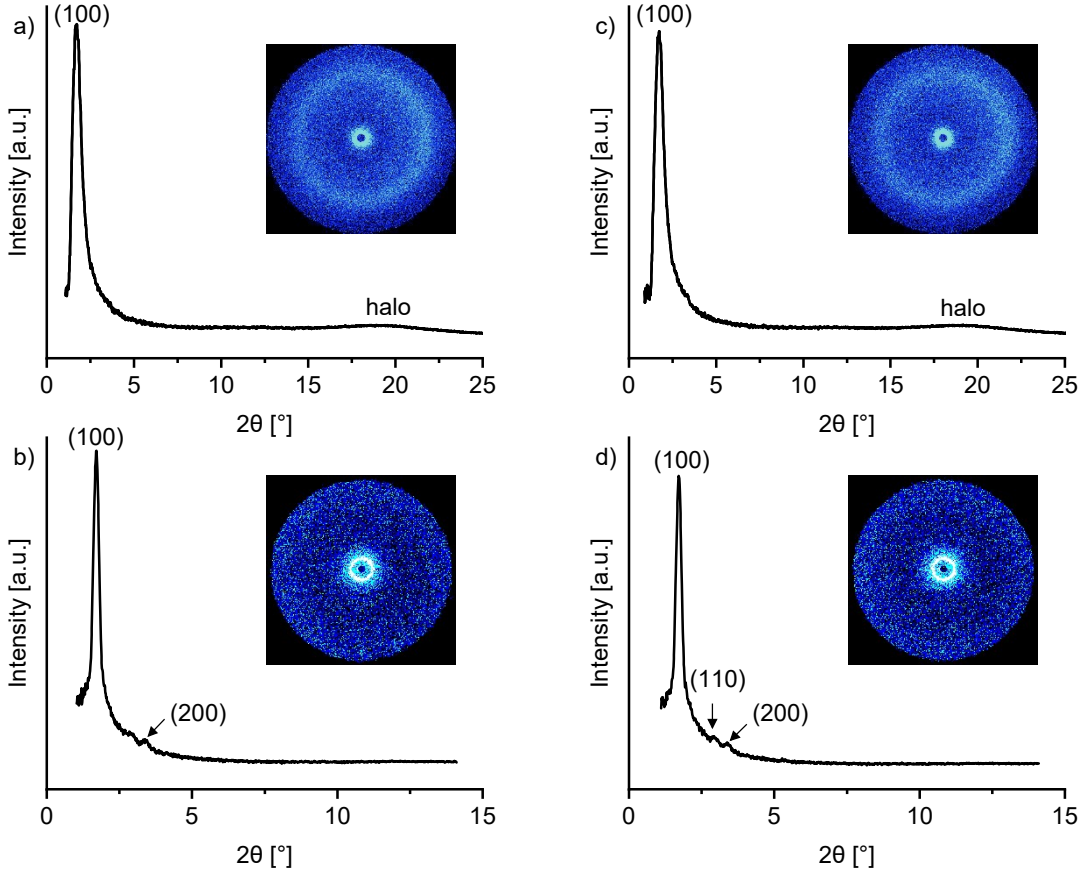

Figure S161: WAXS and SAXS diffractogram of **c-DOPA(16) • KPF_6** at 125 °C (a, b) as well as 130 °C (c, d) with diffraction patterns as inset.

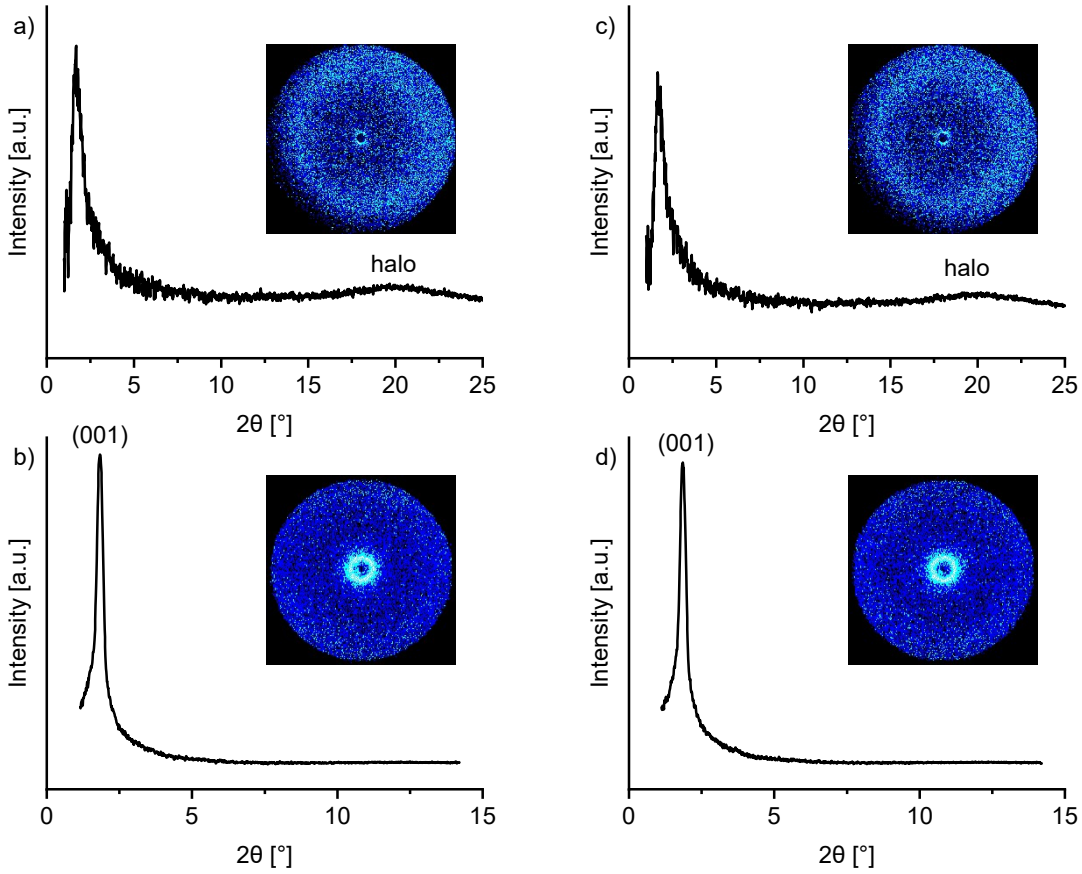

Figure S162: WAXS and SAXS diffractogram of **c-THIQ(14) • KPF_6** at 60 °C (a, b) as well as 65 °C (c, d) with diffraction patterns as inset.

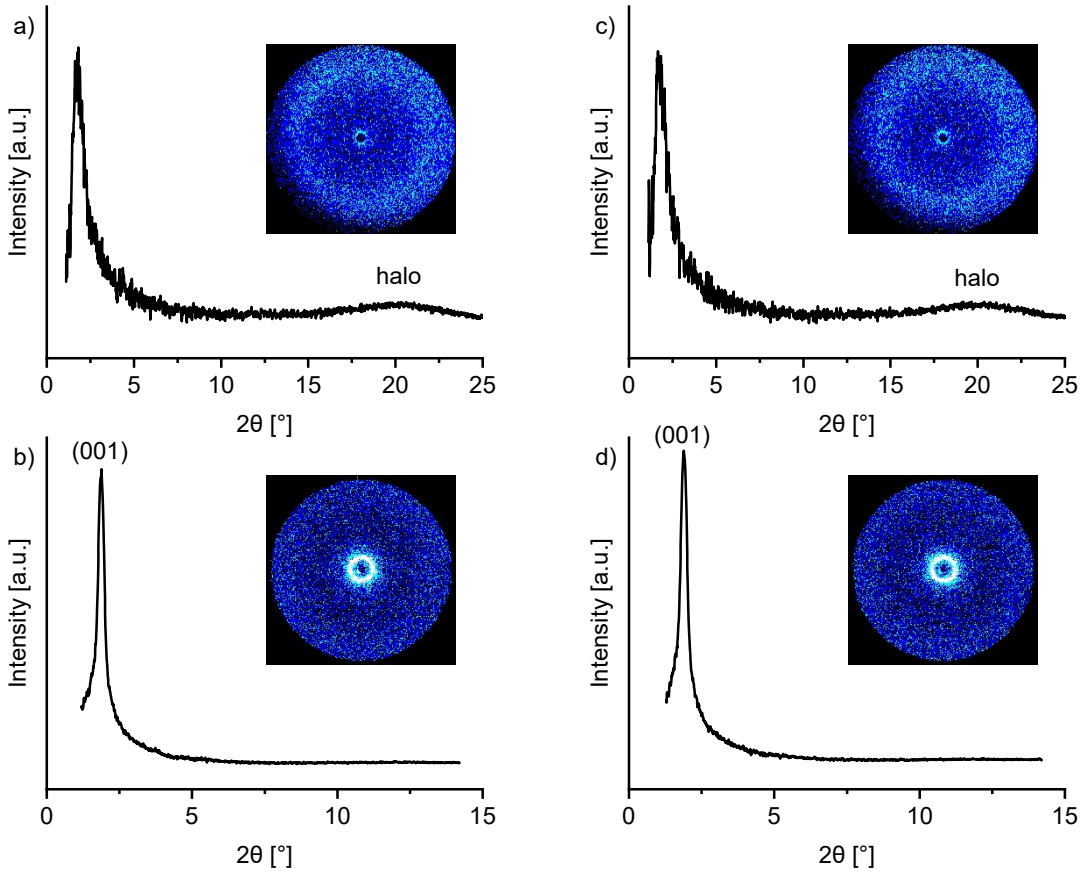

Figure S163: WAXS and SAXS diffractogram of **c-THIQ(14) • KPF_6** at 70 °C (a, b) as well as 75 °C (c, d) with diffraction patterns as inset.

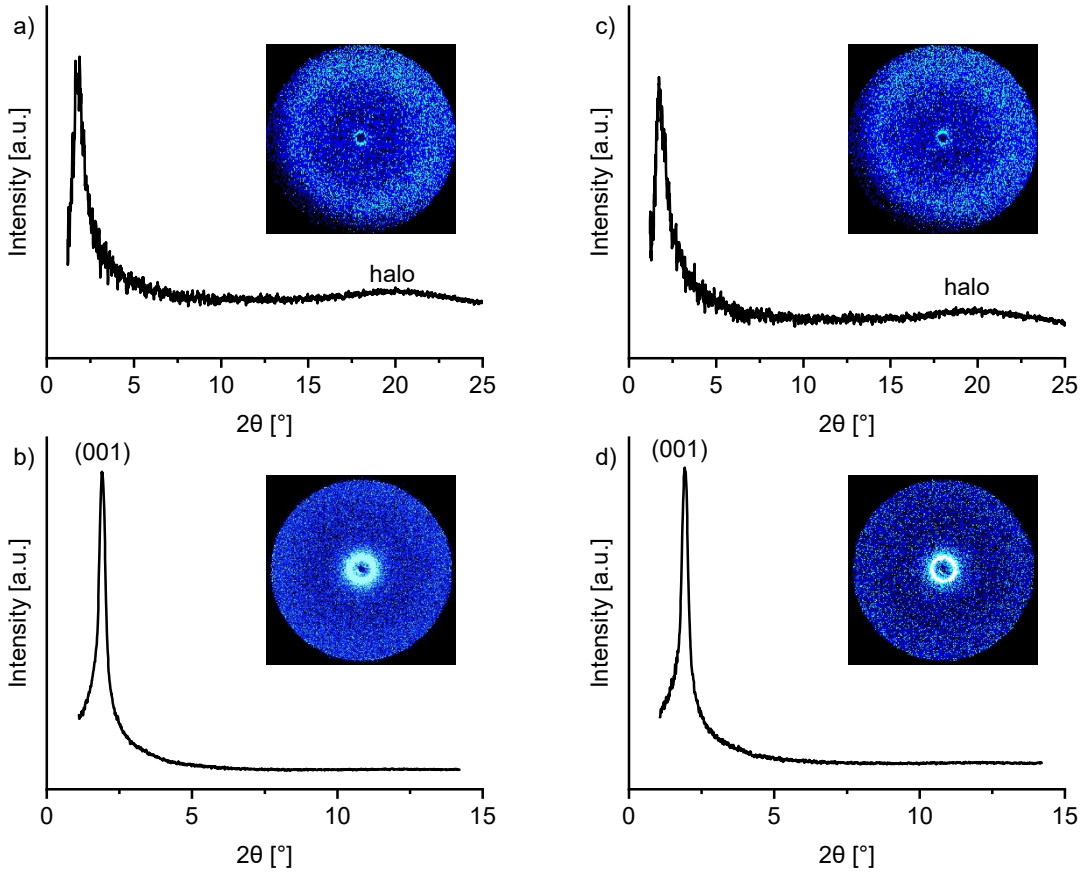

Figure S164: WAXS and SAXS diffractogram of **c-THIQ(14) • KPF_6** at 80 °C (a, b) as well as 85 °C (c, d) with diffraction patterns as inset.

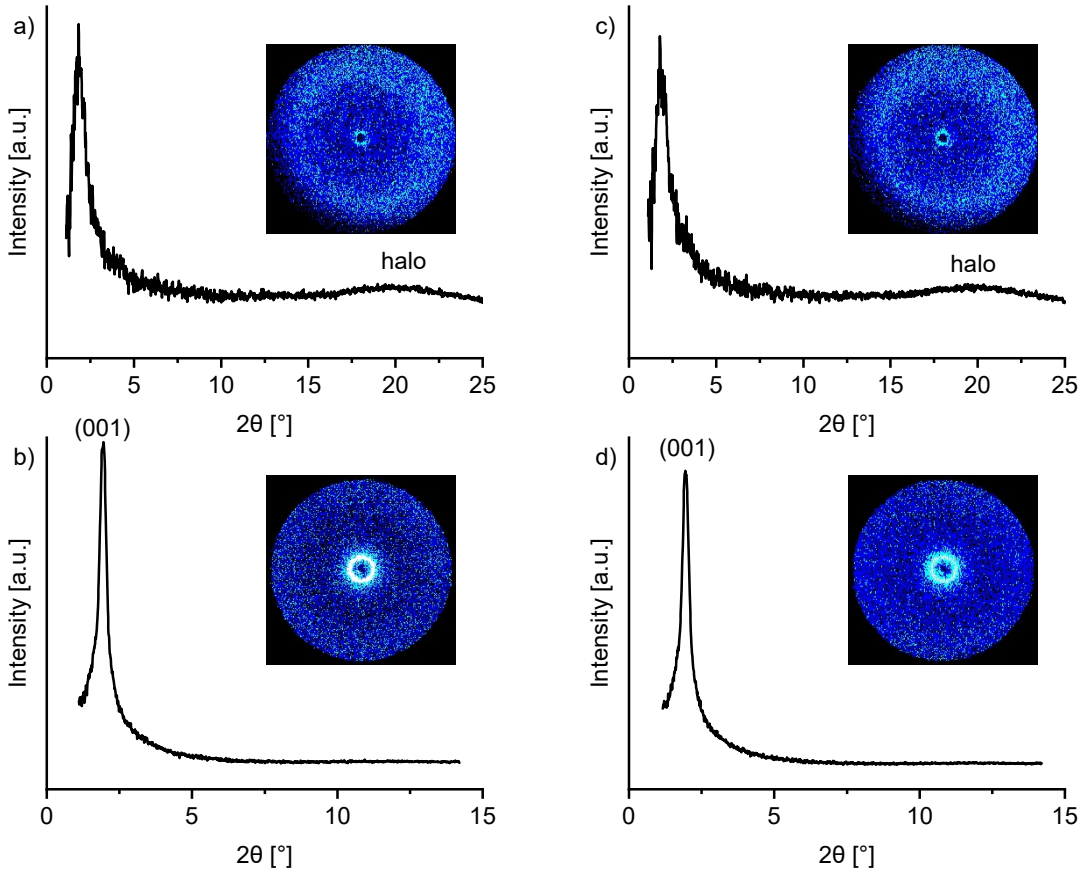

Figure S165: WAXS and SAXS diffractogram of **c-THIQ(14) • KPF_6** at 90 °C (a, b) as well as 95 °C (c, d) with diffraction patterns as inset.

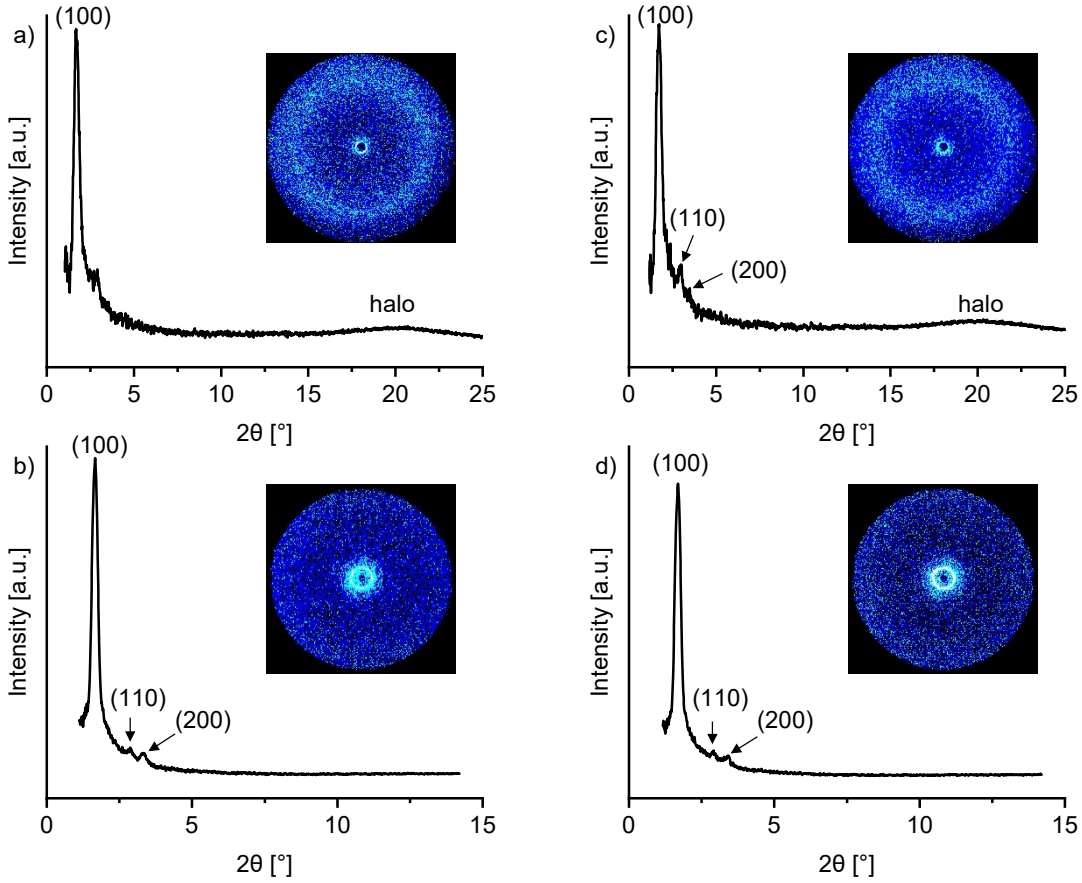

Figure S166: WAXS and SAXS diffractogram of **c-THIQ(16) • KPF_6** at 60 °C (a, b) as well as 65 °C (c, d) with diffraction patterns as inset.

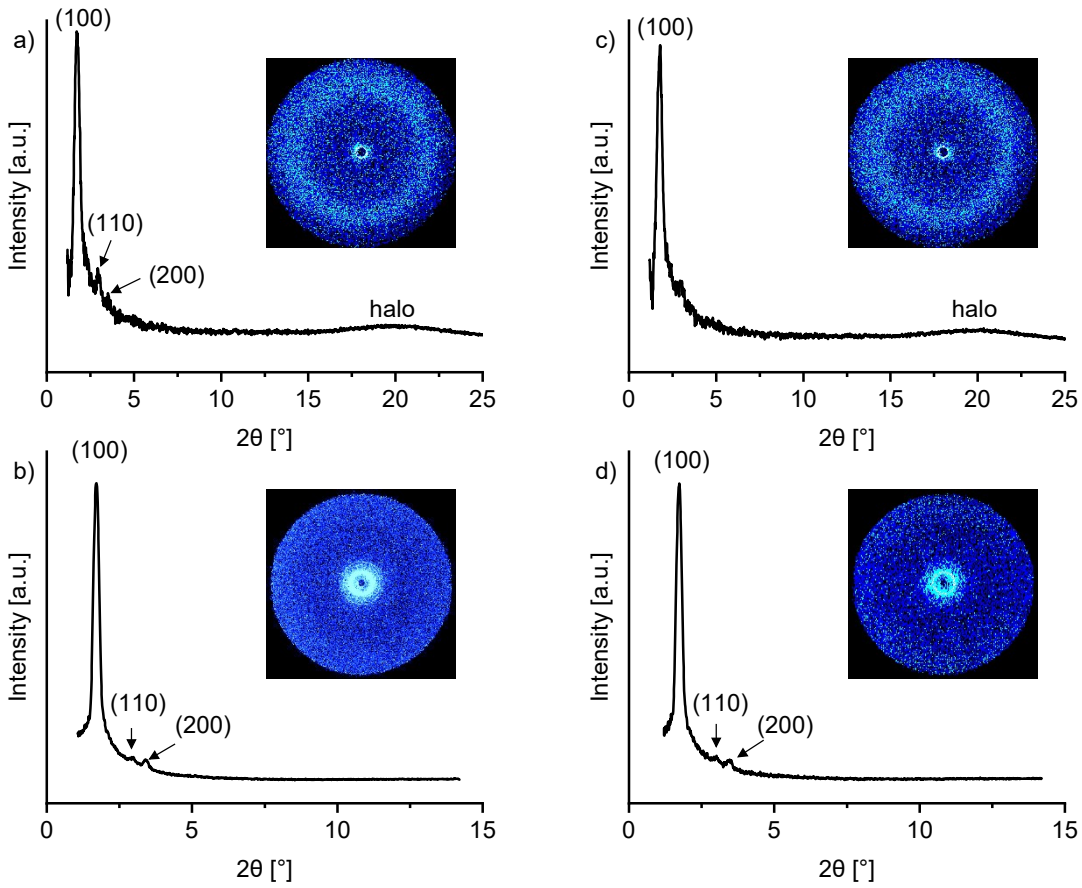

Figure S167: WAXS and SAXS diffractogram of **c-THIQ(16) • KPF_6** at 70 °C (a, b) as well as 75 °C (c, d) with diffraction patterns as inset.

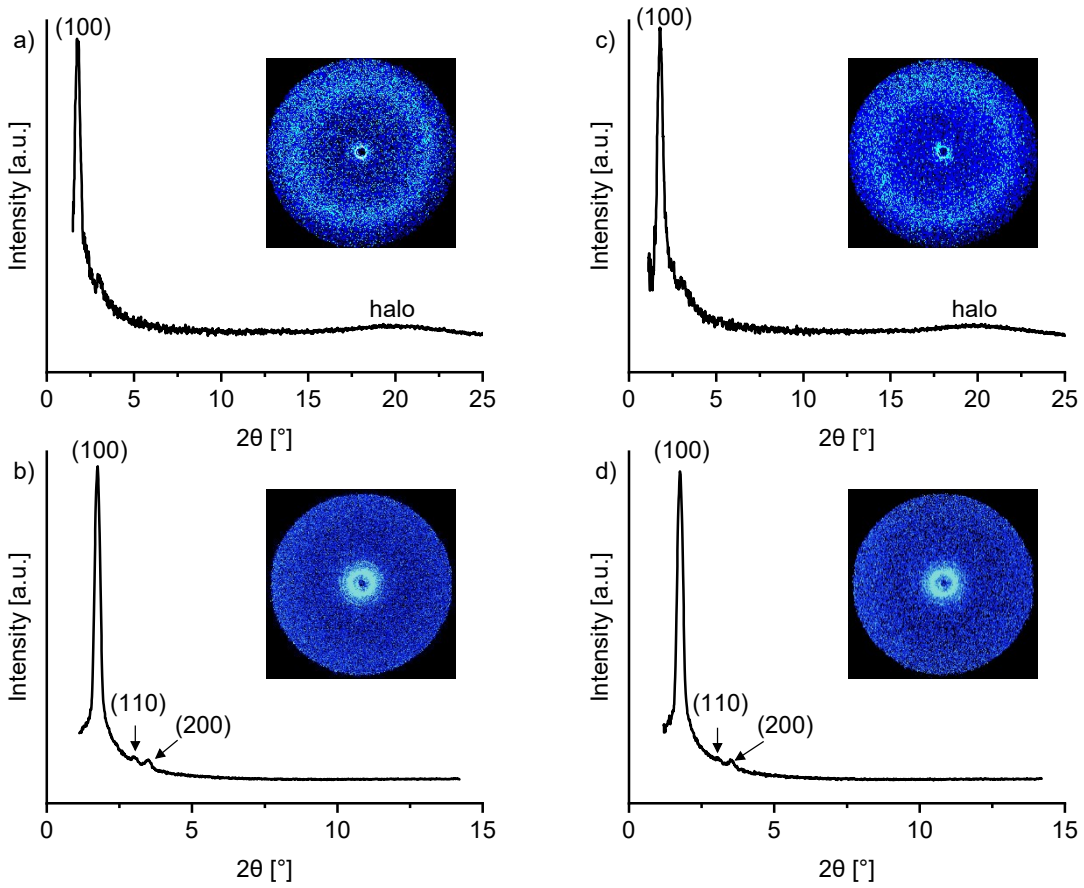

Figure S168: WAXS and SAXS diffractogram of **c-THIQ(16) • KPF_6** at 80 °C (a, b) as well as 85 °C (c, d) with diffraction patterns as inset.

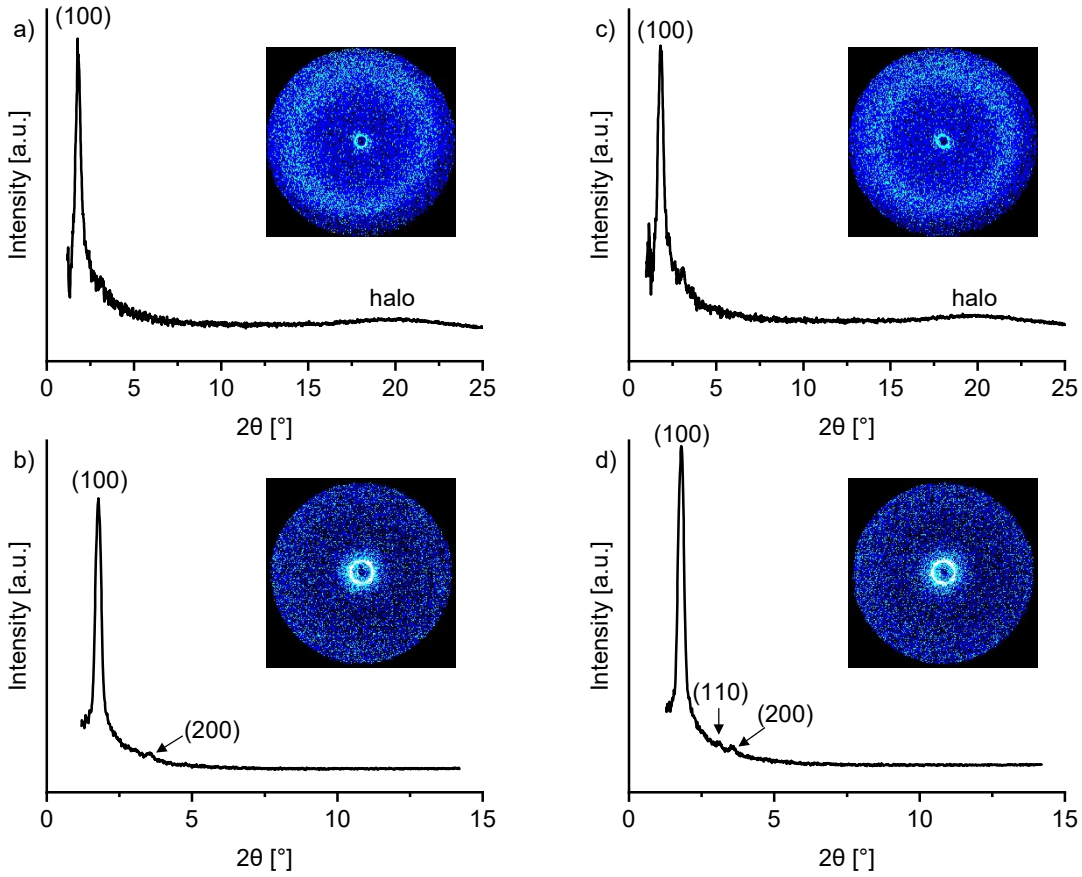

Figure S169: WAXS and SAXS diffractogram of **c-THIQ(16) • KPF_6** at 90 °C (a, b) as well as 95 °C (c, d) with diffraction patterns as inset.

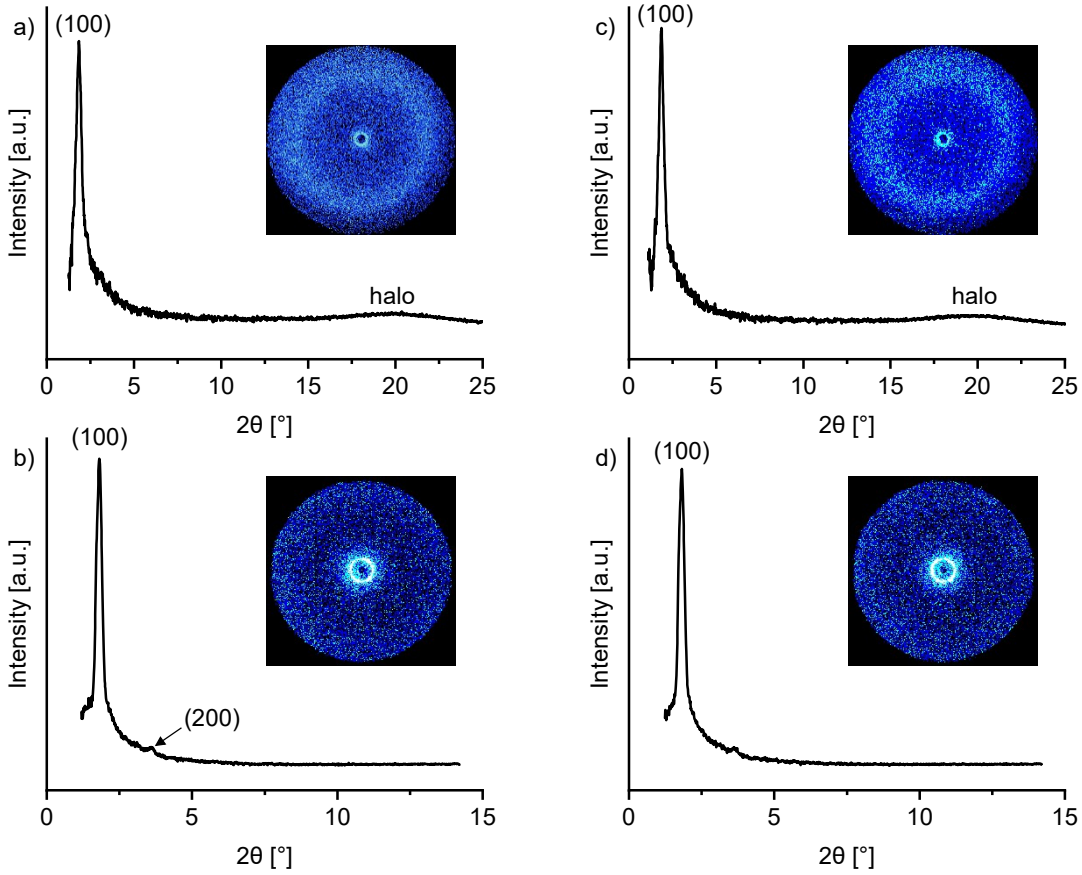

Figure S170: WAXS and SAXS diffractogram of **c-THIQ(16) • KPF_6** at 100 °C (a, b) as well as 105 °C (c, d) with diffraction patterns as inset.

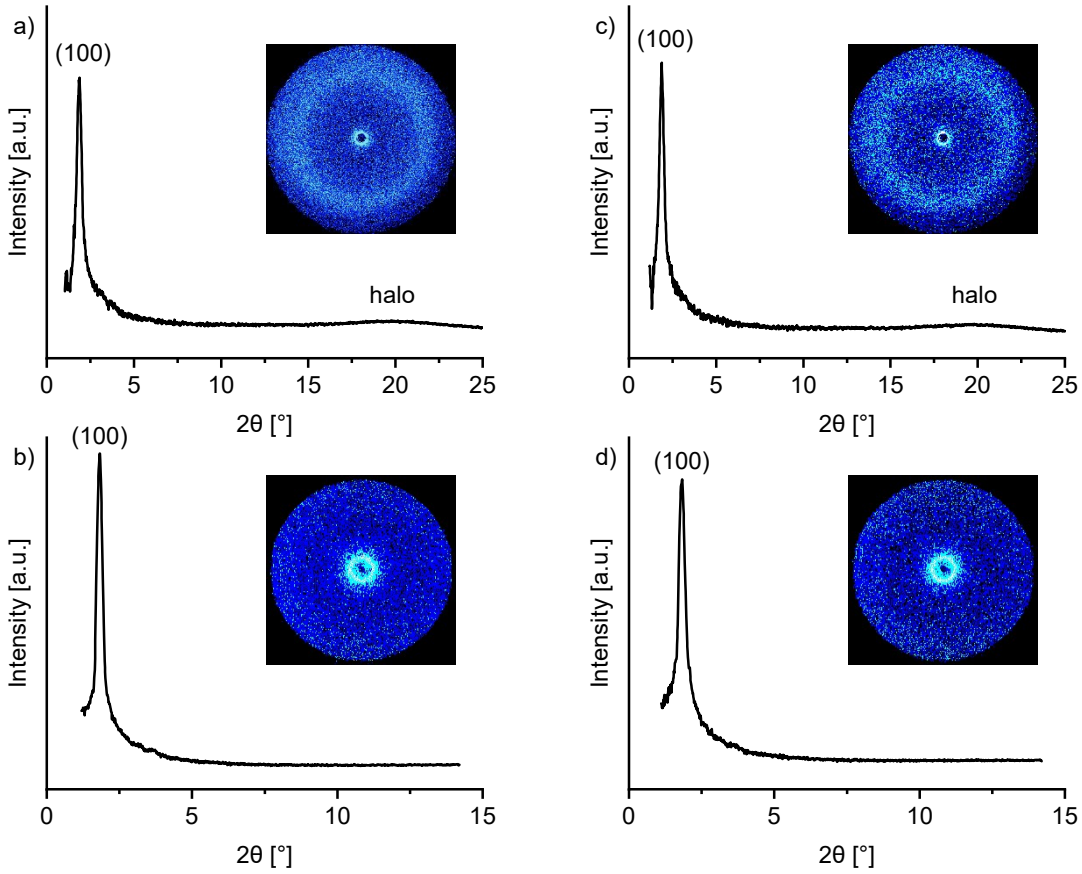

Figure S171: WAXS and SAXS diffractogram of **c-THIQ(16) • KPF_6** at 110 °C (a, b) as well as 115 °C (c, d) with diffraction patterns as inset.

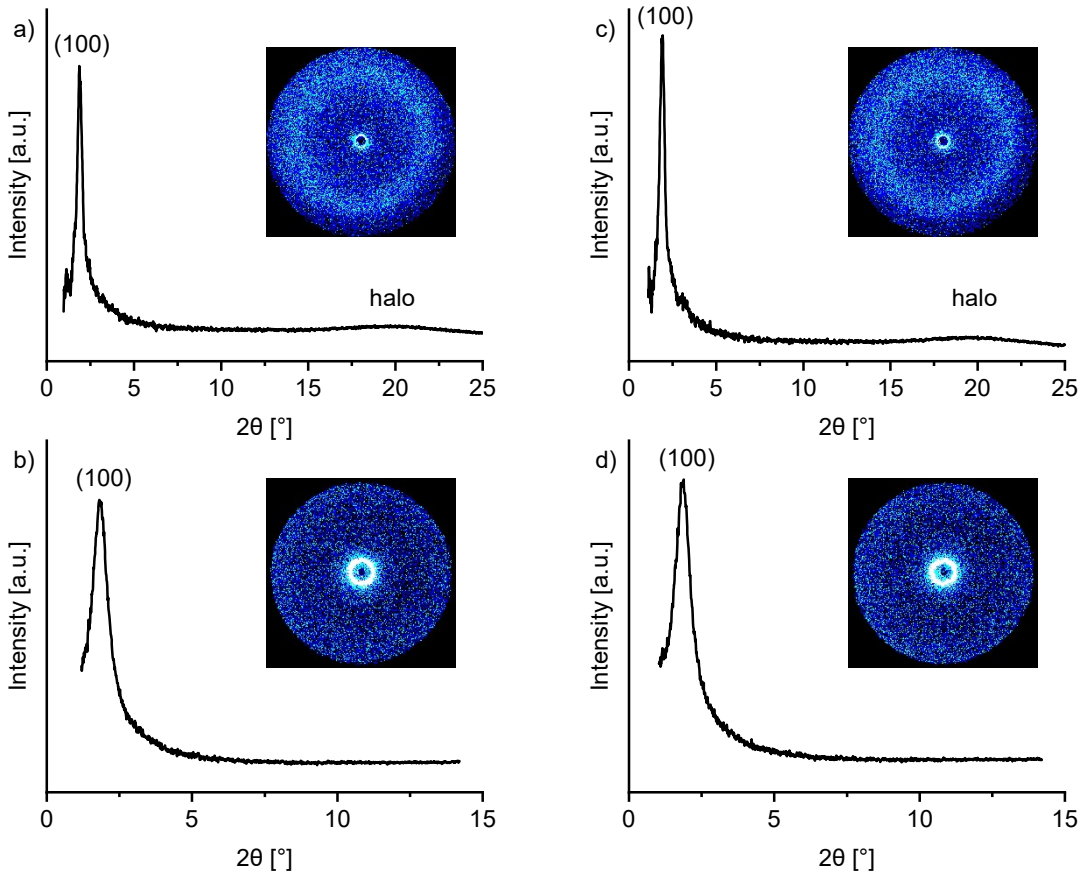

Figure S172: WAXS and SAXS diffractogram of **c-THIQ(16) • KPF_6** at 120 °C (a, b) as well as 125 °C (c, d) with diffraction patterns as inset.

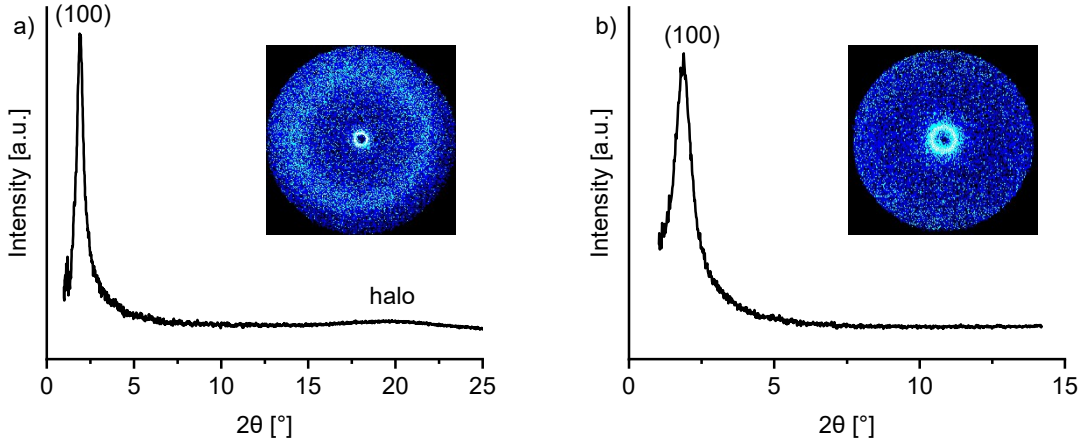

Figure S173: a) WAXS and b) SAXS diffractogram of **c-DOPA(16) • KPF_6** at 80 °C with diffraction patterns as inset.

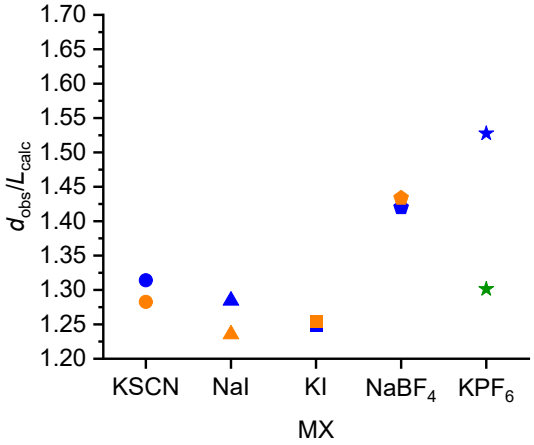

Figure S174: d_{obs}/L_{calc} ratio for smectic complexes **c-DOPA(n) • MX** (n = 12 in blue; n = 14 in orange) and **c-THIQ(14) • KPF_6** (in green); MX = KSCN (circles), NaI (triangles), KI (squares), $NaBF_4$ (pentagons) and KPF_6 (stars).The increase of d_{obs} for **c-DOPA(n) • MX** with the chain length is due to an increase of the molecular length, as evidenced by the almost unaffected d_{obs} / L_{calc} ratio

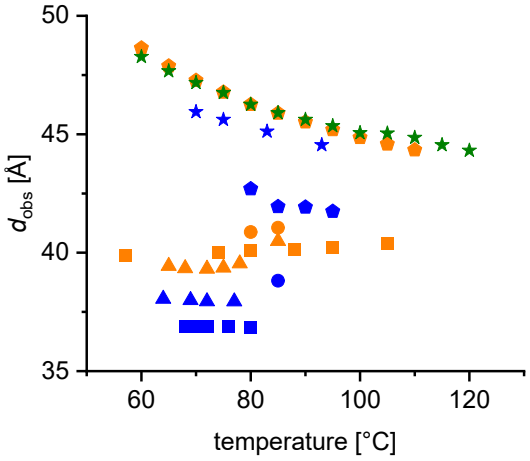

Figure S175: Temperature dependency of d_{obs} for smectic complexes **c-DOPA(n) • MX** (n = 12 in blue; n = 14 in orange) and **c-THIQ(14) • KPF_6** (in green); MX = KSCN (circles), NaI (triangles), KI (squares), $NaBF_4$ (pentagons) and KPF_6 (stars).

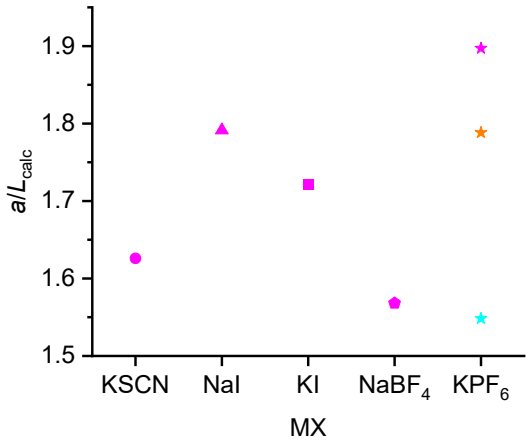

Figure S176: Influence of MX on *a* for columnar hexagonal complexes **c-DOPA(n) • MX** (n = 14 in orange; n = 16 in pink) and **c-THIQ(16) KPF_6** (in cyan); MX = KSCN (circle T = 85°C), NaI (triangle, T = 93°C), KI (square, T = 80 °C), $NaBF_4$ (pentagon, T = 80°C) and KPF_6 (stars, T = 60 °C for **c-DOPA(14)**, 74°C for **c-DOPA(16)**, 80 °C for **THIQ(16)**).

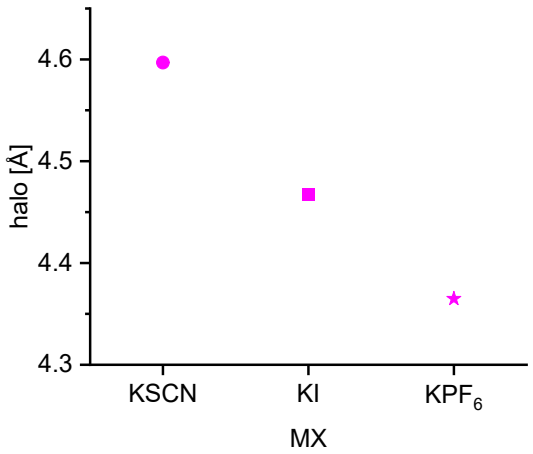

Figure S177: Influence of the anion on the intercolumnar distance of **c-DOPA(16) • KX**, with KX = KSCN (circle, T = 85 °C), KI (square, T = 80 °C) and KPF_6 (star, T = 74°C).

8 Electron density calculations

Table S18: Parameters used for the calculation of the electron density maps depicted in Figure 8. Intensities are Lorentz and Polarization corrected. See ref. 20,21 for further details on the calculation.

Compound	Layer spacing d_{obs} / Å	Miller indices (*hkl*)	Corrected intensity a_{hkl} / arb. units	Phase angle ϕ(*hkl*)
c-DOPA(12) • KI at 72 °C	36.9	(001)	0.8055	0
		(002)	0.2952	0
c-DOPA(14) • KI at 80 °C	40.1	(001)	0.8387	0
		(002)	0.3531	0

Table S19: Parameters used for the calculation of the electron density maps depicted in Figures 12 and 14 as well as Figures S174 and S175. The multiplicity, which describes the number of symmetry equivalent reflections, is 6 for all reflections considered in the calculation. Intensities are Lorentz corrected. See ref. 22 for further details on the calculation.

Compound	lattice parameter *a* / Å	Miller indices (*hkl*)	Corrected intensity a_{hkl} / arb. units	Phase angle ϕ(*hkl*)
c-DOPA(14) • KPF_6 at 80 °C	55.3	(100)	1	0
		(110)	0.2729	0
		(200)	0.2228	0
c-DOPA(16) • KSCN at 85 °C	56.2	(100)	1	0
		(110)	0.2461	0
		(200)	0.2225	0
c-DOPA(16) • NaI at 93 °C	62.0	(100)	1	0
		(110)	0.2438	0
		(200)	0.2231	0
c-DOPA(16) • $NaBF_4$ at 80 °C	54.2	(100)	1	0
		(110)	0.2380	0
		(200)	0.2097	0
c-DOPA(16) • KPF_6 at 80 °C	65.6	(100)	1	0
		(110)	0.2432	0
		(200)	0.2184	0
c-THIQ(16) • KPF_6 at 80 °C	58.5	(100)	1	0
		(110)	0.2307	0
		(200)	0.2044	0

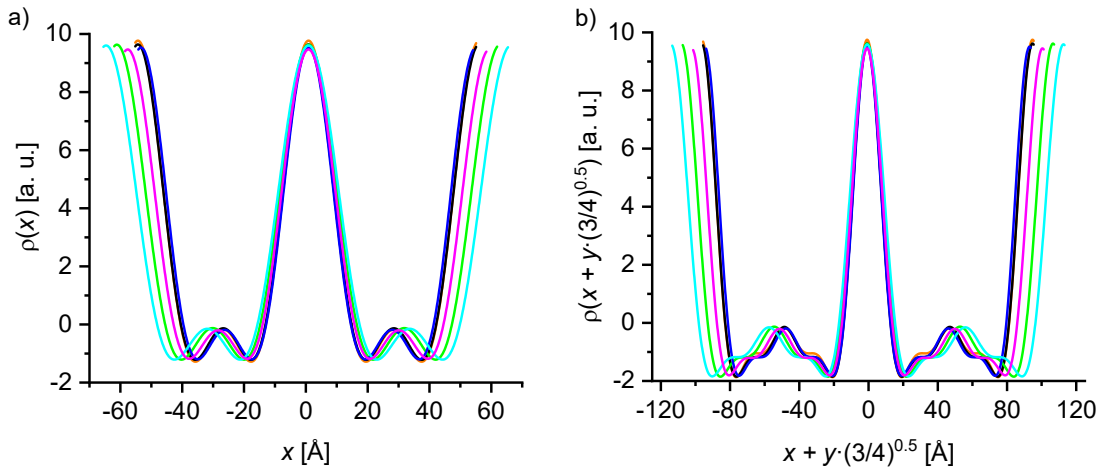

Figure S178: Calculated 1D electron density distributions a) along the lattice parameter and b) along the bisecting line of the hexagonal unit cell of the 2D electron density maps depicted in Figure 16; **c-DOPA(14) • KPF_6** (orange), **c-DOPA(16) • KSCN** (black), **c-DOPA(16) • NaI** (green), **c-DOPA(16) • $NaBF_4$** (blue), **c-DOPA(16) • KPF_6** (cyan), and **c-THIQ(16) • KPF_6** (pink).

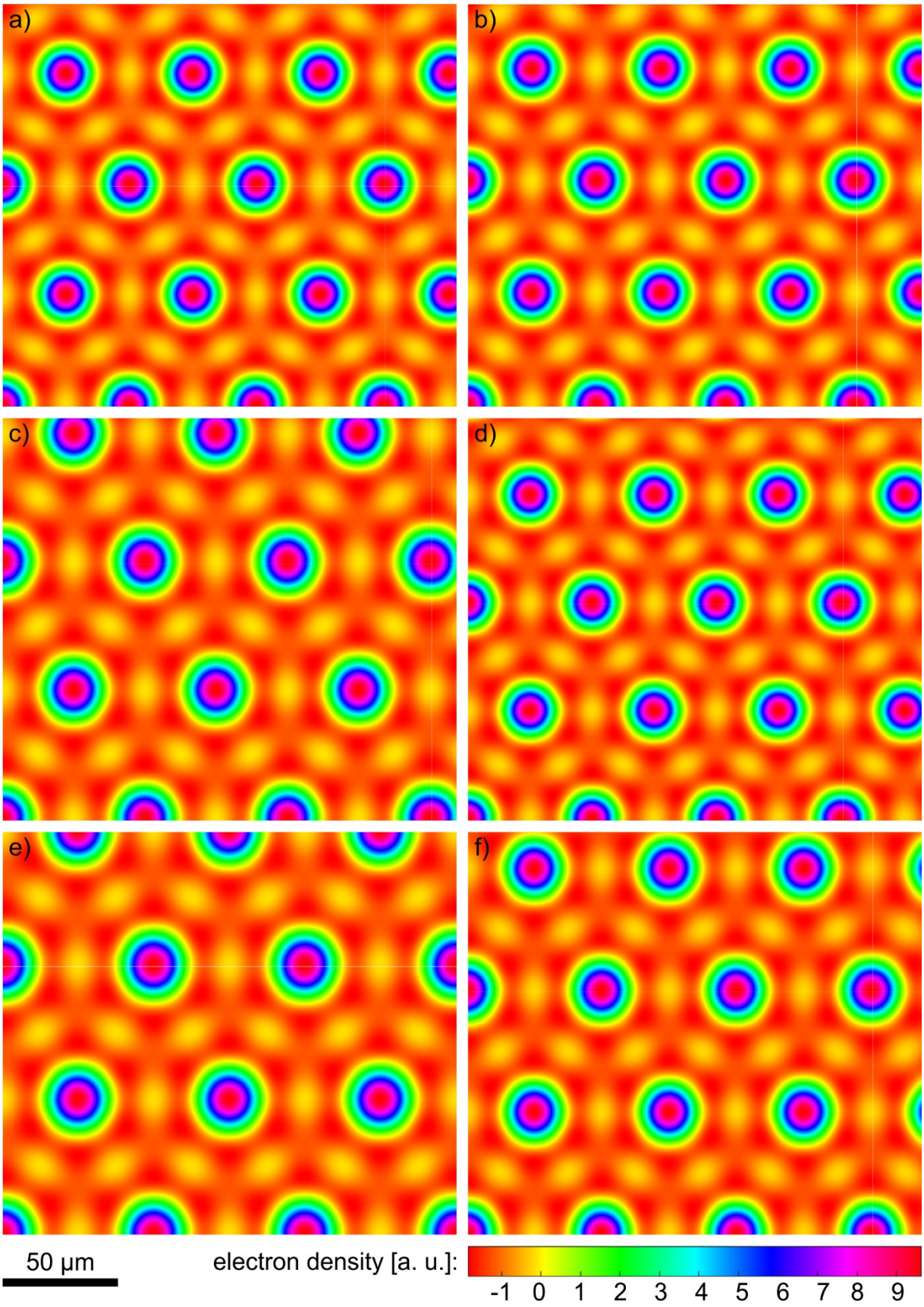

Figure S179: Calculated 2D electron density distribution of a) **c-DOPA(14) • KPF_6**, b) **c-DOPA(16) • KSCN**, c) **c-DOPA(16) • NaI**, d) **c-DOPA(16) • $NaBF_4$**, e) **c-DOPA(16) • KPF_6** and f) **c-THIQ(16) • KPF_6**.

Comparing the calculated electron density distributions of components which only differ in the kind of anion from each other should provide additional insights into the location of the anions. For this, we selected **c-DOPA(16) • $NaBF_4$** and **c-DOPA(16) • NaI** because they differ the most in their atomic form factors.[23] To visualize the differences between the two components we calculated an electron density difference map, after normalizing the lattice parameters to the same value. The resulting difference map in Figure S180 reveals that the electron density of **c-DOPA(16) • NaI** is elevated the most in the center of the columns (pink area) compared to the one of **c-DOPA(16) • $NaBF_4$**, which substantiates the assumption that the anions are mainly located in anion channel in the middle of the columns. The other differences in the electron density are of lower magnitude and might partially arise from the rescaling of the lattice parameter. Unfortunately, construction of a similar electron density difference map for the SmA_d phase is not possible, because in this case only the KI complexes showed more than one scattering peak and thus allowed the calculation of electron density distributions.

Despite the good agreement of Figure S180 with our suggested structure model, the calculated difference map should be handled with caution, considering that the calculated electron densities are only relative, not absolute values.

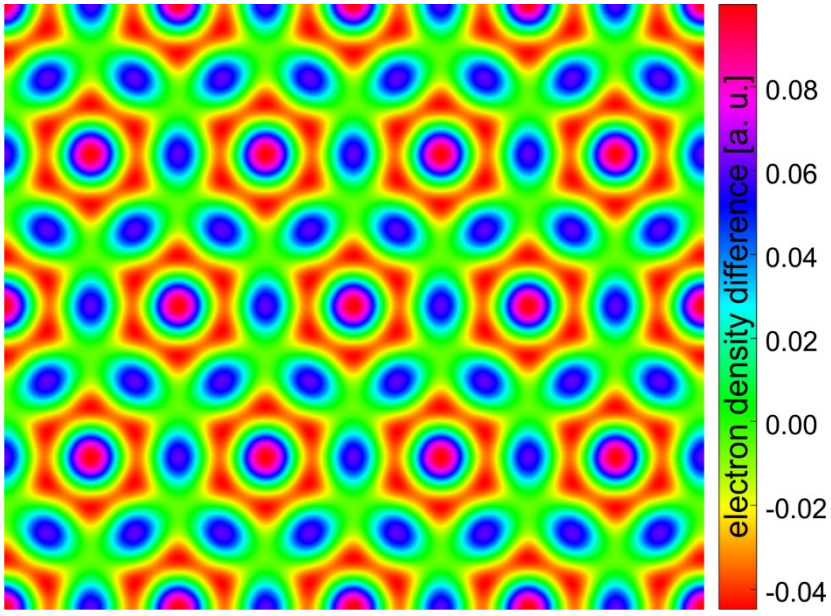

Figure S180: Electron density difference map constructed by subtracting the 2D electron density distribution calculated for **c-DOPA(16) • $NaBF_4$** from the one calculated for **c-DOPA(16) • NaI** (cf. Figure S179). Lattice parameters were normalized prior to subtraction.

9 Retardation experiments

Temperature-dependent optical retardation measurements were conducted to probe the collective thermotropic orientation of the ionic liquid crystal units in the bulk state. Samples in the isotropic phase were filled in liquid crystal test cells (AWAT, Poland) with a cell gap of 1.6 µm. The hydrophobic cells were rubbed on both sides with nylon (thickness = 50 nm). The experimental setup employed a He–Ne laser (λ = 632.8 nm) as a linearly polarised light source. As illustrated in Figure S181, the laser beam first passes through a polariser to ensure linear polarisation at an angle of 45° with respect to the propagation direction. A photoelastic modulator (PEM) introduces a time-modulated phase delay to the beam.

The beam measuring the linear birefringence (Δ-arm) is subsequently reflected by two mirrors and directed through the sample at an incidence angle of α = 36°. After transmission, it passes through an analyser oriented perpendicular to the polariser and is then detected by a photodiode. Two SR830 lock-in amplifiers (Stanford Research Systems, Sunnyvale, USA) are connected to the detector to record the amplitudes of the first and second harmonics, using reference signals at 50 kHz and 100 kHz derived from the modulated light intensities. The corresponding optical retardation is then determined from the measured signal intensities.

Throughout the experiment, the temperature of the sample is varied at a controlled rate of 0.15 K min^{-1} to capture thermotropic transitions. By analysing the optical retardation between the ordinary and extraordinary beams, the collective molecular orientation during heating and cooling within the cells can be inferred. Upon cooling into the liquid crystalline phase, an increase in the retardation value reflects a collective orientation of the discotic units with their rotational axes perpendicular to the pore axis, whereas a decrease in retardation indicates alignment of the rotational axes parallel to the pore axis.

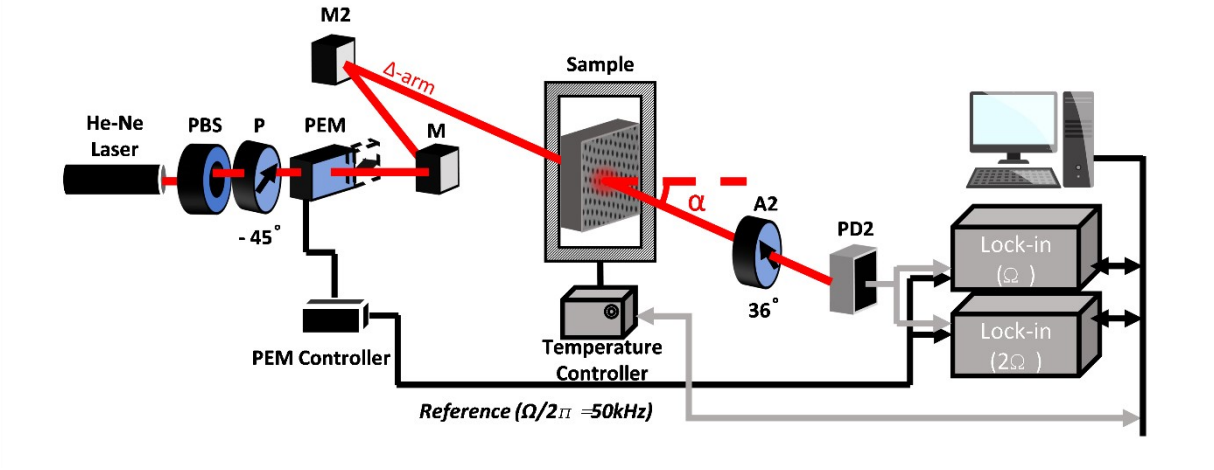

Figure S181: Schematic of the retardation measurement setup. PBS: polarising beam splitter, which divides the laser beam into the Ψ and Δ arms (only the Δ arm is used in this work). P: polariser; PEM: photoelastic modulator; M1 and M2: mirrors; λ/4: quarter-wave plate. The sample is placed in a sealed chamber under an argon atmosphere. A2: analyser, oriented perpendicular to the polariser. PD2: photodiode, which detects the modulated light and sends the signal to the lock-in amplifier for analysis. Reproduced with permission from Zhuoqing Li, ACS Nano, 2024, 18, 22, 14414–14426. Copyright 2024 American Chemical Society.[10]

The optical birefringence $\Delta n = n_e - n_o$ is obtained from the measured optical retardation R by applying Berek's equation for a uniaxial birefringent plate whose optic axis is tilted by an angle θ relative to the direction of the incident light. For a sample of thickness t, probed at wavelength λ, the retardation introduced by the birefringent medium is given by:

$$R = \left(\frac{2\pi t}{\lambda}\right)\left(n - \frac{\Delta n}{3}\right)\left[\sqrt{1 - \frac{\sin^2\theta}{\left(n + \frac{2\Delta n}{3}\right)^2}} - \sqrt{1 - \frac{\sin^2\theta}{\left(n - \frac{2\Delta n}{3}\right)^2}}\right]. \quad \text{(S1)}$$

R is the measured optical retardation (phase difference between the ordinary and extraordinary components), t is the physical thickness of the birefringent sample, λ is the wavelength of the probing light, and θ is the angle between the optic axis of the material and the propagation direction of the incident beam. The ordinary and extraordinary refractive indices are denoted by n_o and n_e, respectively, giving the birefringence $\Delta n = n_e - n_o$. The average refractive index is defined as $n = (2n_o + n_e)/3$. In practice, this expression is evaluated by numerically solving for Δn using the measured values of R, t, λ, and θ. This procedure yields the intrinsic birefringence of the material under the experimental geometry.

However, Eq. S1 contains only parameters that are fixed by the experimental configuration. Thus, the optical retardation R alone is sufficient to evaluate changes in molecular orientation.

Nevertheless, if an effective medium description of the composite is applied, the optical birefringence can be obtained by converting the measured retardation into Δn using Eq. S1.

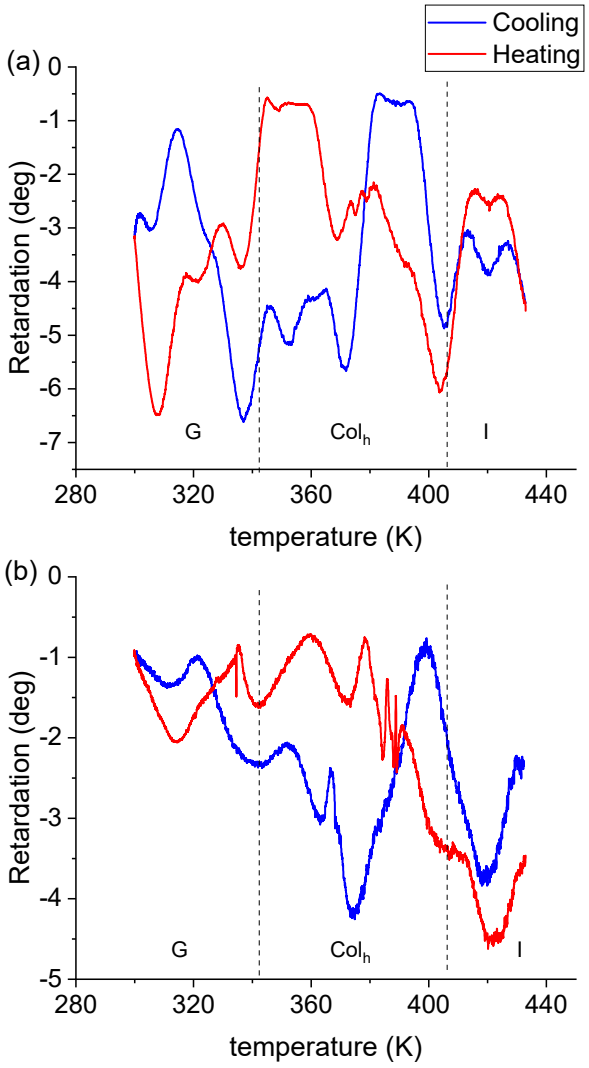

Figure S182: Optical retardation measurements of **c-DOPA(16) • KPF_6** in the bulk state under different surface conditions. a) corresponds to cells with hydrophilic surface treatment, (b) shows results for cells with hydrophobic surface treatment; dashed lines indicate phase transitions measured during 3rd cooling measured by DSC (G: glass, Col_h: hexagonal columnar, I: isotropic).

10 Dielectric measurements

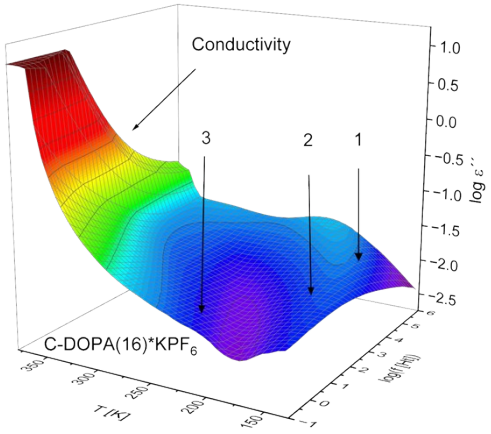

Figure S183: 3D representation of dielectric loss for **c-DOPA(16) • KPF_6** vs. frequency and temperature. The relaxation processes and the conductivity contributions are marked by arrows.

Fitting procedure for the HN model function:

The HN function is mathematically given by[24]

$$\varepsilon^*_{HN}(\omega) = \varepsilon_\infty + \frac{\Delta\varepsilon_{HN}}{(1 + (i\omega\tau_{HN})^\beta)^\gamma} \quad \text{(S2)}$$

ε_∞ denotes the real part of the complex permittivity in the limit $\varepsilon_\infty = \lim_{\omega \gg \tau_{HN}^{-1}} \varepsilon'(\omega)$. The parameter $\Delta\varepsilon_{HN}$ signifies the dielectric strength. The relaxation time, τ_{HN}, is associated with the frequency at which the dielectric loss attains its peak maximum value, referred to as f_p (relaxation rate). The relaxation rate is derived from the relaxation time using the following relationship[25]

$$f_p = \frac{1}{2\pi\,\tau_{HN}}\left[sin\frac{\beta\pi}{2+2\gamma}\right]^{1/\beta}\left[sin\frac{\beta\gamma\pi}{2+2\gamma}\right]^{-1/\beta} \quad \text{(S3)}$$

The parameters β and γ ($0 < \beta$; $\beta\gamma \leq 1$) are used to describe the symmetric and asymmetric broadening of the relaxation spectrum relative to the Debye model.[25] In the fitting process, conductivity is accounted for by incorporating the term $\frac{\sigma_0}{(\omega^s\,\varepsilon_0)}$ into the dielectric loss part of the HN-function. The parameter σ_0 is related to the DC conductivity but also encompasses contributions from Maxwell-Wagner-Sillars effects and/or electrode polarization. The parameter $0 \leq s \leq 1$ characterizes non-ohmic effects in conductivity, with s = 1 indicating ohmic conductivity. The symbol ε_0 represents the permittivity of free space. In the case that several

relaxation processes were observed in the accessible frequency window a sum of HN-functions was fitted to the data of the dielectric measurements. For further details, refer to ref. 25. For all relaxation processes γ was fixed to 1 during the analysis to reduce the number of free fit parameters.

Derivative approach for the evaluation of relaxation process 4 (α-relaxation):

To analyse the α-relaxation the contribution of conductivity needs to be removed. For this the dielectric spectra can be investigated by a so-called conduction free loss approach.[26] For the Debye function it could be shown that

$$\varepsilon_{Deriv}^{''} = -\frac{\pi}{2}\frac{d\,\varepsilon}{d\log(\omega)} = \varepsilon^{''2} \tag{S4}$$

holds. By this approach the contributions of the Ohmic conductivity are removed. Moreover, due to the square in $\varepsilon_{Deriv}^{''}$ the width of the conduction free loss is smaller than that of ε´´ itself. The dielectric data at temperatures above the estimated glass transition temperature of the samples was analysed by this approach. The power of this technique is demonstrated by Figure S184 where the frequency dependence of ε´´ is compared to that of $\varepsilon_{Deriv}^{''}$. A further peak is observed in $\varepsilon_{Deriv}^{''}$ (see Figure S184 b). This peak indicates a further relaxation process, relaxation process 4. The frequency dependence of $\varepsilon_{Deriv}^{''}$ is analysed by fitting the derivative of the real part of the HN-function $\frac{d\,\varepsilon_{HN}^{'}}{d\log\omega}$ to the data. $\frac{d\,\varepsilon_{HN}^{'}}{d\log\omega}$ is given by

$$-\frac{d\epsilon_{HN}^{'}}{dlog\omega} = \frac{1}{ln(10)}\frac{\beta\gamma\Delta\epsilon_{HN}(\omega\tau_{HN})^{\beta}\cos\left(\frac{\beta\pi}{2}\right)(-(1+\gamma)\Psi(\omega))}{\left[1+2(\omega\tau_{HN})^{\beta}\cos\left(\frac{\beta\pi}{2}\right)+(\omega\tau_{HN})^{2\beta}\right]^{\frac{1+\gamma}{2}}} \tag{S5}$$

with

$$\Psi(\omega) = \arctan\left[\frac{\sin\left(\frac{\beta\pi}{2}\right)}{(\omega\tau_{HN})^{-\beta}+\cos\left(\frac{\beta\pi}{2}\right)}\right] \tag{S6}$$

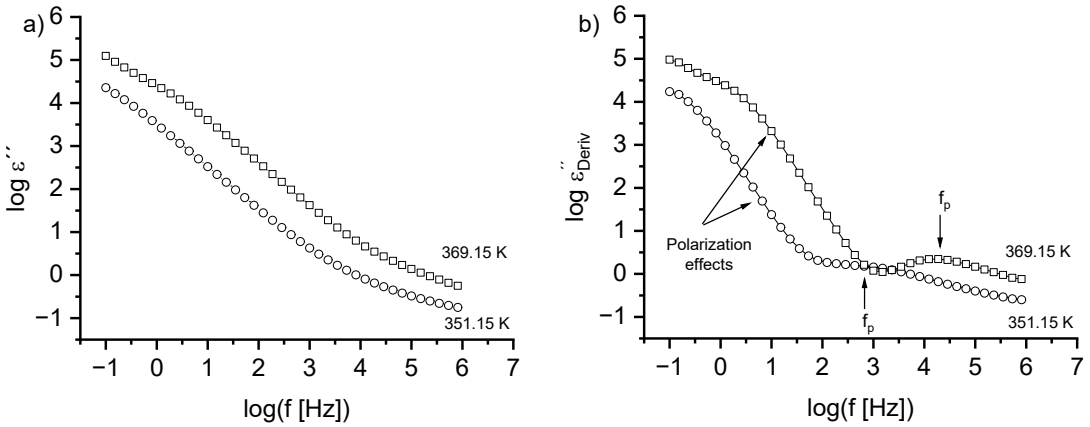

Figure S184: a) Dielectric loss versus frequency for **c-DOPA(16) • KPF_6**: Circles – T = 351.15 K, squares – T = 369.15 K. b) Conduction free dielectric loss versus frequency: Circles – T = 351.15 K, squares – T = 369.15 K.

Fitting procedure for the DC conductivity:

$$\sigma^*(\omega) = \sigma'(\omega) + i\sigma''(\omega) = i\omega\varepsilon_0\varepsilon^*(\omega) \quad \text{(S7)}$$

where σ´ and σ´´ are real and imaginary part of the complex conductivity:

$$\sigma'(\omega) = \omega\varepsilon_0\varepsilon''(\omega) \quad \text{(S8)}$$

$$\sigma''(\omega) = \omega\varepsilon_0\varepsilon'(\omega) \quad \text{(S9)}$$

ε_0 is the permittivity vacuum. Figure S184 depicts the frequency dependence of σ´(f) for the sample **c-DOPA(16) • KPF_6** at different temperatures. The frequency dependence reveals the characteristic features of semi-conductive materials. At high frequencies σ´(f) decreases with decreasing frequency with a power law reaching a plateau which characterizes the DC conductivity σ_{DC}. The further decrease of σ´(f) at even lower frequencies is related to polarization effects.

The DC conductivity is estimated by fitting the Jonscher equation to the frequency dependence of σ´(f) excluding polarization effects.[27] The Jonscher equation reads

$$\sigma'(f) = \sigma_{DC}\left(1 + \left(\frac{f}{f_c}\right)^n\right) \quad \text{(S10)}$$

The exponent n has values between 0.5 and 1. The frequency f_c characterizes the onset of the dispersion. The DC conductivity is a related to f_c by the empirical Barton–Nakajima–Namikawa (BNN) relation.[28]

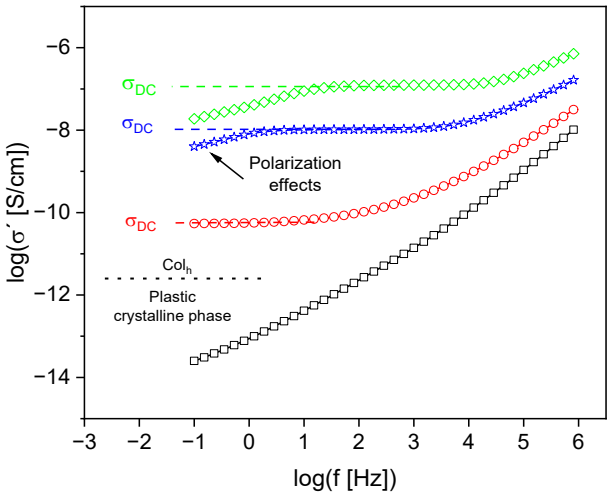

Figure S185: Real part of the complex conductivity versus frequency at T = 304.15 K (black squares), 330.15 K (red circles), 363.15 K (blue asterisk) and 381.15 K (green diamonds).

11 Fast Scanning Calorimetry

Figure S186 gives the heat flow for **c-DOPA(16) • KPF_6** for different heating rates in the range of 4000 K/s to 10^4 K/s. Besides the melting transition and the clearing point which are indicated by peaks, a step-like change is observed in the temperature dependence of the heat flow. This step-like change is assigned to the glass transition in the Col_h phase. With increasing heating rate, the step-like change in the heat flow shifts to higher temperatures as expected for a glass transition.

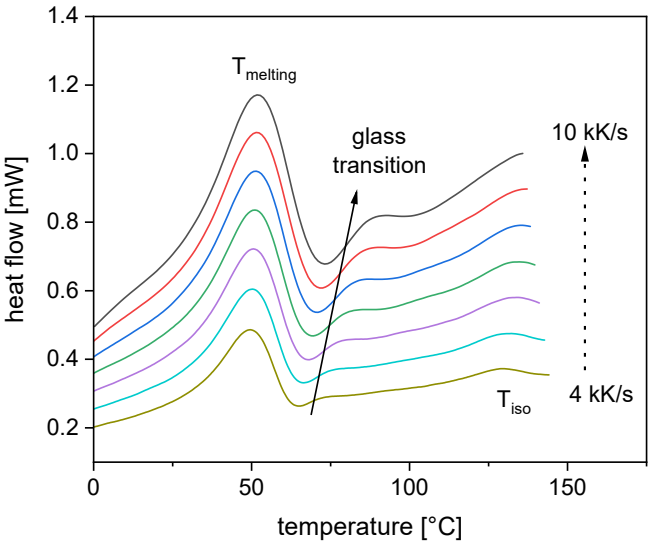

Figure S186: Heat flow versus temperature for the sample **c-DOPA(16) • KPF_6** for different heating rates in the range of 4000 K/s and 10^4 K/s.

Figure S187 gives the heat flow for **c-THIQ(16) • KPF_6** for different heating rates in the range of 2000 K/s to 8000 K/s. Like for **c-DOPA(16) • KPF_6** a step-like change is observed in the heat flow which shifts to higher temperatures with increasing heating rates. Therefore, this step-like change in the heat flow is assigned to the glass transition of **c-THIQ(16) • KPF_6** in the Col_h phase.

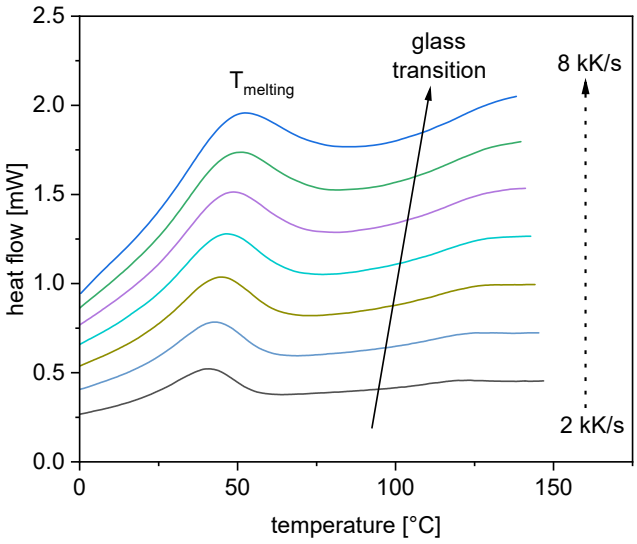

Figure S187: Heat flow versus temperature for the sample **c-THIQ(16) • KPF_6** for different heating rates in the range of 2000 K/s and 8000 K/s.

12 References

1 V. Mathot, M. Pyda, T. Pijpers, G. Vanden Poel, E. Van De Kerkhof, S. Van Herwaarden, F. Van Herwaarden and A. Leenaers, *Thermochim. Acta*, 2011, **522**, 36–45.

2 G. Lindsten, O. Wennerström and R. Isaksson, *J. Org. Chem.*, 1987, **4**, 547–554.

3 M. J. Calverley, J. Dale, A. Jutand, T. Nishida, C. R. Enzell and J.-E. Berg, *Acta Chem. Scand.*, 1982, **36b**, 241–247.

4 V. Calderón, G. Schwarz, F. García, M. J. Tapia, A. J. M. Valente, H. D. Burrows and J. M. García, *J. Polym. Sci. A. Polym. Chem.*, 2006, **44**, 6252–6269.

5 J. S. Moore and S. I. Stupp, *Macromolecules*, 1990, **23**, 65–70.

6 M. P. Chelopo, S. A. Pawar, M. K. Sokhela, T. Govender, H. G. Kruger and G. E. M. Maguire, *Eur. J. Med. Chem.*, 2013, **66**, 407–414.

7 B. M. Rosen, M. Peterca, K. Morimitsu, A. E. Dulcey, P. Leowanawat, A.-M. Resmerita, M. R. Imam and V. Percec, *J. Am. Chem. Soc.*, 2011, **133**, 5135–5151.

8 M. M. Neidhardt, K. Schmitt, A. Baro, C. Schneider, U. Bilitewski and S. Laschat, *Phys. Chem. Chem. Phys*., 2018, **20**, 20371–20381.

9 Y. Azefu, H. Tamiaki, R. Sato and K. Toma, *Bioorg. Med. Chem*., 2002, **10**, 4013–4022.

10 Z. Li, A. Raab, M. A. Kolmangadi, M. Busch, M. Grunwald, F. Demel, F. Bertram, A. V. Kityk, A. Schönhals, S. Laschat and P. Huber, *ACS Nano*, 2024, **18**, 14414–14426.

11 N. Srinivasan, A. Yurek-George and A. Ganesan, *Mol. Divers*., 2005, **9**, 291–293.

12 K. Bader, M. M. Neidhardt, T. Wöhrle, R. Forschner, A. Baro, F. Giesselmann and S. Laschat, *Soft Matter*, 2017, **13**, 8379–8391.

13 M. Kaller, P. Staffeld, R. Haug, W. Frey, F. Giesselmann and S. Laschat, *Liq. Cryst*., 2011, **38**, 531–553.

14 R. D. Shannon, *Acta Cryst. A*, 1976, **32**, 751–767.

15 J. R. Tessman, A. H. Kahn and W. Shockley, *Phys. Rev.*, 1953, **92**, 890–895.

16 M. Li, B. Zhuang, Y. Lu, Z. G. Wang and L. An, *J. Phys. Chem. B*, 2017, **121**, 6416–6424.

17 H. K. Roobottom, H. D. B. Jenkins, J. Passmore and L. Glasser, *J. Chem. Educ*., 1999, **76**, 1570–1573.

18 C. Millot, A. Chaumont, E. Engler and G. Wipff, *J. Phys. Chem. A*, 2014, **118**, 8842–8851.

19 M. C. Simoes, K. J. Hughes, D. B. Ingham, L. Ma and M. Pourkashanian, *Inorg. Chem*., 2017, **56**, 7566–7573.

20 D. M. Smilgies, *Rev. Sci. Instrum*., 2002, **73**, 1706–1710.

21 P. Davidson and L. Strzelecki, *Liq. Cryst*., 1988, **3**, 1583–1595.

22 A.-K. Beurer, S. Dieterich, H. Solodenko, E. Kaya, N. Merdanoğlu, G. Schmitz, Y. Traa and J. R. Bruckner, *Microporous Mesoporous Mat.,* 2023, **354**, 112508.

23 Stephen Seltzer (2005), NIST X-Ray Form Factor, Attenuation and Scattering Tables - SRD 66, National Institute of Standards and Technology, https://www.nist.gov/pml/x-ray-form-factor-attenuation-and-scattering-tables (Accessed 2025-12-15)

24 S. Havriliak and S. Negami, *J Polym Sci, Part C, Polym. Symp*., 1966, **14**, 99–117.

25 A. Schönhals, F. Kremer. Analysis of Dielectric Spectra. In: F. Kremer, A. Schönhals (Eds.), Broadband Dielectric Spectroscopy. Springer, Berlin, Heidelberg, 2003; pp. 59–98.

26 M. Wübbenhorst and J. van Turnhout, *J. Non. Cryst. Solids*, 2002, **305**, 40–49.

27 A. K. Jonscher, *Nature*, 1977, **267**, 673–679.

28 J. C. Dyre and T. B. Schrøder, *Rev. Mod. Phys*., 2000, **72**, 873–892.